STUDIES ON THE INFLUENCE OF ADMIXTURES ON VARIOUS PROPERTIES OF FOAM CONCRETE AND ASSESSMENT OF ITS SUSTAINABILITY MEASURE

A Thesis Submitted

in Partial Fulfilment of the Requirements

for the Degree of

DOCTOR OF PHILOSOPHY

by

WAGH CHANDRASHEKHAR DATTATRAY

DEPARTMENT OF CIVIL ENGINEERING

INDIAN INSTITUTE OF TECHNOLOGY GUWAHATI

GUWAHATI-781039, INDIA

June, 2024

Dedicated to,

My parents,

Dattatray Vitthal Wagh

(Father)

&

Mangal Dattatray Wagh

(Mother)

Indian Institute of Technology Guwahati

Department of Civil Engineering

Statement

I, hereby declare that the content embodied in this thesis entitled ***"Studies on the Influence of Admixtures on Various Properties of Foam Concrete and Assessment of Its Sustainability Measure"*** is the result of investigations carried out by me at the Department of Civil Engineering, Indian Institute of Technology Guwahati, Guwahati, India.

In keeping with the general practice of reporting scientific observations, due acknowledgements have been made wherever the work described is based on the findings of other investigators.

Date: - 11/06/2024

Wagh Chandrashekhar Dattatray

Place: IIT Guwahati

Indian Institute of Technology Guwahati

Department of Civil Engineering

Certificate

This is to certify that the thesis entitled ***"Studies on the Influence of Admixtures on Various Properties of Foam Concrete and Assessment of Its Sustainability Measure"*** *by Wagh Chandrashekhar Dattatray (Roll No: 186104034), to the Indian Institute of Technology Guwahati, India, for the award of Doctor of Philosophy, is a record of bonafide research work carried out by her under my guidance and supervision. The work embodied in this thesis has not been submitted for any other degree or diploma. In my opinion, the thesis is up to the standard of fulfilling the requirements of the doctoral degree as prescribed by the regulations of this Institute.*

Date: - 11/06/2024

Place: IIT Guwahati

G. Indu Siva Ranjani

Dr. G. Indu Siva Ranjani

Assistant Professor

Department of Civil Engineering

Indian Institute of Technology Guwahati

Guwahati-781039, Assam, India

Acknowledgements

This thesis is a result of combination of efforts of so many people who have helped me directly or indirectly during my long journey of PhD. Throughout this long journey, I have gained a lot by learning to preserve despite hardship. I would never have successfully completed this thesis without the assistance of numerous people who I am indebted to. Their direction, advice, support and contributions have proved invariable along the way. I am indebted to many people who had helped me during my research work and it is my privilege to acknowledge them.

At first, I express my deepest sense of gratitude and reverence to my thesis supervisors Dr. Indu Siva Ranjani Gandhi for believing in me. Without her guidance, persistent help, comments, and valuable suggestions, I would not have reached my destination. I thank Dr. Indu Siva Ranjani Gandhi for her dedication, concern, constant encouragement, and being a thrust whenever I was downcast with my Ph.D. I also thank her for instilling in me a craving for perfection. I believe, it will always remain with me in my future life. It has really been a notable working experience with him. Many thanks to her also for initiating and shaping the work of my Ph.D. and constantly shepherding throughout.

I express my sincere thanks to the members of my Doctoral Committee Prof. Laishram Boeing Singh, Prof. G. Pugazhenthi and Dr. Abhishek Kumar, for their valuable suggestions, encouragement, and timely help provided at various stages of the research work.

I thank the head of the civil engineering department (former and present), faculty in-charge of Infrastructure engineering and Management laboratory and Structural Laboratory (former and present) and staff members viz. scientific officer Dr. Arun Ch. Borsaikia, technical superintendent Mr. Pranab Hazarika, Junior Technician Mr. Saurabh Kr. Mudoi and Ms. Juri Jyoti Hazarika, Mr. Mitu Ali for helping me in extensive physical work for providing uninterrupted help accomplishing the Ph.D. work. I also would like to would like to acknowledge the support provided by Central Instruments Facility and Department of Civil Engineering, IIT Guwahati.

I thank my labmates and colleagues and my seniors Dr. Sritam Swapnardashi Sahu, Dr. Selija Khwairakpam, Mr. Abhishek Kamisetty, Mr. Uday Boddepalli, Ms. Nicola Thounaojam, Mr. Maradani Leela Sai Rangarao, Dr. Arya Anuj Jee, Mr. Sathishraj Mani, Dr. Jnyanendra

Kumar Prusty, for the stimulating discussions and the sleepless nights we were working together before deadlines. A very special thanks to Dr. Ketan Kumar Nandi, Mr. Akash Dilip Kamble, Mr. Pankaj Kumar, for their invaluable advice and feedback on my research and for always being so supportive of my work and my juniors for their help in during my Ph.D. I am also thankful to Mr. Ankush Sontakke and Ms. Shweta Kumbhar for their unconditional help and support. I have no words to thank all my friends who have made the stay at IIT Guwahati a memorable one.

Lastly, and the most importantly, I would like to thank my parents, sisters, brothers for all their love and encouragement. I consider myself nothing without them. They gave me enough moral support, encouragement and motivation to accomplish my goals.

Above all, I believe that everything happens for a good reason, so I thank almighty for giving me exposure to such a life changing experience of Ph.D.

Wagh Chandrashekhar Dattatray

Abstract

Almost 40% of the world's total energy demand is utilized to overcome the heat flow and acquisition via surface coating and building wall units. Using materials with low thermal conductivity (T.C) during design and construction of building will help to reduce this energy consumption to a great extent. Foam concrete (FC) which is classified as lightweight concrete (Density 400-1850 kg/m^3) can be considered as one of the suitable material for thermal insulation. It is a cement paste or mortar with air voids entrained by suitable foaming agent. Though low self-weight is considered as a basic property of lightweight foamed concrete but the other additional properties like high flowability, minimal consumption of aggregates, controlled low strength and excellent thermal insulation increases the use of FC in building construction. For instance, the thermal conductivity of LFC typically is 5% to 30% of that of normal weight concrete and range from 0.1 to 0.7 W/mK for dry density values of 400 to 1600 kg/m^3 respectively. Summarization of studies have highlighted the influence of surfactant and foam parameters viz., type of surfactant, dosage of surfactant, foam production technique, foam density, foam capacity, foam stability and bubble microstructure on these exemplary properties of foamed concrete. Hence, selecting appropriate surfactant which provides a stable good-quality foam is the crucial requirement for FC.

The first phase of this study evaluates the role of Xanthan Gum (XG) as an additive in the performance improvement of foam produced with two different surfactants, viz., Hingot (Natural surfactant) and Nonylphenol ethoxylate (NPE) (Synthetic surfactant). Different characteristics of foam and surfactant, such as initial foam density, foam drainage, foam bubble microstructure, surface tension, and viscosity of surfactants, are experimentally evaluated. Hingot surfactant due to its more surface active nature reported its surface tension value 15% lesser than that of NPE. Addition of XG resulted in a 10-fold increment in viscosity for both Hingot and NPE surfactant solutions. The above enhancement in viscosity lead to substantial reduction in bubble size and an increment in lamella thickness. Besides enhancement in viscosity due to XG addition, the lower surface tension value of Hingot surfactant also contributed to the reduction in lamella drainage time and bubble coalescence rate thus improving foam stability. For instance, mere 0.1% addition of XG reduced the drainage of Hingot foam from 90% to 42% at the end of 30 minutes. Further considering the effect of the addition of XG on FC properties, 38 % to 88% reduction in spread flow is noted for FC mixes produced with NPE and Hingot foam. Adding to above, Hingot based FC mixes shows higher

demoulding time when compared to that of NPE because of retarding nature of saponin present in Hingot solution which was further intensified with the addition of XG. Besides improvement in foam performance, a substantial increase in compressive strength and reduction in thermal conductivity of FC is also observed due to XG addition, indicating that foam bubble microstructure has a significant impact. For instance, addition of XG resulted in substantial increase of 51% and 22% in compressive strength of Hingot FC and NPE FC respectively. The best thermal performance is reported for the FC samples prepared with Hingot surfactant and 0.1 % dosage of XG as foam stabilizer. The cost analysis indicates that the production of Hingot surfactant (₹6.83/litre) is significantly more cost-effective than that of NPE surfactant (₹61.56/litre). Therefore, it can be concluded that Hingot + 0.1XG may serve as a cost-effective and better substitute for NPE surfactant.

Having identified the best combination of surfactant and foam stabilizer (Hingot + 0.1% XG), in the next phase, studies on influence of various admixtures viz. Fly ash (FA) as filler replacement, Silica fume (SF) as binder replacement and Polypropylene fiber (PP) as admixture on the FC behavior prepared with aforementioned surfactant combination is carried out. FC with target fresh densities of 600 kg/m^3 and 1000 kg/m^3 are prepared and its performance across stability, consistency, compressive and split tensile strength, thermal properties and microstructure analysis is evaluated. Although all the mixes with target density 1000 kg/m^3 are able to achieve the allowable density ratios (0.95 to 1.05) some of the mixes in 600 kg/m^3 exceeded the allowable density ratio. This may be assigned to the higher foam volume content which leads to longer setting time of the FC mixes causing breakage of foam and instability in the fresh FC further leading to increment in the density of FC. Incorporation of FA, SF and PP fibres reduces the spread flow of the FC to a great extent and hence demands the use of Superplasticizer to maintain the flow. The most significant impact of addition of admixtures is observed on the hardened properties of FC i.e. compressive strength and split tensile strength especially with the incorporation of FA as a replacement to filler. Replacement of sand with 100% FA lead to 368% and 228% increase in compressive strength of FC with design densities 1000 kg/m^3 and 600 kg/m^3 respectively compared to base mix (FC without admixtures) when tested at 90 days. This strength is further increased when used in combination with other admixtures like SF and PP fibre. Similar trend of observations is reported in case of split tensile strength. The combination of 100%FA + 10%SF +0.4%PP fibre reported the highest compressive and splitting tensile strength of 9.83 MPa and 1.671 MPa respectively for density 1000 kg/m^{3}at the testing age of 90 days. The corresponding strength for density 600 kg/m^3 was

3.93 MPa and 0.661 MPa respectively. This can be ascribed to the synergistic effect of combination of all three admixtures along with pozzolanic reaction and superior particle packing ability leading to pore structure improvement and subsequent enhancement of the strength of the FC mixtures. Considering the effect of mix composition on thermal properties, density plays an important role as established in literature. For base mix, with the decrease in density from 1000 kg/m^3 to 600 kg/m^3, the Thermal Conductivity (TC) of FC decreases from 0.3435 W/mK to 0.2476 W/mK. These values are further reduced with the incorporation of the admixtures. For instance, the combination of 100 FA + 0.4% PP fibre reported TC of 0.2959 W/mK and 0.1973 W/mK for densities 1000 kg/m^3 and 600 kg/m^3 respectively. The improvement in concrete pore structure with reduced pore diameter due to particle packing effect of fine FA particles and creation of additional voids due to PP fibres addition contributes to the above mentioned decrease in TC. Based on the performance across various properties evaluated and taking into consideration the economic perspective of mixes, MF2PP2 (FC of 1000 kg/m^3 density with 100 % FA + 0.4% PP fiber) and LF2PP2 (FC of 600 kg/m^3 density with 100 % FA + 0.4% PP fiber) are selected as optimum mixes.

Though FC shows a promising future in terms of huge energy savings when compared to the conventional constructional materials, a detailed life cycle assessment and operational energy cost analysis of using FC as a building component with respect to Indian context needs to be carried out. Thus the third and final phase of this study provides an in-depth investigation on the performance of selected optimum mixes with densities 600 kg/m^3 and 1000 kg/m^3 as a walling material in G+3 residential building for operational energy analysis and its life cycle assessment. Further, comparative analysis of performance of FC with conventional walling materials like standard clay brick and AAC block is also carried out. To evaluate the sustainability of FC prepared using admixtures and hingot surfactant, life cycle assessment (LCA) approach as per the guidelines of ISO 14040 (2006), ISO 14044 (2006) standards is adopted. SimaPro software version 9.3.03 is used for modelling and analysis with the boundary condition limited to cradle to gate of the laboratory facility for 1m^3 of FC serving as the functional unit. Results of the LCA analysis show that the total cumulative energy demand of preparation of 1 kg of Hingot solution is less than that of 1 kg of NPE surfactant solution. The environmental hazard analysis also favours Hingot as a sustainable and economical alternative to NPE surfactant. Results of LCA analysis of FC indicate that FC with densities 1000 kg/m^3 and 600 kg/m^{3}performs better than AAC block and conventional clay brick. The distribution of the cumulative energy demand of production of various constituents involved in the FC

production showed that, maximum cumulative energy demand can be observed for cement, which accounts for almost 70% of total embodied energy. The best performance considering all life cycle assessment categories is provided by the optimum mix of 600 kg/m^3 i.e. LF2PP2 while the clay brick reportedly performed worst of all materials in all the environmental assessment indicators. When compared to AAC block, Mix LF2PP2 showed 33% lower cumulative energy demand and 27% lower global warming potential. On similar lines for Mix MF2PP2 the decrement in cumulative energy demand and global warming potential reported is 23% and 15% respectively when compared to AAC. It is to be also noted that when compared to AAC block and Clay brick, the performance of both the optimum mixes LF2PP2 and MF2PP2 is also better in other environmental impact assessment categories like eutrophication, human toxicity, marine and freshwater ecotoxicity etc.

Further, DesignBuilder software used in this study served as a suitable analysis tool for calculation of operational energy cost of the building. Simulation is carried out to calculate the total annual operational energy incurred when the selected optimum mixes are used as walling and roofing material for buildings across different cities like, Bangalore, Dehradun, Guwahati, Jodhpur, Mumbai and New Delhi representing the various climatic zones of India. Simulation results showed that, of all the materials used in the present study as a walling material, clay brick exhibited highest annual energy consumption while mix LF2PP2 reported the lowest annual energy consumption across all the cities. For instance, in case of New Delhi city mere use of LF2PP2 as a walling and roofing material instead of Clay brick walls provided us with 21% of saving in operational energy. Similarly, the saving for mix MF2PP2 with density 1000 kg/m^3 is observed to be 16%. When compared with performance of AAC block LF2PP2 shows avg. annual energy saving of 11% while MF2PP2 results in savings of 4.5% when used as walling material in New Delhi city. The increased annual energy consumption of clay brick walls and AAC block wall can be attributed to its relatively higher thermal conductivity value, which allows higher average thermal transmittance through the structure.

Keywords: Foam concrete, natural surfactant, hingot, Nonylphenol ethoxylate, xanthan gum, foam stability, sustainability, carbon footprint, thermal comfort, life cycle, operational energy analysis.

TABLE OF CONTENTS

LIST OF FIGURES

LIST OF TABLES

LIST OF ABBREVIATIONS AND NOTATIONS

AAC	Autoclaved aerated concrete
BM	Base mix
C	Calcite ($CaCO_3$)
CMC	Critical micellar concentration
C-H	Calcium Hydroxide
C-S-H	Calcium Silicate Hydrate
DD	Dry density
E	Ettringite ($3CaO\ Al2O_3\ 3CaSO_4\ 32H_2O$)
EDS	Energy Dispersive X-ray spectroscopy
FA	Fly ash
FC	Foam concrete
FER	Foam expansion ratio
FGP	Foam generation pressure
FS	Foam stability
FTIR	Fourier Transform Infrared spectroscopy
GFC	Geopolymer foam concrete
GGBS	Ground granulated blast furnace slag
HM	Hingot mix
LCA	Lifecycle assessement
LICA	Lifecycle impact assessement
LWAC	Light weight aggregate concrete
LWC	Light weight concrete
NPE	Nonyl phenyl ethoxylate
P	Portlandite ($Ca(OH)_2$)
PP	Polypropylene fiber
PVA	Polyvinyl alcohol
Q	Quartz (SiO_2)
SEM	Scanning electron microscopy
SF	Silica fume
SLS	Sodium Lauryl Sulphate
SLES	Sodium lauryl ether sulfate

SP	Super plasticizer
TC	Thermal conductivity
TGA	Thermogravimetric analysis
IFD	Initial foam density
w/c	Water-cement ratio
w/s	Water-solids ratio
WRA	Water reducing admixture
XG	Xanthan gum
XRD	X-ray diffraction

CHAPTER 1 INTRODUCTION

1.1 General

Foresight groups around the world have identified the future need for construction materials that are light, durable, simple to use, economical, and yet more environmentally sustainable. Therefore, a special concrete, namely foam concrete (FC), which has the density ranging from 300 to 1850 kg/m^3 based on application, can be considered an alternative (Amran et al., 2015). Although FC was initially envisaged as an insulation material, there has been increasing widespread use in structural and semi-structural applications in the last few years (Jones and McCarthy, 2005a). Low range densities are generally designed for insulation purposes, whereas high range densities are envisaged for structural and semi-structural applications. Apart from these, high flowability, low self-weight, and excellent thermal and acoustic insulation are some key attributes of FC.

1.2 Foam concrete and its historical background

FC, which can be classified as a type of cellular concrete, is produced by introducing stable voids within the hardened cement paste or mortar, resulting in cellular structure in concrete. American Institute of Concrete (ACI Committee 523, 2014) defines cellular lightweight concrete as "a mixture of cement, water and preformed foam". The purpose of the foam is to provide a high ratio of air cells which, when mixed with cement, produce a porous solid. There are two different methods to create a cellular structure. (i) By chemical reaction, where gas can be generated within the mix during its plastic condition using expansive agents like aluminium(Al) powder and H_2O_2 (Gas concrete) (ii) By mechanical intrusion of air using foaming agents (FC). Gas concrete, also known as autoclaved aerated concrete (AAC), is a widely recognized and extensively utilized material in the production of wall panels and blocks. However, its utilization is constrained by the necessity of a substantial autoclaving factory setup, which incurs significant cost and lacks flexibility. This has limited AAC usage for precast units (Just and Middendorf, 2009). FC on other hand, can be used for both onsite production as well as precast applications. A schematic representation that represents the diverse ways of cellular concrete production is showed in Figure.1.1.

Although the Portland cement based FC was first patented by Axel Eriksson in 1923, FC has surprisingly a way long history (Valore, 1954a). There are evidences that suggest that two thousand years ago, the Romans had used animal blood as air entrainer which made the mix more workable and durable. They had even added horse hair into mixes to reduce shrinkage, much like fibres that are used nowadays in concrete (Amran et al., 2015). There is also evidence of use of this technology by the Egyptians over 5000 years ago, with similar results. Although these very early air entrained concretes were extremely basic with no control over air content, they cannot be considered as FC in true sense (Jones and McCarthy, 2005a). The lack of specialised materials and equipment had limited its use to small-scale projects and its application as an insulation material. But over the past 20 years a significant improvement was observed in production equipment and better quality surfactants (foaming agents). This has not only enabled the use of FC on a larger scale but also over a wide range of applications.

FC is now extensively used in Netherland, Sweden Germany, Switzerland, USA and UK (Cox, 2005; Wimpenny, 1996). In the year 1997, a successful trial was attempted in Delhi, India by G. B. Singh, who had constructed a G+3 storey building with FC (Singh, 2005). Recently, researchers have tried various techniques for improvement in strength of FC. Basically, uniform cellular structure is a key factor for producing concrete with good mechanical properties. Hence a significant way to improve concrete strength was witnessed by introducing additive that leads to protection of the bubbles from collapse leading to uniform cellular structure (Siva et al., 2015).

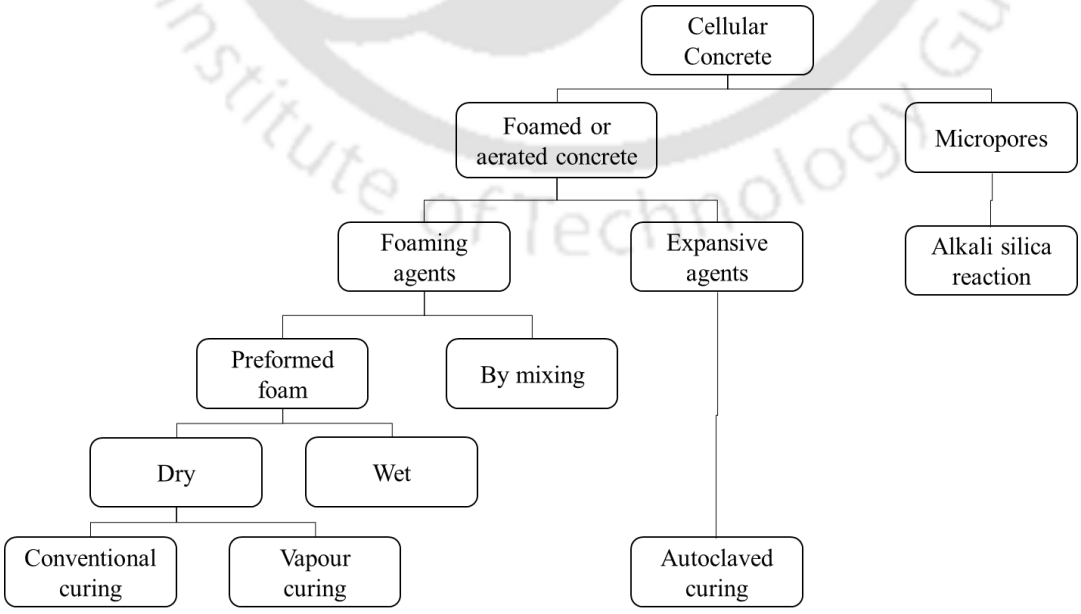

Figure 1-1: Classification of lightweight cellular concrete (Chica and Alzate, 2019)

1.3 Advantages and applications of foam concrete

The most important advantage of FC over its adversaries like AAC lies in the fact that construction elements in FC can be fabricated on construction site. Production of AAC blocks is restricted to factory which requires high initial investment cost and energy consuming process when compared to FC. In addition, large amount of industrial wastes (up to 70% fly ash) can be used in FC production without dramatically changing its mechanical properties, thus providing a means of economic and safe disposal of these waste residues (Just and Middendorf, 2009; Kearsley and Mostert, n.d.). Apart from this the other advantages associated with the several applications of FC are as follows: -

Variable density The density of FC ranges from 300 to 1850 kg/m^3, as compared to 2400 to 2600 kg/m^3 for conventional concrete. Therefore, the weight of a structure built with FC would undoubtedly be reduced significantly, leading to tremendous savings in the use of reinforcement steel in the foundations and structural members (Jones and McCarthy, 2005b).

Application: High density FC ranging from 1200 to 1800 kg/m^3 is reckoned as structural grade material and can be utilized for the construction of load carrying structural elements like walls, slabs, pre-cast blocks. In year 1997, a four storey high building was made using in-situ pouring of FC at Delhi, India, with density ranging from 1200 to 1600 kg/m^3. The walls were nominally reinforced cellular lightweight concrete cross walls having a uniform thickness of 150 mm throughout (Singh, 2005). Medium density FC ranging from 800 to 1000 kg/m^3 can be utilized for making pre-cast blocks for non-load-bearing walling masonry for internal and/or external walls in framed structures. Low densities of 400 to 600 kg/m^3 are ideal for thermal insulation applications like roof insulation.

Thermal insulation Thermal insulation is a major contributor and obvious practical and logical first step towards achieving energy efficiency especially in buildings located in sites with harsh climatic conditions. It has been reported that thermal conductivity of FC typically is 5% to 30% of that of normal weight concrete and ranges from 0.1 to 0.7 W/mK for concrete with dry density values ranging from 600 to 1600 kg/m^3 (Wagh et al., 2021).

Application: Due to superior thermal insulation property, FC was used for roof insulation in middle east and South Africa. In the middle far east, almost 3000 houses were built between 1948 and 1958 using 1100 to 1500 kg/m^3 density of FC (Giannakou and Jones, 2002; Jones and McCarthy, 2005a). The conditions of these dwellings when assessed later were found to have performed better than contemporary timber or brick and concrete houses. Approximately

250,000 m^3 of FC is used annually in Korea as an essential component in floor heating system (Yang et al., 2014).

Savings in Material and Manpower A reduction in dead weight contributes substantially to savings in reinforcement steel in foundations. For working with FC construction, only few semi-skilled workers are needed to produce FC for the casting/pouring of panels, blocks, or even to complete walls for houses.

Self- Levelling Concrete Properties Due to the absence of gravel and the ball-bearing effect of the foam, FC possesses a high degree of flow-ability. No vibration is thus required. FC completely fills all gaps and voids in the concrete or mould, fully embedding hoses, tubes, electrical conduits, windows and door frames, when cast in place.

Application: Due to its self-flowing nature, FC has been used in two of the largest FC void filling projects in the UK viz., (i) the Heathrow railway tunnel and (ii) Coombe Down mines. For the former, 14,500 m^3 of FC of 1400 kg/m^3 density were pumped into the ground over a period of 14 days to stabilise it, following the collapse of the railway express tunnel at Heathrow airport in 1994 (Jones and McCarthy, 2005a) .

Fast Track Construction Method The rapid mixing and high fluidity of FC facilitates speedy construction of cast-in-place building structure. With the application of vertical formwork to cast complete houses in place, omission of vibrating equipment results in the entire walls and roof slab of a building being filled in one step.

Application: In Richards Bay, considered as South Africa's busiest port, FC of density 500 kg/m^3 was used for backfilling (600 mm deep fill) to reduce the settlement and erosion and to facilitate speedy construction. Since the construction at port needed to be carried out quickly, FC was chosen as a material due to its self-flowing nature with less placement time.

1.4 Thermal Comfort and Operation Energy of Buildings

Thermal comfort is the condition of the mind that expresses pleasure with the thermal surroundings. Development in technology and extreme global temperatures is responsible for triggering mechanical means to control temperature in places like homes, offices, hospitals, malls etc. which provides a person with best possible comfort. This pursue for thermal comfort has led to huge consumption of energy. Operational energy of a building generally consists of energy consumed in heating/cooling, lighting and other electrical equipment operations. Operational energy is main part of energy used in general run of a building. Generally, in places with extreme weather, the heating and cooling operation contributes a major fraction in

operational energy usage. Thus, the pursue of thermal comfort and high operational energy usage has opened a vast field of research which ranges across disciplines. FC which is classified as lightweight concrete (density 400 to 1850 kg/m^3) can be considered as one of the most suitable material in modern building industry from thermal insulation point of view. Air being poorest conductor of heat, FC which signifies greater porosity due to air entrainment possess lower thermal conductivity which varies according to the degree of porosity.

1.5 Life cycle assessment

One of the main concerns on concrete production is the environmental impact produced throughout its upstream. Life Cycle Assessment (LCA) is used as a tool to assess the environmental impacts of a product, process or activity throughout its life cycle; from the extraction of raw materials through to processing, transport, use and disposal. LCA study includes thorough energy and material inventory, which is required throughout the product, process, and service value chain industry, and calculates the relevant environmental emissions.

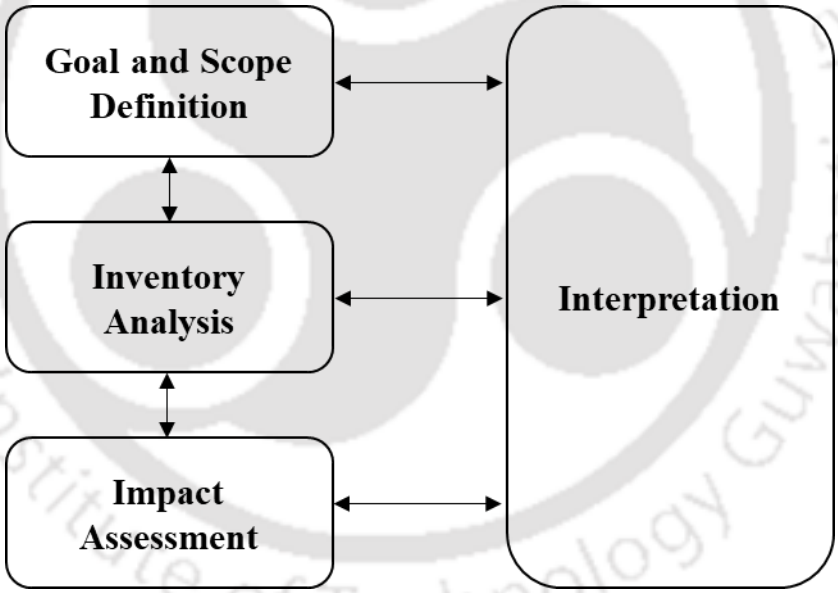

Figure 1-2 Illustration of the phases of a life-cycle assessment, as described by ISO 14040

The recent push towards sustainable development leads to the application of LCA in the construction industry. ISO 14040-2006 and ISO 14044-2006 specifies requirements and provides guidelines and framework for LCA. As per this, LCA is performed in four stages. The four steps include: goal and scope definition; inventory analysis; life-cycle impact assessment (LCIA); and interpretation as represented in Figure. 1.2.

1.6 Organization of report

The contents of this report are organised into seven chapters, followed by bibliographical references. For clarity of presentation, each chapter is divided into sections and sub-sections, as required. A brief overview of the contents of various chapters is as follows:

Chapter 2 Provides a review of literature from various standard journals, conference papers and books. It is categorised into four sections-

First section reviews literature on constituent materials of FC, surfactant and foam stability, and preparation methods of FC

Second section discusses various properties of FC and factors affecting it with special emphasis on the thermal properties of FC and its measurement methods.

Third section gives a detailed review on the role of insulating walling materials in thermal comfort and its effect on operational energy cost analysis of buildings

Fourth section addresses a systematic review on LCA, its implications in construction and building material field, current scenario of LCA of FC from the Indian perspective.

Chapter 3 provides the research objectives, scope of the work and brief outline of methodology to be carried out.

Chapter 4 depicts a more in-depth experimental programme on the comparative analysis of the influence of additive xanthan gum (XG) in performance improvement of foam produced with two surfactants viz., Nonyl phenol Ethoxylate (NPE) and Hingot and its role in enhancement of FC properties.

Chapter 5 discusses the influence of various admixtures (fly ash, silica fume, polypropylene fiber) on the different properties of FC. Fresh state characteristics, compressive strength, splitting tensile strength, thermal properties and microstructure of FC is discussed in detail. Further based upon the overall performance and considering cost efficiency, the optimum mixes are selected.

Chapter 6 provides an in-depth investigation into the performance of selected optimum FC mixes as a walling material and roofing material with varying densities (600 kg/m^3 to 1000 kg/m^3) in G+3 residential building with respect to operational energy analysis and its LCA. Further, comparative analysis of performance of FC with conventional walling materials like standard clay brick and AAC block is also carried out.

The last chapter (***Chapter 7***) summarises the typical conclusions drawn from the studies and the scope for future research.

CHAPTER 2 LITERATURE REVIEW

2.1 General

Chapter 1 provided a brief introduction to lightweight concrete, highlighting FC, its history, advantages and applications. It came to light that though the FC was introduced in 1924 by Axel Eriksson, however the first initial comprehensive review was conducted by Valore on cellular concrete only in 1954 (Valore, 1954a, 1954b). Further, a detailed review on FC production by Rudnai, Short & Kinniburgh came in 1963, summarizing the composition, properties, and uses (Short and Kinniburgh, 1963). Since then, there have been several studies and reviews on properties, application of FC (Amran et al., 2015; Ramamurthy et al., 2009), foam characteristics, and surfactants for use in FC (Sahu et al., 2018). Chapter 1 also provided a brief idea about the thermal comfort in buildings and its relation with operational energy of building, followed by an introduction to the concept of LCA. This chapter further attempts to review the existing academic journal papers and other available literature to provide the current research trend predominantly focusing on the functional properties and LCA of FC. Hence, this chapter is divided into four parts. The first part provides a short review of FC's constituent materials and preparation methods. The second part focuses on the properties of FC. Third part discusses in detail with respect to operational energy analysis. While the last part throws some light on the very few LCA studies carried out on FC till now.

2.2 Review on constituent materials and preparation methods of foam concrete

2.2.1 Surfactant

Surfactants, typically organic compounds, serve the purpose of reducing the surface tension or interfacial tension between various states of matter, such as gas-liquid or liquid-solid interfaces. Surfactants possess both hydrophobic and hydrophilic groups within their molecular structure. The hydrophobic group, which is not soluble in water, has the ability to extend beyond the aqueous environment and interact with either the gaseous phase or the oil phase. Meanwhile, the water-soluble head group remains confined within the aqueous phase (Wiley, 2010). Surfactants exhibit a diverse array of applications across various industries. These compounds play a crucial role as indispensable additives in the production of materials that find widespread utilization in our everyday lives. Notably, surfactants are integral components in the

formulation of laundry detergents, industrial cleaners, and cosmetics, among other products. Surfactants, which are widely employed in various industries such as pharmaceutical, textile, food, and petroleum, serve multiple functions including wetting, emulsifying, defoaming, and solubilizing (Sahu et al., 2018). In this line it also finds application in the production of stable foam, specifically for its utilization in FC (Ramamurthy et al., 2009). It has been observed that not all surfactants exhibit the ability to generate a stable foam suitable for the production of FC. The selection of surfactants plays a crucial role in determining the characteristics of foam, including its density, output rate, capacity, and stability. These factors, in turn, have a direct impact on the properties of FC. Based on their origin, surfactants can be categorized into two main groups, namely synthetic and natural.

Synthetic surfactants, also known as artificial surfactants, are artificially synthesized compounds that are readily manufacturable. The susceptibility of synthetic surfactants/ foaming agents for application is increased by their high productivity, its rigorous regulation over composition and extended shelf life, as noted by Sahu et al., (2018). Sodium Lauryl Sulphate (SLS) (Ranjani and Ramamurthy, 2010), Cetyltrimethylammonium bromide (CTAB) (Samson et al., 2017), Nonylphenol ethoxylate (NPE) (Sahu and Gandhi, 2021a) etc. are some of the synthetic type foaming agents commonly used in FC production. One of the drawbacks associated with synthetic surfactants, as documented in various studies, pertains to their lack of compatibility with other admixtures. Moreover, it should be noted that the production of synthetic surfactants necessitates the utilization of strict conditions, such as high pressure, nitrogen protection (ethoxylation), and blended catalysts (alkylation, oxidation, ethoxylation, condensation, and polymerization) which can have detrimental effects on the environment. Also, synthetic surfactants derived from petrochemical sources often give rise to by-products or isomers of the primary compounds like disulfonates in petrosulfonates or methyl ester sulfonates, causing environmental, or ecological problems (Nnanna et al., 2001). Since 1970, it has been established in scientific literature that synthetic surfactants have the potential to induce chronic and sub-lethal toxic effects on aquatic organisms (Lewis, 1991). Furthermore, research has also indicated that these surfactants can pose health hazards to human beings (Zhou et al., 2013). The aforementioned drawbacks associated with synthetic surfactants have encouraged the investigation and preference for surfactants derived from natural and renewable sources.

Natural surfactants are derived from a diverse range of waste materials, encompassing both animal and vegetable origins. Several studies have been conducted on the extraction of natural

surfactants from different sources, such as Glycyrrhiza Glabra (Arabloo et al., 2015) and Zyziphus Spina Christi (Shahri et al., 2012), specifically for their application in oil recovery. Additionally, Sapindus Mukorossi (Siva et al., 2017) and Phytolacea Dodecondra (Retta, 1991) have been investigated for their potential use in FC. It is worth noting that many plant products possess inherent surface-active properties due to the presence of a compound called "saponin." Saponin can be found in various parts of numerous plant species. Notable examples of saponin-rich plant species include soaproot (Chlorogalum pomeidianum), soapbark (Quillayasaponaria), soapberry (Sapindus saponaria), soapnut (Sapindus mukurossi), and soapjacob (Glinus lotoides) (Oleszek and Hamed, 2010; Siva et al., 2017). Recently pericarp of the soapnut fruit has been used successfully by (Siva et al., 2017) as a foaming agent in FC. Further saponin based surfactant derived from hingot fruit (Balanites aegyptiaca) was successfully developed by Khwairakpam and Ranjani Gandhi, (2020) and their output highlighted its potential to be used as surfactant in the FC. Researchers have also reported that protein based foaming agent produce uniformly distributed smaller size bubbles with viscous liquid around lamellar layer resulting in more stable foam (Kearsley and Wainwright, 2002; Nambiar and Ramamurthy, 2007a) which resulted in 20% increase in compressive strength of FC when compared to synthetic surfactant (D K Panesar, 2013). Natural surfactants are known for their environmentally friendly characteristics, as they possess low toxicity levels and are readily biodegradable. Despite these advantages, the application of natural surfactant is limited due to its intricate nature of the manufacturing process, limited storage life and inconsistency in composition due to variability in raw material.

2.2.2 Foam

A foam is commonly defined as a dispersion of gas bubbles in a liquid (Walstra, 1989). Foam is an important component of the FC. The dosage of foam controls the concrete density through the amount of air bubbles created in the cement paste mixture. The properties of foam are greatly influenced by the characteristics of foam, surfactant and method of production as discussed in subsequent sections.

Properties of foam and methods of its measurement

Important properties of foam are foam texture, foam density and foam stability;

Foam texture is commonly referred as the shape and size of bubbles in the foam (Osei-Bonsu et al., 2016). It has a significant influence on the foam stability and foamability. The shape of foam bubbles can be characterised as spherical or polyhedral (Vijayaraghavan et al., 2009).

According to minimum energy principle, bubbles will tend to become spherical in shape. Generally, the foam with smaller size bubbles are reported to be more stable and leads to reduction in rate of drainage. Numerous studies in the literature demonstrated that bubble size distribution is correlated with drainage rate (Magrabi et al., 1999). Also, more uniform bubble size distribution enhances foam stability (Miles et al., 1945; Sheng, 2013). From the above observation it is clear that the foam with fine texture (small spherical bubbles) is required to produce uniform and closed cellular microstructure.

Foam density is referred to a unit weight of foam. It is the governing parameter to calculate the foam volume for a given density of FC. As per ASTM C796-19, guidelines, the recommended foam density for use in preformed FC usually range from 30 to 65 kg/m^3 depending on the foaming agent used. This range could be adjusted according to the manufacturer's recommendation. Foam density depends on various factors like type of surfactant, concentration of surfactant, additives, viscosity of foaming solution, thickness of lamellae and foam generation pressure (Sahu et al., 2018). Researchers reported that a minimum lamellar thickness of 5–15 nm is necessary to sustain the pressure within the bubbles (Myers, 2020). Generally, the foam with higher density has thicker lamellae layer than the foam with lower density. Hence, when the thickness of lamellae layer around the bubble is greater than the critical thickness required, the stability of foam is reported to be good.

Foam expansion ratio (FER) is the ratio of volume of foam formed to the volume of foaming solution used to generate the foam (Magrabi et al., 2002). It is the measure of foam capacity or foamability of the foaming solution (Vananuvat and Kinsella, 1975). FER depends on the properties of surfactant and foam production parameters i.e. concentration of surfactant and foam generation pressure (FGP). The foam that is to be used in FC production should have FER in the range of 1:15.6 to 1:31.25 as derived from the foam density range recommended by ASTM C796M – 12. Foam with very high expansion ratio (greater than 1:50) has very thin lamellae layer resulting in foam with less stability. These over expanded foams of low foam density are likely to collapse and increase the FC density. On the other side, foam with less expansion ratio (less than 1:15) has less amount of air resulting in poor quality foam generally referred to as wet foam (Ranjani, 2011).

Stability of aqueous-based foam refers to the ability of foam to withstand spontaneous collapse or breakdown due to external causes. It reflects the life of the generated foam's lamellae (Laukaitis et al., 2005). Stability of foam is also dependent on the chemical and physical

properties of the surfactant-stabilized water film separating the bubbles of foam. Foam breakdown is due to excessive thinning and rupturing of foam liquid films with time and a result of diffusion of gas from smaller bubbles into the larger bubbles, thus increasing the bubble size of foam. Foam lamellae stability depends on various factors like gravity drainage, capillary suction, surface elasticity, viscosity, electric double-layer repulsion, steric repulsion, and coalescence of adjacent bubbles due to rupture of inter-bubble lamellae (Sahu et al., 2018). Foam stability is an essential parameter for FC production to ensure a uniform cellular microstructure of concrete as the bubble should remain stable till the concrete sets (I. S. Ranjani and Ramamurthy, 2010). The stability of foam is often characterized by drainage rate, which can be measured either as free drainage or forced drainage. Stability of foam could be enhanced through addition of additives like bone glue and viscosity enhancing agent. Foam stability can also be enhanced by the use of fine fillers like fly ash (FA) and pulverized sand in FC as the fine material forms a uniform coating around the lamellae and prevent the coarsening effect.

Need for a stabilized foam

Summarization of studies on correlation of foam and FC behaviour identified the influence of following parameters viz., type of surfactant, dosage of surfactant, foam production technique, foam density, foam capacity, foam stability, viscosity of foam and bubble microstructure on concrete properties (Falliano et al., 2018; Kunhanandan Nambiar and Ramamurthy, 2008; Kuzielová et al., 2016; D. K. Panesar, 2013; G. I. S. Ranjani and Ramamurthy, 2010; Siva et al., 2015; Sun et al., 2018). Hence, it should be realised that the production of FC with desired properties like low density, high strength to weight ratio, impact resistance, low shrinkage, better thermal and acoustic insulation is governed by incorporation of a stable and good quality foam for which appropriate surfactant is the key requirement (ASTM C796-19, 2019; Sahu et al., 2018; Samson et al., 2017). Therefore, judgement regarding the selection of surfactant is very critical for FC production. One of the important requirement of foam is that, the foam must be firm and stable so that it resists the pressure of the mortar until the cement takes its initial set and a strong skeleton of concrete is built up around the void filled with air (Ramamurthy et al., 2009). In order to enhance the foam performance in terms of density, stability, lamella thickness, additives such as foam stabilizers, viscosity enhancing agent and thickening agents have been identified by various researchers. The performance of sodium lauryl sulphate (SLS), a commonly reported anionic surfactant in many studies on FC, was enhanced through addition of various additives such as carboxymethylcellulose sodium (CMC) (Colak, 2000), $MgCl_2$ (Angarska et al., 1997), polymer (vinylpyrrolidone) (Folmer and Kronberg, 2000), alkyl alcohol

(Sharma et al., 1984), sodium salts like NaCl, $NaCO_3$, NaOH (Siva et al., 2015), edible starch (Y. Zhang et al., 2015), xanthan gum (Yu et al., 2020), which improved different foam characteristics including foam density, foam drainage, foam film thickness, foam film stability, and foam film lifetime. Xanthan gum (XG) which is a kind of microbial exopolysaccharide produced by fermentation of Xanthomonas campestris with carbohydrate as the primary raw material (like corn starch), is reported to act as an efficient foam stabilizer with surfactants like SLS (Bueno et al., 2014; Dário et al., 2011; Moffat et al., 2016; Sheng et al., 2021; Yu et al., 2020). Investigations of Hajimohammadi et al. (Hajimohammadi et al., 2018) and Zhu et al. (Zhu et al., 2020) have shown that the addition of a very small dosage of XG as a foam stabilizer to surfactant solution significantly reduced the drainage rate and subsequently improved the pore structure and mechanical properties of FC.

2.2.3 Binder

Cement is the most dominant binder used across various studies in FC. Studies have reported use of various types of cement in the FC viz., ordinary Portland cement (Mydin, 2011), rapid hardening Portland cement (Pan et al., 2014), calcium sulfoaluminate cement (Kearsley and Mostert, n.d.), and high alumina cement (Tarasov et al., 2010). However, other supplementary materials such as silica fume (SF), FA, lime, incinerator bottom ash and Lytag can also be used as cement replacement at dosage ranging between 10% and 75% (Ganesan et al., 2015; Pan et al., 2007). The supplementary materials are used to improve mix consistency, long term strength and to reduce costs (Pan et al., 2007). Each supplementary material may contribute to properties of FC in different fashion. For instance, the purpose of using SF is to strengthen the FC in a short time due to their filler characteristics and pozzolanic behaviour, while FA needs a longer time to reach the maximum strength when compared to cement (Gökçe et al., 2019). Therefore, the choice of supplementary materials as partial replacement can be made according to desirable FC properties.

2.2.4 Aggregate

Various studies have proved that use of conventional coarse aggregate and coarse sand affects the stability of foam and eventually has negative impact on pore structure and strength of FC (Ibrahim et al., 2013; E. K. K. Nambiar and Ramamurthy, 2006a). Since the coarse aggregate phase is mostly absent in the FC, the filler mainly consists of only fine aggregate. Hence, many studies have been reported on the replacement of normal sand with similar other finer materials like FA, lime, tyre crumbs, palm oil fuel ash, limestone dust etc. (Ameer A. Hilal et al., 2015;

Kashani et al., 2017; Kumar et al., 2018; Lim et al., 2013). These replacements have resulted in improvement in various properties like compressive strength, tensile strength, thermal insulation, permeability etc. Limited studies have proved that partial or complete replacement of sand with FA results in higher strength to density ratio due to pozzolanic activity of FA. Jones and McCarthy (Jones and McCarthy, 2005c) opted for 100% replacement of sand with FA and reported strength up to six times higher than those of corresponding control mixes with sand, with differences becoming increasingly larger with increasing test ages due to the relatively slow nature of the pozzolanic activity of the FA. Though natural coarse aggregate due to their high specific gravity and angular shape are not preferred in FC but experimental evidences have showed that in order to improve the properties of FC, researchers have used lightweight aggregate manufactured from FA, expanded clays, oil palm shells, ceramsite etc. (Johnson Alengaram et al., 2013; Q.X. Wang*, Y.X. Shi*, J.B. Shi, Y.G. Zhang, 2015; Weigler and Karl, 1980).

2.2.5 Admixtures and its compatibility

Researchers have reported that for achieving higher strengths at a given FC density it is recommended to use low water to cementitious materials ratio (Bagheri and Samea, 2018). Hence use of water reducing admixtures becomes a necessity (Cong and Bing, 2015; Ameer A. Hilal et al., 2015; Jones and McCarthy, 2005b). Despite the importance, reported work on use of water reducing admixtures in FC have showed foam instability in some cases. Saucier et al. (Saucier et al., 1990) studied the effect of addition of superplasticizer (SP) and found that that addition of SP destabilized the air void system produced by the air entraining admixtures (AEA) by modifying the relationship between the air content and the spacing factor. It was recommended by Brady et al. to limit the dosage of SP to 0.2% of the weight of binder content when similar outcomes were reported. They found that addition of SP resulted in the reduction of stability of foam which led to the segregation in FC. While studying the effect of chemical and mineral admixtures on the foam indexes, which governs foaming ability and foam stability of cement-based materials incorporated with AEA, Huang et al. (Huang et al., 2019) recommended to use slag over FA as partial replacement of cement due to its better compatibility with foam. It was also worth noting that when air entraining admixture's (AEA) were used with Naphthalene SP and polycarboxylate ether (PCE) based SP, comparatively the PCE based SP provided more stable foam. Similar instability issues were reported by Nambiar and Ramamurthy (Kunhanandan Nambiar and Ramamurthy, 2008) while working with FA as replacement for sand, in which the adhesion between the bubbles and FA particles in the

mixture increased the stiffness of the mix, which caused the bubbles to break during mixing affecting the stability of mix. Compatibility issues were also reported between shrinkage reducing admixtures (SRA) and surfactant based AEA and polymer based AEA. Research outcome indicated that out of the two AEA's used, surfactant based AEA performed better showing less instability(Pendergrass et al., 2017).

2.2.6 Foam concrete preparation techniques

As represented in Figure. 2.1, there are predominantly two techniques that are widely used for the production of the FC; pre-foaming method and mix-foaming method. Both methods control the mixing process and the quality of FC (Karl and Worner, 1993)(Zulkarnain and Ramli, 2011). In pre-foaming method a stabilized foam is prepared separately from a surfactant mixed aqueous solution and then later blended into base mix (consisting of cement, sand and water). The pre-formed foam could be produced by either dry or wet method. The dry foam is generated with the help of air compressor in which the foaming agent solution is pushed over sequences of high density constraints and by pushing compressed air concurrently inside a mixing chamber. The dry foam generated from this method is quite stable and the bubbles size generated is smaller than 1 mm. The small sized bubbles facilitate stable and uniform blend of foam with the base material in order to produce pumpable FC (Aldridge and Ansell, 2001). The wet foam is generated by spraying the foam agent solution through a fine mesh. The wet foam bubble size is generally between 2 mm and 5 mm and the foam produced is somehow less stable compared to the dry foam [66]. In the mixed foaming method, the surface active agent is practically mixed along with base-mix constituents specifically cement slurry (Pugh, 1996). Generally pre-formed foaming is preferred over mix-forming technique due to the following advantages: (i) lower foaming agent requirement and (ii) a close relationship between amount of foaming agent used and air content of mix (Valore, 1954a). Most common types of mixers (tilt drum or pan mixer used for concrete or mortar) are suitable for FC. The type of mixer and batching and mixing sequences of FC depends upon pre-formed foam method or mix-foaming method (Karl and Worner, 1993).

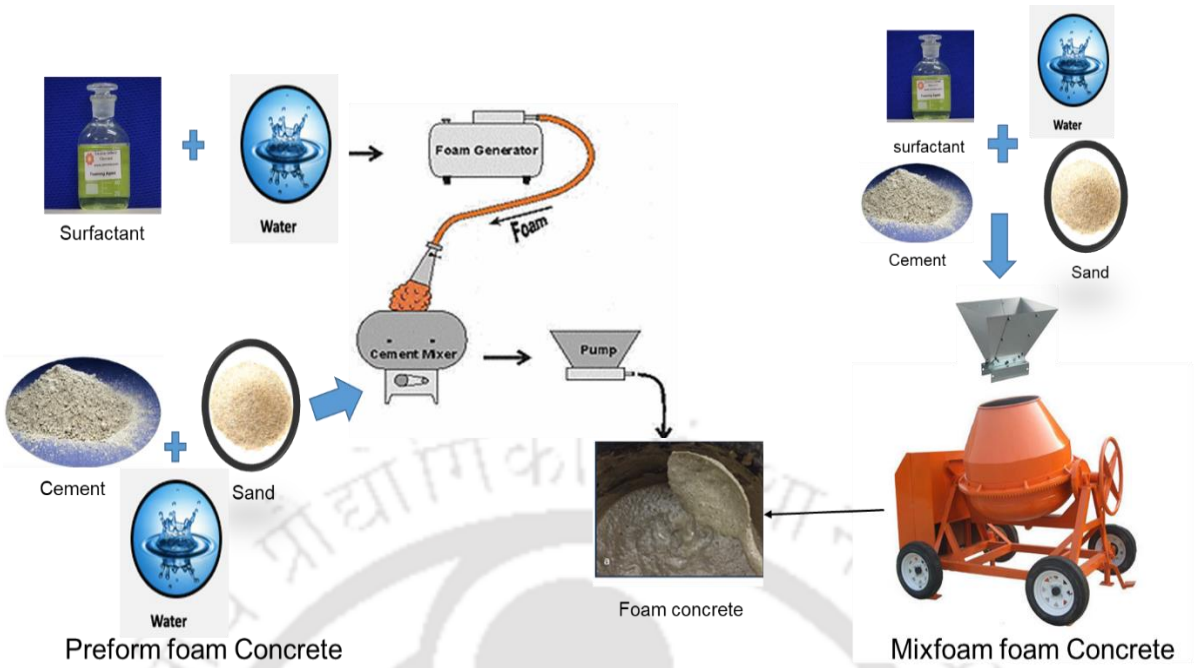

Figure 2-1: Production methods of foam concrete

2.3 Foam concrete properties

2.3.1 Fresh state properties

In the fresh state, the FC mix has a flowing and self-compacting rheology. Different parameters such as consistency and stability are considered. These parameters are mostly influenced by the selection of water to cement (w/c), supplementary materials, fine aggregate, and the volume of foam and type of foam agents.

Consistency is measured by standard flow cone test and the marsh cone flow test to investigate the FC mixture performance. The performance of consistency of FC is acceptable when the spreadability % of fresh concrete mixes is limited between 40% and 60% of the flow spread % i.e. 140 mm to 160 mm of flow (Amran et al., 2015). The flowing time through marsh cone should be within 20 s for a satisfactory mix to be placed into molds and get self-compacted without any external aid. One important factor that affects rheology and consistency of the fresh FC is the water content in the mix design. It was recommended that the water to cement ratio should be minimized because the excessive volume of water causes segregation of FC during casting which affects the workability performance. The consistency of fresh FC reduces with an increase in volume of foam in the mix, which may be attributed to the (i) reduced self-weight and greater cohesion resulting from higher air content and (ii) adhesion between the bubbles and solid particles in the mix increases the stiffness of the mix (Ramamurthy et al., 2009).

Stability of FC is defined as the state of the mix at which the density ratio is closer to unity (i.e. measured fresh density/design density =1). It depends on the consistency of the base mix, water–solids ratio and varies with filler type (Kunhanandan Nambiar and Ramamurthy, 2008; E. K. Nambiar and Ramamurthy, 2006). Thus the consistency of the base mix to which foam is added is an important factor, which affects the stability of mix. When foam is added to the base mix, the "consistency of FC" is reduced. The stability of test mixes is assessed by comparing the (i) calculated and actual quantities of foam required to achieve a plastic density within ±50 kg/m^3 of the design density value and (ii) calculated and actual w/c ratios (Ramamurthy et al., 2009). Hence there is a need for determining the water–solids ratio, which would satisfy both stability and consistence of the mix.

2.3.2 Mechanical properties

The compressive strength of FC is influenced by multiple factors such as mix constituents including the w/c ratio, filler type, binder type, binder-filler ratio, foaming agent, foam production parameters, foam volume and curing method. The predominant factor controlling compressive strength is the quantity of air voids, determining concrete density (Falliano et al., 2018). Lower-density mixes are particularly impacted by entrained air voids, significantly influencing the strength (Falliano et al., 2018; Jiang et al., 2016). While the w/c ratio traditionally influences strength in normal weight concrete, however in FC, density has a greater impact than the w/c ratio (Mccormick, 1967). In this regard, studies by Falliano et al., (2018) observed that increasing the w/c ratio from 0.3 to 0.5 remarkably increased strength due to enhanced cement hydration. Piotrowski and Prochoń, (2018) found an optimum w/c ratio for maximum strength in Geopolymer FC. Compressive strength decreases with increase in void diameter for dry densities between 500 and 1000 kg/m³ (E. P. Kearsley and Wainwright, 2001a). Falliano et al., (2018) noted that a higher w/c ratio reduces foam content requirement for a target density. Additionally, the amount and fineness of sand influence pore structure and, consequently, compressive strength (E. K. Nambiar and Ramamurthy, 2006; Nambiar and Ramamurthy, 2007b). Moreover, surfactants and foam properties significantly impact the microstructure of concrete, influencing its strength. Various studies (Falliano et al., 2018; Kuzielová et al., 2016; Liu et al., 2019; D. K. Panesar, 2013; Sun et al., 2018) have demonstrated that foam stability governs pore size, subsequently affecting the strength of FC. For instance, (Falliano et al., 2018) established that certain protein-based surfactants, leading to foam with a higher fluid phase, enhance cement hydration, thereby promoting strength development compared to synthetic surfactants. Additionally, the relationship between the

water-to-cement (w/c) ratio and compressive strength in FC is contingent on the foaming agent type. Moreover, the incorporation of foam stabilizers like CMC, XG, and $Ca(OH)_2$ enhances foam stability by aggregating the plateau border and increasing the viscosity of the surfactant solution, resulting in improved concrete strength (Hajimohammadi et al., 2018; Sritam Swapnadarshi et al., 2021; Yuanliang et al., 2021). Further researchers have tried the inclusion of various fillers such as fine recycled glassy aggregates, expanded shale aggregate, lime, FA, clay and quarry dusts aggregates to augment the foam stability and subsequently the strength of FC (Al-Shwaiter et al., 2022; Gencel et al., 2021; Jones et al., 2003; Jones and McCarthy, 2005c; Lim et al., 2017; Roslan et al., 2013; Wagh et al., 2021). Jones and McCarthy, (2005c) chose to completely substitute sand with FA and observed a strength increase of up to six times compared to control mixes containing sand. The differences in strength became more pronounced as the test ages increased, which can be attributed to the relatively slow pozzolanic activity of the FA. Similar observation was reported by Nambiar and Ramamurthy, (2006b) where they have reported 200% increase in compressive strength at 90 days for 70% replacement of sand with FA. Gandhi et al., (2023) in their studies reported an improvement in strength of 120% and 61% for densities 1500 kg/m^3 and 1000 kg/m^3 respectively for 45% replacement of sand with FA. The improvement in strength was reported due to the combined action of pore structure densification and pozzolanic reaction caused due to incorporation of FA. In addition, the use of cement replacements such as SF and FA alters the compressive strength of the mix over time. A study found that, a high volume replacement of up to 65% of cement with FA is possible without any decrease in strength (E. P. Kearsley and Wainwright, 2001b). The reported replacement level of cement with of SF was minimal, however, its long-term strength gain was boosted due to its pozzolanic action. According to reports, the use of a combination of SF and FA in a binary mix resulted in a 25% increase in compressive strength (Gökçe et al., 2019).

Examining through the literature, it is evident that studies reported on the tensile properties of FC is limited. FC exhibits reduced splitting tensile strength compared to conventional normal weight and lightweight aggregate concrete mixes. Notably, mixes with sand surpass those with FA in terms of tensile strength, which can be attributed to enhanced shear strength between sand particles and the paste, as suggested by (Jones and McCarthy, 2005a). The incorporation of polypropylene fibres (PP fibre) in concrete is known to elevate tensile and flexural strength, provided the fibres do not interfere with the behaviour of freshly poured concrete or its self-compaction, according to (Kearsley and Mostert, 1997). A flexural strength to compressive

strength ratio of 0.25 to 0.35 has been reported for cellular concrete, as documented by (Valore, 1954b).

Modulus of elasticity

The static modulus of elasticity of FC is said to be much lower than that of normal weight and lightweight concrete, with values ranging from 1.0 to 8.0 kN/mm^2, for dry densities between 500 and 1500 kg/m^3 respectively (Jones and McCarthy, 2005b). Normal weight concrete exhibited E-values that were up to four times greater than FC of equivalent strength. According to reports, FC that contains FA as fine aggregate has a lower E-value than FC that contains sand. The E-value has been found to increase by two to four times when PP fibre is used (Jones and McCarthy, 2005b).

2.3.3 Functional characteristics – Thermal properties

In the past, more attention was paid by researchers to the mechanical properties of FC. However, in recent years, studies evaluating the thermal properties as well as mechanical properties of FC is prioritized by researchers due to the importance of energy saving in buildings (Wagh et al., 2021). Thermal conductivity (TC), Thermal Diffusivity (TD) and Specific Heat (SH) are considered as thermo-physical properties of FC. Thermal diffusivity (α-value) expresses the rate of heat spread through materials while specific heat (C-value) represents the heat storage capability of material (Bejan, 1995). The TC (k-value) which refers to heat transfer by conduction through material is considered as most important property of all (Silva, 2004). TC (k-Value) is commonly used to check the energy performance of buildings and conducting energy audits of the existing buildings (Ficco et al., 2015; Giannakou and Jones, 2002). Considering this most of the researchers tried to address factors affecting TC.

Thermal conductivity measurement methods for foam concrete

TC which demonstrates heat conduction capability of material is measured primarily by two approaches namely steady state methods and transient methods which have different heat transfer conditions across materials (Bindiganavile et al., 2012; Tong, 2011; W. Zhang et al., 2015). A constant heat transfer approach is adopted by steady state methods, where in the temperature or heat flow is not dependent on time while transient method is dependent on time and temperature changes over time. A graphical representation of different available TC measurement methods of FC is shown in Figure 2.2. It was observed that in recent years most researchers are selecting transient methods to measure the thermal performance of FC and other materials. Though it may not specify its greater accuracy over steady state methods however

very less experiment measurement time, compactability, and the ability to measure moist specimens can be considered as some factors compelling the researchers for using transient methods rather than steady state (Wagh et al., 2021).

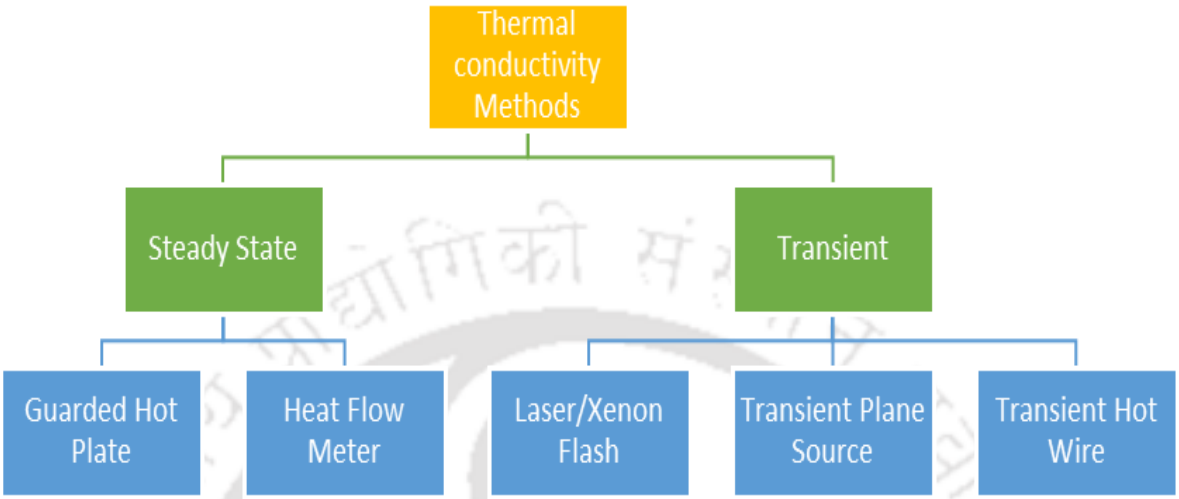

Figure 2-2: Different thermal conductivity measurement methods.

Factors affecting Thermal Properties of foam concrete

Table 2.1 summarizes the literature addressing various factors influencing the thermal properties of FC. Also it should be noted that, most researchers have investigated the TC rather than focusing on all thermal properties for FC as observed in Table 2.1. The subsequent section reviews the influence of various factors related to materials, mix composition and microstructure on thermal properties of FC.

Influence of air void system and density

One of the most substantial factors influencing thermal properties is the density and subsequently porosity. Many of the earlier studies have established the correlation that thermal resistance is indirectly proportional to density of FC (Mydin, 2011; Shrivastava, 1977; Weigler and Karl, 1980). In this line, Pan et al. (Pan et al., 2014) prepared a super low density FC with density in range of 150 to 300 kg/m^3 and hence was able to achieve a very low TC of 0.05 to 0.07 W/mK. This was possible due to use of rapid hardening cement and accelerators which prevented the foam collapse by quick setting. Similar research was carried out by Jiang et al. (Jiang et al., 2016) on very low density FC. Adding to above Chen and Liu (Chen and Liu, 2013) in their research replaced foam with EPS (expanded polystyrene) beads in FC. It was observed that there was a significant increase in TC as well as compressive strength of concrete, though the density of the mixes remained almost similar. Hence the above finding proved that

apart from density, properties of mix constituents also plays an important role in TC of FC. Wei et al. (Wei et al., 2013) explored the effect of porosity level on thermal properties and established that at high porosity levels radiation heat transfer becomes a considerable factor while with decrease in porosity the radiation influence starts to diminish. TC is also predominantly influenced by directional homogeneity of pore distribution. Pores when arranged perpendicular to heat flow allowed more heat to pass through, thus improving thermal resistance. However layer of pores when populated in parallel to heat flow direction offered lower thermal resistance (Hajimohammadi et al., 2017).

Influence of moisture content, temperature and curing condition

Studies on influence of moisture content on TC of FC proved that TC increases with increase in moisture content (Valore, 1954b). For instance every 1% increment in moisture content led to increase in TC value by 6% (Ameer A. Hilal et al., 2015). This can be ascribed to the fact that TC of water is 25 times higher than that of air (Bessenouci et al., 2014). While investigating the influence of temperature variation on thermal properties of FC, Richard et al. (Richard et al., 1975) noted that rate of increase in TC with increase in density was lesser at lower temperature. Hence the thermal insulation property of FC was improved with reduction in temperature. On similar lines Othuman and Wang (Othuman and Wang, 2011) investigated the thermal properties of FC at different temperatures ranging from 20°C to 250°C. Their experimental outcomes indicated that the TC remained constant with gradual increase in temperature till 90°C after which it started to decrease rapidly till 170°C. This can be attributed to evaporation of the available moisture in the pores of specimen. Beyond 170°C the increase in temperature resulted in gradual increase in TC due to the radiation in pores. Hence moisture content in pores of FC plays an important role in thermal properties. It was also noted that specific heat was very less sensitive to temperature changes as compared to TC.

While studying the influence of curing conditions on TC, Zhao et al. (Zhao et al., 2015) subjected FC specimens to four different curing conditions namely 28-day air, 7-day water + 21-day air, 28-day natural weather and 7-day water + 21-day natural weather. The 28-day air cured FC exhibited the lowest TC. This was due the lowest amount of moisture present in 28-day air cured specimens where in curing temperature and humidity was kept constant at 30°C and 65% respectively. Further Ji et al. (Ji et al., 2019) reported that FC specimens cured at higher temperature showed lower TC. This could be attributed to the increased porosity resulting from increase in curing temperature.

Influence of aggregate/filler substitution

Since the coarse aggregate phase is mostly absent in the FC, the filler mainly consists of only fine aggregate and the replacement of which also affects the thermal properties to a great extent. Researchers have tried to incorporate different waste materials such as recycled tyre crumbs (Kashani et al., 2017), waste limestone slurry (Kumar et al., 2018), granulated blast furnace slag (Oren et al., 2020) , palm oil fuel ash (POFA) (Lim et al., 2013) etc. as replacement for filler in FC. Their experimental outcomes indicated that the thermal insulation properties were improved in most cases due to increase in porosity. However, use of POFA as filler replacement resulted in increase in TC due to densification of microstructure. Li et al. (P. Li et al., 2019) were able to prepare a high performance aerogel FC by using aerogel powder of extreme low density as filler which resulted in dry density of 198 kg/m^3 and TC of 0.049W/Mk with better compressive strength and decreased porosity. Salvini et al. (Salvini et al., 2012) proposed that use of porous ceramics as filler material for preparation of FC could result in insulating refractory composite with an acceptable TC.

Though natural coarse aggregate due to their high specific gravity and angular shape are not preferred in FC but experimental evidences have showed that in order to improve the properties of FC, researchers have used lightweight aggregate composed of expanded clays and expanded shales as coarse aggregate providing a filler effect (Weigler and Karl, 1980). This not only resulted in better mechanical properties but also improved the thermal resistivity of FC. On similar lines oil palm shells (OPS) were used as coarse aggregate for preparing FC. The physical and thermal properties were found to be on par with concrete prepared with expanded perlite aggregates as OPS itself are porous aggregates having large number of micropores (Demirboğa and Gül, 2003; Johnson Alengaram et al., 2013; Liu et al., 2014) . Wang et al. (Q.X. Wang*, Y.X. Shi*, J.B. Shi, Y.G. Zhang, 2015) prepared a new type of FC with a density of 600 kg/m^3 by incorporating ceramsite as lightweight coarse aggregate which resulted in concrete with best thermal and mechanical behaviour.

Table 2-1; Factors affecting the Thermal conductivity

Factor	Type of Additive	Foaming agent used	Observation	Density (kg/m^3)	Thermal properties	Other properties studied	Ref.
Air void system and density	None	Noraite PA-1 (protein based)	Lower density FC indicates greater porosity and hence lower TC.	650-1200	k= 0.23-0.39	Porosity and pore size	(Mydin, 2011)
	Ultrafine GGBS and PF	Hydrogen peroxide	TC achieved was significantly lower than that of normal weight concrete (1.7 W/mK)	150-300	k= 0.05-0.07	CS, water absorption	(Pan et al., 2014)
	Foam replaced with EPS	Protein based	Increase in EPS % not only increased the strength but also decreased the TC	400-800	k= 0.07-0.15	Porosity CS, TS	(Chen and Liu, 2013)
	None	NA	Super low density concrete with porosity ranging from 88% to 95% was achieved with extremely lower TC values	110-270	k= 0.036-0.063	Rheological tests, porosity, CS	(Jiang et al., 2016)
	None	Protein based	In case of high porosity FC radiation heat transfer is a considerable factor affecting TC. However the radiation influence starts diminishing as the porosity decreases.	252-1870	k= 0.065-0.5	Microstructure study, porosity	(Wei et al., 2013)
Moisture content and temperature	None	Noraite PA-1 (protein based)	The TC values of FC were less for high temperatures due to lower moisture content.	650-1850	k= 0.226-0.484	Moisture content, Fire resistance.	(Othuman and Wang, 2011)
	S.F as cement and F.A as filler replacement	EABASSOC (chemical)	TC of prepared FC was more in saturated state compared to specimens in dry state due to presence of moisture.	1280-1870	k= 0.475-0.962	CS, TS	(Ameer A. Hilal et al., 2015)
	GGBS	Synthetic	FC specimen with air dried curing showed the best thermal performance.	1167-1293	K=0.62-0.72	CT, Ultrasonic pulse velocity	(Zhao et al., 2015)

Aggregate/ Filler Substitution	RTC	NA	Addition of RTC made concrete more thermal resistive due to improvement in porosity.	600 ±25	k= 0.15-0.2	Porosity, Acoustic. Water absorption and CS	(Kashani et al., 2017)
	OPS	Naphthalene Sulfonated (Synthetic)	The TC was on par with FC prepared with expanded perlite aggregate and very less compared to clay brick and blocks.	1100-1600	k= 0.4-0.57	CS	(Johnson Alengaram et al., 2013)
	LS	Natural Protein based	TC values were way less than normal brick and concrete	800-1000	k= 0.32-0.34 C= 1.025-1.07 α= 0.32-0.35	CS, Porosity	(Kumar et al., 2018)
	OPS	Sika AER 50/50 (Synthetic)	The porous structure of OPS aggregates resulted in better thermal resistivity of OPS GFC compared to conventional materials	1300-1700	k= 0.47-0.54	Sorpitivity, porosity, CS TS and UPV	(Liu et al., 2014)
	AP	NA	With the porosity maintained constant, the TC could be efficiently decreased by increasing the AP content and decreasing the cement content.	700-200	k= 0.164-0.049	CS, porosity	(P. Li et al., 2019)
	POFA	Synthetic foaming agent	Replacement of sand with POFA as filler increased the TC due to densification of FC.	1300±50	k= 0.65-0.74	CS, TS	(Lim et al., 2013)
Binder/Cement and pozzolanic materials	PFA, POFA, SF,WA	Noraite PA-1 (protein based)	Use of S.F as mineral admixture resulted in less TC than PFA. But when PFA mixed with optimum WA is used it exhibited better heat resistant behaviour.	700-1400	k= 0.24-0.74 C= 0.879-0.794 α= 0.39-0.69	None.	(Ganesan et al., 2015)

	S.F and F.A	Hydrogen peroxide	TC of FC has much relevance with dry density	190-470	k= 0.05-0.085	CS	(Cui et al., 2014)
	FA, SF and slag	Protein based	TC depends mainly on porosity rather than mix constituents.	1490-430	k= 0.72-0.16	CS	(Pan et al., 2007)
	FA, SF	Synthetic based	SF introduction resulted in superior compressive strength/TC ratios than FA introduction.	873-1998	k= 0.238-0.942	CS, water absorption, porosity	(Gökçe et al., 2019)
	MPC	Hydrogen peroxide	TC of the MPC FC is higher than that of OPC for a given dry density	300-1000	k= 0.08-0.23	Porosity, CS, water absorption	(T. Li et al., 2019)
Mix Cement + Filler replacement	Soil as filler and SF and QL as cement replacement	Protein based	Addition of SF decreased TC while quick lime increased the TC	800-1800	k= 0.19-0.755	Hygroscopic properties, CS,	(Cong and Bing, 2015)
	FA and lime as filler replacement, PF	Noraite PA-1 (protein based)	Addition of FA and PF decreased TC	600-1400	k= 0.19-0.59 C= 0.54-0.98 α= 0.35-.60	CS, flexural strength, porosity	(Mydin et al., 2012),(Awang et al., 2012)
	S.F as cement and F.A as filler replacement	EABASSOC (chemical)	Addition of S.F and F.A leads to slightly increased TC in the dry state. However TC in the saturated state was slightly lower due to better microstructure.	1280-1870	k= 0.475-0.962	CS, TS	(Ameer A. Hilal et al., 2015)
Influence of Fibers and Admixtures	Fibres- Steel, Polypropylene, coconut.	Noraite PA-1 (protein based)	Among various types of fibres studied coconut fibres showed lowest TC.	700-1400	k= 0.24-0.74 C= 0.879-0.794 α= 0.39-0.69	None.	(Ganesan et al., 2015)

	HPMC	Modified sodium alcohol ether sulfate	Addition of HPMC decreases TC to a great extent.	181-409 151-180	k= 0.059-0.078 k= 0.050-0.055	Porosity	(Sang et al., 2015)
	Newspaper	Synthetic	Addition of 0.05g/cm^2 newspaper, sandwiched in FC panels were able to reduce the TC by 20%	1100-1700	k= 0.303-0.621	CS.	(Ng and Low, 2010)
	Water repellents	Protein based	The addition of potassium trimethylsilanolate (PT) and calcium stearate (CS) showed an increasing trend while siloxane-polymer (SP) showed irregular trend in case of TC	550	k= 0.149-0.159	CS, Sorpitivity and Hygroscopicity	(Ma and Chen, 2016)
Geopolymer Foam concrete	GGBS, FA	Protein based	Type of activator used in GFC does not affect the TC,	325-492	k= 0.088-0.129	Porosity, CS	(Yang et al., 2014)
	FA	Protein based	TC performance of alkali activated system was comparable with normal OPC FC system	940-1310	k= 0.23-0.31 C= 1.18-1.69 α= 0.18-0.20	None.	(Stolz et al., 2018)
	Class F-FA, GGBS	NA	GFC exhibits better thermal insulation property than normal FC with similar density range.	585-1370	k= 0.15-.048 α= 0.27-0.34	CS, acoustic	(Z. Zhang et al., 2015)

k – Thermal conductivity (W/mK), C – Specific heat (J/g K), α – Thermal Diffusivity (mm^2/s)

FC-foam concrete, OPS- Oil palm shells, LS- Limestone slurry, FA-flyash, SF- silica fume, QL- Quick Lime, GFC- Geopolymer foam concrete, POFA- palm oil fuel ash, HPMC- hydroxypropyl methyl cellulose, MPC- magnesium phosphate cement, PFA -Pulverized Fly ash, Wood ash-WA, EPS-Expanded Polystyrene, PF- polypropylene fibre, RTC- Recycled tyre crumb, AP- Aerogel powder, CS-compressive strength, TS-Tensile strength.

Influence of binder/cement and pozzolanic materials

The chemistry of cement plays a significant role on the thermal performance of FC. To date very few research works have been undertaken on influence of type of binder on thermal properties of FC. Based on the extensive studies, researchers have established that higher heat of hydration of cement also have a significant role on thermal performance of FC (Jones and McCarthy, 2006; Tarasov et al., 2010). Hence the above problem can be addressed by optimum use of cement and its replacement with pozzolanic FA with lower heat of hydration. In a study by Li et al. (T. Li et al., 2019) magnesium phosphate cement (MPC) was used instead of OPC and the prepared FC was found to have higher TC along with higher compressive strength for a given dry density.

Studies on use of FA and silica fume as additive in FC showed slight increase in TC. However a significant increase in the mechanical properties was observed and this could be attributed to the densification of microstructure due to addition of additives (Gökçe et al., 2019; Pan et al., 2007). The above increment in TC was more significant for SF concrete when compared to FA blended concrete. However the TC range reported for SF concrete was on par with similar density range of non-autoclaved cellular gas concrete produced with perlite (Fabien et al., 2019). Ganesan et al. (Ganesan et al., 2015) based on their comparative studies on the various possible binder replacements such as Pulverized fuel ash (PFA), Silica Fume (SF), Palm oil fuel ash (POFA) and Wood ash (WA), found out that replacement with combination of PFA and wood ash provided the best thermal performance of all.

Influence of cement + filler Replacement

In order to optimize the performance as well as cost of FC, researchers have tried to replace the cement as well as filler with various substitutes. Similar such attempt was made when SF was used as cement replacement and FA as fine sand replacement (Ameer A. Hilal et al., 2015). This led to better mechanical properties but a slight increase in TC was observed for oven dried specimens due to dense microstructure. On contrary, in case of saturated specimens the TC observed was lower and this could be attributed to reduced water absorption resulting from improved microstructure of SF-FA concrete. In same line, Cong and Bing (Cong and Bing, 2015) based on comparative studies on use of SF and quick lime as cement replacement with soil as filler in FC, proved that addition of quick lime resulted in poor thermal performance. This was because in mixes with quick lime, foam collapse occurred due to consumption of water from foam surface by quick lime while mixing and eventually leading to increase in

concrete density. Awang and Mydin (Awang et al., 2012; Mydin et al., 2012) replaced the filler with lime and cement with FA and found out that lime as aggregate replacement did not contribute much on mechanical behaviour but good in thermal performance by improving all three thermo-physical properties.

Influence of addition of fibers and admixtures

Generally, fibers and admixtures though added in small quantities leave a good impact on the properties of FC. Use of fibres in FC resulted in better thermal as well as shrinkage resistance performance. This was due to ability of fibres to form small and uniform pores by swelling and shrinking in a concrete during mixing and drying (Awang et al., 2012; Mydin et al., 2012). Researchers have tried the incorporation of various synthetic fibers such as PP fibre, alkaline resistance glass, kenaf, steel, basalt, chrysotile asbestos and also natural fibers like oil palm fibre, coir (coconut) fibres etc. in FC. Ganesan et al. (Ganesan et al., 2015) studied the relative performance of different fibres such as steel, PP and coir and their experimental outcomes proved that coir fibres showed the best performance of all. Based on a similar comparative study of fibres such as PP, alkaline resistance glass, kenaf, steel and oil palm fibre Ahmad and Awang (Ahmad and Awang, 2013) reported that PP fibres turned out to be better. On the same note, Li et al. (Li et al., 2020) studied the seismic and thermal behaviour of FC pre-cast self-insulation shear wall panels with PP fibres incorporated in the mix and reported that the TC was very much lesser than previous related research. On contrary another study on synthetic fibers showed that thermal performance of PP was relatively poor than basalt and chrysotile asbestos fibre (Aleksandr I. Kudyakov; Aleksei B. Steshenko, 2014).

Experimental results presented by Ng and Low (Ng and Low, 2010) showed that mere addition of 0.05g/cm^2 newspaper, sandwiched in FC panels were able to reduce the TC by 20% for same density. Sang et al. (Sang et al., 2015) found that the mere inclusion of 4% of hydroxypropyl methyl cellulose (HPMC) in FC led to decrease in TC to a great extent due to increase in porosity. Ma and Chen (Ma and Chen, 2016) used water repellents in FC and found out that the addition of potassium trimethylsilanolate (PT) and calcium stearate (CS) showed an increasing trend while siloxane-based polymer (SP) showed constant trend in case of TC.

Geopolymer foam concrete (GFC)

Yang et al. (Yang et al., 2014) studied the properties of alkali activated GGBS FC prepared with three different types of activators. Based on their studies it was concluded that TC of alkali activated GGBS FC was found to be more dependent on density rather than on type of activator

used. Liu et al. (Liu et al., 2014) evaluated the thermal properties of geopolymer FC (GFC) in which crushed oil palm shells were used as coarse aggregates. The obtained results established that the foamed geopolymer concrete was superior in thermal resistivity compared to conventional blocks and bricks available in market. While investigating the thermal properties of GFC made from class F FA along with partial slag substitution researchers reported. better thermal insulation properties than normal Portland cement FC at the same density (Stolz et al., 2018; Z. Zhang et al., 2015). This was due to the low proportion of chemically bound water in the geopolymer gel, providing a more discontinuous gel structure in these material. The thermal diffusivity and specific heat values were also on the lower side, thus recommending GFC as excellent thermal insulation building material. A commercially viable and environmentally-friendly GFC was synthesized with a mix composed of a hollow cenospheres exhibiting high strength/density ratio. The material thus prepared reported a strength of 17.5 MPa at density of 978 kg/m^3 with TC value to be around 0.28W/mK which is comparable to normal FC (Hajimohammadi et al., 2019).

2.3.4 Microstructural characteristics

The literature study indicates that there is a scarcity of studies about the microstructure and chemical analysis of FC. This section focuses on the chemical properties and methods used to determine them. The chemical analysis of FC is often conducted using X-ray diffraction (XRD), Energy Dispersive X-ray spectroscopy (EDS), and Fourier Transform Infrared (FTIR) spectroscopy. X-ray diffraction (XRD) provides information about the atomic-scale structure of cement paste and crystalline materials (Ungkoon et al., 2007). Nevertheless, XRD is incapable of identifying the existence of the amorphous phase. However, it can be measured indirectly using the Quantitative XRD approach (De La Torre et al., 2001). The Rietveld Method, a widely employed technique, was applied to measure the identified phases using X-ray diffraction (QXRD). The Rietveld method provides the total proportion of crystalline phases, excluding the amorphous material, expressed as a percentage normalized to 100 percent. XRD analysis conducted by the Xian et al., (2022) showed the presence of main hydration products like ettringite, calcium hydroxide, and Calcium Silicate Hydrate (CSH) along with di calcium silicate (C_2S) and tri calcium silicate (C_3S). Further (Chung et al., 2020) in his investigation on influence of supplementary cementitious materials, found that the incorporation of FA and SF lead to decrement in portlanditie (CaOH) peaks thus indicating the occurrence of pozzolanic reaction. The presence of other compounds like ettringite (E), gypsum (G), portlandite (PTL), alite (C_3S), belite (C_2S), quartz (QTZ), calcite (CC), and dolomite (DO)

along with CSH was also noted. On similar lines X-ray diffraction (XRD) analyses revealed that the incorporation of SF in concrete results in a chemical reaction between SF and the free calcium hydroxide (CH) present in hydrated cement. This reaction leads to the formation of a more rigid and long-lasting calcium silicate hydrate (C-S-H) gel, which contributes to the development of a uniform FC with improved distribution of solid particles and voids, as well as a densely packed arrangement of cement particles. Consequently, FC containing SF exhibits higher compressive strength compared to mixtures without SF. It also showed the reduction in ettringite content reduces when silica fume/cement ratio increases; thus SF decreases the risk of sulphate attack in FC (Reisi et al., 2017). Ranjani and Ramamurthy, (2012) in their XRD study revealed that a majority of the portlandite underwent conversion into ettringite, leading to substantial expansion of FC when exposed to sulphate solution. Consequently, the intensity of the ettringite peak was significantly larger, while the portlandite peak was lower in FC exposed to extremely severe sulphate conditions.

For microstructural and pore structural analysis several authors have used scanning electron microscope (SEM). In their study, Hilal et al., (2015) utilized scanning electron microscopy (SEM) to assess pore size and shape parameters. Their research focused on the impact of various additives on the strength performance of FC (FC). The findings revealed that the incorporation of additives significantly improved the pore structure of the FC slurry when compared to a traditional mixture. Despite the additives leading to an increase in the number of pores, the overall strength was higher due to a reduction in pore size and connectivity. SEM images of FCs with densities of 500 kg/m^3 and 1000 kg/m^3, showed that in concretes with high air content, air pockets tend to become closer to each other, causing larger air pockets. The size of the air voids increased due to lack of enough paste to prevent the joining of air voids. This observation is more important in concrete with a plastic density of less than 900 kg/m^3, where the corresponding foam content is 52%. The average air void size increases significantly for paste content less than 48% since the cement paste content is not enough to prevent air voids from coalescing (Gencel et al., 2022; Wei et al., 2013b). Besides porosity SEM analysis have also helped to observe and confirm the presence of various compounds altering the microstructure of FC like ettringite, C-S-H, CH (CaOH), portlandite, $CaCO_3$ (Ahmad et al., 2019; Chung et al., 2020).

2.4 Operational energy analysis

The operational energy of a building typically encompasses the energy utilized for heating/cooling, lighting, and the operation of various electrical equipment. The utilization of operational energy constitutes a significant component of overall energy consumption within the typical operation of a building. In regions characterized by severe climatic conditions, it is widely observed that the operation of heating and cooling systems constitutes a significant proportion of the overall energy consumption. The pursuit of thermal comfort and the optimization of operational energy usage have fostered a broad and interdisciplinary realm of research into thermal insulating building materials. There have been many attempts to calculate and compare operational energy of different walling materials and residential buildings (Hamidul Islam D, 2012; Islam et al., 2014; Udawattha and Halwatura, 2016). However, there are only limited studies done in tropical climatic conditions where the walling materials is very important to achieve the thermal comfort and reduce the operational energy cost (Dissanayake et al., 2017; Udawattha and Halwatura, 2017). Further it is to be noted that most of these studies are based on general industry used walling materials such as brick, hollow concrete block, AAC block etc. Thermal modelling via various simulation software's was applied to investigate the cost in most of the researches carried out (Islam et al., 2014; Udawattha and Halwatura, 2017) . Table 2.2 provides the brief summary of the work carried out by various researchers and the simulation platform used by them for contemplating the operational energy of the building.

2.4.1 Role of insulating walling materials in thermal comfort

Materials with better insulation should be given priority in selection for brand new construction or retrofitting existing buildings when the emphasis is on energy efficiency. Insulation in buildings is an important factor to attain thermal comfort for its occupants for winters and warm summers in composite weather. Insulation influences internal thermal conditions of building envelope as it loses less heat in cold weather and gains less heat in hot weather thus providing user thermal comfort (Ezema, 2019) . Insulation is the key factor which can help to achieve the operational energy efficiency in building. Insulation reduces unwanted heat loss or advantage and decreases the energy needs of heating and cooling structures. The thermal insulation in walls and roofs contributes to decreasing the desired air-conditioning system size and reducing the annual energy cost in buildings (Antonelli et al., 2020). Additionally, it extends the durations of thermal comfort without reliance on mechanical air-conditioning, especially at some point of inter-season periods. Better insulation in buildings also brings extra benefits in

lower energy bills and protective the environment via reducing CO_2 emissions (Kumar and Suman, 2013). Adopting proper thermal insulation strategy is one of the effective methods to lessen building cooling and heating energy consumption (Wang et al., 2016).

Table 2-2: List of Simulation tools used by various researchers

Author	Building Type	Work	Simulation Platform
(Subbarao, 1988)	Residential Buildings	short-term testing for predicting long-term performance of residential buildings	PSTAR
(Kossecka and Kosny, 2002)	Wood, concrete, steel framed walls	energy performance of buildings containing massive exterior building envelope components	DOE-2.1E
(Brown et al., 2014)	Residental Buildings	Quick design analysis for improving building energy performance	EnergyPlus (DesignBuilder)
(Reddy et al., 1999)	commercial building	Development of an inverse method to estimate overall building and ventilation parameters of large commercial buildings	DOE-2
(Yoon et al., 2003)	Large Commercial Building	Calibration procedure of energy performance simulation model for a commercial building	DOE-2.1E
(Coakley et al., 2012)	University Building	Calibration of Whole Building Energy Simulation Models: Detailed Case Study of a Naturally Ventilated Building Using Hourly Measured Data	EnergyPlus (DesignBuilder)
(Jusoh et al., 2015)	Office Building	Computational analysis of thermal building in a no-uniform thermal environment	CFD
(Westphal and Lamberts, 2005)	Office Building	Building simulation calibration using sensitivity analysis	EnergyPlus (DesignBuilder)

2.4.2 Review on operational energy cost analysis of buildings

Adopting the right thermal insulation material is one of the effective ways to reduce building cooling and heating energy consumption. To reduce the power consumption of buildings, as the walls have an important role to play with respect to thermal comfort, hence the choice of suitable materials for walls need to be carefully done. With the publication of energy-saving design standards, building energy-saving requirements have become more stringent, thus making use of thermal insulation materials a necessity in building construction (Wang et al.,

2016). In the studies carried out by Marwan, (2020), two styles of the building were investigated, building-1 constructed with conventional brick and building-2 constructed with modern cellular lightweight brick (CLC). The investigation found out that the heat transfer coefficient of building-1 was higher than building-2. Under a monetary mathematical version, the power cost of the air conditioning for building-1 was way higher than building-2. Hence walling materials can be manipulated by replacing the traditional construction blocks by more energy efficient blocks like replacing clay brick with FC or adding a separate insulating layer. Table 2.3 shows that the walling material Cabook with higher U value resulted in higher total energy cost compared to the brick wall which has relatively lower U value (Udawattha and Halwatura, 2017). Further a study carried out by (Mahlia et al., 2007) showed that about 32% saving in average annual energy consumption can be achieved with the mere use of better insulating material with lower TC.

Table 2-3 – Total energy cost for different block (Udawattha & Halwatura, 2017)

Parameters	Brick	Cabook
Wall Thickness	225 mm	200 mm
U Value	2.110 W/m^{2}K	3.756 W/m^{2}K
Total Energy Cost	$37,598.99	$47,139.36

On a similar note, another study was performed at NIT Hamirpur Campus, Himachal Pradesh, India. The structure taken for study had 3 floors with RCC framework, bricks and aluminium frame and partition walls. It had a gross floor area of 3960m^2 and was assumed to have a life time of 50 years. A life cycle cost analysis was done in the study to compute the energy associated with construction, maintenance and operation energy (Table 2.4). It was observed that operational usage, compared to other categories was the highest and contributed to a major share of 59.38% of the total energy use (Varun et al., 2012). The result showed that operational energy consumption is a huge fraction of the total energy usage and establishes the point that there is a need of alternative materials that can bring down the operational energy usage.

Table 2-4 – Category wise energy consumption (Varun et al., 2012)

Phases	Energy used (MJ)	Energy usage %
Construction	10,512,410.8	39.82
Maintenance	210,248.22	0.80
Operation	15,675,675.68	59.38

2.5 Life cycle assessment

2.5.1 Recent LCA approach and methods

Though there are number of studies on the LCA of concrete, the available literature on FC is very limited. Namsone et al. (Namsone et al., 2017) carried out a comparative study on LCA for AAC blocks and FC produced by two different methods, one with the traditional pre foaming method while in other method intensive mixing technique was followed. The LCA results showed that CO_2 emission was highest for AAC blocks, while lowest emission was observed for FC prepared with intensive mixing technique. This was due to the reduction in amount of water, sand and energy required for production of FC by intensive mixing technique. On similar line, a study was conducted by Zimele et al. (Zimele et al., 2019) on LCA of FC produced in Latvia. In their study they compared life cycle impact assessment of FC with hollow ceramic block over 11 different impact categories and found that FC mixtures performed poor. Chen et al. (Chen et al., 2019) also established a similar trend when they compared the LCA of pervious concrete with FC indicating higher CO_2 emission for FC. In the above mentioned studies, majority of CO_2 emission came from the extensive use of Ordinary Portland cement (OPC). Hence, in line with the recommendations reported in previous studies on LCA of conventional normal weight concrete, partial replacement of OPC with other pozzolanic materials will reduce the environmental impact by lowering energy demand and CO_2 emissions (Gettu et al., 2019; Panesar et al., 2019; Yao et al., 2019). Life cycle studies of FC also saw similar approach when OPC was replaced with waste materials like quarry dust (Lim et al., 2017) and eggshell powder (Tiong et al., 2020). Their results showed reduced CO_2 emission and lower energy consumption values compared to OPC based FC.

Various LCA software tools have been developed in different regions: GaBi, SimaPro and Umberto NXT in Europe and ATHENA in the US and Canada (Islam et al., 2014). Similarly, many life cycle inventory (LCI) databases are available (i.e. ATHENA, Eco-Invent etc.). Although any LCA software can be used for analysis, generally it is preferred to use region specific LCI data. For example, several recent Indian LCA studies were conducted using SimaPro software (Gettu et al., 2019; Pillai et al., 2019; Ram et al., 2020) while some used Umberto NXT(Sangwan et al., 2018a) but region specific data for LCI was taken from Ecoinvent database. One study in Canada (Panesar et al., 2019) was conducted using GaBi software while most of the researchers around the world preferred SimaPro (Braga et al., 2017; Islam et al., 2014; Tait and Cheung, 2016). Though the outcomes of these studies are valid for

their region, the limitation is that they cannot be compared to studies done in other regions. Hence, the choice of LCI database is a key decision in any LCA study as the outcomes of any study are generally valid only for that particular region. In LCA studies the assumptions, system boundaries and methods adopted for impact assessment varies significantly. The selection of impact category indicators depends on the study focus. GHG (Greenhouse gas like CO_2) and CED (Cumulative Energy Demand like Embodied energy) are most commonly used indicators. Most of the researchers have followed cradle-to-gate system for LCA (Lim et al., 2017; Tiong et al., 2020; Zimele et al., 2019). In this system, activities start from raw material extraction and end with the production. A common limitation of most studies is that they did not consider the implications of life cycle cost in their analysis. Table 2-5 provides the brief review on the LCA studies carried across the world with respect their location, their impact categories studies, their boundary conditions and the software utilised by them.

2.5.2 Life cycle assessment in India

Singh et al., (2017) performed the LCA on concrete using waste marble powder as partial replacement of cement and sand using UMBERTO-NXT software for modelling. They used the Ecoinvent database 3.0 for inventory data. The carbon footprint per ton of concrete was reduced from 410 kg/m^3 to 350 kg/m^3 by replacing 15% of cement with marble powder.

Pradhan et al., (2019) compared the environmental impact of natural aggregate with recycled aggregate using LCA. Inventory data for fuel (diesel), electricity, water consumption, cement production, loading operation (loader or excavator), and transportation were obtained from the Ecoinvent 3.01 database. While LCI for the production of natural coarse aggregate and recycled coarse aggregate was prepared by collecting the necessary data from the crushing plant and recycling plant, respectively. The result shows that cement contributed the most in each of the impact categories in GWP followed by transportation.

Performance of mortars with waste from steel and iron industry as replacement of cement was evaluated by (Palod and Ramtekkar, 2019). LCA was used as one of the parameters to compare the sustainability of these mortars. Iron and steel waste was taken from Bhilai Steel Plant, Chhattisgarh, India. Indian database from GaBi software was used for the input materials. The optimum mix was obtained by replacing cement with steel slag and GGBS each at 20% replacement level, and the above mix was reported to reduce the carbon dioxide emission.

Table 2-5: Software and approaches adopted by various researchers for LCA

S no	Study	Author and year	Location	Approach used	Impact category	Software used
1	LCA of concrete using marble waste	M. Singh et al., (2017)	India	Cradle to grave	Climate Change, Human Toxicity, Agricultural Land Use, Stratospheric Ozone Depletion, Fossil depletion, Particulate matter and Water depletion.	UMBERTO-NXT
2	LCA of natural and recycles aggregate	Pradhan et al., (2019)	India	Cradle to gate	Abiotic depletion, Global warming potential, Ozone layer depletion, Formation of tropospheric ozone photochemical oxidants (POCP), Acidification potential, and Eutrophication potential.	Simapro
3	LCA utilizing steel and iron industry waste in mortar.	Palod & Ramtekkar, (2019)	India	Cradle to gate	Abiotic depletion, Acidification Potential, Eutrophi- cation Potential, Global Warming Potential, Human Toxicity, Marine Aquatic Ecotoxicity Potential, Ozone layer Depletion Potential.	GaBi
4	EIA of fly ash and silica fumes in geopolymer concrete	Bajpai et al., (2020)	India	Cradle to grave	Climate Change, Human Toxicity, Agricultural Land Use, Stratospheric Ozone Depletion, Fossil depletion, Particulate matter and Water depletion.	UMBERTO-NXT
5	Sustainability assessment of brickwork	Joglekar et al., (2018)	India	Cradle to gate	Water depletion, Energy usage, Fuel depletion, GWP	GaBi
6	The environmental benefit of construction and demolition debris using LCA	Ram et al., (2020)	India	Cradle to gate	Ozone layer depletion, Respiratory organics, Land occupation, Aquatic acidification, Global warming, Non-renewable energy, Aquatic ecotoxicity, Terrestrial ecotoxicity	Simapro

6	CO_2 emission of light weight materials in construction	Kalyana et al., (2020)	India	Cradle to gate	GHG emission, Global warming, Natural resource depletion.	Simapro
7	LCA of new construction material from stainless steel slag	Maria & Maria, (2018)	India	Cradle to gate	Abiotic depletion, Acidification, Eutrophication, Freshwater aquatic ecotoxicity, Global warming potential, Human toxicity, Ozone layer depletion, Terrestrial ecotoxicity, Marine aquatic ecotoxicity	GaBi
8	LCA of concrete using fly ash and copper tailings in concrete as partial replacement of cement	Dandautiya & Singh, (2019)	India	Cradle to grave	Climate Change, Human Toxicity, Agricultural Land Use, Stratospheric Ozone Depletion, Fossil depletion, Particulate matter and Water depletion	UMBERTO-NXT
9	LCA of concrete wuth recycled course aggregate and fly ash	Kurda et al., (2018)	Portugal	Cradle to gate	Abiotic Depletion Potential, Global warming potential, Photochemical ozone creation, Acidification potential, eutrophication potential, Cumulative Energy Demand	Simapro
10	Environment impact of different concrete design using bottom ash instead of sand	Pushkar, (2019)	Israel	Cradle to gate	GWP, Terrestrial ecotoxicity, Fossil resource scarcity, and water consumption	Simapro
11	LCA of manufacture of EPS granulates and light weight concrete with EPS and high density boards	(Gomes et al., (2020)	Portugal	Cradle to gate	Global warming potential, Ozone depletion potential, Acidification potential of soil, Eutrophication potential, Photochemical ozone creation potential, Depletion of abiotic resources.	Simapro

12	LCA of self-compacting concrete containing fly ash and limestone powder	Celik et al., (2015)	Turkey	Cradle to gate	GWP, CO_2 equavalent, CO, NOx, Perticulate matter, SO_2.	-
13	Effect of transportation of Fly ash on Sustainability of concrete.	Panesar et al., (2019)	Canada	Cradle to grave	Ecotoxicity, Human toxicity, Resources and fossil fuels, GWP.	GaBi
14	Used eggshell as partial replacement of cement in foam concrete and perform LCA.	Tiong et al., (2020)	Malaysia	Cradle to gate	Acidification, Climate change, Fossil fuel, Photo- chemical oxidation, Eutrophication, and Ozone layer depletion	-
15	Perform LCA of Concrete of six different mix having include construction and demolition wastes (CDW), marble sludge, rice husk and bagasse ash as a partial replacement of cement	Khan & Ali, (2019)	Pakistan	Cradle to gate	CO_2, CO, NOx, SO_2 emission.	Simapro

Gettu et al., (2019) studied the influence of supplementary cementitious materials on the sustainability parameters of cement and concretes in the Indian context. The author compared the three approaches of LCA i.e. (i) Ground to Gate, (ii) Gate to Gate, and (iii) Cement Sustainability Initiative systems (CSI) for production of cement. The impact on sustainability was assessed in terms of CO_2 emissions. LCA for cement production in Chennai for different types of cement was done by (Gettu et al., 2018). The Carbon footprint (kg CO_2 eq./tonne of cement) and embodied energy (MJ/tonne of cement) for Ordinary Portland cement (OPC), Portland pozzolanic cement(PPC), Portland slag cement (PSC), and limestone calcined clay cement (LC3) obtained were 930 and 5945, 690 and 4690, 550 and 3840, 610 and 4850 respectively. They concluded that the incorporation of fly ash in cement and concrete has a significant benefit. Further, portland slag cement showed the lowest CO_2 emissions and embodied energy. Also, the use of GGBS as an SCM and its impact on sustainability in Indian conditions should be further studied

Bajpai et al., (2020), Dandautiya & Singh, (2019) performed LCA of concrete with various cement replacement materials such as Fly ash, Silica fumes, and GGBS. They concluded that these materials have the potential to reduce the GHG (Greenhouse Gas) effect when replaced with cement. But unavailability of these materials nearby caused increased transportation distance which subsequently resulted in negative environmental effect (Panesar et al., 2019).

Ramesh et al., (2012) calculated the life cycle energy (LCE) demand of a residential building with a usable floor area of about 85.5 m^2 located at Hyderabad (Andhra Pradesh). LCE savings were significant when insulation was added to the external wall and roof. Saving varied from 10% to 30% depending on the climatic conditions Aerated concrete (AC), as wall material, has better energy performance over other materials as aerated concrete is porous in nature and provided better thermal and sound insulation.

Praseeda et al., (2015) calculated embodied and operational energy of urban residential buildings in India constructed with different building materials. Their studies found out that dwellings using materials like stabilized soil blocks, rammed earth, etc. for walls have embodied energy below 2.0 GJ/m^2 and those with burnt clay brick masonry walls have embodied energy in the range of 2.40 - 2.90 GJ/m^2. The embodied energy rose to 10.5 GJ/m^2 when the RC frame and monolithic RC walls were used.

Amongst the various raw materials, cement manufacturing had the highest environmental footprint, which was responsible for the consumption of about 74% of energy while also producing 88% GHG emissions. Further, the energy required to produce 1 ton of concrete is 1.4 GJ, which is mainly generated by the burning of fossil fuels. The embodied carbon dioxide (CO_2) for concrete is approximately 5% to 13% of its total weight (Singh et al., 2020).

Praseeda et al., (2015) estimated the embodied energy of different building materials that are used in the construction industry of India. The values were assessed based on actual industrial survey data. Also, the authors examined the suitability of two basic methods; process analysis and input-output method, and concluded that process analysis is more appropriate for embodied energy (EE) assessment in the Indian context. The building materials and building products that were included in the study were sand, coarse aggregate, cement, concrete block, burnt clay brick, laterite block, steel, ceramic tile, glass, clay roofing tile, aluminium, polished granite slabs, and polished marble slabs.

Oglekar et al., (2018) performed a sustainability assessment of burnt clay bricks and bricks made of industrial and agro wastes used for brickwork in a low-cost house. Three different bricks using paper mill waste, cotton mill waste, and risk husk ash mixture were prepared and their sustainability was compared with standard burnt clay bricks and fly ash bricks. Brick made of cotton mill waste showed the best sustainability index of (0.94). Clay brick was found out to be the least environmentally sustainable.

Sangwan et al., (2017) assessed the environmental impact of vitrified ceramic floor tile supply chain by performing LCA using the endpoint and mid-point assessment method and found that the manufacturing stage of the supply chain is generating the highest impact on the environment in all the categories.

Bhatia, (2014) compared the two walling systems viz. kiln burnt brick and AAC block based on environmental impact category by performing LCA. The author concluded that AAC blocks having lower density has low raw material impact and embodied energy. Also, the CO_2 emission of AAC block is 40% lower than kiln burnt bricks.

2.6 Major Gaps in Research Work

Based on the literature review carried out, the major research gaps are identified which could serve as future research directions. The various issues that were predominantly highlighted, which could serve as future research directions are visualised as follows; -

1. Necessity of stabilized foam: Production of FC especially very low density requires an incorporation of a stable good-quality foam for which appropriate surfactant is the crucial requirement. XG has the potential to be used as an effective foam stabilizer for production of FC however its potential in the construction industry is not explored in detail. Further, to the best of author's knowledge the available limited literature is only focused on the effect of XG on anionic surfactants, hence more investigations are needed concerning its performance with other categories of surfactants.
2. Addressing the compatibility issues and influence of admixtures in FC: Suitability of the surfactant and its foam to be incorporated should be checked for its compatibility with the admixtures. Incorporation of admixtures have potential to enhance the properties of FC significantly however optimization of dosage of admixture is the major issue that needs the dire attention. Despite the fact the FA is the most widely used industrial residue, its suitability as filler in FC need to be explored in detail and surprisingly, only scanty literature is available in this regard.
3. Thermal behaviour of FC: Thermal properties of FC is influenced by various factors related to materials, mix composition and microstructure. There are very few literature available on studies related to thermal behaviour of FC from Indian context. Evaluation of the thermal behaviour of FC and its influence on the energy consumption of buildings in different weather conditions can lead to huge energy savings. However, the studies reported relevant to above is scanty.
4. Life cycle assessment: Researchers can explore the potential environmental hazards or benefits that FC can provide when compared to the conventional materials that are in use in construction industry. As of now, very few researchers have worked on LCA of FC and hence there is a lot of potential for significant research in this area particularly from Indian context.
5. Operational energy cost analysis: Cost implication of the use of FC in buildings over an operational period of time can be evaluated. Till now there is no study conducted on the operational energy cost analysis of FC from Indian context. Thus this becomes a major research area that is yet to be explored.

2.7 Motivation for the Research

The literature review, highlights existing research trends, underlines several areas which could serve as motivation for future studies on the potential of FC in structural and non-structural applications. Globally, use of FC is increasing nowadays over a wide range of applications.

Even in India it is gaining a suitable ground in structural and non- structural applications. Despite this renewed interest of FC, one of its major limiting factors with low density FC is the low strength, low durability, high drying shrinkage and high cost of production coupled with its tedious production technicalities. Studies have revealed that FC behaviour is influenced by factors such as surfactant type, dosage, foam generation process, foam density, foam capacity, foam stability, foam viscosity, and bubble microstructure. Therefore, the production of FC with desirable characteristics necessitates a stable high-quality foam produced with appropriate surfactant. (Sahu et al., 2018; Samson et al., 2017). The studies conducted by (Hajimohammadi et al., 2018) and (Zhu et al., 2020) have demonstrated that incorporating a small quantity of XG as a foam stabilizer into a surfactant solution has a notable effect on reducing the drainage rate and improvement in foam stability. This, in turn, leads to enhancements in the pore structure and mechanical properties of FC. However, the existing literature is only concentrated on the impact of XG on anionic surfactants and, its potential in the construction industry is not explored in detail. Therefore, further research is required to examine its effectiveness with other types of surfactants. Present study assesses the role of additive XG in performance improvement of foam produced with two surfactants viz., NPE (synthetic) and Hingot (natural). Performance is studied through evaluation of essential foam and surfactant characteristics such as foam density, foam stability, bubble microstructure, viscosity and surface tension of surfactant. Further the effect of XG on the FC performance in terms of fresh state properties (stability and consistency) and hardened properties such as compressive strength and TC is also studied. This experimental study is probably the first study to be reported on the suitability of additive XG with surfactants NPE and Hingot for use in FC. Also, in order to improve FC properties like strength, durability and shrinkage behaviour and to make it economical, researchers have been optimising the FC mix by incorporating various admixtures in it. However, evidence from literature shows that incorporation of different admixtures may cause foam stability issues thus affecting the properties of FC. With respect to FC a sizeable amount of literature is available on FA as a binder replacement. However, the literature pertaining to the FA as filler (i.e. sand) replacement is rather limited and this has been reported to give more positive effect on the strength (Gandhi et al., 2023; Jones and McCarthy, 2005c; Kearsley and Mostert, n.d.; E. K. K. Nambiar and Ramamurthy, 2006b, 2006a). Also studies carried out on FC incorporating polypropylene fibres and SF is scanty. Hence as a part of present study, systematic investigations on the effect of replacement of sand with class F FA, cement with SF and addition of PP fibres on fresh properties, compressive strength, split tensile strength and thermal

behaviour of FC shall be evaluated. Further, the variation of above mentioned characteristics with density of concrete is also studied. Two different densities of FC are being chosen i.e. 1000 kg/m^3 and 600 kg/m^3. Which can be recommended for non-structural applications like roof insulation and walling material as a sustainable alternative to clay bricks.

Further in the current scenario, with harsh climatic conditions in most of the places in the world, it is to be noted that most people spend 90% of time living indoor for which 40% of the energy is consumed to overcome the heat flow and acquisition via surface coating and building wall units (Costa et al., 2013). Hence usage of FC with good thermal insulating properties, in a long run can result in huge energy savings when compared to the conventional constructional materials. Operational energy cost analysis can provide an accurate anticipation of those savings. Still there are no studies reported on operational energy cost analysis of FC with respect to Indian climatic zone. Review of literature in the concerned area has pointed out that DesignBuilder software can provide a platform to evaluate the operational energy requirement for the various climatic zones in India. Hence the present study will simulate the operational energy performance of residential building with FC as walling and roofing material. Further, it is to be noted that LCA of a FC varies as per the region. However, most existing databases and inventories for emissions and energy demand do not have information pertinent to emerging economies like India, resulting in unreliable reporting or no reporting at all. Since there have been no study conducted as of now on LCA in India with respect to FC, a framework for assessing sustainability parameters, especially CO_2 emissions and energy demand, in the Indian context is required. The application of which can be extended to all situations where such evaluation is in its infancy. Simapro software can be used to contemplate the performance of the FC across various environmental impact categories. This will be first of its kind of LCA evaluation of FC production across various environmental impact categories for Indian subcontinent. This will help to assess its sustainability measure of FC and to compare with equivalent products available in market.

2.8 Summary of Literature Review

Generally, to enhance the characteristics of FC, admixtures such as FA, SF, plasticizers, and fibres can be integrated. Further, enhancement in the properties of FC can be achieved through the use of longer curing, adoption of novel mixing techniques, incorporation of pozzolanic materials, and adjustment of water-to-cement ratios. The stability of foam directly impacts the strength characteristics of FC. The choice of foaming agent, aggregate, and the amount of water

utilized has a direct impact on the stability of the foam. The increase in the foam volume significantly reduces the consistency, and the increased air voids overlap and increase the amount of combined pore. The strength is influenced by the spacing, morphology, and dimensions of the air voids and pore network. Utilizing waste materials, such as FA, as a filler has a beneficial impact on the strength characteristics. However, due to its pozzolanic abilities, it provides later strength growth. FC faces instability issues due the foam collapse resulting from compatibility issues of admixtures with the surfactant used for production of foam. Different admixtures show different levels of compatibility, like PCE based SP is more compatible than lignin based SP. In recent years, considering the importance of energy efficiency in building sector, researchers have prioritized studies on thermal properties of FC. Out of all three thermos-physical properties, it is observed 80% of researchers had studied TC of FC. Review on factors affecting thermal properties of FC indicates that density and the air void system are the most substantial factors. Studies indicated that thermal resistance is indirectly proportional to density and directly proportional to porosity of FC. Moisture content, temperature and curing conditions also have a considerable impact on thermal properties of FC. FC prepared with lightweight aggregates not only improves mechanical properties but also significantly improve the thermal resistivity of FC. Fibres and admixtures though added in small quantities but affect the micro structure and porosity to a great extent in FC thus reducing the TC. Geopolymer FC not only on par but in some cases resulted in better insulating properties than normal FC.

The microstructure of FC plays a crucial role in determining its properties. Apart from thermal behaviour of FC, studies on life cycle assessment of FC is necessary in order to quantify the environmental impacts and to identify the materials that are more environmentally sustainable. CO_2 emission and embodied energy of FC is more due to the high cement content, which can be reduced to a great extent by partial replacement with pozzolanic materials. Role of insulating materials in thermal comfort has a due importance. Adopting proper thermal insulation form is one of the effective ways to reduce building cooling and heating energy consumption. Limited studies had proved that buildings with light weight concrete bricks provided better energy consumption when compared to traditional bricks. Further, LCA in combination with operational energy cost can highlight where impacts and costs fall in different phases of a building's life cycle and can reveal which building assemblage will result in minimum environmental impact and economic cost.

CHAPTER 3 OBJECTIVE AND SCOPE OF THE PRESENT STUDY

3.1 General

The previous chapter highlighted the necessity for a comprehensive investigation into the identification of cost-effective foaming agents which can lead to a stable foam for the production of a sustainable FC. Further it recommended towards the use of admixtures for the overall improvement in the performance of FC for its application towards an efficient walling material and roof insulation. Based on a review of prior research and development in the field of FC, the goals and extent of the current investigation have been established as described in the subsequent sections.

3.2 Objectives

The objectives of present study are:

1. To enhance the performance of the surfactant and foam (viscosity, foam density, foam drainage, bubble microstructure) for its applicability in production of FC, especially with lower densities.
2. To study the influence of various chemical and mineral admixtures on fresh state (spread flow behavior) and hardened state properties (compressive strength, split tensile strength and thermal behavior) of FC.
3. To conduct the LCA of FC for assessing sustainability parameters, especially global warming potential in terms of kg eq. of CO_2 emissions and embodied energy demand, with respect to the Indian context.
4. To carry out operational energy cost analysis of G+3 residential building with FC as walling and roofing material over its life time, located at different locations falling under various climatic zones of India.

3.3 Scope of work

The scope of the study is limited to the following with respect to raw materials and methods to be adopted.

- Studies on enhancement of surfactant performance are limited to following two surfactants, one for each category- 1) Synthetic surfactant- NPE; 2) Natural Surfactant- Hingot

- The study of influence of admixtures on various properties of FC is restricted to FC with two different densities viz. 600 kg/m^3 and 1000 kg/m^3 made by preformed foaming method. Ordinary Portland cement conforming to IS 12269-1987 and pulverized river sand finer than 300 μm will be used. For the entire study *w/s* is set as 0.35 for 600 kg/m^3 and 0.30 for 1000 kg/m^3.

- For making cost effective FC, different levels of FA shall be incorporated as partial replacement of sand along with Polycarboxylate ether based superplasticizer to achieve a better strength and to maintain a constant spread percentage of 40% to 60% (i.e. slump flow of 140 mm to 160 mm).

- In the LCA analysis, Cradle to gate boundary i.e. from the extraction of raw material till the production phase of FC is considered in the present study. This study is carried out with more focus on Guwahati region.

- The operational energy analysis carried out in the present study considers only the energy consumption during the operational phase of the building. This analysis did not consider the energies involved in the construction, maintenance and disposal phase which also contributes to total energy consumed in a building's life cycle.

3.4 Outline of research

The current study is conducted by adopting the following methodology. Further an brief outline of the experimental program carried out is depicted in Figure 3.1: -

- An in-depth review on the surfactant, properties of foam and influence of foam stability on the performance of FC is carried out. Further, a review on the various available foam stabilizers is done and its role in improving the properties of foam and consecutively FC properties is also conducted.

- To begin with, one surfactant in each surfactant category (Synthetic- NPE and Natural-Hingot) is selected for the experimental program. Further based on preliminary studies, XG is selected to be the foam stabilizer. The optimum levels of XG incorporation for both the surfactants will be derived by evaluating essential characteristics such as foam density,

foam drainage, foam stability and surface tension and viscosity of surfactant solution. Also, the correlation between various surfactant and foam properties such as viscosity vs initial foam density, viscosity vs initial foam drainage, viscosity vs lamellar thickness, surface tension vs average foam bubble size is established. Further ascertainment of the performance of these surfactants at the optimized dosage of XG will be carried out based on the assessment of FC properties such as fresh state characteristics, setting behaviour, compressive strength and thermal properties. The best surfactant combination based on the overall performance and cost effectiveness shall be selected for the further experimental evaluation.

- The selected best combination of surfactant and stabilizer (Hingot + XG) shall be used further for extensive experimental investigations on the influence of various types of admixtures (fly ash, silica fume, polypropylene fibre) on FC properties. Firstly, the influence of admixtures on the fresh state properties (stability and consistency) of FC for mixes with two different foam volumes is studied. This is followed by studies on the mechanical behaviour and the thermal properties of FC. The optimum mix proportions at which the fresh concrete characteristics, mechanical properties, and thermal characteristics are satisfactory are selected for both the densities of FC. Further studies on microstructure are used to justify the experimental results.
- The selected optimum mixes are subjected to to LCA and operational energy analysis. The LCA studies is carried out by using SimaPro software version 9.3. Boundary conditions and various environmental impact categories to be considered for the present study are finalised. Further the obtained results are compared with the similar building materials like AAC block and clay brick which are available in the database of the software.
- For the operational energy analysis, the selected optimum mixes are modelled as a walling and roofing material in G+3 residential building by using DesignBuilder software version 6.1.7.007. The building is simulated considering different cities in India representing various climatic zones as per National building code (NBC) guidelines. The reported annual operational energy consumption is then converted to operational energy cost by considering the respective rates per unit kWh, provided by the corresponding power supply companies in the cities. Comparison with similar walling materials like AAC block and traditional clay brick is also carried out to check the efficiency and sustainability of the selected optimised FC mixes.

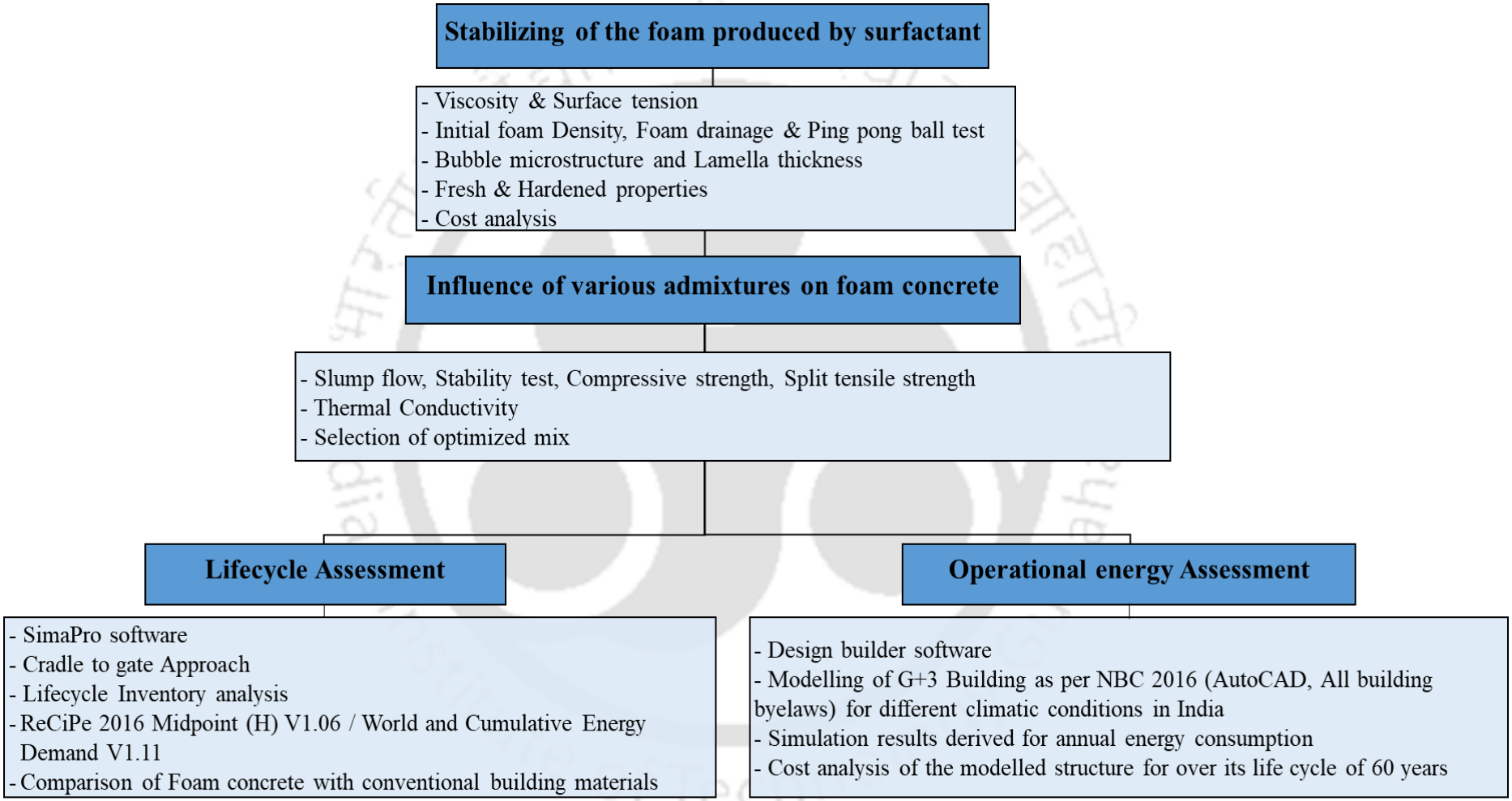

Figure 3-1: Outline of the proposed methodology

CHAPTER 4 INVESTIGATIONS ON THE PERFORMANCE OF XANTHAN GUM AS A FOAM STABILIZER IN FOAM CONCRETE PRODUCTION

4.1 General

The properties of FC are greatly influenced by the quality of the foam used. The stability of the foam is a vital property that needs dire attention when selecting surfactant. The review indicates that researchers have developed diverse foaming agents, categorized as either synthetic or natural. Additionally, numerous research studies have recognized additives, including foam stabilizers, viscosity enhancers, and thickening agents, aimed at improving foam performance in aspects like density, stability, and lamella thickness. However, studies on incorporation of these foaming agents in combination with the foam stabilizers for production of FC is rather limited.

Hence, this chapter assess the role of additive xanthan gum (XG) in performance improvement of foam produced with two surfactants viz., NPE and Hingot. The experimental study in this chapter is divided into two parts. The first part of this chapter is about the assessment of influence of XG on relative performance improvement of two surfactants NPE and Hingot. Different characteristics of foam and surfactant, such as Initial Foam Density (IFD), foam drainage, foam bubble microstructure, surface tension, and viscosity of surfactants, are experimentally evaluated. The second phase of this chapter will focus on the effect of XG on the FC performance in terms of fresh state properties (stability and consistency) and hardened properties such as setting time, compressive strength and TC for two different densities viz., 1000 kg/m^3 and 1500 kg/m^3. Further to evaluate the efficiency of the surfactants from economic perspective cost analysis is carried out to determine the unit production cost for each surfactant combination.

4.2 Experimental investigation on properties of surfactant and foam

4.2.1 Surfactant and foam production methodology

Two different types of surfactants are used in this study viz., i) Hingot Solution (saponin based), which is an in-house produced natural surfactant and ii) Nonylphenol ethoxylate (NPE), which is a commercially available non-ionic synthetic surfactant supplied by Loba Chemie, Mumbai.

Hingot surfactant is synthesised as per the methodology reported by Khwairakpam et al., (2023) (Figure 4.1). The prominent steps involved in production process include drying and particle size reduction of Hingot fruit pericarp (obtained from Bhopal, Madhya Pradesh). Further, the dried and pulverised Hingot powder is blended with water at a concentration of 6% (i.e. 6 grams of surfactant is added to 100 ml of water). The prepared Hingot solution is heated and stirred with a magnetic stirrer at a temperature of 90°C for four hours to promote the saponin extraction (Khwairakpam et al., 2023a; Khwairakpam and Ranjani Gandhi, 2020; Majinda, 2012). In the finally extracted saponin solution, the actual concentration of saponin will be lower than the initial 6% and it will vary depending on several factors, including the extraction method employed, the source and quality of the hingot fruit, and any purification steps undertaken during the extraction process. Hence, in order to reduce the variations in the present study, the material is collected in November season and procurement is made from one vendor. Overall, while the initial concentration of 6% hingot powder may serve as a guideline, the actual concentration of saponin in the final solution will be determined by the efficacy of the extraction and purification processes, as well as the inherent characteristics of the plant material used. After cooling down, the solution is filtered with muslin cloth and mixed with different concentrations of XG procured from Loba Chemie, Mumbai. XG is used as an additive to increase the viscosity of surfactant solution and subsequently to enhance the foam stability. In order to study the effect of XG on surfactant and foaming properties, the dosage of XG is varied between 0% to 0.3% by weight of prepared surfactant solution.

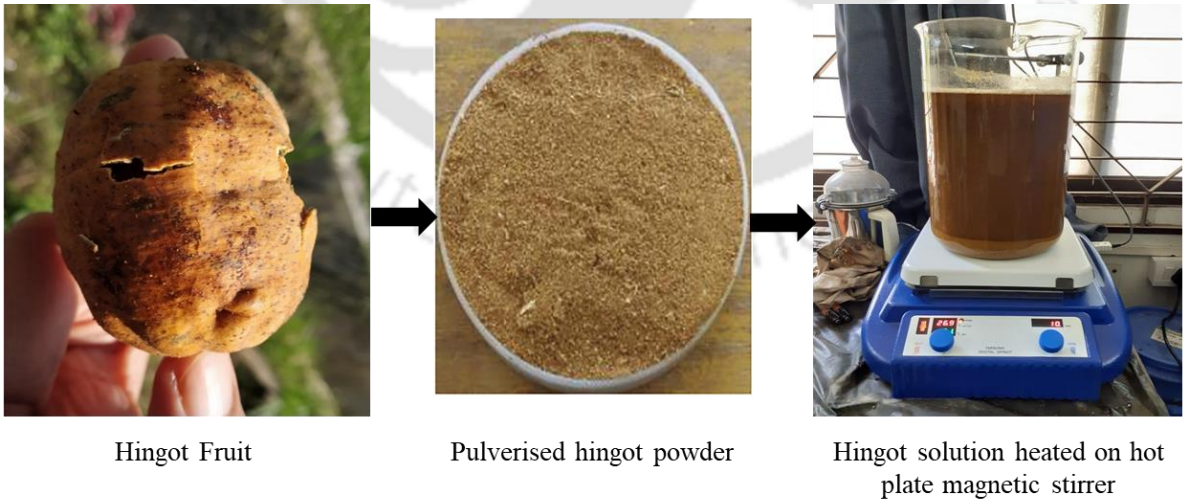

Figure 4-1: Steps involved in preparation of Hingot surfactant solution

On a similar trend, for preparing NPE surfactant solution, 9.5 moles of NPE surfactant is mixed with water at a concentration level of 6% (i.e. 6 grams of surfactant is added to 100 ml of water)

with the help of electric stirrer. Further in the prepared solution, XG is added at different dosages for analysis of its performance. Properties of XG and both the surfactants used in the present study is provided in Table 4.1. A laboratory-scale foam generator with a 200-litre-per-minute output rate is used to aerate various surfactant combinations using the compressed air method.

Table 4-1: Properties of Xanthan gum and foaming agents

Material	Chemical formulae	pH value	Charge	Application/ Role
NPE	$C_{15}H_{24}O$	6 - 8	Non-ionic structure	Surfactant
Hingot	$C_{58}H_{94}O_{27}$	4 - 5	Non-ionic structure	Surfactant
Xanthan gum	$C_{35}H_{49}O_{29}$	6 - 8	anionic structure	Additive

4.2.2 Surfactant and Foam characterization methodology

The characteristics of surfactants have a significant influence on foam properties. For this reason, surfactant characterization is also an essential part of this study. As a part of surfactant characterization, the viscosity of surfactant solution is evaluated using Anton Par, Physica MCR 101 rheometer with concentric cylinder (CC) geometry, operated at constant rotation speed of 150 rpm and constant temperature of 25 °C. The surface tension of surfactant is determined using the tensiometer from Kyowa Interface Science Co. Ltd., model no. DY-300, by Whilmey plate method at a constant temperature of 25°C as shown in Figure 4.2. In line with above studies, foam density, also referred to as the unit weight of the foam, is calculated as per the guidelines recommended by ASTM C796-19 (2019) (ASTM C796-19, 2019). The foam density test is conducted six times for every surfactant combination, and the average of all six trials is reported. The recommended range of IFD as prescribed by ASTM C796-19 is 30 to 65 kg/m^3. Foam stability refers to the ability of foam to resist breakdown from external causes and it is assessed based on the drainage of foam, also referred to as the bleeding rate of foam. The drainage of foam is recorded as per Def Standard 42-40 (Standard, n.d.), which is a commonly adopted method as mentioned in multiple previous works of literature (I. S. Ranjani and Ramamurthy, 2010; Sahu and Gandhi, 2021a; Siva et al., 2015; Sritam Swapnadarshi et al., 2021). The foam drainage is measured at 5 min time interval for a time duration of 30 minutes with the apparatus as shown in the Figure 4.3. The ping pong ball test is another way to assess the foam's stability. The ability of foam to support the weight of a ping pong ball is

contemplated in this test using the sinking time. This test is carried out using a test setup similar to the one reported by Hashim and Tantray (2021) and Sun et al. (2018). A 5000 mL beaker is used to collect freshly generated foam from the foam generator. A ping pong ball with a diameter of 40 mm and a weight of 2.7 g is gently placed on top and the time taken by the ball to reach the beaker's bottom surface is recorded (Figure 4.3). In addition, tracking of intermediate readings of the distance travelled by the ball at every 5-minute interval is also done.

(a) (b)

Figure 4-2: (a) Anton Par, Physica MCR 101 Rheometer (b) Kyowa DY-300 Tensiometer

Further to study the foam microstructure, freshly premade samples of foams with varying XG concentration are spread on a thin dish and kept below Meiji Trinocular Stereo Zoom Microscope (Model EMZ-13 TR). The images of the foam bubbles are captured at different time intervals after generation of foam viz., 5, 15 and 30 min. To analyse the impact of XG concentration on the foam bubble size and lamellar thickness, optical microscope is set at 10x zoom and 40x zoom respectively. Foam texture is analysed through optical image analysis, which involves examining the morphology, size, distribution, and lamella thickness of bubbles present in the liquid phase. The open-source image analysis software FIJI Image-J is utilised for this purpose (Schindelin et al., 2012). The present study involves the calibration of a digital image, which is originally obtained in pixel units, through the adoption of a standard scale. Subsequently, the image in question is subjected to a conversion process to produce 8-bit

format, followed by a thresholding procedure to obtain a binarized image. The extracted information pertaining to the bubble size distribution and lamella thickness is obtained.

(a) (b) (c)

Figure 4-3: (a) Initial foam density test setup, (b) Foam drainage test setup, (c) Pingpong ball test setup

4.2.3 Results on Impact of stabilizer on surfactant and foam characteristics

Viscosity and Surface tension

The key role of any surfactant is to lower the surface interfacial tension and facilitate foam formation. The surface tension of the tap water used for production of the surfactant solution in the present study is found out to be 67.19 mN/m. However, the surface tension of the pure water as reported in literature is 71.99 mN/m at 25°C (Pallas and Harrison, 1990). Comparative analysis of two different surfactant solutions indicate that Hingot is more surface active in nature and its surface tension is found to be 15% lesser than that of NPE (Figure 4.4). For instance, NPE and Hingot surfactant solutions when used at 6% concentration, decreases the surface tension of water to 33.31 mN/m and 28.92 mN/m respectively. Figure 4.4 shows the influence of XG dosage on surface tension and viscosity of NPE and Hingot surfactant solution. A general observation is that, XG, not being an interfacial active polymer, does not tend to show a significant effect on the surface tension, though a slight increase in the surface tension of both NPE and Hingot surfactant solutions can be seen with the increase in XG dosage. This phenomenon can be attributed to the presence of a weak interaction between polymer like XG and non-ionic surfactant in bulk. Similar behaviour is reported by various researchers while

studying the interaction between the XG and non-ionic surfactants (Asnacios et al., 2000; Krstonošić et al., 2019; Sheng et al., 2016).

Comparative analysis of viscosity of both the surfactants shows that NPE is highly viscous in nature with its viscosity 49% higher than that of Hingot. Figure 4.4 shows the influence of XG dosage on the viscosity of foaming solution at constant shear rates. It can be noted from the graph, that the impact of XG on the viscosity of surfactant solution is more predominant when compared to surface tension. XG being anionic polymer is found to be more compatible with both the non-ionic surfactants (Berninger et al., 2021). Hence a 10-fold increment in viscosity is observed when XG concentration is varied from 0% to 0.30% for both Hingot and NPE surfactant solutions. For instance, increase in XG, results in increase in viscosity from 1.84 mPa-s to 18.24 mPa-s for Hingot surfactant while the corresponding variation for NPE surfactant is from 2.75 mPa-s to 23.42 mPa-s. Graphs indicate uniform rate of increase in the viscosity with respect to increase in the XG concentration indicating that it is an efficient viscosity enhancing agent even at a lower concentration.

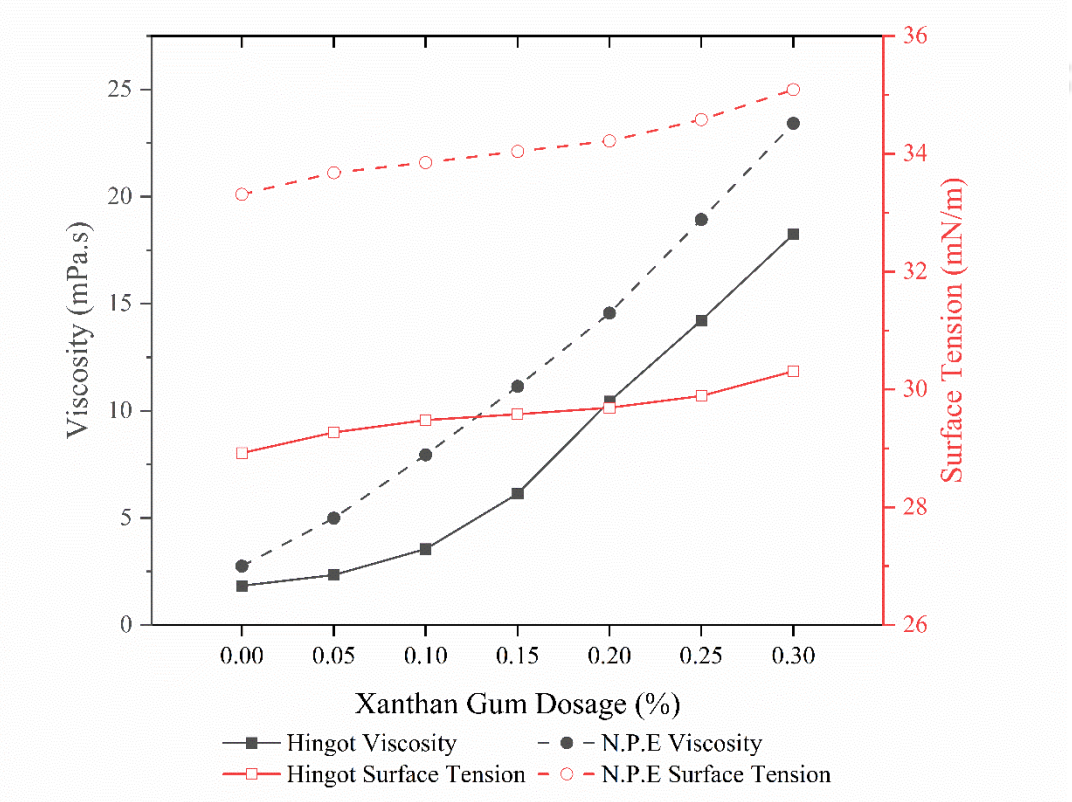

Figure 4-4: Variation of viscosity and surface tension of surfactant solution with XG dosage

Initial foam density

General observation shows that IFD of pure solution of NPE (without XG addition) is higher than that of Hingot, however both the surfactants meet the ASTM C796-19 (2019) requirements. From the Figure 4.5, it is evident that increase in XG concentration from 0% to 0.3% results in significant increase of 140% to 175% in IFD for both the surfactants. XG being viscosity enhancing agent has a key role in enhancement of viscosity of surfactant solution which consequently results in foam with thicker liquid film and higher density. This is supported by the literature that reports that higher viscous surfactant solution results in foam with high initial density and stability (Porter, 1994; Siva et al., 2015). However, the dosage of XG needs to be carefully selected as the increase in XG concentration beyond levels of 0.20% and 0.15% for surfactants Hingot and NPE respectively results in foam with IFD not conforming to ASTM recommendation.

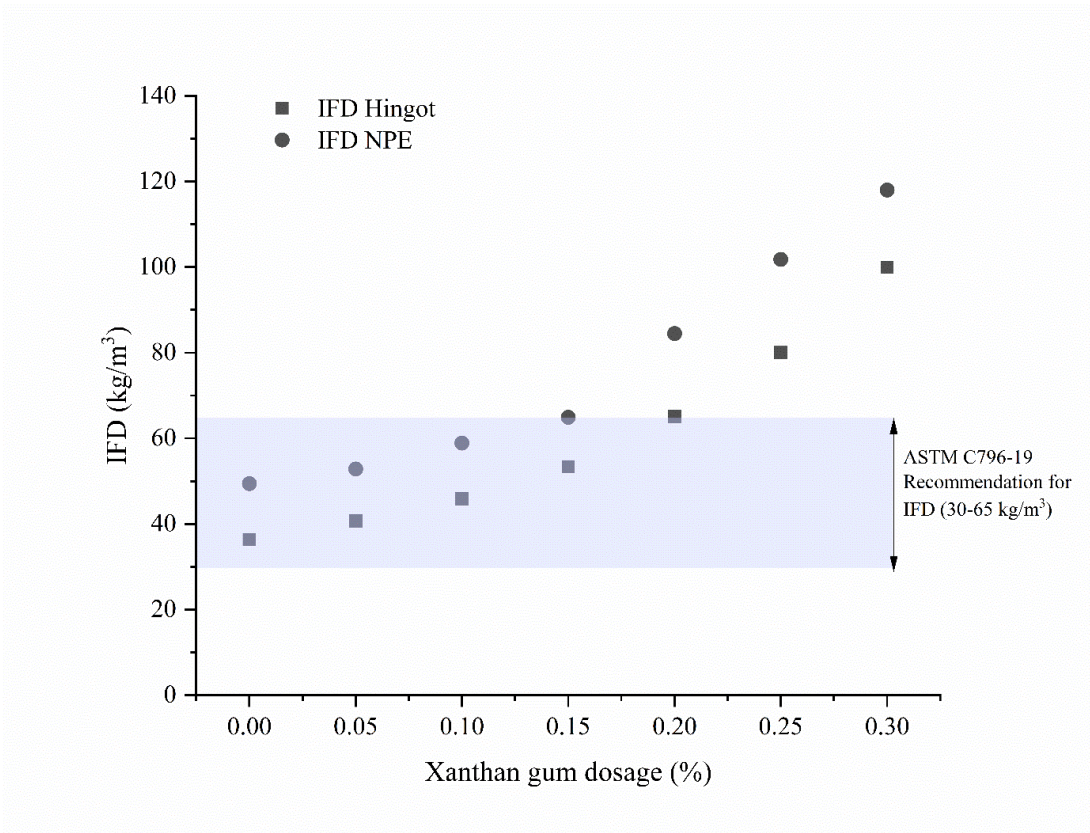

Figure 4-5: Variation in initial foam density with XG dosage

Foam stability

Comparative analysis of foam drainage results for pure surfactant solutions (without XG addition) shows that the early foam drainage (@5 min) is significantly lesser for Hingot when

compared to that of NPE (Figure 4.6). The lower surface tension of the Hingot surfactant contributes to its enhanced foam stability characteristic, thus making it a desirable foaming agent in the first place. Further, addition of XG results in a substantial reduction in the foam drainage which can be attributed to the significant increase in solution viscosity. For instance, addition of a small dosage of 0.05% of XG to both the surfactant solution results in almost no drainage in first 5 minutes. However, Hingot+XG combination outperform NPE+XG combination with very much reduced later drainage (15 min and 30 min). Closer examination of the variation in drainage, shows that increase in XG concentration from 0% to 0.15% results in a steep reduction of 70% in drainage (15 min) for both the surfactants. However, increase in XG concentration beyond 0.15% does not result in further significant reduction in drainage in 15 min for both the surfactants. In line with the other studies reported earlier, if 50% drainage in 30 min is considered as desirable critical limit for foam stability then the experimental outcomes indicates that addition of 0.1% and 0.2% of XG are found to be satisfactory for surfactants Hingot and NPE respectively. Further the above selected levels of XG are also found to satisfy the ASTM C796 (ASTM C796-19, 2019) foam density requirement of 30 to 65 kg/m^3 in 30 min (Figure 4.7).

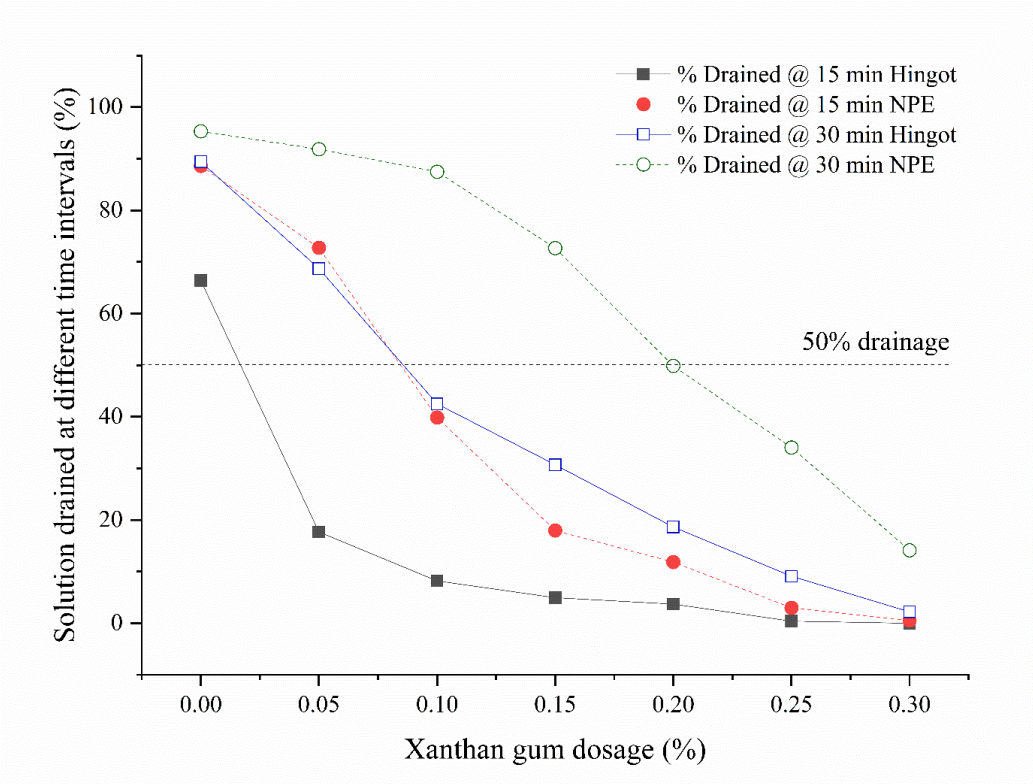

Figure 4-6: Variation of percentage solution drained with XG dosage

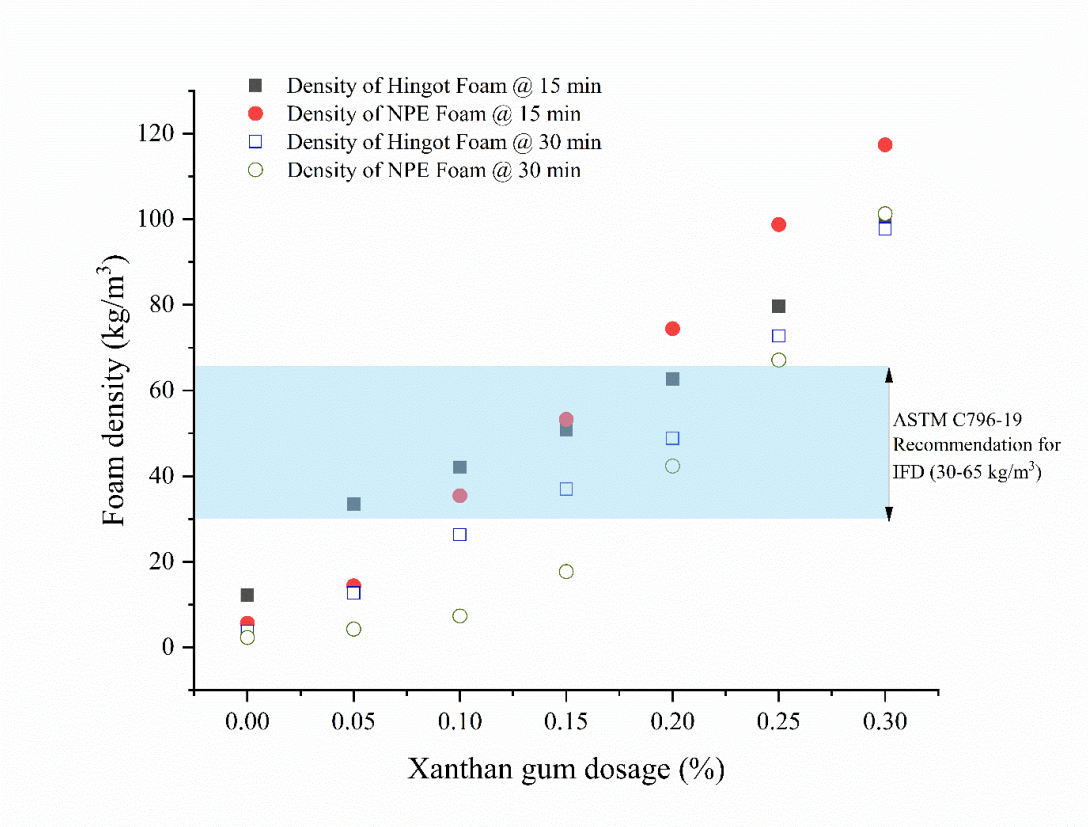

Figure 4-7: Variation in foam density at different time intervals with XG dosage

Besides the conventional foam drainage test, the ping pong test gives additional information about the weight sustaining capability of the foam which can be closely related to the stability of the foam. In line with the above observation on foam drainage test, the results of ping pong ball test as shown in Figure 4.8, indicate that the time taken by ball to reach the bottom of beaker is 32% more for pure Hingot surfactant solution (without XG addition) when compared to NPE. The addition of XG further increases the time taken by the ping pong ball to settle down. A linear increase in time for settlement of ball is observed with the increment in the dosage of XG and this can be closely correlated to the trends seen above for the foam drainage study. An almost 200% increment in time is recorded for both the surfactants when XG dosage is increased from 0% to 0.3%. Moreover, the combination of Hingot surfactant and XG shows better results when compared to that of NPE and XG. From the Ping-Pong ball test results, it can be inferred that the improvement in foam stability upon addition of XG is due to increase in viscosity of surfactant solution and subsequent increase in foam lamella thickness. Hence studies on foam bubble microstructure is warranted for thorough understanding of the influence of XG on foam stability.

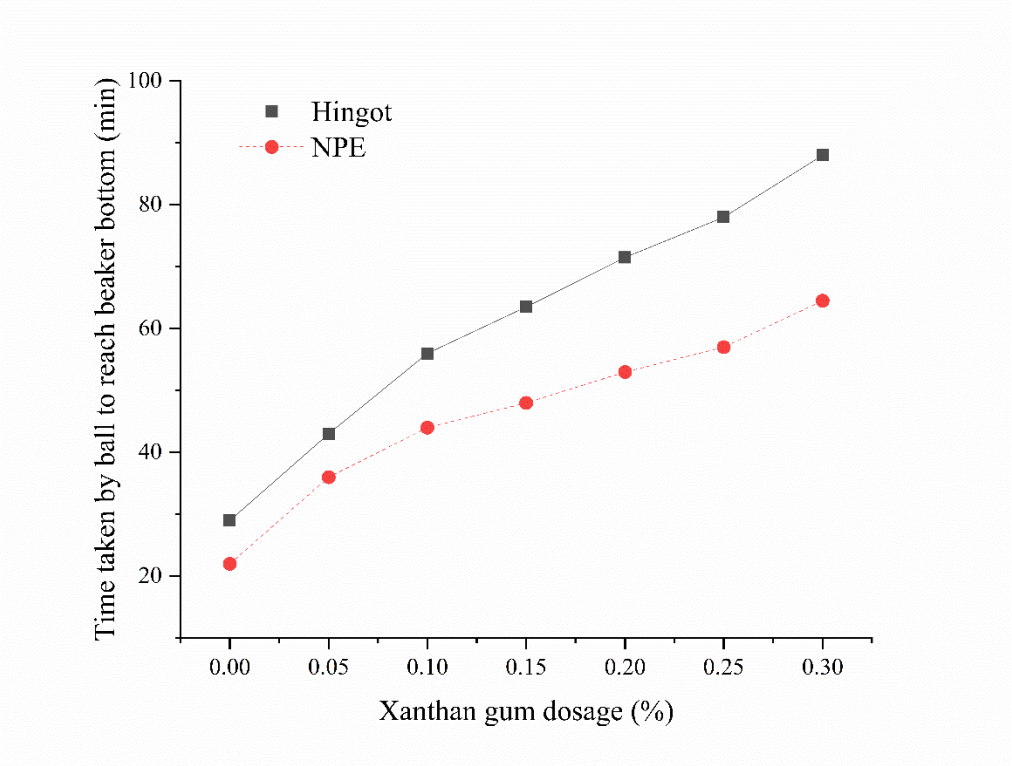

Figure 4-8: Variation in the foam sustaining ability with XG dosage (Ping pong ball test)

Bubble size distribution and Lamellar thickness

Figure 4.9 shows the effect of the of XG dosage on the mean bubble size at different time intervals. At a given time, interval after the foam generation, the mean bubble size of the Hingot surfactant is found to be smaller than that of the NPE surfactant. The above observation on bubble size is contradictory to the trend on viscosity discussed in earlier section. Though the viscosity of the NPE solution is higher than that of the Hingot, the bubble size of NPE foam is found to be larger than that of Hingot. This can be attributed to the predominant influence of surface tension over viscosity. According to research findings, surface tension and viscosity both, tends to have greater influence on bubble size, however, particularly surface tension is the initial driving force in bubble coalescence (Kováts et al., 2020; Sun et al., 2022). Also, the foaming ability of Hingot surfactant with reduced surface tension is very much higher subsequently resulting in production of larger volume of foam from unit quantity of foam concentrate when compared to that of NPE surfactant. Adding to above, viscosity also impedes the bubble coalescence and enhances stability resulting in reduced bubble size (Khwairakpam et al., 2023a; Sun et al., 2022). Further, it is to be noted that foaming, as seen in the context of NPE and Hingot foam, is affected by the interplay between liquid viscosity and surface tension, impacting the stability and size of bubbles in the foam. Hingot surfactant with reduced surface tension is relatively more surface active in nature and this coupled with enhanced viscosity due

to addition of XG further leads to its superior foam stability, reduced coalescence and reduced bubble size when compared to that of NPE (Khwairakpam et al., 2023a). The nuances of how these factors contribute to bubble size discrepancies, especially between NPE foam and Hingot foam, is explored further by considering the variation in average foam bubble size with XG dosage at different time intervals. With increase in XG dosage from 0 to 0.3%, the mean bubble size is reduced from 807 microns to 429 microns for NPE. The corresponding variation in mean bubble size for Hingot foam due to XG addition is from 717 microns to 404 microns. Increase in viscosity and lamella thickness due to XG addition contributes to the above mentioned reduction in bubble size. Further, for a time-lapse from 5 min to 30 min, foam coarsening with time is clearly evident due to bubble coalescence. For instance, a significant increase of 200% in mean bubble size is observed for NPE surfactant solution (without XG addition) and the corresponding increment for Hingot foam is 174%. However, with XG addition the rate of coarsening is reduced for both the surfactants and the above effect is more predominant in Hingot. For instance, at time interval of 30 minutes after foam generation, the mean bubble size of H+0.3 X is 49% lesser that that of NPE+0.3 X. Further, it is to be noted that the mean bubble size of H+0.1X concentration itself is lower than that of NPE+0.3X at time interval of 30 minutes after foam generation as can be evident from Figure 4.10. It can be clearly noted that the difference in the average bubble size of NPE and Hingot foam is lower when considering the initial time phase. However, as the time passes Hingot foam due to reduced rate of bubble coalescence exhibited much lower average bubble size when compared to NPE. The above difference can be ascribed to the reduced surface tension of Hingot when compared to NPE which contributes to more saponin adsorption at lamellar interface. Interestingly, the above observations are in line with previous studies which have showed that the surfactants with lower surface tension exhibited improved lamella drainage time and reduced rate of bubble coalescence (Djabbarah and Wasan, 1985). Adding to above, enhancement in viscosity of solution also retards the drainage and bubble coalescence leading to higher foam stability (Mohanan et al., 2020). Having studied the impact of XG addition on bubble size, in the following section, the effect on the interface that exists between two bubbles within a foam known as lamella is elucidated clearly.

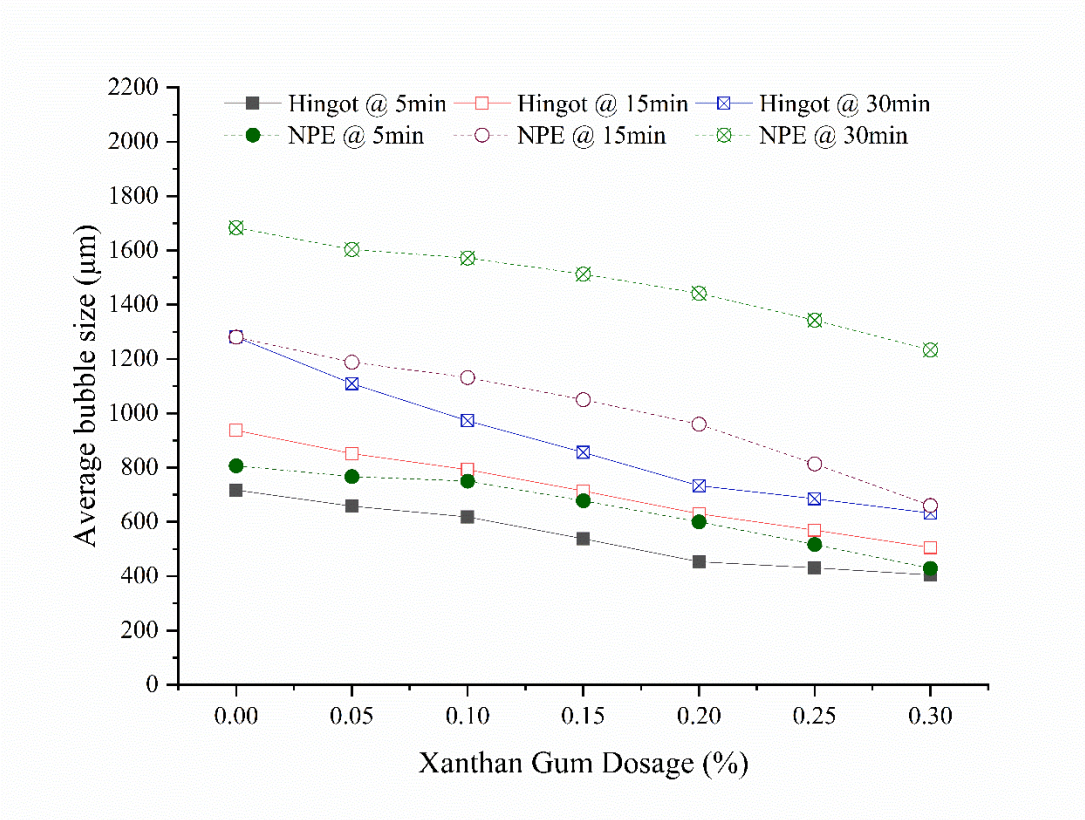

Figure 4-9: Variation in average foam bubble size with XG dosage at different time intervals

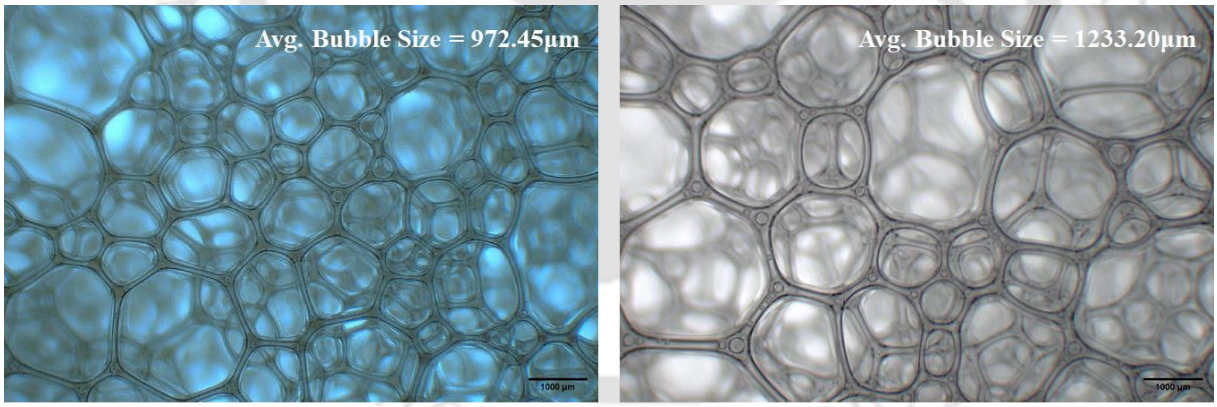

(a) (b)

Figure 4-10: Average bubble size @ 30 min (a) Hingot + 0.1 XG (b) NPE + 0.3XG

Figure 4.11 depicts a standard representation of the foam lamella. Basically, the lamella thickness is denoted by the minimum fluid length between two bubbles, while the node is where three or more bubbles converge. Further, the effect of addition of XG on the lamella thickness at different time intervals after foam generation is illustrated in Figure 4.11 and Figure 4.12. Over the whole 30-minute test period, at any XG dosage, the lamella thickness is found to increase with time. The increase in lamella thickness with time can be ascribed to the bubble growth over time owing to Ostwald ripening and coalescence effect (Stevenson, 2012), which

lowered the interface area and released additional fluid to the bulk. At any given measurement time, lamella thickness is found to increase with XG dosage. For instance, increase in XG concentration from 0% to 0.3% leads to almost 200% increase in the lamella thickness (51 µm to 121 µm) for NPE foam. Interestingly, similar trend is noted in the Hingot foam where increase in XG concentration from 0% to 0.3% enhances lamellar thickness from 43 µm to 98.66 µm. This may be due to the fact that increase in XG concentration, improved the molecular entanglement and thereby increased viscosity and subsequently enhanced the fluid storing ability of lamella (Gelman and Barth, 1981). In this line Raj et. al. (Raj et al., 2022) also highlighted that the addition of XG enhanced the viscosity, IFD and foam stability.

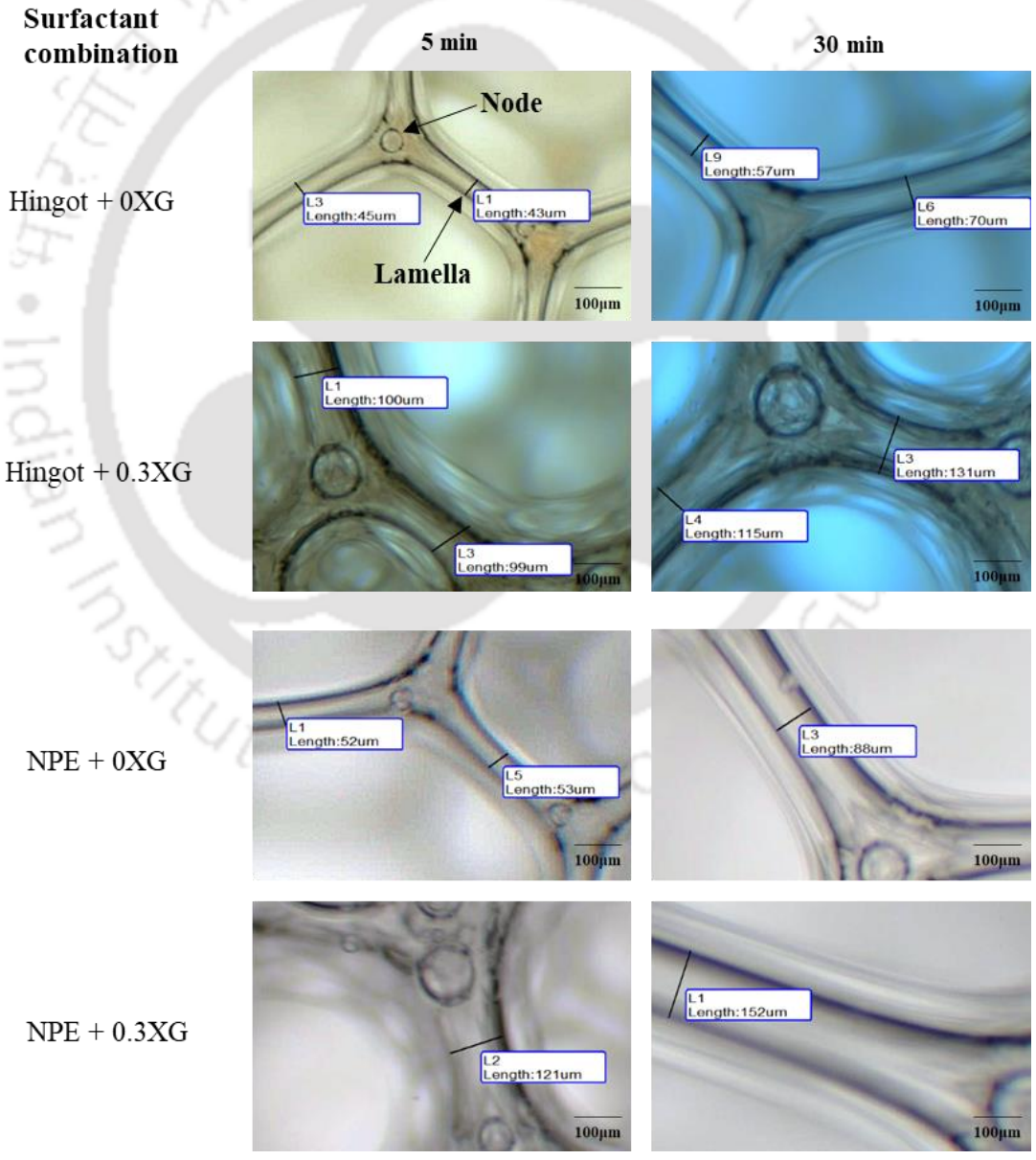

Figure 4-11: Impact of time and XG on thickness of lamellae

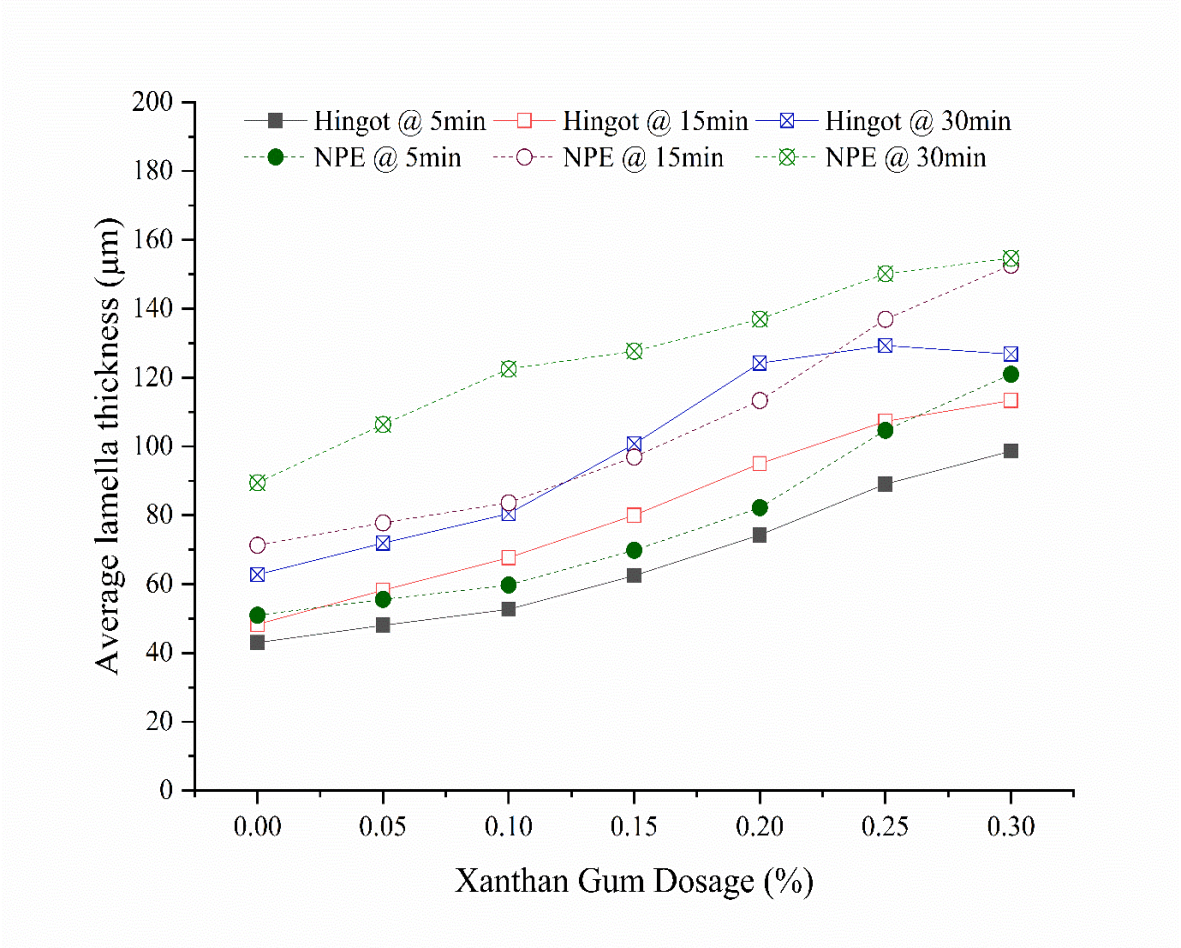

Figure 4-12: Variation in lamellae thickness with XG dosage at different time intervals

4.3 Experimental investigation on properties of FC

4.3.1 Materials and mix proportioning

The freshly premade foams of different surfactant combinations (as discussed in previous section) are mixed with ordinary portland cement of 43 grade (conforming IS 269:2015) supplied by Dalmia cement Ltd. and river sand finer than 300µm. In Table 4.2, the chemical composition and physical properties of cement are presented. Further, the particle size gradation of river sand (Specific gravity of 2.65 and fineness modulus of 1.96), Hingot powder and cement is shown in Figure 4.13.

Table 4-2: Chemical composition and physical properties of cement

Chemical Composition %								
CaO	SiO_2	Al_2O_3	Fe_2O_3	MgO	SO_3	K_2O	Na_2O	LOI
64.63	20.19	5.02	1.45	3.2	2.22	0.5	0.28	2.51
Physical properties								
Specific gravity :- 3.14		Specific Surface Area :- 288 m^2/kg				28 days compressive strength:- 50 MPa		
Initial setting time:- 110 min				Final Setting time :- 220 min				

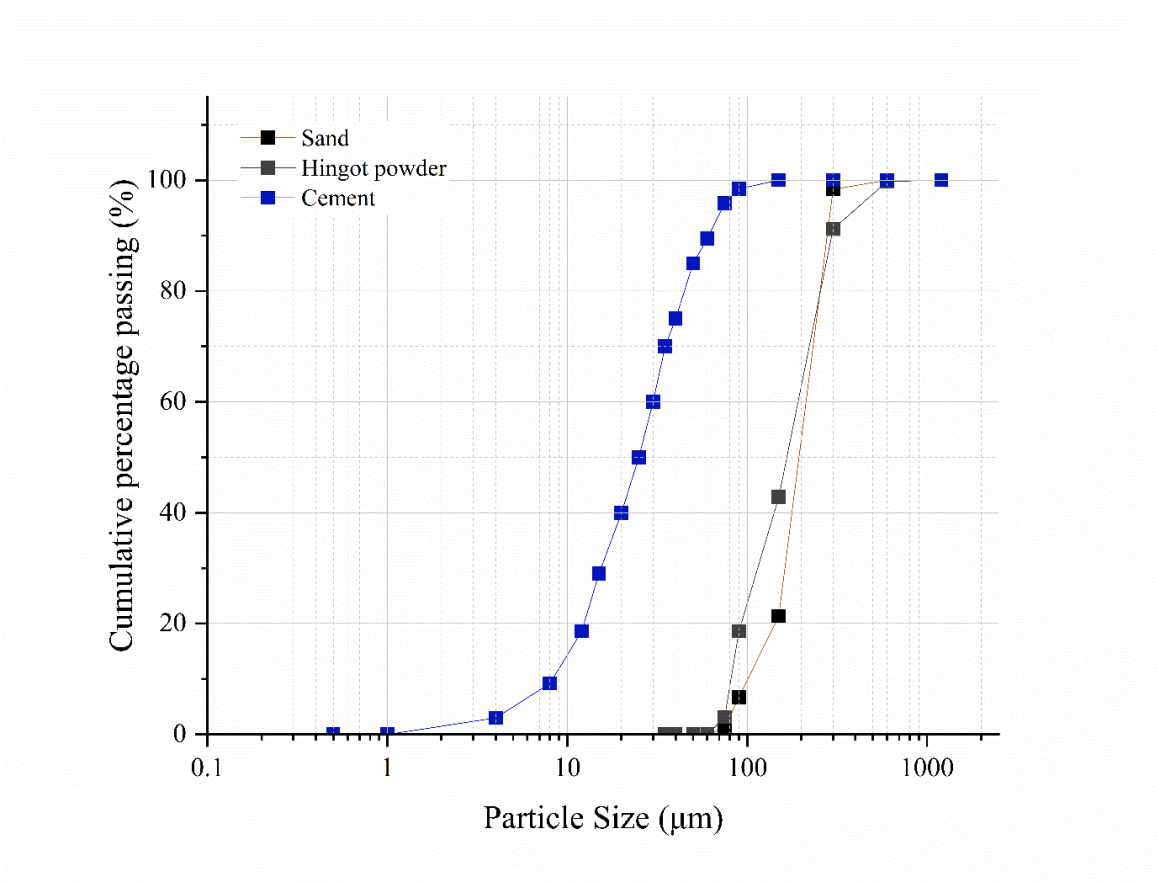

Figure 4-13: Particle size distribution of fine sand, Hingot powder and cement used in the present study

FC mixes with two different design fresh densities viz. 1500 kg/m^3 and 1000 kg/m^3 are prepared for this study by varying foam volume between 51% and 24%. Contrary to normal concrete, where the mix design is based on the target strength required, FC mix design is based on the target density. It is due to the fact that the density and air volume of the FC directly affect the

strength and other properties of the FC. To design FC with desired properties, various methods have been employed and proposed over the years, however none of them can be considered as the only standard practice. Some methods such as trial and error process, rational proportioning method based on solid volume calculations, selection of cement content and water–cement ratio based on plastic density and compressive strength relation for a given strength and density are used by the researchers for production of FC (Aldridge, n.d.; Mccormick, 1967). The guidelines provided in ASTM C 796-19 "*Standard Test Method for Foaming Agents for Use in Producing Cellular Concrete Using Preformed Foam*" is the most commonly used method for calculation of foam volume and mixture constituents for the foam cement paste of given density (ASTM C796/C796M − 19, 1967)(E. K. K. Nambiar and Ramamurthy, 2006b) and is being adopted in the current study. Even though the strength of FC primarily depends on its density, for a given density, the strength can also be modified by altering the mix composition. Most of the methods proposed, help in calculation of batch quantities if the mix proportions are known (Ramamurthy et al., 2009). Since there is no standard procedure for mix proportioning of FC, hence the method prescribed by ASTM C796-19 has been modified for mortar of known target design density and w/s ratio to calculate amount of ingredients. A constant cement to the sand ratio of 1:2 by weight is considered throughout the study. The water to solids ratio is fixed at 0.3 and is maintained for all the FC mixes to facilitate rational comparison. Table 4.3 and Table 4.4 provides the mix proportioning details for FC mixes made with different surfactant combinations adopted in this study. The initial phase of the mixing procedure involves the production of a homogeneous base mix of binder and filler slurry in a horizontal shaft paddle type mixer machine as shown in Figure 4.14. Subsequently, a predetermined quantity of foam is introduced into the mixture. The mixing process is continued for a minimum of five minutes or until the foam is homogeneously incorporated into the slurry. In Table 4.4. the mix code 10 indicates 1000 kg/m^3 target density, 15 indicates 1500 kg/m^3 target density, H indicates Hingot, N indicates NPE and XG indicates xanthan gum. It is to be noted that the dosage of Hingot and NPE are fixed at 6% throughout the study. However, the dosage of XG is varied from 0.05% to 0.3% for various mixes according to the foam behaviour. For instance, 10H+0.15XG indicates FC of target density of 1000 kg/m^3 with Hingot surfactant and xanthan gum dosage of 0.15%.

Table 4-3: Derivation of Mix proportions for cement sand FC mixes

Target fresh density (kg/m^3)	**1000**		**1500**	
	Hingot	NPE	Hingot	NPE
W/S	0.3		0.3	
Cement (kg)	256.41		384.62	
Sand (kg)	512.82		769.23	
Volume of air V_a (litres)	$V_a^* = 1000 - \left(\frac{256.41}{3.14} + \frac{512.82}{2.65} + \frac{230.77}{1}\right)$		$V_a^* = 1000 - \left(\frac{384.62}{3.14} + \frac{769.23}{2.65} + \frac{346.15}{1}\right)$	
Foam volume V_f (m^3)	$V_f = \frac{V_a}{1000 - IFD} = \frac{494.31}{1000 - IFD}$		$V_f = \frac{V_a}{1000 - IFD} = \frac{241.47}{1000 - IFD}$	
Wt. of foam W_f (kg)	$W_f = V_f \times IFD$		$W_f = V_f \times IFD$	
Water (kg)	$= 230.77 - W_f$		$= 346.15 - W_f$	

*Volume of Air V_a (litres) = 1000 – (Total volume of solids + Total volume of water),

(here vol. of water also includes the liquid present in foam)

IFD - Initial foam density for different surfactant combinations as discussed in section 4.2.3

Table 4-4: Mix design proportions (constituents) per 1 m^3 of FC mixes

Mix name	**Target fresh density (kg/m^3)**	**Composition of mixture per m^3**			
		Cement (C) (kg)	Sand (S) (kg)	Water (kg)	Foam (F) (kg)
10H	1000	256.41	512.82	212.11	18.66
10H+0.05XG		256.41	512.82	209.81	20.96
10H+0.1XG		256.41	512.82	207.01	23.76
10H+0.15XG		256.41	512.82	202.91	27.86
10H+0.2XG		256.41	512.82	196.36	34.41
10H+0.25XG		256.41	512.82	187.77	43.00
10H+0.3XG		256.41	512.82	175.88	54.89
10N		256.41	512.82	205.07	25.70
10N+0.05XG		256.41	512.82	203.19	27.58

10N+0.1XG		256.41	512.82	199.84	30.93
10N+0.15XG		256.41	512.82	196.45	34.32
10N+0.2XG		256.41	512.82	185.15	45.62
10N+0.25XG		256.41	512.82	174.75	56.02
10N+0.3XG		256.41	512.82	164.64	66.13
15H		384.62	769.23	337.04	9.11
15H+0.05XG		384.62	769.23	335.91	10.24
15H+0.1XG		384.62	769.23	334.54	11.61
15H+0.15XG		384.62	769.23	332.54	13.61
15H+0.2XG		384.62	769.23	329.34	16.81
15H+0.25XG		384.62	769.23	325.14	21.01
15H+0.3XG	1500	384.62	769.23	319.34	26.81
15N		384.62	769.23	333.59	12.56
15N+0.05XG		384.62	769.23	332.68	13.47
15N+0.1XG		384.62	769.23	331.04	15.11
15N+0.15XG		384.62	769.23	329.38	16.77
15N+0.2XG		384.62	769.23	323.87	22.28
15N+0.25XG		384.62	769.23	318.78	27.37
15N+0.3XG		384.62	769.23	313.84	32.31

*10- 1000 kg/m^3 H- Hingot, N-NPE, XG-Xanthan gum

Figure 4-14: FC production setup

4.3.2 Characterization of Fresh and Mechanical properties of FC

To assess the stability of FC, the plastic or fresh density is calculated by weighing the prepared FC mix in a standard container of known volume. The density ratio is then calculated by comparing the actual fresh density with the target fresh density. A tolerance on fresh density is set at ±50 kg/m^3 of the target design density, as per typical industrial practice, ASTM C796-19 (2019) and various earlier reported literature (Jones and McCarthy, 2005b). The spreadability of the freshly prepared FC is measured as per ASTM C230/C230M-21 (2021) (ASTM C230/C230M-21, 2021). The spread is measured at four locations for each mix and the average spread flow is expressed as percentage of base diameter of standard flow cone. Marsh cone test which is considered to be a reliable method for studying the rheological behaviour of cement and mortar is modified for the suitability of FC. The test is carried out as per modifications suggested by Jones et.al. (Jones et al., 2003), where Modified marsh cone with orifice diameter of 12.5 mm is filled with 1.5 litres of fresh mix. Then, the time taken for 1.0 litre of FC to flow through the constricted orifice is noted down.

To study the influence of XG addition on setting behaviour of concrete, demoulding test is carried out instead of conventional setting time test. The demouldability of 50 mm FC cube specimens are assessed based on its ability to retain the shape after demoulding. Twelve number of 50 mm cubes are casted for each mix and the demouldability is checked at four-hour time interval. The minimum time required for demoulding cubes without affecting the shape is noted for all the mixes. Compressive strength test is performed on 50 mm size concrete cube specimens according to ASTM prescribed guidelines (ASTM C495/C495M-12(2019); ASTM C796-19, (2019)). Six number of specimens are tested for each mix after 28 days of curing. The TC and thermal diffusivity of FC with densities 1000 kg/m^3 and 1500 kg/m^3 are measured using TC kit supplied by C-therm technologies (ISO 22007-2, 2008) based on the principle of transient plane source method (TPS). For each composition, four number of 50 mm size cube samples were prepared, polished flat and parallel, and cleaned with compressed air to ensure good contact between the TPS element and the sample. The probe for the analysis is inserted between the polished surfaces of two samples. To achieve a relatively precise result, each pair of samples are tested three times at three different surfaces and the average value is reported.

4.3.3 Results on Impact of stabilizer on fresh and Hardened state properties of foam concrete

Consistency of FC

The consistency of FC mixes is measured using flow cone test and modified marsh cone for different design densities. Figure 4.15 depicts the spreadibility of FC mixes measured with flow cone for FC with design densities of 1500 kg/m³ and 1000 kg/m^3 at a constant w/s ratio of 0.3. The fluidity and consistency of the FC mixes are mainly dependent on the foam content and quantity of water in the mixes (Lim et al., 2017). The experimental outcome shows that the decrease in FC density results in decrease in spread values due to increase in foam content. For instance, decrease in FC density from 1500 to 1000 kg/m^3 results in 20% reduction in spread for NPE and Hingot based FC mixes. The above observations are consistent with results reported in literature which stated that increase in foam content resulted in increase in cohesiveness of mix and reduction in consistency (Kunhanandan Nambiar and Ramamurthy, 2008; Lim et al., 2017; Sahu and Gandhi, 2021a). Further, NPE based FC mixes exhibits higher spread value when compared to Hingot FC mixes. The above observations on spread is slightly counterintuitive as the viscosity of NPE surfactant solution is higher than that of Hingot. The possible explanation for greater spread of NPE based FC mixes can be attributed to its higher foam density (Sahu and Gandhi, 2021a). The higher foam density of the NPE is due to the higher liquid fraction in the foam of NPE surfactant. This higher liquid fraction leads to relatively wet foam which further leads to higher flow of the FC. The above observations are in line with the results of work reported by Othman et.al. (Othman et al., 2021) and Panesar D. K. (D. K. Panesar, 2013) .

Further examination of effect of XG, shows that increase in XG concentration from 0% to 0.3% results in significant reduction of 88% and 75% in spreadability of Hingot based FC mixes with densities 1000 kg/m^3 and 1500 kg/m^3 respectively. Nevertheless, the corresponding reduction in spread for NPE based mixes ranged from 53% to 38%. The above reduction can be ascribed to 10-fold increment in viscosity of surfactant solution resulting from addition of XG. The reduction in spread due to XG addition is relatively lesser for NPE surfactant and the possible reason can be the higher foam density of NPE which is due to the presence of higher liquid fraction in the foam lamella of NPE as mentioned earlier. When NPE+XG foam is incorporated in the FC due to higher liquid fraction present in the NPE foam, the effect of XG on restriction of flow of concrete is slightly compromised. However, in case of Hingot foam, since it is a

relatively dry foam, the combination of Hingot+XG tends to provide a rather sticky foam and the flow arresting nature of XG is very much evident in the FC as can be seen in Figure 4.16. On a similar note, many researchers have reported about the negative effect of addition of viscosity enhancing foam stabilizers on the consistency of the FC (Sritam Swapnadarshi et al., 2021; J. Zhang et al., 2020). Hence, it can be recommended that the optimum value of XG needs to be checked from the point of view of workability and stability of FC mixes.

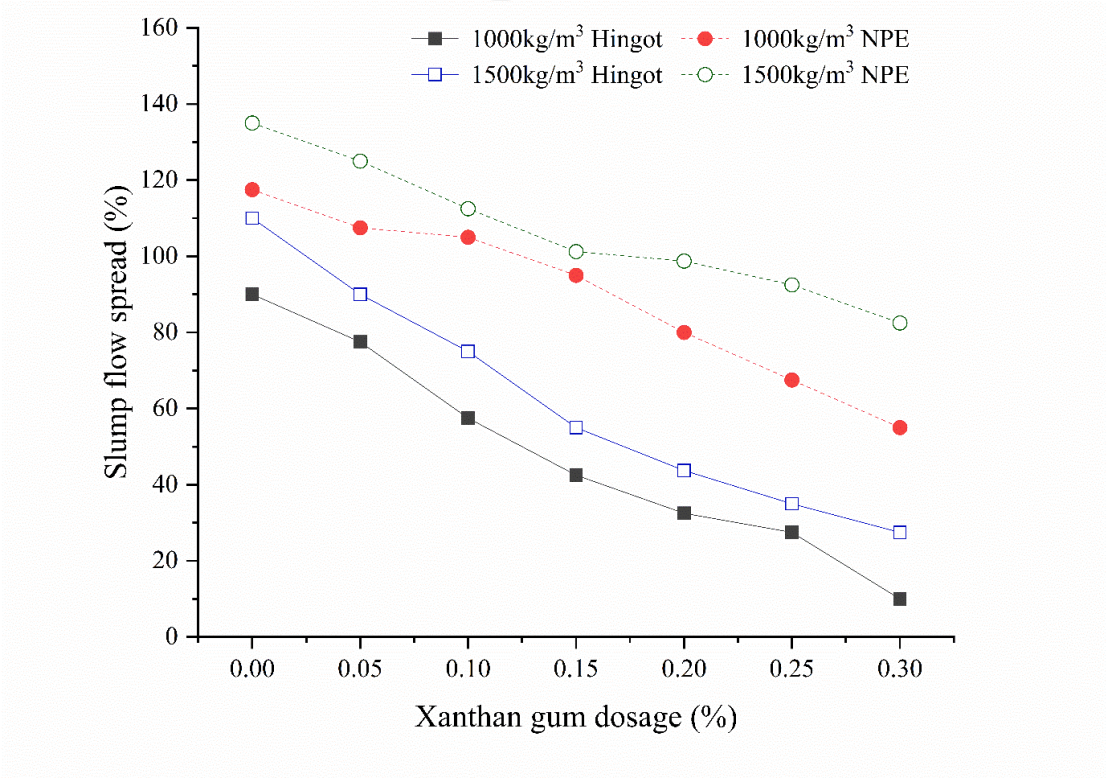

Figure 4-15: Variation of Slump flow spread % of FC with XG dosage

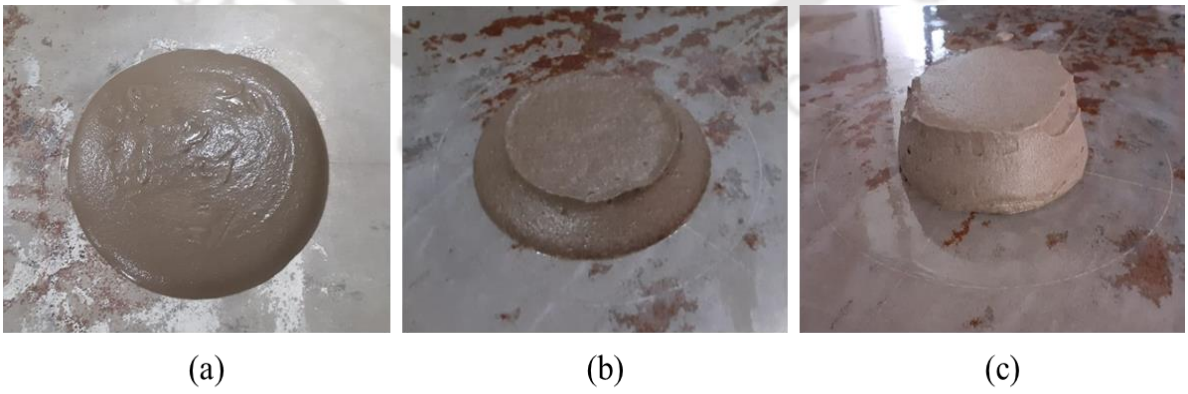

Figure 4-16: Slump flow for different dosages of XG (a) Slump flow of 10H (b) Slump flow of 10H+0.15XG (c) Slump flow of 10H+0.30XG

Figure 4.17 shows the variation of marsh cone flow time value for various FC mixes. The observations on flow time concurred with the trend of spread. As expected for the parameters investigated the greater spread flow values corresponds to smaller flow time. Increase in XG concentration up to 0.3% results in significant increase of 300% to 500% in flow time for Hingot based FC mixes. Particularly for XG dosage greater than 0.1%, significant increase in flow time is observed. However, in line with earlier discussions on spread, the corresponding increment in flow time for NPE based mixes ranges from 33% to 75% for different design densities studied. The flow time for FC of density 1000 kg/m^3 with Hingot+0.3XG dosage could not be determined and the non flowability of the above mix correlates well with the almost zero slump flow spread obtained in slump flow cone test as discussed above and can be noted in Figure 4.16.

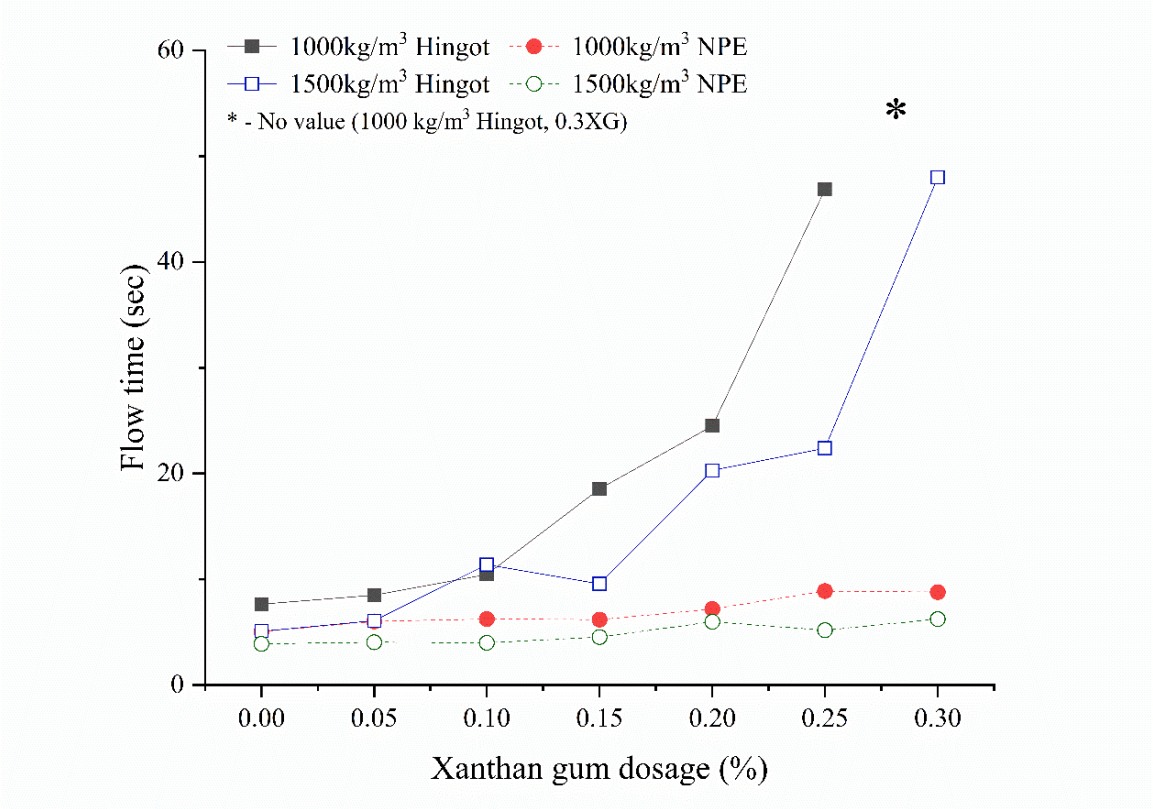

Figure 4-17: Influence of XG admixture dosage on marsh cone flow time of FC

Setting behaviour of FC

Figure 4.18 shows the typical representation of the good demouldable FC specimens with proper shape, sharp and intact edges along with specimens that are not ready for demoulding at a given particular time. The experimental analysis on the effect of XG on demoulding time of FC cubes indicates that the addition of XG increases the demoulding time. This can be ascribed to the retarding nature of XG (Qi et al., 2019). Further, from Figure 4.19 the comparative

analysis indicates that, Hingot based FC mixes shows higher demoulding time when compared to that of NPE. Hingot being saponin based surfactant shows the tendency of delayed setting with cement and concrete mixes and XG addition further intensifies the retarding effect (Siva et al., 2017). Also it should be noted that the lower density concrete mixes took longer time to set when compared to higher density concrete and this can be accounted for the higher foam content as well as its internal self-insulating property (Jones and McCarthy, 2006; Sritam Swapnadarshi et al., 2021). Based on the various studies on foam and surfactant, the desirable upper limit of XG is recommended as 0.15% in case of Hingot and 0.20% in case of NPE.

Figure 4-18: Images of demoulded specimen (a) Specimen with intact shape and edges (b) Specimen with distorted edges and shape

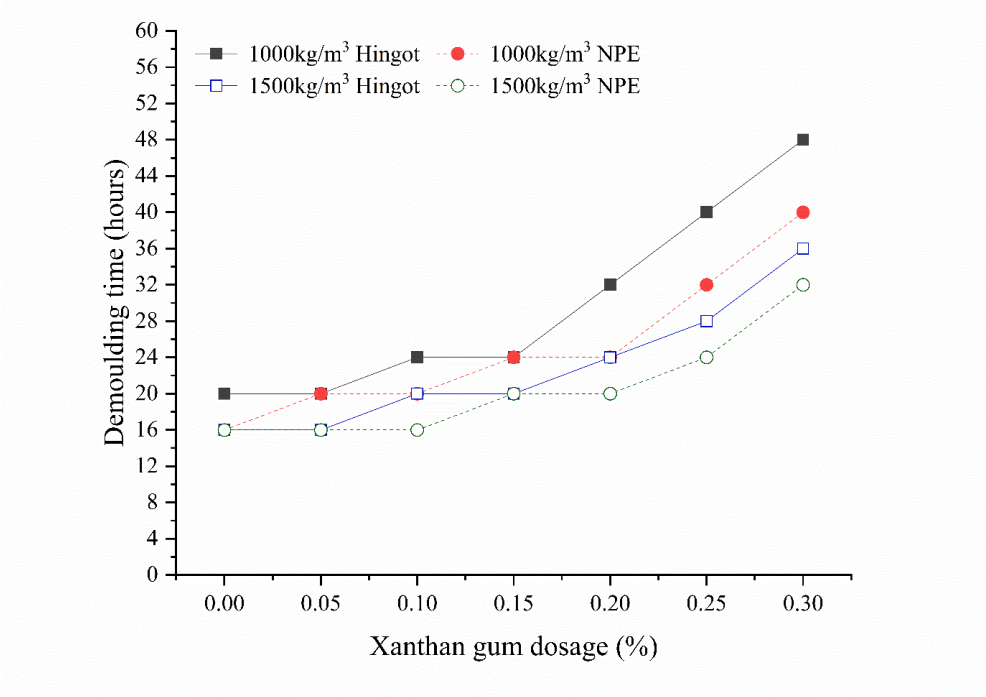

Figure 4-19: Variation of demoulding time of FC with XG dosage

Compressive strength and thermal conductivity of FC

Having studied the influence of XG on the consistency and setting behaviour of FC mixes, as a next step, studies on compressive strength and TC of FC mixes are carried out. Based on the earlier studies, upper limit of XG has been fixed as 0.15% and 0.20% for surfactants Hingot and NPE respectively for further studies. It is to be noted that the addition of XG beyond above mentioned limits is futile, as there is no significant improvement in foam stability at very high dosages. Furthermore, adoption of higher dosages of XG affects the consistency and demouldability of FC significantly. Considering the above concerns, further studies are carried out with the above mentioned limits of XG.

While addition of XG have shown a significant impact on lowering liquid drainage and foam collapse time, its influence on foam stability during the mechanical mixing process, pouring, and handling of FC samples is also noteworthy. Due to the fragility of the foam produced without addition of XG, some foam collapse is observed during mechanical mixing operation while preparing FC mix. In addition, gradual coarsening of the bubbles is also noted after pouring the samples into the moulds. However, the stabilised foams with XG are found to be relatively much stable throughout the process of preparation of concrete. This effect is more easily quantifiable; as additional quantity of foam is necessitated to achieve targeted densities for FC samples without XG, particularly in case of 1000 kg/m^3 NPE (w/o XG) FC mix. Also it is worth noting that even after incorporation of additional foam, settling of the mixes poured in moulds is observed particularly for 1000 kg/m^3 made with NPE (w/o XG) foam, thus leading to overall increase in demoulded density as well as oven dry density (Figure 20). The above finding highlights the importance of stabilized foams in FC preparation.

The results for 28day compressive strength of FC for densities 1000 kg/m^3 and 1500 kg/m^3 is represented in Figure 4.20. The strength results for mixes with density 1000 kg/m^3 ranged in between 1.2 MPa to 2.5 MPa while mixes with density 1500 kg/m^3 reported the strength between 4.6 MPa to 6.3MPa. These results are in line with the similar studies carried out by researchers where sand was incorporated as the basic filler material (Jones and McCarthy, 2005c; Lim et al., 2013; E. K. Nambiar and Ramamurthy, 2006; E. K. K. Nambiar and Ramamurthy, 2006b; Sahu and Gandhi, 2021b; Selija and Gandhi, 2022). It's important to note that ASTM standards typically provide guidelines and testing procedure to measure compressive strength (ASTM C869 and ASTM C796) and does not provide any recommendations with respect to average compressive strength values for various densities.

However, ASTM C869 which covers foaming agents specifically formulated for making preformed foam for use in the production of cellular concrete recommends a minimum strength requirement of 1.4 MPa for foamed cement paste with a density of 641 kg/m^3. The aforementioned strength was achieved by both Hingot (Khwairakpam et al., 2023b) as well as NPE (Sahu and Gandhi, 2021b) surfactant.

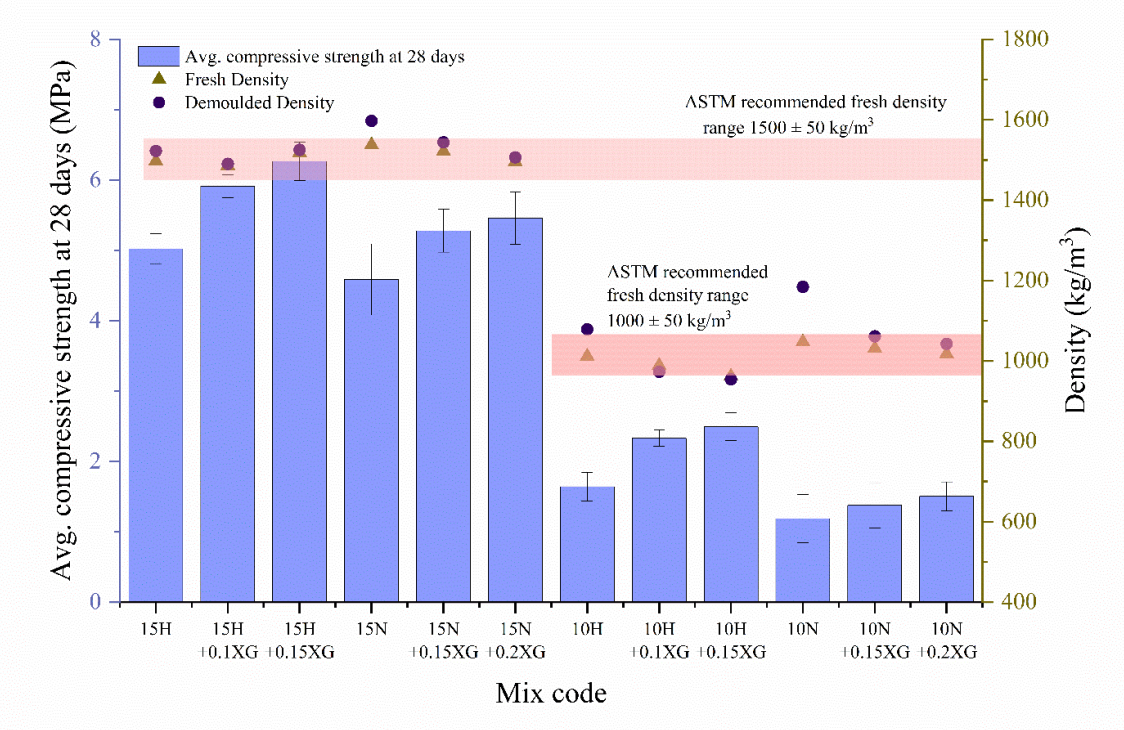

Figure 4-20: Influence of XG on the compressive strength of FC

Further, comparative analysis of compressive strength results for both the aforementioned densities indicate higher compressive strength for specimens prepared with natural saponin based Hingot surfactant. FC specimens of density 1000 kg/m^3 and 1500 kg/m^3 prepared with Hingot surfactant (w/o XG) exhibits 38% and 10% higher compressive strength respectively when compared to the similar density specimens prepared with NPE (w/o XG) as surfactant. The compressive strength of FC seems to be influenced by the smaller bubble size microstructure of Hingot foam. Also in case of NPE FC mix particularly for 1000 kg/m^3 density, foam collapse which occurred during mixing operation and subsequent additional foam requirement and poor bubble microstructure with larger bubble sizes could be one of the possible reasons for relatively lesser strength of NPE FC. The addition of XG as a foam enhancer is found to improve compressive strength of FC mixes prepared with both Hingot as well as NPE surfactant. Though it is worth noting that the improvement in properties of mixes casted with Hingot surfactant is better than NPE surfactant mixes. Detailed analysis of

compressive strength results for mixes with stabilized Hingot foam reveals that mere addition of 0.1% and 0.15% XG to Hingot surfactant results in increase in compressive strength by 42% and 51% respectively for mixes with density of 1000 kg/m^3. However, in case of 1500 kg/m^3 density the corresponding improvement in strength is recorded as 15% and 22% respectively. NPE foam stabilized with addition of 0.15% and 0.2% XG reports an increment in strength of 16% and 27% respectively for 1000 kg/m^3 density specimens whereas for 1500 kg/m^3 density specimen the improvement is reported as 15% and 19% respectively. Improvement in strength with addition of XG is more predominant for Hingot surfactant mixes and this can be attributed to the improved concrete pore structure and lower foam content (Hajimohammadi et al., 2018; Zhu et al., 2020). There are many studies reported in literature stating that concrete with uniform pore structure can be achieved with good quality of foam and this can subsequently result in improvement of the thermo-mechanical properties of FC (Ameer A Hilal et al., 2015; E P Kearsley and Wainwright, 2001; Nguyen et al., 2017; Sun et al., 2018). In line with the above literature, based on the limited studies carried on the pore structure of concrete as a part of present study, it is evident that uniform pore size distribution with reduced pore sizes can be achieved in FC mixes produced with XG modified foam (Figure 4.21).

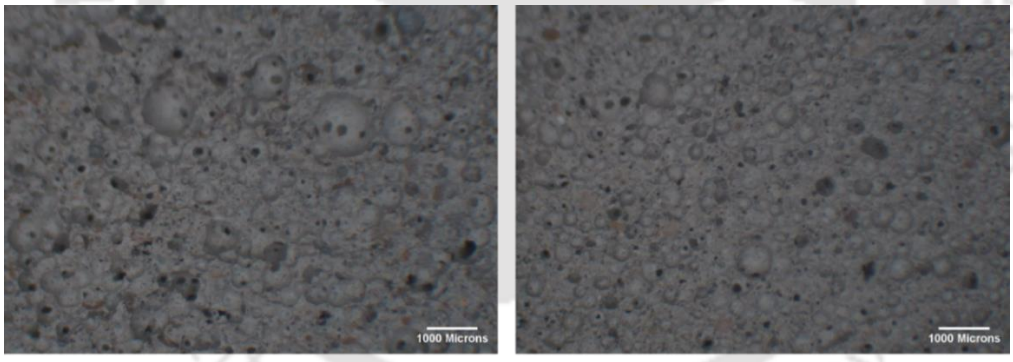

Figure 4-21: Cross section of FC sample (a) FC mix of 1000 kg/m^3 density with Hingot surfactant
(b) FC mix of 1000 kg/m^3 density with Hingot surfactant + 0.1% XG

Having discussed the results on compressive strength, as a next step, thermal behaviour of FC need to be analysed. Similar to that of strength, thermal properties of FC are also known to be very much dependent on pore morphology and structure (Wagh et al., 2021). In the present study, thermal behaviour is assessed based on TC which quantifies the effectiveness of a material as an insulator against heat loss (Zhang et al., 2022). For FC prepared with Hingot and NPE, Figure 4.22 depicts a linear relationship between the oven dry density and TC of the

material. As the oven dry density of FC is increased from 832 kg/m^3 to 1464 kg/m^3 the TC significantly increases from 0.315 W/mK to 0.735W/mK. The foregoing observations are consistent with previous studies that thermal resistance is indirectly proportional to the density of FC (Gökçe et al., 2019). On comparative analysis of FC prepared with pure Hingot and NPE surfactants (without XG addition) the specimens with Hingot surfactant tends to show lower TC than that of NPE. For instance, TC values of Hingot samples with target densities 1000 kg/m^3 and 1500 kg/m^3 are reported to be 22% and 10% lower than that of NPE samples respectively with similar density range. The stabilized samples of FC with XG reportedly shows reduction in TC of samples prepared with both the surfactants. Mere addition of 0.15% of XG lead to decrement of 13% and 17% in TC of Hingot FC and NPE FC respectively. The best thermal performance is reported for the FC samples prepared with Hingot surfactant and 0.1% dosage of XG as foam stabilizer. This can be ascribed to the better pore structure achieved with Hingot surfactant and it supports the fact reported in literature that natural foaming agent produces better pore structure with smaller isolated spherical air bubbles (D. K. Panesar, 2013). Further, addition of XG also contributes to improvement in foam pore structure through increase in lamellae thickness and reduction in bubble size which subsequently influenced the TC of concrete (Falliano et al., 2018; Gołaszewski et al., 2022; Hajimohammadi et al., 2018; D. K. Panesar, 2013; Zhu et al., 2020).

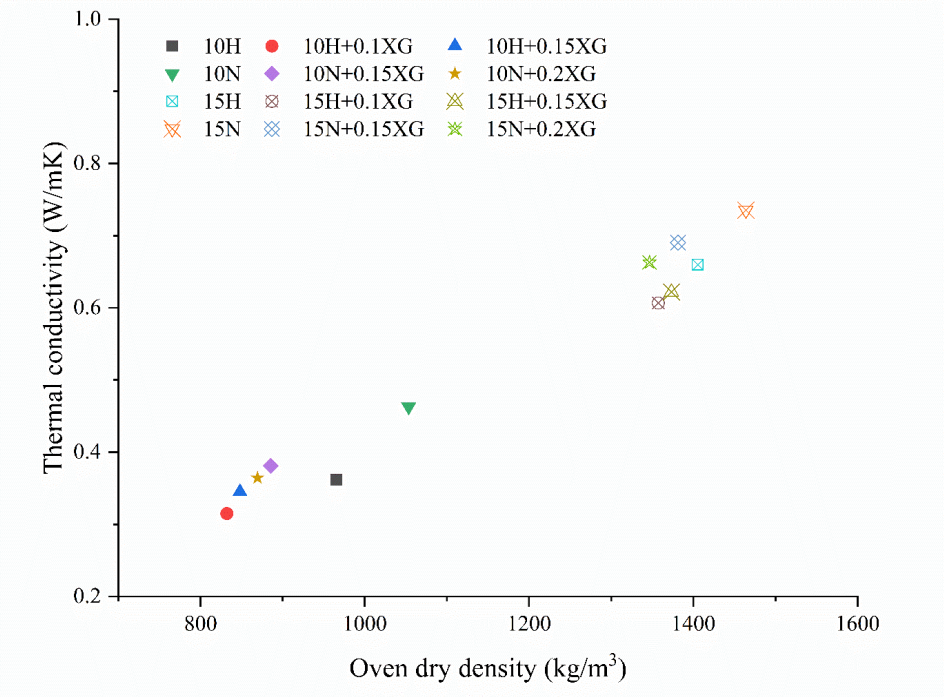

Figure 4-22: Correlation of Thermal conductivity of FC with density

4.4 Cost analysis

The cost analysis has been conducted for the combinations of HX0.10 and NPEX0.15 for producing a single batch (20 litres) as presented in Table 4.5. The pricing for Hingot, NPE, and XG is carried out in accordance with the vendor's quotation, which encompasses transportation costs. The rate offered by Assam Power Distribution Company Limited (APDCL) for commercial use is taken into account when determining electricity cost. Further, the water charges have been incorporated in accordance with the rates set by the Guwahati Municipal Corporation (GMC). The cost of cement and sand is ₹8.60/kg and ₹1.50/kg respectively. The cost analysis indicates that the production of Hingot surfactant is significantly more cost-effective than that of NPE surfactant. The cost of one litre of NPE surfactant is approximately nine times higher than that of Hingot surfactant. Therefore, it can be concluded that Hingot may serve as a cost-effective substitute for NPE surfactant. Further, using the aforementioned surfactant combinations, an approximate material cost estimate for FC with densities 1000 kg/m^3 and 1500 kg/m^3 is carried out. Production of one cubic meter of FC for densities 1000 kg/m^3 and 1500 kg/m^3 with NPE surfactant (i.e. 10N+0.15XG and 15N+0.15XG) is reported to be ₹5,267.90/m^3 ($64.23/m^3) and ₹5,585.00/m^3 ($68.09/m^3) respectively. Correspondingly the production cost of FC for densities 1000 kg/m^3 and 1500 kg/m^3 Hingot surfactant (i.e. 10H+0.10XG and 15H+0.10XG) came out to be ₹3,140.30/m^3 ($38.29/m^3) and ₹4,546.00/m^3 ($55.43/m^3) respectively. FC with Hingot surfactant is almost 40% and 19% cheaper than that of FC with NPE surfactant for densities 1000 kg/m^3 and 1500 kg/m^3 respectively. The higher density of NPE surfactant necessitates the use of a greater amount of foam to achieve the desired density of FC. Consequently, this higher foam density of NPE surfactant, coupled with its higher surfactant cost, results in a higher production cost for FC, making it significantly more expensive than FC produced with Hingot surfactant. Further, a more comprehensive analysis of FC in comparison to the commercially available standard clay brick and AAC block reveals that the clay brick, which has a density ranging from 1800 kg/m^3 to 2000 kg/m^3 and is priced between ₹6000 ($$73.10) and ₹8000 ($97.47), is comparatively more expensive than FC. The AAC blocks, which have a density ranging from 600 kg/m^3 to 800 kg/m^3 and are priced between ₹4000 ($48.75) and ₹5000 ($60.92), can be considered comparable to the FC made with Hingot surfactant.

Table 4-5: Detailed cost analysis of 20 litres of surfactant and stabilizer solution (HX0.10 and NPEX0.15)

Sl.No.	Item	Quantity Required for 20 litres	Rate (In ₹)	Amount (In ₹)	Total Cost
			Hingot Solution		
1.	Hingot Powder	1.2 kg	60/kg	72.00	₹ 136.58/20liter **(₹6.83/litre $ 0.083/litre)**
2.	Electricity	6.8125 kWh	6.50/kWh	44.28	
3.	Water	20 litres	15/kilolitre	0.30	
4.	Xanthan Gum	20 gm	1000/kg	20.00	
			NPE Solution		
1.	NPE	1.2 kg	1000/kg	1200.00	₹ 1231.23/20litre **(₹61.56/litre $ 0.75/litre)**
2.	Electricity	0.142 kWh	6.50/kWh	0.923	
3.	Water	20 Litres	15/kilolitre	0.30	
4.	Xanthan Gum	30 gm	1000/kg	30.00	

4.5 Summary

The study assessed the influence of XG on the characteristics of two surfactants, namely Hingot (Natural) and Nonylphenol ethoxylate (NPE) (Synthetic). A comprehensive investigation on the important surfactant and foam characteristics such as viscosity, surface tension, IFD, foam drainage, foam bubble microstructure was carried out. It is observed that, the introduction of Xanthan gum leads to a tenfold increase in viscosity for both Hingot and NPE surfactant solutions. This amplified viscosity significantly reduces bubble size and increases lamella thickness. Notably, the addition of XG does not cause a noticeable change in the surface tension of the surfactant solution. Besides enhancement in viscosity due to XG addition, the lower value of surface tension of Hingot surfactant also contributes to improvement in lamella drainage time and reduction of rate of bubble coalescence.

Further, the combination of these surfactants with XG was utilized to investigate the consistency, setting behaviour, compressive strength, and thermal conductivity of FC at two different densities: 1000 kg/m³ and 1500 kg/m³. The addition of XG resulted in reduction of spread for FC mixes and lead to higher demoulding time due to retarding nature of XG. However, on positive side, addition of of XG is found to result in substantial increase of

compressive strength of both Hingot FC and NPE FC respectively when similar densities are compared indicating that foam bubble microstructure has greater impact on strength.

The combination of Hingot+0.1% XG was found to be most suitable option outperforming NPE+XG combination in most of the properties evaluated. In addition, it was also found that, the cost of one litre of NPE+XG is approximately nine times higher than that of Hingot+XG surfactant. Therefore, it can be concluded that Hingot may serve as a cost-effective surfactant when compared to NPE.

CHAPTER 5 INFLUENCE OF VARIOUS ADMIXTURES ON FOAM CONCRETE BEHAVIOUR

5.1 General

Having identified the best combination of surfactant and foam stabilizer (Hingot+0.1XG), as a next step, studies on influence of various admixtures (fly ash, silica fume, polypropylene fiber) on the FC behavior is carried out in this chapter. To enhance foam concrete (FC) properties such as strength, durability, and shrinkage behaviour while maintaining cost-effectiveness, researchers have focused on optimizing the FC mixture by introducing various admixtures. However, literature suggests that the inclusion of diverse admixtures may lead to stability issues, impacting FC properties. While there is ample literature on using fly ash (FA) as a substitute for binders in FC, there is a scarcity of research on utilizing FA as a replacement for sand. Furthermore, studies exploring FC with the incorporation of polypropylene (PP) fibres and silica fume (SF) are relatively limited. Hence, for this study, class F FA is used as replacement for sand at different levels viz., 0%, 50% and 100%, SF is being used as cement replacement levels viz. 0%, 10% and 20%. PP fiber are added at two different dosages viz. 0.2% and 0.4% by total volume. Mixes with two different densities 600 kg/m^3 and 1000 kg/m^3 are prepared for the study. The aforementioned admixtures are incorporated in mixes as single admixture, combination of two (i.e. binary) admixtures and combination of all three (i,e. ternary) admixtures. The influence of admixtures on the fresh state characteristics is assessed by evaluating its stability through measurement of density ratio (both in fresh and demoulded states). Further flow table test is used to evaluate the spread % of the FC with different admixtures combination is carried out. Furthermore, the effect of the admixtures on the hardened state properties, viz. compressive strength, splitting tensile strength and thermal properties are evaluated. Finally, an optimized mix is selected each for both the densities considering its performance across all the parameters evaluated and assigning the appropriate weightages to it.

5.2 Properties of Materials

The basic components of FC consist of binder, fine aggregate, foaming agent, and water to produce a lightweight cellular concrete structure. Based on the initial part of the work carried

out, which primarily focused on the stabilization of the hingot foaming agent with XG as stabilizer, desirable surfactant-stabilizer combination is derived as 6% hingot surfactant and 0.1% dosage of XG and this combination will be adopted throughout the study. For the current experimental study, supplementary components or admixtures, such as FA, PP fibers, SF and plasticizers are added to achieve desired properties of FC. The effects of these materials are summarized in the literature review.

For this experimental study OPC 43 grade cement is used as binder in all the mix samples. Chemical composition and physical properties of cement are given in Table 5.2, Table 5.1 represents the source and the basic properties of various materials used in the present study. Figure 5.1 represents the particle size distribution of different materials used. Table 5.2 presents the chemical composition and physical properties of the materials used. Quality of water also plays important role in FC mixes. Hence, clean tap water is used for mix preparation and curing. In the present study, the particle size of aggregate has greater impact on the stability of the FC. Hence, for this experiment, fine sand passing through 300-micron sieve is used. For this experiment, class F FA is used as replacement for sand at different levels viz., 0%, 50% and 100%. SF tends to reduce the setting time of the FC and subsequently provide better microstructure and enhanced strength and hence its addition is necessary particularly for the FC with low density. For this experiment, admixture SF purchased from ELKEM is being used as cement replacement at following replacement levels viz., 0%, 10% and 20%. PP fiber used for this study is Alkali resistant synthetic PP fibre conforming to ASTM C1116 with specific gravity - 0.91, aspect ratio – 545 and length- 12 mm, tensile strength- 400–500 MPa and surface area- 250 m^2/kg. For the current study PCE based super-plasticizer from FOSROC constructive Solutions is used. Further, to enhance the stability of low density FC mixes, addition of Viscosity Modifying Agent (VMA) is essential. For the present study, Hydroxy Propyl Methyl Cellulose (HPMC) is used as VMA and is procured from Foroly Commercio Pvt. Ltd. Further as per the technique described in the research paper (Khwairakpam and Ranjani Gandhi, 2020; Selija and Gandhi, 2022) and as discussed in the previous section *4.2.1*, the surfactant extraction from hingot fruit and the foaming operation is carried out accordingly.

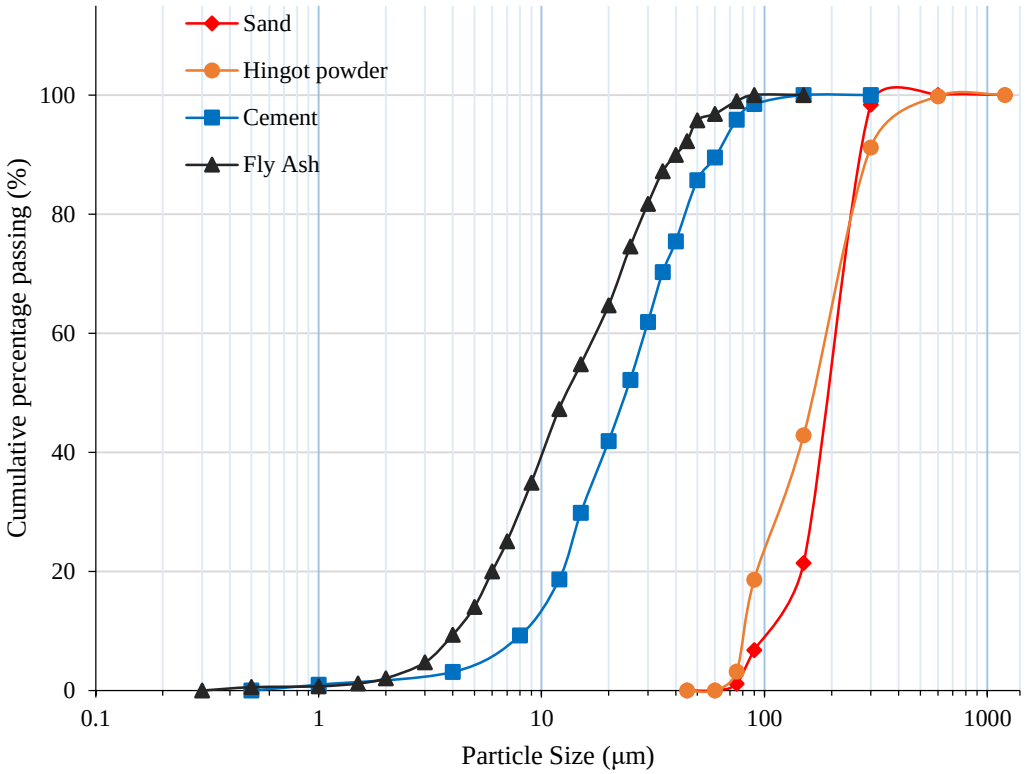

Figure 5-1: Particle size distribution of cement, sand, fly ash and hingot powder

Table 5-1: Properties of the material used for the experimental study

MATERIAL	REMARK	SOURCE	Specific Gravity	Application
Cement	OPC 43 conforming to IS 8112 – 2013, Bulk Density = 1610 kg/m^3	Dalmia cement plant Morigaon, Baghjhap Assam	3.15	Binder/cementing ingredient
Sand	IS 383-2016, Pulverized sand finer than 300 microns, Bulk density = 1628 kg/m^3	Brahmaputra river sand. Dudhnoi, Goalpara Assam	2.65	Aggregate
Fly ash	Class F passing through 75 µm sieve conforming to ASTM C 618, Bulk Density = 995 kg/m^3	NTPC Bongaigaon, Kokrajhar Assam	2.16	Mineral Admixture
Silica Fume	Conforming to IS 15388:2003, Bulk Density 500 kg/m^3	AKJ engineers PVT. Ltd Behrabari, Guwahati.	2.17	Mineral Admixture
Polypropylene Fibres	Polypropylene fibres with length 12 mm and 22 µm diameter, synthetic, monofilament, alkali resistant with tensile strength of 400-500 MPa	Jogani Reinforcement, Mumbai.	0.91	Admixture
Hingot	Desert fruit with extractable saponin	Madhya Pradesh		Surfactant
Water	-	From IITG treatment plant	1.0	-
Xanthan gum	Naturally occurring microbial exopolysaccharide, produced by fermentation of Xanthomonas campestris	From Loba chemicals	-	Foam Stabilizer
Hydroxy Propyl methyl Cellulose HPMC	Model : HS 1218, PH -7, Viscosity 160000 Mpa.S	Foroly Commercio Pvt. Ltd.	0.37-0.42	Viscosity Modifying agent (VMA)
Super plasticizer (SP)	Model: Fosroc Auramix 300, pH > 6.5, conforming to ASTM C494 and IS 9103-2007	Fosroc constructive solutions, Guwahati	1.085	PCE based Super plasticizer

Table 5-2: Chemical composition and physical properties of OPC cement, fly ash and silica fume

Chemical Composition	Cement (%)	Fly ash (%)	Silica Fume (%)	Physical properties	Cement	Fly ash	Silica fume
CaO	64.63	1.59	0.32	Specific gravity	3.14	2.16	2.17
SiO_2	20.19	55.60	93.4	Specific surface area	288 m^2/kg	364 m^2/kg	20,150 m^2/kg
Al_2O_3	5.02	29.80	0.63	28 days compressive	50	-	-
Fe_2O_3	1.45	5.91	0.60	strength	Mpa		
MgO	3.2	1.08	0.82	Initial Setting time	110	-	-
SO_3	2.22	0.45	0.18		min		
K_2O	0.5	1.94	0.76	Final Setting time	220	-	-
Na_2O	0.28	0.23	0.38		min		
LOI	2.51	0.47	1.3				

5.3 Mix Proportioning

In this study performance of FC mixes produced by variation of FA content, PP fibers, and SF is compared with base mixes (FC without any admixture), for two different design densities (600 kg/m^3 and 1000 kg/m^3). Sand is replaced with FA at two different levels namely 50% and 100%, while SF is used as a partial replacement of binder i.e. cement at two different variations of 10% and 20%. PP fibers are added by percentage of volume at two different dosages of 0.2% and 0.4%. As presented in Table 5.3 to Table 5.6, for each density, a total of twenty-seven mix samples of FC (including sample of base mix) are made for studying the fresh and mechanical properties. These mix samples are further divided into three different levels. Level one replacement mixes are the single admixture replacement mixes where effect of incorporation of only one admixture at various proportions is studied. Level 2 mixes are binary mixes where synergistic effect of incorporation of combination of two admixtures at various percentages is studied. Level three mixes include ternary mixes where combination of three different admixtures at varying proportion is studied for various fresh and mechanical properties of FC. In the mix code, alphabet 'M' and 'L' signifies the densities 1000 kg/m^3 and 600 kg/m^3 respectively while 'B' signifies the base mix for the aforementioned densities of FC. The alphabets 'F', 'S' and 'P' signify FA substitution, SF substitution and addition of PP fiber in the mix codes, respectively.

The proportioning of the mixes is done as per the procedure given in ASTM C796-19, (2019), which is further modified to include the additional component of sand, FA and SF. The mix

proportioning method is discussed in detail in the previous section 4.3.1 of chapter 4. Table 5.4 and Table 5.6 provides the mix proportions details for densities 600kg/m^3 and 1000 kg/m^3 of FC. For this experiment, the *w/s* is maintained at 0.35 for 600 kg/m^3 design density, and, 0.3 for 1000 kg/m^3 design density. This *w/s* ratio has been arrived based on literature (Sahu and Gandhi, 2021a) and preliminary trials to achieve design density. Binder to filler ratio (*b/f*) has been maintained at 1:2 by weight for all mixes with design density 1000 kg/m^3, while for density 600 kg/m^3 the *b/f* is adopted as 1:1. The *b/f* is finalised based upon the preliminary studies while taking into consideration the economic perspective and the stability of FC. In the preliminary studies it is found that FC with *b/f* of 1:2 results in unstable FC mix particularly for lower density i.e. 600 kg/m^3. Hence *b/f* of 1:1 is adopted for lower density i.e. 600 kg/m^3 in the present study. Replacement of sand with FA and cement with SF is done on weight basis and consequentially the adjustment in volumes for calculated slurry components and air volume is done. PP fibers are added by percentage of total volume.

Foam is produced by aerating produced surfactant solution through a pressurizing unit at a pressure of 550 kPa. The IFD of hingot surfactant is found to be 45±2 kg/m^3. Superplasticizer (SP) content expressed as percentage of binder content is varied for different mixes in order to maintain a minimum slump flow in range of 150 mm ± 10mm. The above range of desired consistency has been fixed considering the stability of FC in preliminary studies and as reported by various researchers (Nambiar and Ramamurthy, 2009). The mixing process begins with a homogenous base mix of binder and filler slurry prepared in a horizontal shaft paddle type mixer machine. The mixing sequence for both densities are similar for mixes with similar material composition. For mixes without fibre, the mixing sequence constitutes of first combining cement with water in mixer. Then depending on composition, materials are added based on particle size, i.e. smallest (SF) to highest (fine sand), in the mixer and are mixed for 3 minutes until a homogeneous slurry mix is achieved. For the mixes with fibre reinforcement, the fibres are mixed in water before pouring in the mixer such that they are evenly suspended in water without settling at bottom of water container. This is done to achieve homogeneity in mix since fibres have behaviour of clumping while mixing with solid components. Mixing with liquid beforehand separates the individual fibres and encourages homogeneity of base mix. To the slurry mix thus prepared, the necessary volume of preformed foam is introduced and thereafter mixed for at least 2 or 3 minutes in order to get uniform distribution of mix. The entire mixing procedure is continued for at least 5 minutes, or until the foam is uniformly incorporated into the slurry.

Table 5-3: Mix constituents and mix code preferences of FC with target fresh density 1000 kg/m^3

Mix Type	Density: 1000 kg/m^3			
Base Mix (FC without admixtures)	MB0			
	Level 1 Replacement mixes			
FC with admixture Fly ash	MF1 (50% FA)		MF2 (100% FA)	
FC with admixture Silica Fume	MS1 (10% SF)		MS2 (20% SF)	
FC with admixture PP Fibre	MPP1 (0.2% PP)		MPP2 (0.4% PP)	
	Level 2 Replacement mixes			
FC with admixture Fly ash and Silica Fume	MF1S1 (50% FA+ 10% SF)	MF2S1 (100% FA+ 10% SF)	MF1S2 (50% FA+ 20% SF)	MF2S2 (100% FA+ 20% SF)
FC with admixture Fly ash and PP Fibre	MF1PP1 (50% FA+ 0.2% PP)	MF2PP1 (100% FA+ 0.2% PP)	MF1PP2 (50% FA+ 0.4% PP)	MF2PP2 (100% FA+ 0.4% PP)
FC with admixture Silica Fume and PP Fibre	MS1PP1 (10% SF+ 0.2% PP)	MS2PP1 (20% SF+ 0.2% PP)	MS1PP2 (10% SF+ 0.4% PP)	MS2PP2 (20% SF+ 0.4% PP)
	Level 3 Replacement mixes			
FC with admixture Fly ash, Silica Fume and PP Fibre	MF1S1PP1 (50% FA+ 10% SF + 0.2% PP)	MF2S1PP1 (100% FA+ 10% SF + 0.2% PP)	MF1S2PP1 (50% FA+ 20% SF + 0.2% PP)	MF2S2PP1 (100% FA+ 20% SF + 0.2% PP)
	MF1S1PP2 (50% FA+ 10% SF + 0.4% PP)	MF2S1PP2 (100% FA+ 10% SF + 0.4% PP)	MF1S2PP2 (50% FA+ 20% SF + 0.4% PP)	MF2S2PP2 (100% FA+ 20% SF + 0.4% PP)

Table 5-4: Mix design proportions (constituents) per 1 m3 of FC sample with target fresh density 1000 kg/m3

Mix code	Cement (kg/m^3)	Sand (kg/m^3)	Fly-ash (kg/m^3)	Silica fume (kg/m^3)	PP fibre (kg/m^3)	Water (kg/m^3)	SP Dose (kg/m^3)	Foam (kg/m^3)	Foam volume (%)
MB0	256.410	512.821	0.000	0.000	0.000	206.934	0.000	23.835	51.815
MF1	256.410	256.410	256.410	0.000	0.000	207.993	0.769	22.776	49.514
MF2	256.410	0.000	512.821	0.000	0.000	209.051	1.538	21.718	47.213
MS1	230.769	512.821	0.000	25.641	0.000	207.146	0.513	23.623	51.355
MS2	205.128	512.821	0.000	51.282	0.000	207.358	1.026	23.411	50.895
MPP1	255.897	511.795	0.000	0.000	1.820	206.989	0.512	23.780	51.695
MPP2	255.385	510.769	0.000	0.000	3.640	207.044	2.043	23.725	51.576
MF1S1	230.769	256.410	256.410	25.641	0.000	208.204	1.026	22.565	49.054
MF1S2	205.128	256.410	256.410	51.282	0.000	208.416	2.051	22.353	48.594
MF2S1	230.769	0.000	512.821	25.641	0.000	209.263	2.564	21.506	46.753
MF2S2	205.128	0.000	512.821	51.282	0.000	209.475	3.590	21.295	46.293
MF1PP1	255.897	255.897	255.897	0.000	1.820	208.046	2.047	22.724	49.399
MF1PP2	255.385	255.385	255.385	0.000	3.640	208.099	2.554	22.671	49.284
MF2PP1	255.897	0.000	511.795	0.000	1.820	209.102	1.791	21.667	47.103
MF2PP2	255.385	0.000	510.769	0.000	3.640	209.153	4.086	21.617	46.992
MS1PP1	230.308	511.795	0.000	25.590	1.820	207.201	1.535	23.569	51.236
MS1PP2	229.846	510.769	0.000	25.538	3.640	207.255	2.554	23.514	51.117
MS2PP1	204.718	511.795	0.000	51.179	1.820	207.412	2.047	23.357	50.777
MS2PP2	204.308	510.769	0.000	51.077	3.640	207.466	3.575	23.303	50.659
MF1S1PP1	230.308	255.897	255.897	25.590	1.820	208.046	2.047	22.724	49.399
MF1S1PP2	229.846	255.385	255.385	25.538	3.640	208.099	3.065	22.671	49.284
MF1S2PP1	204.718	255.897	255.897	51.179	1.820	208.468	3.071	22.301	48.481
MF1S2PP2	204.308	255.385	255.385	51.077	3.640	208.520	3.575	22.249	48.367
MF2S1PP1	230.308	0.000	511.795	25.590	1.820	209.102	4.094	21.667	47.103
MF2S1PP2	229.846	0.000	510.769	25.538	3.640	209.153	4.597	21.617	46.992
MF2S2PP1	204.718	0.000	511.795	51.179	1.820	209.524	4.606	21.245	46.184
MF2S2PP2	204.308	0.000	510.769	51.077	3.640	209.574	5.618	21.195	46.076

Table 5-5: Mix constituents and mix code preferences of FC with target fresh density 600 kg/m^3

Mix Type	Density: 600 kg/m^3			
Base Mix (FC without admixtures)	LB0			
	Level 1 Replacement mixes			
FC with admixture Fly ash	LF1 (50% FA)		LF2 (100% FA)	
FC with admixture Silica Fume	LS1 (10% SF)		LS2 (20% SF)	
FC with admixture PP Fibre	LPP1 (0.2% PP)		LPP2 (0.4% PP)	
	Level 2 Replacement mixes			
FC with admixture Flyash and Silica Fume	LF1S1 (50% FA+ 10% SF)	LF2S1 (100% FA+ 10% SF)	LF1S2 (50% FA+ 20% SF)	LF2S2 (100% FA+ 20% SF)
FC with admixture Flyash and PP Fibre	LF1PP1 (50% FA+ 0.2% PP)	LF2PP1 (100% FA+ 0.2% PP)	LF1PP2 (50% FA+ 0.4% PP)	LF2PP2 (100% FA+ 0.4% PP)
FC with admixture Silica Fume and PP Fibre	LS1PP1 (10% SF+ 0.2% PP)	LS2PP1 (20% SF+ 0.2% PP)	LS1PP2 (10% SF+ 0.4% PP)	LS2PP2 (20% SF+ 0.4% PP)
	Level 3 Replacement mixes			
FC with admixture Flyash, Silica Fume and PP Fibre	LF1S1PP1 (50% FA+ 10% SF + 0.2% PP)	LF2S1PP1 (100% FA+ 10% SF + 0.2% PP)	LF1S2PP1 (50% FA+ 20% SF + 0.2% PP)	LF2S2PP1 (100% FA+ 20% SF + 0.2% PP)
	LF1S1PP2 (50% FA+ 10% SF + 0.4% PP)	LF2S1PP2 (100% FA+ 10% SF + 0.4% PP)	LF1S2PP2 (50% FA+ 20% SF + 0.4% PP)	LF2S2PP2 (100% FA+ 20% SF + 0.4% PP)

Table 5-6: Mix design proportions (constituents) per 1 m3 of FC sample with target fresh density 600 kg/m3

Mix code	Cement (kg/m^3)	Sand (kg/m^3)	Fly-ash (kg/m^3)	Silica fume (kg/m^3)	PP fibre (kg/m^3)	Water (kg/m^3)	SP Dose (kg/m^3)	Foam (kg/m^3)	Foam volume (%)
LB0	222.222	222.222	0.000	0.000	0.000	122.283	0.000	33.272	72.331
LF1	222.222	111.111	111.111	0.000	0.000	122.742	0.889	32.814	71.334
LF2	222.222	0.000	222.222	0.000	0.000	123.200	1.778	32.355	70.337
LS1	200.000	222.222	0.000	22.222	0.000	122.375	0.444	33.181	72.132
LS2	177.778	222.222	0.000	44.444	0.000	122.467	0.889	33.089	71.932
LPP1	221.778	221.778	0.000	0.000	1.820	122.315	0.887	33.240	72.261
LPP2	221.333	221.333	0.000	0.000	3.640	122.348	1.328	33.208	72.191
LF1S1	200.000	111.111	111.111	22.222	0.000	122.834	1.333	32.722	71.135
LF1S2	177.778	111.111	111.111	44.444	0.000	122.925	1.778	32.630	70.935
LF2S1	200.000	0.000	222.222	22.222	0.000	123.292	3.111	32.263	70.138
LF2S2	177.778	0.000	222.222	44.444	0.000	123.384	3.556	32.172	69.938
LF1PP1	221.778	110.889	110.889	0.000	1.820	122.773	2.218	32.782	71.266
LF1PP2	221.333	110.667	110.667	0.000	3.640	122.804	3.099	32.751	71.198
LF2PP1	221.778	0.000	221.778	0.000	1.820	123.231	2.661	32.325	70.271
LF2PP2	221.333	0.000	221.333	0.000	3.640	123.261	4.427	32.294	70.205
LS1PP1	199.600	221.778	0.000	22.178	1.820	122.407	1.331	33.149	72.062
LS1PP2	199.200	221.333	0.000	22.133	3.640	122.439	2.656	33.117	71.993
LS2PP1	177.422	221.778	0.000	44.356	1.820	122.498	1.774	33.057	71.863
LS2PP2	177.067	221.333	0.000	44.267	3.640	122.530	3.099	33.025	71.794
LF1S1PP1	199.600	110.889	110.889	22.178	1.820	122.773	1.774	32.782	71.266
LF1S1PP2	199.200	110.667	110.667	22.133	3.640	122.804	3.541	32.751	71.198
LF1S2PP1	199.600	221.778	0.000	22.178	1.820	122.956	2.218	32.599	70.868
LF1S2PP2	199.200	221.333	0.000	22.133	3.640	122.987	3.984	32.568	70.801
LF2S1PP1	199.600	0.000	221.778	22.178	1.820	123.231	3.548	32.325	70.271
LF2S1PP2	199.200	0.000	221.333	22.133	3.640	123.261	4.427	32.294	70.205
LF2S2PP1	177.422	0.000	221.778	44.356	1.820	123.414	4.436	32.142	69.873
LF2S2PP2	177.067	0.000	221.333	44.267	3.640	123.444	5.312	32.112	69.808

5.4 Test Methodology

5.4.1 Fresh state properties

Under fresh properties, the plastic or fresh density is calculated by weighing the prepared FC mix in a standard container, as shown in Figure 5.2 (b).

(a) (b)

Figure 5-2: Measurement of fresh density (a) collection of pre-formed concrete mix in standard container, (b) weigh measurement of the container

The density ratio is then calculated by comparing measured fresh density with the target density. The closer the density ratio to one, the more stable is the mix. A tolerance on plastic density was set at ±50 kg/m^3 of the target design density, as per ASTM C 869-91. Other than density ratio for determining of consistency, spreadability is measured using flow table. In accordance to ASTM C1437, the flow table test or flow cone test is adopted to determine spreadability of fresh concrete. Spreadability is measured with a ASTM standard flow cone as presented in Figure 5.3. The cone is filled with FC soon after mixing, and is lifted and the average flow of concrete is measured without any shocking motion of the flow table as it would affect the entrained air bubbles. The spread of concrete is measured at four locations for each composition and the average spread flow is expressed as percentage of base diameter of standard cone.

Figure 5-3: Flow table test

5.4.2 Test methods for measurement of hardened state properties

The mixes passing tolerance limit of fresh density (i.e. at ±50 kg/m^3 of the target design density, as per ASTM C 869-91) are then collected and poured into moulds. Specimens of different mix composition with varying density and different replacement levels of admixtures are casted by adopting the mix proportion presented in Table 5.3 to Table 5.6. Specimens are demolded after 24 hours and then subjected to water curing till 3 days prior to testing age. For the remaining 3 days till the testing age, specimens shall be subjected to air curing. For measurement of mechanical properties, standard compression testing machine (Figure 5.4) is used. Details of these tests are further explained in the following sections:

Mechanical and water permeation characteristics

To study compressive strength, twelve cubes (for each mix type) of size 50 mm are casted. The specimens are then subjected to water curing till 3 days prior to testing age. For the remaining 3 days till the testing age, specimens shall be subjected to air curing. The compressive strength tests are carried out in accordance with ASTM C 796 at various ages of specimens viz., 14 days, 28 days and 90 days.

Figure 5-4: Compressive strength testing machine with a maximum capacity of 50KN

For determining the split tensile strength, the specimens are made for all mix types and cured as per ASTM standards (ASTM C495/C495M-12, 2019; ASTM C796-19, 2019). Cylindrical specimen of size 100 mm diameter × 200 mm height are made, four for each mix type, and tested at 28 day and 90 day. The average split tensile strength is then calculated based on the result of 4 specimens casted for each FC mix.

Water absorption is defined as the amount of water absorbed by a material and is calculated as the ratio of the weight of water absorbed to the weight of the dry material. To study the water absorption, six cubes of size 50 mm are cast and moist cured for 28 days. Water absorption (% by weight) is measured based on the increase in weight of oven-dried specimens (to a constant mass) after immersion in water for 24h as per IS 1124-1974.

Thermal Properties

Thermal properties are determined using transient plane source (TPS) method based C Therm-Technologies Thermal Conductivity (TC) Kit, in compliance with ISO 22007 part2-2015 (ISO 22007-2, 2008). As per the equipment manual, the minimum sample size should be 10 mm thick and 30 mm diameter/edge. For thermal conductivity test, six number of cubical specimens of size 50 mm are sliced half and then tested by sandwiching the flexible 13 mm FLEX TPS-based sensor in between two samples as represented in Figure 5.5. An electric current is passed through the sensor's spiral heating element, heating the specimen samples. As the temperature changes, the resistance of the spiral also changes, and the resulting voltage drop is measured. By measuring the current and voltage drop through the sensor over a period of time, the thermal properties of the specimen is calculated. In order to ensure good contact between the TPS element and the sample surface, all samples surfaces were polished flat and parallel, and cleaned with compressed air to minimize the influence of contact resistance. Also additional suitable weight is placed on top of the stack to ensure good contact between sample and sensor. Since, moisture content of the sample has an important impact on the measured thermal properties therefore before testing, all specimens were kept in a hot air oven at 60 °C until they attained constant weight. Properties like thermal conductivity (W/m*k), thermal diffusivity (mm^2/s) and specific heat (MJ/m^3K) is assessed for various FC mixes.

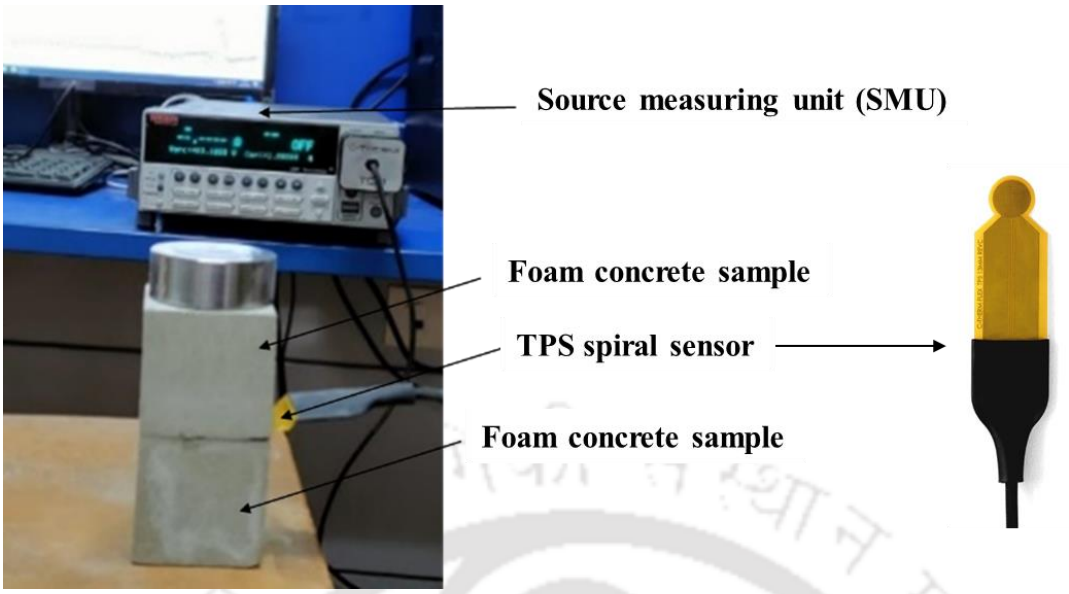

Figure 5-5: Thermal conductivity test setup

5.4.3 Microstructure analysis

XRD Analysis

X-ray diffraction (XRD) technique is used to investigate the hydration products by recording the XRD patterns in Rigaku high power X-ray diffractometer (model - Micromax-007HF) with Cu Kα radiation (λ = 1.54184 Å) operating at 50 kV and 100 mA. The samples are obtained by crushing the concrete specimens and then the powder is sieved through 75 μm' sieve. The concrete powder sample is scanned from 5° to 60° (2θ) at scan speed of 5° per minute. The mineral phases of the samples are analyzed through Xpert High Score Plus software (Version 3.0) and the peak intensities at different angles are compared with ICDD (International Centre for Diffraction Data) database. For better understanding of the concrete microstructure, Energy Dispersive Spectroscopy (EDS) technique is also used for elemental analysis. The process is carried out according to ASTM C1365.

FESEM Analysis

Field Emission Scanning Electron Microscopy (FE-SEM) is an advanced technology used to capture the microstructure image of the materials. FE-SEM is typically performed in a high vacuum because gas molecules tend to disturb the electron beam and the emitted secondary and backscattered electrons is used for imaging. A field-emission cathode in the electron gun of a scanning electron microscope provides narrow probing beams at low and high electron energy, resulting in improved spatial resolution and minimized sample charging and damage. In order to characterize the specimens in this study, Zeiss Crossbeam 340 was used to capture the

microstructure image. The specimens (except powder) were cut into smaller sizes of about 5×5×5 mm and coated using aurum prior to the morphological observation. In addition to FE-SEM, energy-dispersive X-ray (EDX) was conducted on the same specimens for further analysis. EDX is an X-ray technique used to identify the elemental composition of materials. These systems are attachments to electron microscopy instruments where the imaging capability of the microscope identifies the specimens of interest. The process is carried out according to ASTM C 1723.

5.5 Results on fresh state properties

5.5.1 Density ratio

As FC mix designs are solely based on target density required, the observations of density help in determining the stability of mixes based on the density ratio. Many authors in preliminary studies have shown that design density is achieved only at a particular consistency of the base mix (E. K. K. Nambiar and Ramamurthy, 2006b). Consistency values either lower (mixture is too stiff causing the bubble to break) or higher (slurry becomes too thin to hold the bubbles resulting in segregation) than the appropriate value leads to an increase in density. Thus the "stability of FC", is the state of the mix at which the density ratio (ratio of measured fresh density to target fresh density) is closer to unity (Kunhanandan Nambiar and Ramamurthy, 2008). Also, as per ASTM C 869-91, the permissible range for deviation in actual density of fresh mix is limited to ±50 kg/m^3 of the target density.

Table 5.7 and Table 5.8 shows the test results related to the fresh and demoulded density and its ratio with respect to target density for various FC mixes as achieved in this study. For all FC mixes, the density ratios for both measured fresh and demoulded density with respect to target densities are expected to be closer to 1. The allowable range of density ratios (both fresh and demoulded) for mixes with target density 1000 kg/m^3 is 0.95 to 1.05. Similarly, the allowable range of density ratios (both fresh and demoulded) for mixes with target density 600 kg/m^3 comes out to be between 0.916 to 1.083. Almost all FC mixes with target density 1000 kg/m^3 tends to show both measured fresh and demoulded density ratio close to 1. However, in case of FC mixes with 600 kg/m^3 a notable variation in density ratio is reported, particularly for demoulded density ratio of mixes LB0, LF1, LF2 and LS1. The aforementioned mixes showed higher demoulded density ratio in the range of 1.10 to 1.19 (662 kg/m^3 to 713 kg/m^3). This may be assigned to the fact that mixes with very low density have higher foam volume which in turn leads to breakage of foam and subsequent increment in the density of FC (Jones et al., 2016).

Also, higher foam volume content leads to longer setting time of the FC mixes which in this case is observed to be around 48 hours. Researchers have assigned this instability in the fresh FC to the collapse of foam bubbles which continues with time until the mortar paste solidifies and forms a constrictive network around the bubbles (Dhasindrakrishna et al., 2021). This collapse of foam bubbles can be attributed to three primary mechanisms. The phenomenon of coalescence referring to the merging of adjacent bubbles in an effort to minimize the energy associated with the interface between air and liquid. Ostwald ripening effect, involving the dissolution of smaller bubbles as a result of air diffusion from regions of higher pressure to regions of lower pressure within larger bubbles. Lastly, drainage linked to the gravitational flow of the liquid medium through the interconnected channels created by the Plateau border network, which serves to separate the gas and liquid phases (Tran et al., 2022; Walstra, 1989). The magnitude of this collapse can vary, encompassing coarser inhomogeneous pores as well as observable instances of partial or complete collapse, characterized by a drop in level or settlement, within the solidified FC resulting in increment of demoulded density (Dhasindrakrishna et al., 2021; Jones et al., 2016). However, FC mixes of density 600 kg/m^3 incorporating SF and PP fibres shows both the density ratios with in allowable range and hence stable at both fresh and in demoulded state. This can be ascribed to the rapid setting behaviour of mixes with SF which subsequently forms a solidified paste network before the collapse of foam. This can be noted from the demoulding time of the FC mixes with SF which is reported in between 24 hours to 36 hours against the previous 48 hrs reported for mixes without SF. While the mixes incorporated with PP fibres shows formation of three dimensional PP fibre mesh network homogeneously incorporated into the cement mortar paste system which, in the fresh state, leads to stability improvements withstanding the collapse and also retarding the merging of the bubbles (Falliano et al., 2022). The effect of SF and PP fibre in maintaining the stability of the FC is observable for all the mixes i.e. in combination of binary and ternary mixes as well.

5.5.2 Flow Table Test and SP dosage

The important fresh state properties of FC are its ability of self-compaction, workability, and stability. Stability can be determined by density ratios, whereas spreadability test is carried out to measure the consistency or workability of FC. Based on Table 5.7 and Table 5.8 of the observed density related data, it is evident that the fresh state properties of FC are influenced by the foam volume, mix constituents and superplasticizer (SP) dosage, as observed in previous

studies (Kunhanandan Nambiar and Ramamurthy, 2008)(Mccormick, 1967). In this section, the effect of addition of foam, FA, SF and fibres can be seen on the test results of slump flow

Table 5-7: Test results on fresh state properties of FC with design density 1000 kg/m3

Mix code	Slump flow before adding foam (mm)	Slump flow after adding foam (mm)	Required SP dosage (%)	Fresh density (kg/m^3)	Fresh density ratio	Demoulded density (kg/m^3)	Demoulded density ratio
MB0	172.50	150.00	0.00	975.83	0.98	958.63	0.96
MF1	207.50	152.50	0.30	970.00	0.97	951.23	0.95
MF2	270.00	157.50	0.60	1046.00	1.05	986.67	0.99
MS1	170.00	152.50	0.20	991.00	0.99	976.00	0.98
MS2	167.50	150.00	0.40	987.55	0.99	956.63	0.96
MPP1	155.00	140.00	0.20	957.00	0.96	952.67	0.95
MPP2	157.50	145.00	0.60	955.04	0.96	957.33	0.96
MF1S1	290.00	155.00	0.40	974.00	0.97	960.00	0.96
MF1S2	250.00	160.00	0.80	973.00	0.97	970.67	0.97
MF2S1	305.00	157.50	1.00	1008.00	1.01	994.67	0.99
MF2S2	320.00	155.50	1.40	985.50	0.99	1026.67	1.03
MF1PP1	277.50	157.50	0.80	989.15	0.99	1018.67	1.02
MF1PP2	270.00	152.50	1.00	978.29	0.98	951.33	0.95
MF2PP1	320.00	162.50	0.70	979.85	0.98	1024.00	1.02
MF2PP2	305.00	157.50	1.60	989.92	0.99	968.00	0.97
MS1PP1	170.00	155.00	0.60	965.12	0.97	970.67	0.97
MS1PP2	172.50	155.00	1.00	970.84	0.97	965.33	0.97
MS2PP1	162.50	140.00	0.80	1008.23	1.01	962.67	0.96
MS2PP2	160.00	142.50	1.40	992.25	0.99	976.00	0.98
MF1S1PP1	305.00	140.00	0.80	1006.98	1.01	997.33	1.00
MF1S1PP2	240.00	157.50	1.20	968.22	0.97	962.67	0.96
MF1S2PP1	262.50	155.00	1.20	1010.91	1.01	952.00	0.95
MF1S2PP2	230.00	145.00	1.40	975.97	0.98	1002.67	1.00
MF2S1PP1	325.00	150.00	1.60	1008.53	1.01	1090.67	1.09
MF2S1PP2	285.00	160.00	1.80	986.05	0.99	968.00	0.97
MF2S2PP1	305.00	162.50	1.80	958.14	0.96	948.43	0.95
MF2S2PP2	285.00	155.00	2.20	964.34	0.96	953.33	0.95

Table 5-8: Test results on fresh state properties of FC with design density 600 kg/m^3

Mix code	Slump flow before adding foam (mm)	Slump flow after adding foam (mm)	Required SP dosage (%)	Fresh density (kg/m^3)	Fresh density ratio	Demoulded density (kg/m^3)	Demoulded density ratio
LB0	210.00	155.00	0.00	581.01	0.97	682.00	1.14
LF1	280.00	150.00	0.40	624.42	1.04	712.67	1.19
LF2	325.00	162.50	0.80	598.06	1.00	704.67	1.17
LS1	220.00	150.00	0.20	580.20	0.97	662.00	1.10
LS2	255.00	147.50	0.40	635.00	1.06	635.33	1.06
LPP1	197.50	147.50	0.40	602.72	1.00	592.67	0.99
LPP2	192.50	145.00	0.80	578.66	0.96	539.33	0.90
LF1S1	325.00	155.00	0.60	585.66	0.98	568.67	0.95
LF1S2	320.00	160.00	0.80	619.00	1.03	595.33	0.99
LF2S1	335.00	157.50	1.40	572.63	0.95	551.33	0.92
LF2S2	347.50	155.00	1.60	571.23	0.95	543.00	0.91
LF1PP1	320.00	155.00	1.00	568.60	0.95	530.67	0.88
LF1PP2	232.50	145.00	1.40	610.53	1.02	571.33	0.95
LF2PP1	340.00	150.00	1.20	594.86	0.99	560.67	0.93
LF2PP2	250.00	147.50	2.00	603.28	1.01	560.67	0.93
LS1PP1	197.50	150.00	0.60	601.16	1.00	560.67	0.93
LS1PP2	165.00	152.50	1.20	592.20	0.99	554.67	0.92
LS2PP1	195.00	147.50	0.80	611.24	1.02	563.33	0.94
LS2PP2	167.50	140.00	1.40	565.16	0.94	546.67	0.91
LF1S1PP1	305.00	150.00	0.80	565.46	0.94	538.00	0.90
LF1S1PP2	215.00	147.50	1.60	584.38	0.97	548.00	0.91
LF1S2PP1	295.00	145.00	1.00	570.16	0.95	549.33	0.92
LF1S2PP2	205.00	137.50	1.80	587.21	0.98	566.00	0.94
LF2S1PP1	300.00	155.00	1.60	580.26	0.97	550.85	0.92
LF2S1PP2	280.00	140.00	2.00	600.28	1.00	579.33	0.97
LF2S2PP1	322.50	145.00	2.00	587.20	0.98	540.33	0.90
LF2S2PP2	252.50	140.00	2.40	614.86	1.02	603.33	1.01

Level 1 Replacement

Figure 5.6 represents the effect of incorporation of single admixture i.e. FA or SF or PP fiber on the spread % of FC with densities 1000 kg/m^3 and 600 kg/m^3. Bar graph represents the spread % of FC mixes before adding foam and spread % obtained after adding foam. Markers with triangle and square shape represents the required SP dosage to maintain the spread % between 50 ±10% (i.e. slump flow 140 mm to 160 mm) for FC with densities 1000 kg/m^3 and 600 kg/m^3 respectively. As observed from Figure 5.6, density of FC plays a significant role in the fresh properties of FC. In order to maintain the spread % of 50±10% for the base mix the required w/s ratio comes out to be 0.30 for M series (FC with density1000 kg/m^3) while for L series (FC with density 600 kg/m^3) it comes out to be 0.35. The above observation is in line with earlier studies which reported higher water demand for mixes with more foam (Sahu and Gandhi, 2021a; Selija and Gandhi, 2022).The adoption of aforementioned w/s ratio leads to spread of 72.50% in M series base mix mortar before addition of foam which reduces to 50% after foam incorporation. However, in case of L series base mix mortar, incorporation of foam results in significant reduction of spread from 110% to 55%. Previous studies (Kunhanandan Nambiar and Ramamurthy, 2008)(Raj et al., 2019) have indicated this reduction in consistency for FC with the increase in foam volume is due to reduction in the self-weight of FC sample and increase the cohesion in FC mix with higher air content. The above mentioned trend of greater amount of reduction in spread of L series mortar mix after addition of foam compared to that of M series is consistently noticed for all the Level 1 Replacement mixes.

Incorporation of FA affects the slump flow of FC to a great extent compared to other admixtures (SF and PP fiber). Incorporation of FA as a replacement of sand increase the water demand required for achieving the stable mix. This increase in water demand is compensated by the use of SP. The demand for SP to attain stable mixes (without increase in water content) exhibits a positive correlation with the percentage replacement of sand with FA and foam volume. For instance, in M series mixes, a dosage of 0.3% of SP by weight of cement is needed for a 50% replacement of sand with FA, and a dosage of 0.6% of SP is required for a 100% replacement. While, In the case of L series mixes, it has been observed that the dosage of SP required for FC increases to approximately 0.4% and 0.8% when 50% and 100% of sand is replaced with FA, respectively. This increase in dosage of SP is necessary to ensure the stability and spread of 50± 10% for the fresh FC mixes incorporating FA. The combined effect of SP and FA can be seen evidently on the spread of FC mixes before and after incorporation of foam. For instance, spread of 108% and 170% is noted for M series F1 and F2 mixes and a spread of 180% and

220% for L series F1 and F2 mixes respectively before addition of foam. However, after addition of foam, the foam restricted the ball bearing action of FA particles limiting the spread to a range of 50% to 62.5% for both the series mixes. Similar phenomenon is reported for mixes with SF where SP dosage in range of 0.2% to 0.4% is required to maintain the spreadability of 50 ±10% after incorporation of foam. Incorporation of PP fiber tend to show higher demand of SP for maintaining the consistency. In case of PP1 mixes, SP demand is reported to be 0.2 and 0.4% for M series and L series respectively. While in case of PP2 mix the SP demand is increased to 0.6% and 0.8%. This can be due the creation of 3-Dimensional spatial network structure which consumes mortar paste to cover the fibers resulting in lower flow than FC without PP fiber (Gencel et al., 2021). The highest SP demand in case of Level 1 replacement mixes is reported to be 0.8% in case of L series and 0.6% in case of M series.

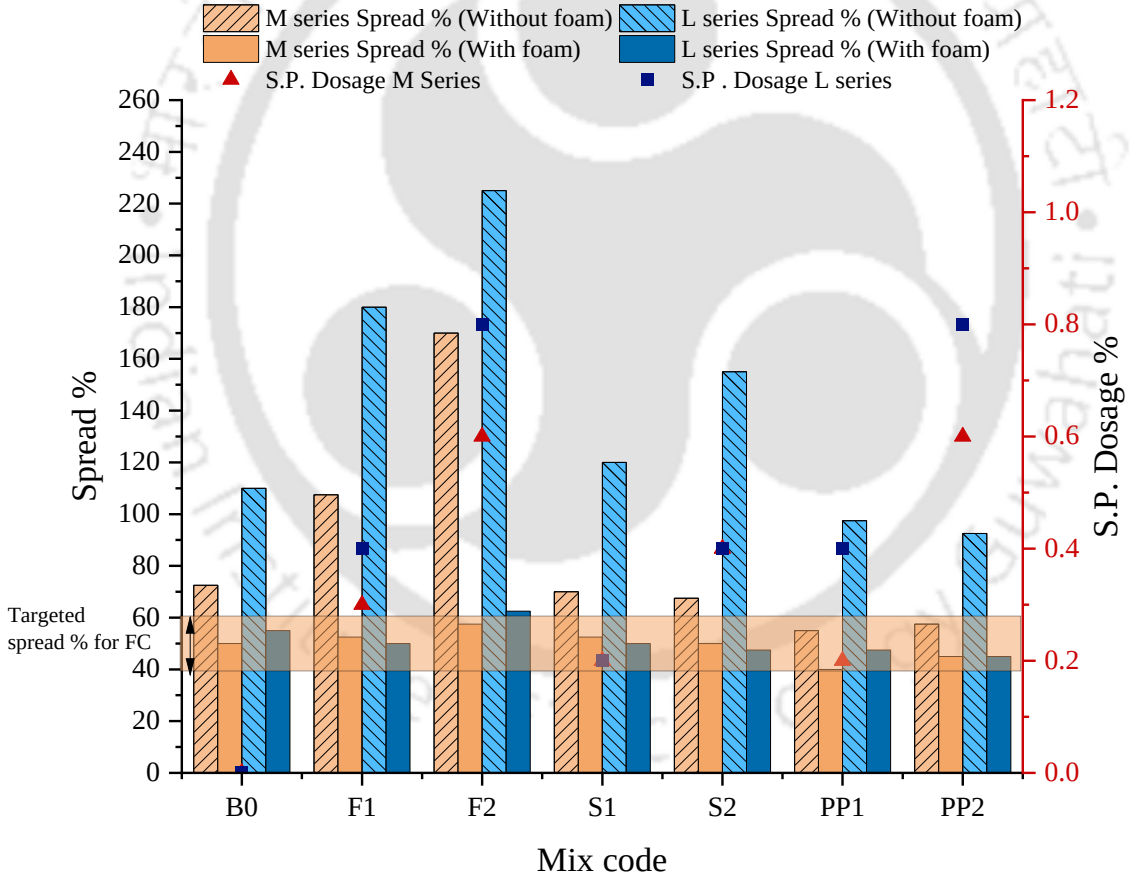

Figure 5-6: Spread% and SP dosage for level 1 replacement

Level 2 Replacement

Effect of the combination of two admixtures (FA and SF / SF and PP fibre / FA and PP fibre) on the flow properties and SP dosage requirement is represented in Figure 5.7. The synergistic effect of the combination of two admixtures causes the increment in the SP demand for both M

series and L series mixes compared to Level 1 replacement mixes. The mixes with the combination of 100% FA and 0.4% PP fibre shows the highest SP demand of 1.6% for M series mixes and 2.0% in case of L series mixes. Further, the mixes with combination of FA and SF shows significant spread flow before addition of foam in the range of 140% to 240%. On a similar note, the incorporation of FA in combination with PP fibres also shows a notable spread flow of 130% to 230%. However, the range of spread flow for mixes without FA i.e. combination of SF and PP fibres is relatively less say 60% to 97.5% before incorporation of foam. For all the level 2 replacement mixes the spread % ranges between 40% to 60% after addition of foam.

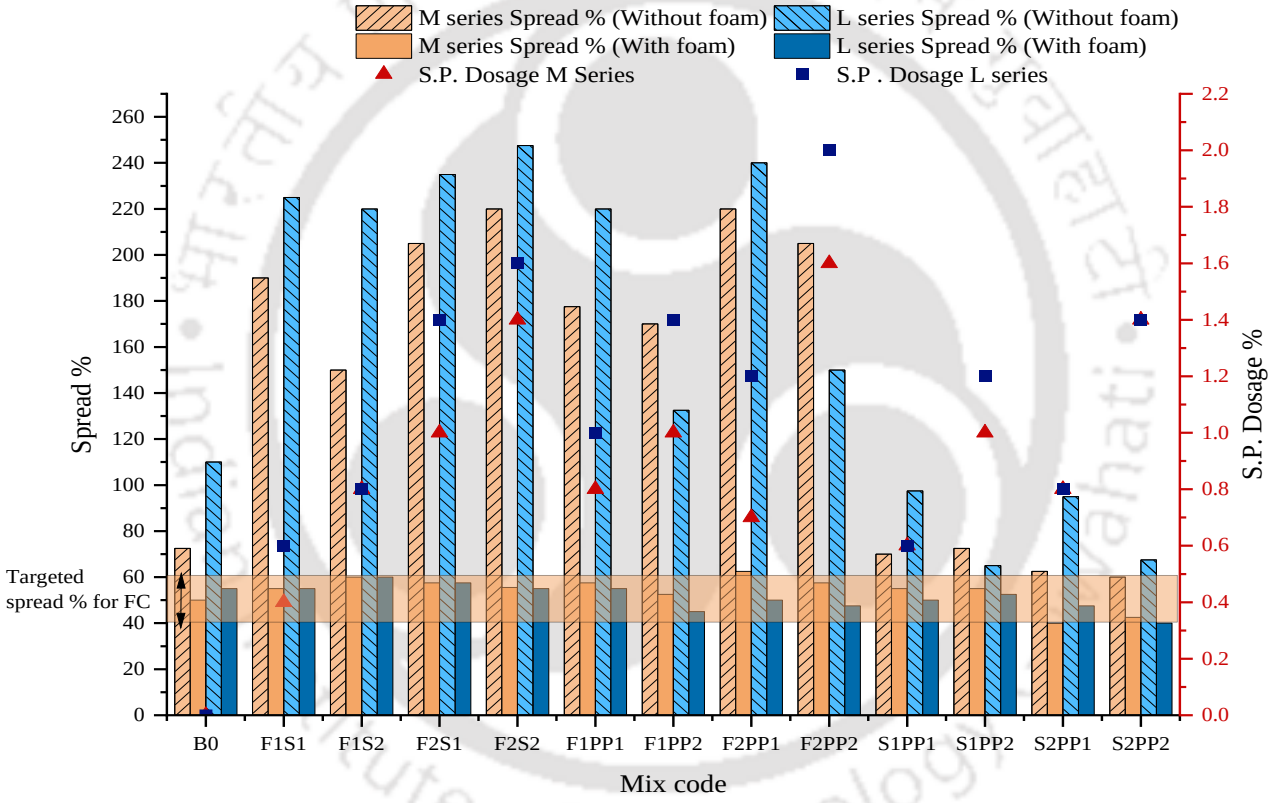

Figure 5-7: Spread% and SP dosage for level 2 replacement

Level 3 Replacement

The results on the spread flow % of FC mixes comprising of ternary admixture i.e. combination of FA + SF + PP fiber is shown in Figure 5.8. Additionally, Figure 5.8 also shows the SP demand for various mixes. As level 3 replacement mixes comprises of combination of all three admixtures, the SP demand reported is highest compared to level 1 and level 2 mixes. The highest SP demand of 2.2% is noted for M series mix with F2S2PP2 (100FA+20%SF+0.4%PP fiber) combination while the corresponding value for similar L series mix is 2.4%. Since all the

mixes in this category incorporates FA replacement in the range of 50% or 100% the effect of ball bearing action of FA can be clearly noted in the all the level 3 mixes before addition of foam. The spread flow of the M-series mixes is reported to be in the range of 130% to 225% while for L series mixes the spread flow is found to be 105% to 222.50% before addition of foam. All the above mentioned mixes exhibits a significant reduction of spread with final spread of 40% to 60% after addition of foam.

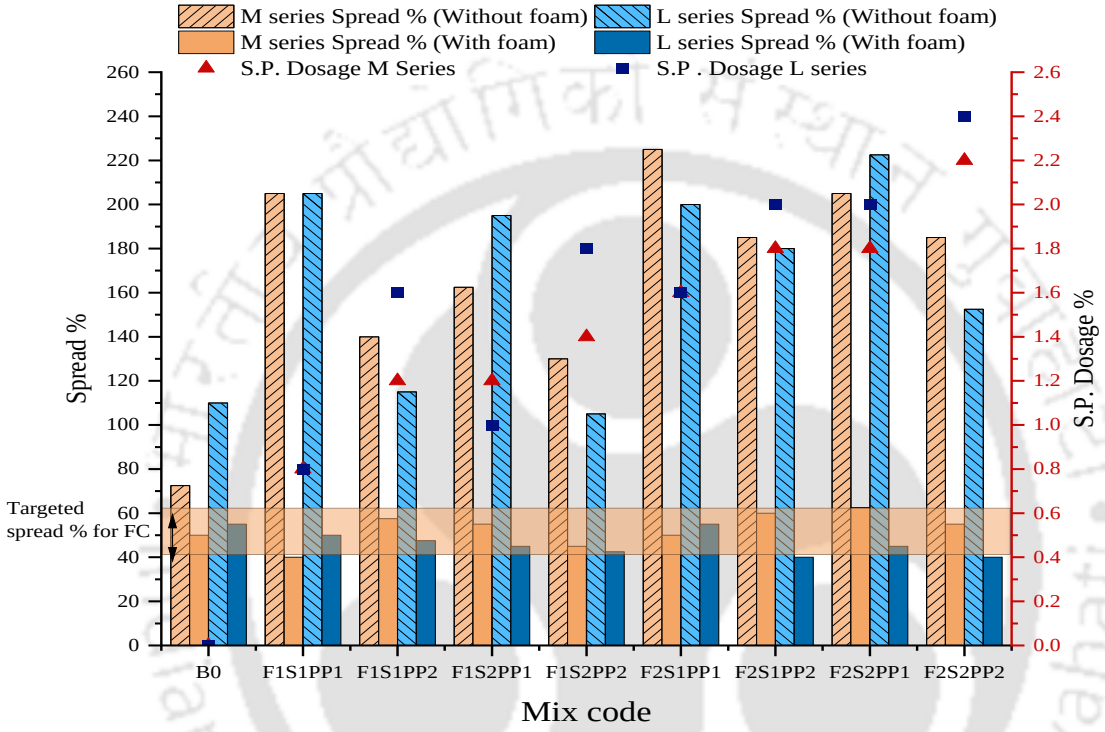

Figure 5-8: Spread% and SP dosage for level 3 replacement

5.6 Results on hardened state properties of FC

5.6.1 Compressive strength

Level 1 Replacement

Table 5.9 provides the results for compressive strength for mixes incorporating single admixture. Table 5.9, also provides the percentage increment in strength w.r.t. base mix at the respective ages. Figure 5.9 and Figure 5.10 represents the effect of incorporation of single admixture i.e. FA or SF or PP fiber on the compressive strength of FC (at different testing ages 14 days, 28 days and 90 days) with design densities 1000 kg/m^3 and 600 kg/m^3 respectively. Further mixes are required to achieve a minimum compressive strength criterion of 5 MPa and 1.5 MPa for FC with design density 1000 kg/m^3 and 600 kg/m^3 respectively as per IS

2185:1984. Line no. 1 represented by red color represents the minimum compressive strength criterion for the respective densities.

Table 5-9: Results on compressive strength of FC with single admixture

Mix code	Compressive strength at 14 days (N/mm^2)	% increase w.r.t base mix (14 days)	Compressive strength at 28 days (N/mm^2)	% increase w.r.t base mix (28 days)	Compressive strength at 90 days (N/mm^2)	% increase w.r.t base mix (90 days)
MB0	1.10	0.00	1.72	0.00	1.79	0.00
MF1	1.37	24.82	2.06	19.71	3.25	82.09
MF2	3.05	176.76	4.40	155.93	8.36	367.91
MS1	1.77	61.14	2.28	32.74	2.25	26.12
MS2	1.65	49.64	1.67	-2.83	2.08	16.42
MPP1	1.07	-3.27	1.64	-4.58	1.73	-2.99
MPP2	1.40	27.00	1.57	-8.77	1.85	3.73
LB0	0.79	0.00	0.93	0.00	1.04	0.00
LF1	1.58	101.10	1.64	76.34	2.47	137.67
LF2	2.16	174.89	2.77	197.84	3.41	227.88
LS1	1.49	89.65	1.64	76.34	1.72	65.38
LS2	1.00	26.65	1.13	21.51	1.09	4.81
LPP1	1.09	38.11	1.54	65.69	1.77	70.53
LPP2	0.90	14.54	1.37	47.80	1.42	36.26

As established in literature, it is evident that the strength of FC increases exponentially with increase in density. From Figures 5.9 and 5.10, it can be noted that for base mixes corresponding to FC of design density 1000 kg/m^3 and 600 kg/m^3, the highest compressive strength reported is 1.79 MPa and 1.04 MPa at the age of 90 days respectively. The increase in density from 600 kg/m^3 to 1000 kg/m^3 in case of base mixes results in increase of strength by 85% and 72% at ages 28 days and 90 days respectively. The highest compressive strength for FC with single admixture replacement for both the design densities i.e. 1000 kg/m^3 and 600 kg/m^3 is reported for mixes with 100% FA replacement at 90 day age which is 8.36 MPa and 3.81 MPa respectively. This corresponds to about 120% increment in strength with the increment in density.

Compressive strength of the FC increases by adding the FA to the mixture. The trend followed by compressive strength with increase in FA replacement level when compared to base mix can be noted in Figures 5.9 and 5.10. Replacement of 50% of sand with FA results in increase in compressive strength by 82% for M series mix and 138% for L series mix, at a testing age of 90 days. Further increase in replacement level say 100% FA results in significant increase of compressive strength by 368% for M series mix and 228% for L series mix at testing age 90

days. The observed initial increase in strength, (at the 14-day and 28-day), can be attributed primarily to the enhanced packing within the structure owing to the smaller particle size of FA compared to sand. However, delayed pozzolanic reaction of FA particles along with superior particle packing ability leads to major strength enhancement observed at 90 days age (Al-Shwaiter et al., 2022; Jones and McCarthy, 2005c). This can be verified with the help of XRD analysis as shown in Figure 5.11. Decrease in portlandite peaks with the increase in FA levels can be clearly noted in the XRD results of 14 days and 28 days. With the further increase in age up to 90 days, a significant reduction in portlandite peak intensity is observed thus indicating the utilization of calcium hydroxide in the formation of CSH gel due to pozzolanic reaction leading to improvement in compressive strength. Also it can be noted that ettringite formation is observed specially in the FC mixes with FA at 90 days age. Figure 5.12 shows the SEM images of the mixes MB0 and MF2 at ages of 28 days and 90 days. In the SEM analysis of base mix samples clear presence of portlandite ($Ca(OH)_2$), Calcite ($CaCO_3$) can be seen. While 28 day SEM image of MF2 shows the abundant presence of unreacted FA particles (Figure 5.12 b) proving that the physical effect i.e. particle packing predominantly influences strength enhancement. Further SEM analysis of MF2 mixes at 90 days reports the presence of Calcium Silicate Hydrate (C-S-H) gel formation along with mineral named Ettringite which is calcium sulfoaluminate ($3CaO\ Al_2O_3\ 3CaSO_4\ 32H_2O$), normally found in Portland cement concretes (Figure 5.12 c). Under microscopic examination, needle-like crystals of ettringite are often observed lining air voids or cracks.

Figures 5.9 and 5.10 illustrates the pattern of compressive strength development with increase in SF replacement level. The partial replacement of cement by SF causes a gradual increase in compressive strength till 10% replacement level. When compared to base mixes, mixes with 10% SF reports an almost 61%, 33% and 26% increase in compressive strength for M series and 90%, 76% and 65% increase is observed in L series mixes at ages 14 days, 28 days and 90 days respectively. The addition of 20% SF lead to improvement in strength at age of 14 days by 50% and 27% for M series and L series respectively. However, the corresponding increment in strength at 90 days age is 16% and 5% for M series and L series respectively when compared to base mix. It is observed that, mixes with 20% SF incorporation shows lower compressive strength when compared to mixes with 10% SF at all testing ages. This makes 10% replacement of SF as the optimum dosage. There are two possible reasons for the above trend. Firstly, the foam in FC intends to collapse and merge in the presence of excessive SF which may affect the microstructure and compressive strength of FC. Secondly, increased fineness and higher water

demand of SF affects the hydration process of cement when excessive amount of SF is present in mix (Gong et al., 2020).

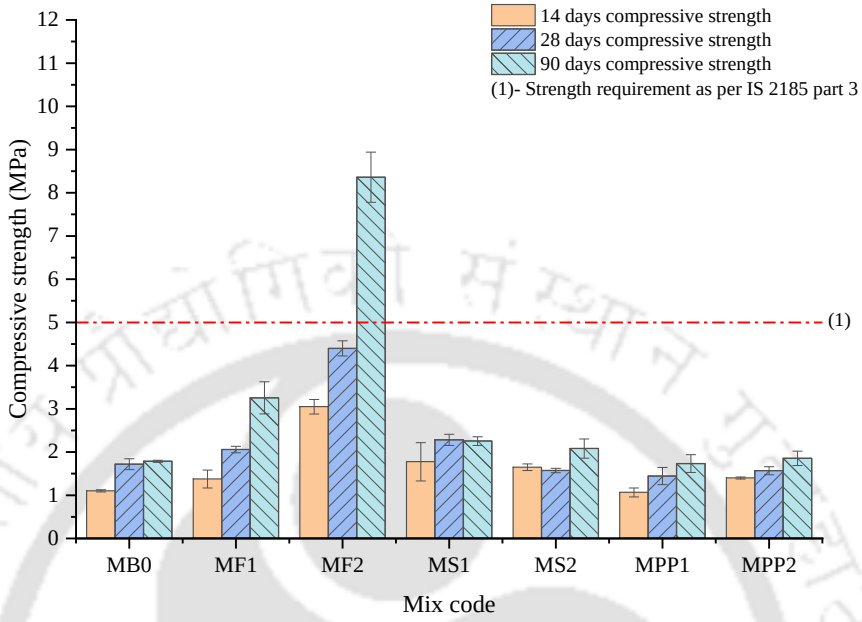

Figure 5-9: Effect of Single admixture on compressive strength of FC with design density 1000 kg/m^3

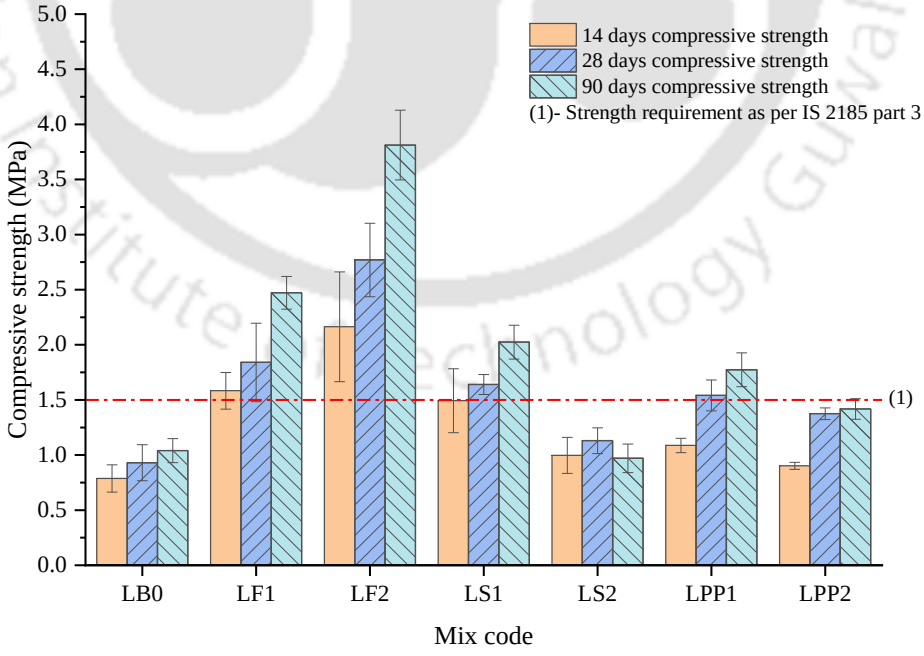

Figure 5-10: Effect of Single admixture on compressive strength of FC with design density 600 kg/m^3

Further the improvement in strength of SF mixes when compared to base mix, can be attributed to the improved aggregate matrix bond along with formation of dense micro structure of FC. Also it can be noted that at testing age of 14 days and 28 days maximum percentage improvement in strength is observed while in the later ages the rate of gain of strength is slowed down. For e.g. The Mix LS2 represents the FC mix with density 600 kg/m^3 and partial replacement of cement with silica fume by 20%. When compared to base mix, the addition of 20% SF in L series mix lead to improvement in strength at age of 14 days by 27%. However, the corresponding increment in strength at 90 days age is 5%. The incorporation of silica fume in concrete or mortar may not provide a statistically significant increase in strength from 14 days to 90 days due to several factors. In presence of SF the Hydration of cement is getting accelerated in the presence of fine SF particles. Silica fume primarily enhances early-age strength development, resulting in significant improvements in strength within the first few days. After the initial curing period, the rate of strength gain may slow down, leading to minimal additional strength increase between 14 days to 90 days, as observed in some studies (Ahmad et al., 2022). Other factors such as pozzolanic reaction reaching its limit, reduced availability of reactive materials, or optimization of microstructure mix design, curing conditions, and concrete composition may also influence the rate of strength gain over time, potentially masking the effects of silica fume beyond the early-age period (Duval and Kadri, 1998; Ameer A. Hilal et al., 2015; Pan et al., 2007). This phenomenon can be verified in Figure 5.13, where XRD pattern shows that with the SF incorporation, a higher intensity of portlandite peak is reported at the early age (14 days and 28 days). These high intensity portlandite peaks at early age indicate higher rate of hydration of the mixes with SF. However, it should be noted that the maximum portlandite peak intensity is observed for MS2 mixes (20% SF) indicating occurrence of more hydration in the MS2 mix compared to MS1 mix at early age (14 days and 28 days). Further, a slight reduction in portlandite peaks of the SF mixes can be observed from XRD patterns at 90 days age. This indicates the occurrence of pozzolanic reaction in the later ages of FC mixes with SF.

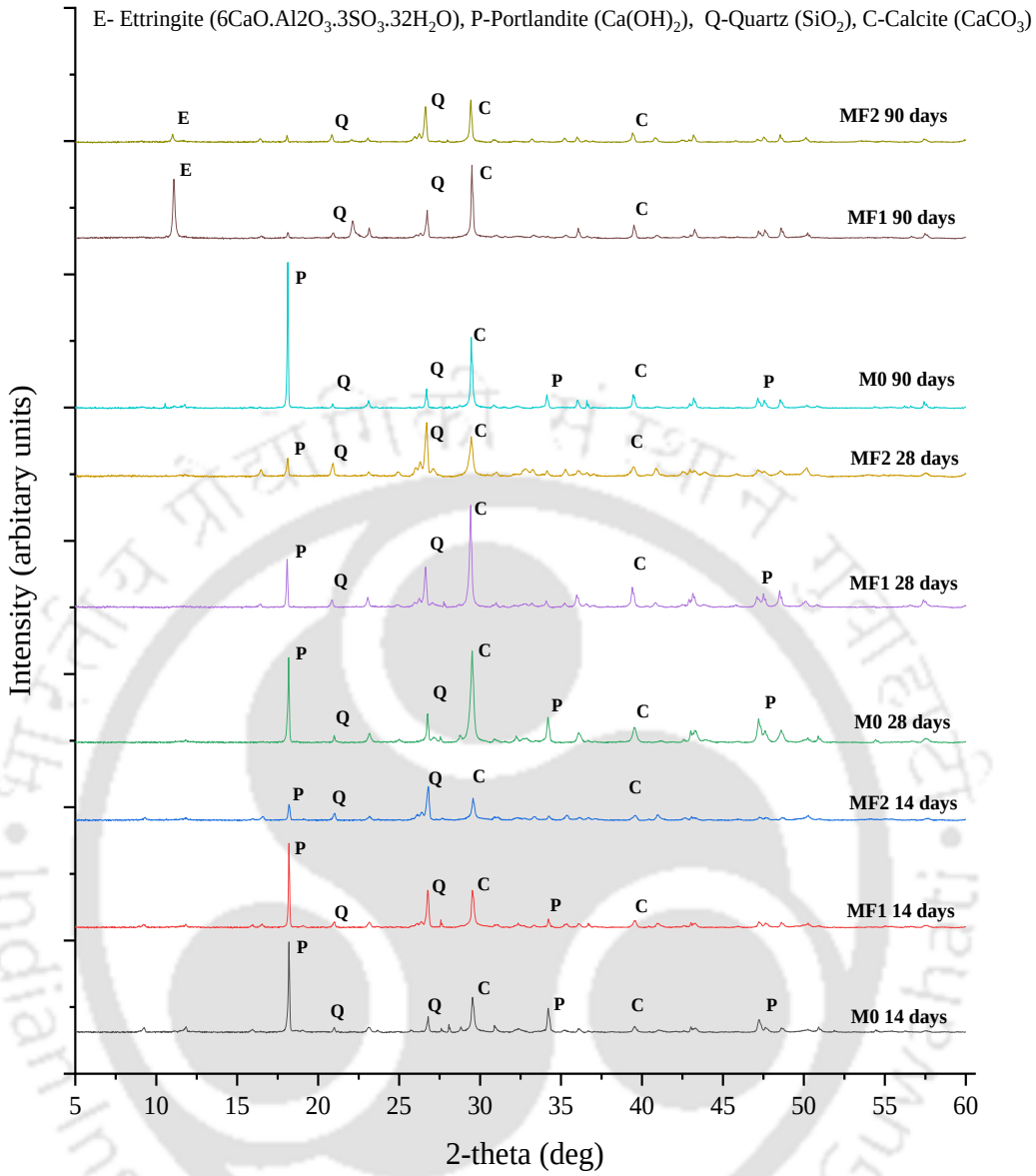

Figure 5-11: XRD pattern of FC with varying fly ash replacement levels

The effect of addition of PP fibers on compressive strength of FC is shown in Figures 5.9 and 5.10. The compressive strength of FC has not significantly changed due to addition of PP fibers when compared to FA and SF. Apart from this in M series mixes a slight decrement of 9% to 5% in strength is noted at 28 days when compared to base mix. The above reduction can be attributed to the creation of more pores in the concrete structure due to the water retaining ability of hydrophobic PP fibres combined with the orientation of fibres (Gencel et al., 2021). However, in case of L series mixes the incorporation of PP fibers plays a significant role in strength gain and lead to an increase of 71% in compressive strength at the age of 90 days. The increment in strength can be assigned to the enhancement of bonding between the fibres and

paste in L series concrete mixes due to adoption of cement to sand ratio of 1:1 as compared to 1:2 of M series. Also the negative effect of creation of more voids due to addition of PP fibres in lower-density FC is not affecting the compressive strength significantly as the above negative effect is subsided by the positive effect of homogenous incorporation of three dimensional PP fibre mesh network into the cement mortar paste system (Jhatial et al., 2021). Also, the creation of air voids due to fiber addition adds to porosity at minor level only when compared to already existing higher proportion of voids in lower density FC mixes. However, the addition of PP fiber may lead to early hydration as evident from the XRD plot (Figure 5.14). The higher intensity of the portlandite peaks with incorporation of PP fibers clearly indicates the formation of more $CaOH_2$ due to better hydration of the cement in FC mixes. The presence of additional pores at the interface between the fiber and matrix may contribute to the establishment of interconnectivity among the voids generated by the foam as shown in Figure 5.15. Consequently, this interconnectivity can enhance the availability of water for hydration of cementt during the early stages for the PP fiber mixes. Here only mix MF2 in M series and LF1, LF2 and LS1 in L series are able to meet criteria for minimum strength requirement of IS 2185 part3.

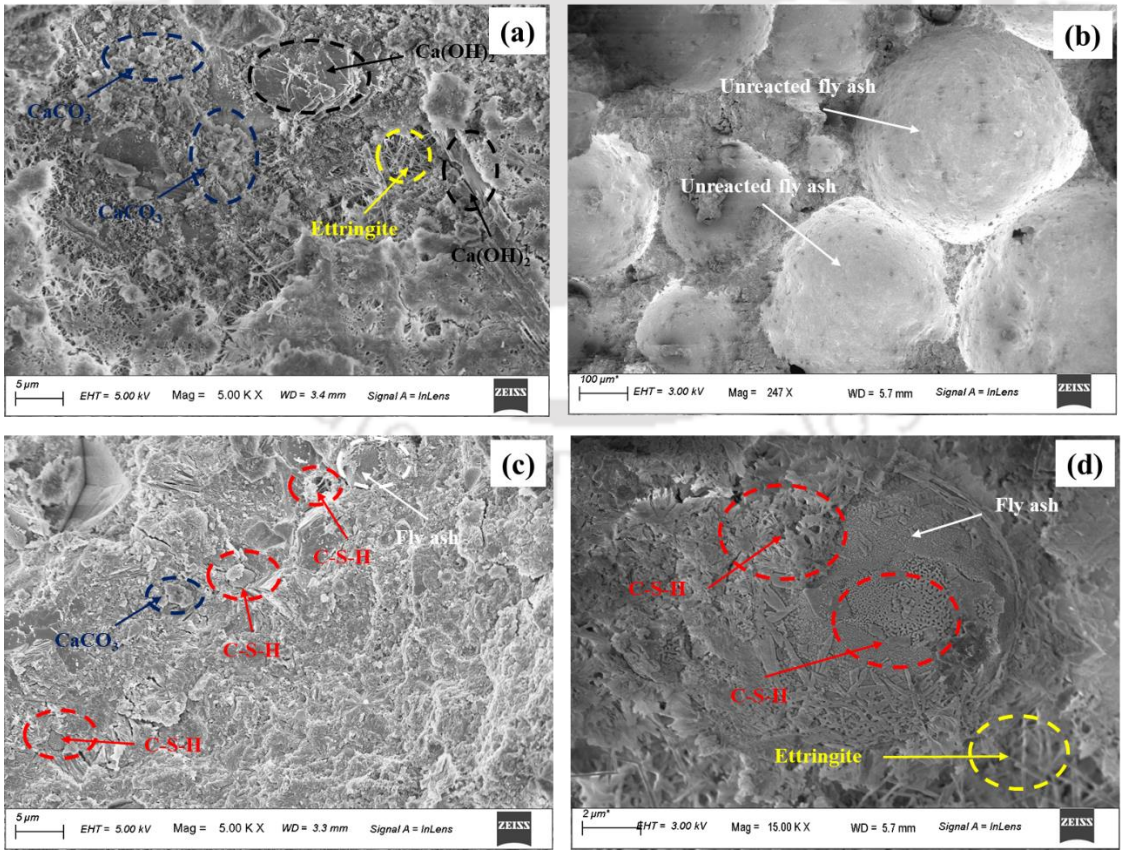

Figure 5-12: SEM images of (a) MB0 at 28 days age (b) MF2 at 28 days age (c) MF2 at 90 days age (d) MF2 at 90 days age with higher magnification

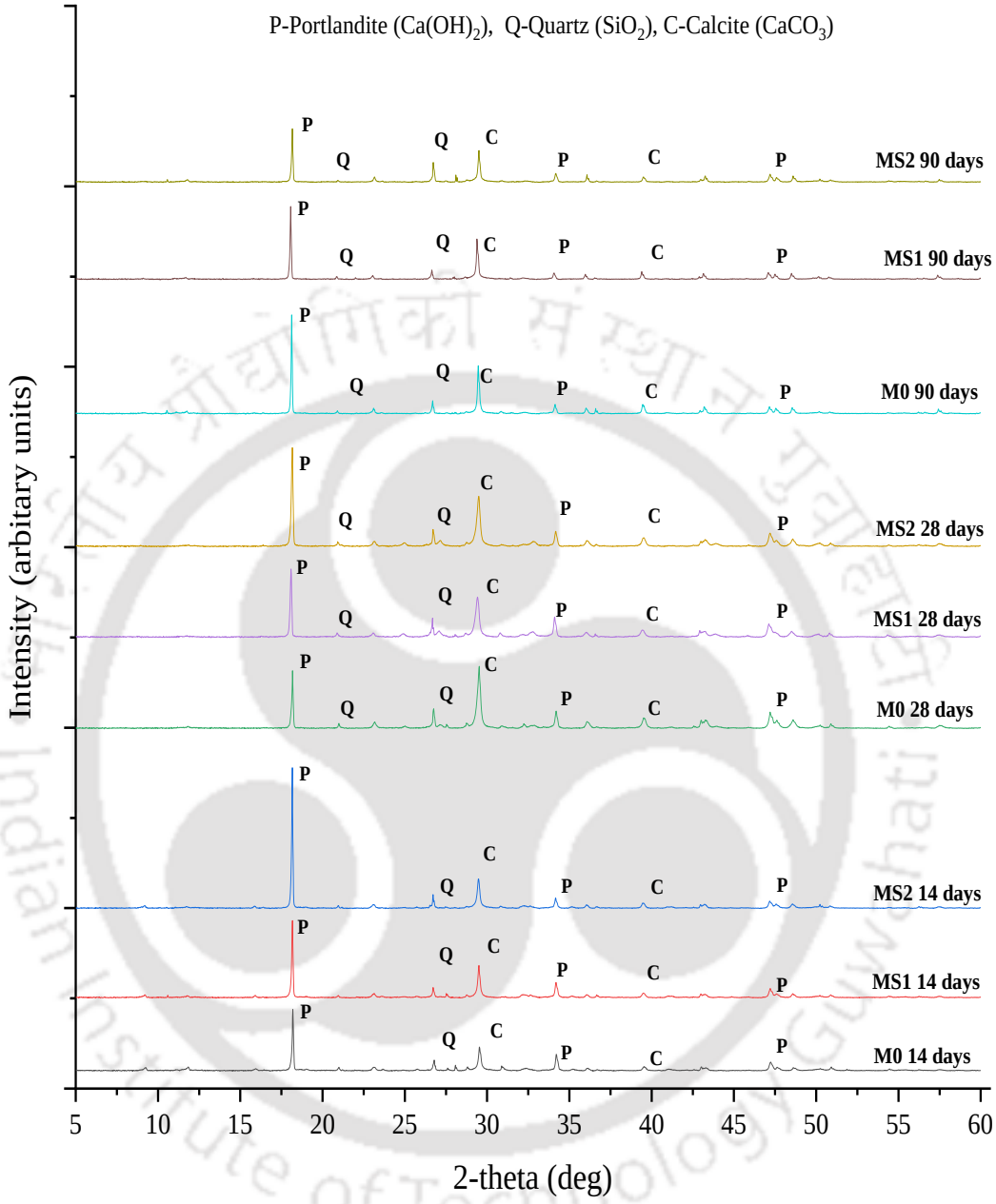

Figure 5-13: XRD pattern of FC with varying SF replacement levels

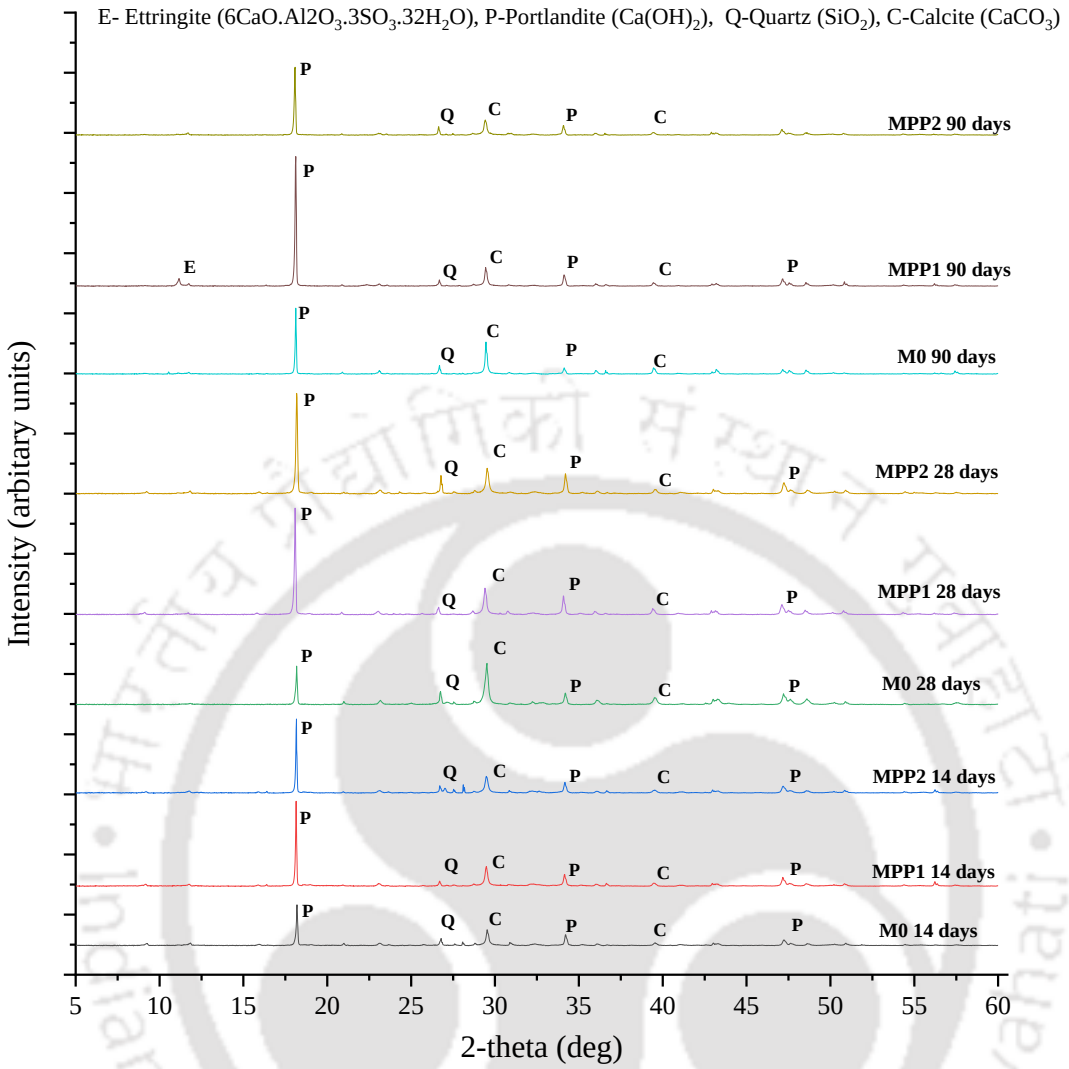

Figure 5-14: XRD pattern of FC with varying PP fibre addition levels

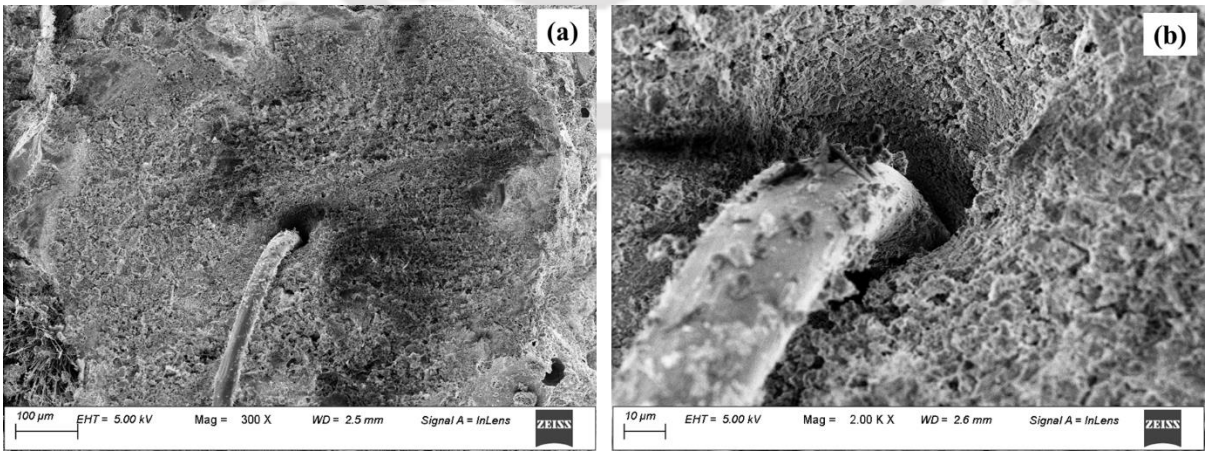

Figure 5-15: SEM images of (a) MPP2 at 28 days age (b) enlarged view of the void around fibre of MPP2

Level 2 Replacement

The results on compressive strength of mixes comprising binary (combinations of two) admixtures are shown in Table 5.10. Additionally, Table 5.10 also shows the % increase in strength with respect to base mix at the corresponding ages. Figure 5.16 and Figure 5.17 represents the effect of incorporation of binary admixture i.e. FA + SF or FA + PP fiber or SF + PP fiber on the compressive strength of FC (at ages 14 days, 28 days and 90 days) with design densities 1000 kg/m^3 and 600 kg/m^3 respectively. The mixes must meet a minimum compressive strength requirement of 5 MPa and 1.5 MPa for FC with design densities of 1000 kg/m^3 and 600 kg/m^3 respectively, according to IS 2185 Part 3 (1984).

Table 5-10: Results on compressive strength of FC with binary admixture

Mix code	Compressive strength at 14 days (N/mm^2)	% increase w.r.t base mix (14days)	Compressive strength at 28 days (N/mm^2)	% increase w.r.t base mix (28days)	Compressive strength at 90 days (N/mm^2)	% increase w.r.t base mix (90days)
M0	1.10	0.00	1.72	0.00	1.79	0.00
MF1S1	1.81	63.92	2.64	53.61	4.44	148.51
MF1S2	1.73	56.66	2.46	42.90	3.89	117.91
MF2S1	3.21	191.16	5.17	200.70	9.66	440.75
MF2S2	3.47	215.13	4.73	175.17	8.69	386.57
MF1PP1	2.38	116.10	3.71	115.59	5.72	220.15
MF1PP2	2.92	165.38	3.74	117.46	4.92	175.37
MF2PP1	3.92	256.30	5.09	196.43	9.16	412.69
MF2PP2	4.50	308.35	7.48	335.45	8.25	361.92
MS1PP1	2.11	91.65	2.37	37.86	1.83	2.24
MS1PP2	1.67	51.33	1.45	-15.59	1.65	-7.46
MS2PP1	1.37	23.97	1.42	-17.46	1.93	8.21
MS2PP2	1.73	56.78	1.83	6.44	2.09	17.16
LB0	0.79	0.00	0.93	0.00	1.04	0.00
LF1S1	1.05	33.70	1.39	49.66	1.58	51.83
LF1S2	0.93	18.18	1.02	9.68	1.31	25.96
LF2S1	1.57	99.78	1.45	55.63	2.62	152.33
LF2S2	1.88	138.77	1.89	102.78	2.34	125.17
LF1PP1	0.83	5.73	1.36	45.94	1.42	36.45
LF1PP2	2.04	158.81	2.22	138.94	2.66	156.03
LF2PP1	1.48	88.33	1.68	80.97	1.51	44.79
LF2PP2	2.69	292.51	3.69	277.61	3.90	244.06
LS1PP1	0.99	26.43	1.00	7.54	1.33	28.17
LS1PP2	1.19	50.88	1.50	61.59	1.22	17.35
LS2PP1	0.93	17.62	0.87	-6.62	1.17	12.67
LS2PP2	0.84	6.61	0.89	-4.20	1.00	-3.92

The highest compressive strength for FC with binary admixture replacement with density 1000 kg/m^3 is reported for mix with 100% FA and 10% SF, while for 600 kg/m^3 density, mix with 100% FA and 0.4% PP fibre shows the highest strength at 90 days age. The corresponding strengths are 9.66 MPa and 3.90 MPa, which is about 440% and 275% higher than that of the base mixes respectively. Also the highest strength mixes in Level 2 replacement category reports 16% and 14% improvement in strength when compared to the mixes exhibiting highest strength in level 1 replacement category for densities 1000 kg/m^3 and 600 kg/m^3 respectively.

The effect of incorporation of combination of FA and SF in FC mixes with densities 1000 kg/m^3 and 600 kg/m^3 can be observed in Figure 5.16 and Figure 5.17 respectively. The incorporation of 100% FA (F2) and 10% SF (S1) is reported to be optimum dosage in case of combination of FA and SF mixes for both the design densities. For instance, F2S1 mixes provides a compressive strength of 9.66 MPa and 2.62 MPa at the age of 90 days for densities 1000 kg/m^3 and 600 kg/m^3 respectively which is 440% and 152% higher than that of base mixes with corresponding densities. This can be due to the delayed pozzolanic reaction occurring in the F2S1 mixes leading to the significant increase in the strength. Similar to level 1 replacement mixes, here in level 2 replacement category also mixes in combination with 100% FA provides better strength than that of mixes with 50% FA. Also its to be noted that in level 2 replacement category, mixes in combination with 10% SF provides better results than that of 20% SF except in 600 kg/m^3 density where higher strength is observed for LF2S2 mixes for 14 days and 28 days, however at 90 days the strength observed is lower than that of LF2S1.

Figures 5.16 and 5.17 illustrates the pattern of compressive strength development with the incorporation of FA in combination with PP fibers for densities 1000 kg/m^3 and 600 kg/m^3. In case of M series i.e. 1000 kg/m^3 density mix, MF2PP2 reports a higher early age strength of 4.50 MPa and 7.48 MPa at age of 14 days and 28 days respectively. However, at 90 days the MF2PP1 reports the highest ultimate strength of 9.160 MPa in this combination for M series. For L series, the highest strength reported in this combination and entire Level 2 replacement category is for the combination of 100% FA and 0.4% PP fiber, at all ages. The strength reported for mix LF2PP2 is 3.09 MPa, 3.51 MPa and 3.58 MPa at ages 14 days, 28 days and 90 days respectively. The corresponding increment in strength is found to be 293%, 278% and 244% more than that of the base mix. This may be due to the fact that in very low density mix like 600 kg/m^3 the paste content itself is very low occupying only 30% and hence the strength is governed mainly by the homogeneous incorporation of three dimensional PP fibre mesh

network into the cement mortar paste system rather than paste having predominant effect as observed in higher densities. When considering the early age strength development in level 2 replacement category, it is observed that for both the densities, mixes with combination of 100% FA and 0.4% PP fibre reports the highest strength among all mixes at ages 14 days and 28 days. The strength observed is more than that of the mixes in combination with SF. This can be attributed to the creation of additional pores on the fibre-matrix interface which leads to the interconnectivity between the voids created by foam and in turn aids pozzolanic reaction by facilitating water availability for hydration in the early ages for the F2PP2 mixes (Kamisetty et al., 2023). The above observation can be supported by the % strength development over ages where MF2PP2 and LF2PP2 reported an initial 14-day strength of 4.50 MPa and 2.69 MPa against MF2 and LF2 which reported a strength of 3.05 MPa and 1.96 MPa respectively. Further, a significant increment of 66% and 41% in strength is noted from 14 days to 28 days for MF2PP2 and LF2PP2, while mixes MF2 and LF2 reports an increment in strength of 44% and 21% respectively. However, it is to be noted that for the mixes MF2PP2 and LF2PP2, later age strength gain is affected seriously where only 11% and 3% strength gain is reported over a testing age from 28 days to 90 days while in case of MF2 and LF2 the corresponding strength gain reported is 90% and 44% respectively. This phenomenon can be observed in the XRD graph of the MF2PP2 vs MF2 (Figure 5.18) where higher intensity of portlandite peaks are observed for MF2PP2 mixes at 14 days and 28 days thus indicating better hydration of cement when compared to MF2 mix. These peaks further completely disappear at 90 days age indicating conversion of C-H into C-S-H gel due to pozzolanic reaction. Figure 5.19 shows the SEM analysis of MF2PP2 mix at ages of 28 days and 90 days. The interconnectivity of the pore created due to the incorporation of the PP fibre can be observed in the Figure 5.19 (a). This void around the pore gets filled over a period of time which is represented in Figure 5.19 (b) where Calcite deposits can be noted around the void of the pore thus leading to further improvement in strength

Experimental outcomes indicate that the combination of SF and PP fibre do not show significant impact on strength development of FC when compared to other combination mixes. The highest compressive strength achieved by these combination mixes viz., MS1PP1 and LS1PP2 are 2.41 MPa and 1.53 MPa at the age of 90 days respectively. The corresponding increment in strength reported is 35% and 47% when compared to base mix at same age. Here mixes MF2S1, MF2S2, MF1PP1, MF2PP1 and MF2PP2 are able to meet minimum strength requirement criteria of IS

2185 part3. while in case of L series mixes LF1S1, LF2S1, LF2S2, LF1PP2, LF2PP1, LF2PP2 are able to meet the codal provision for minimum strength.

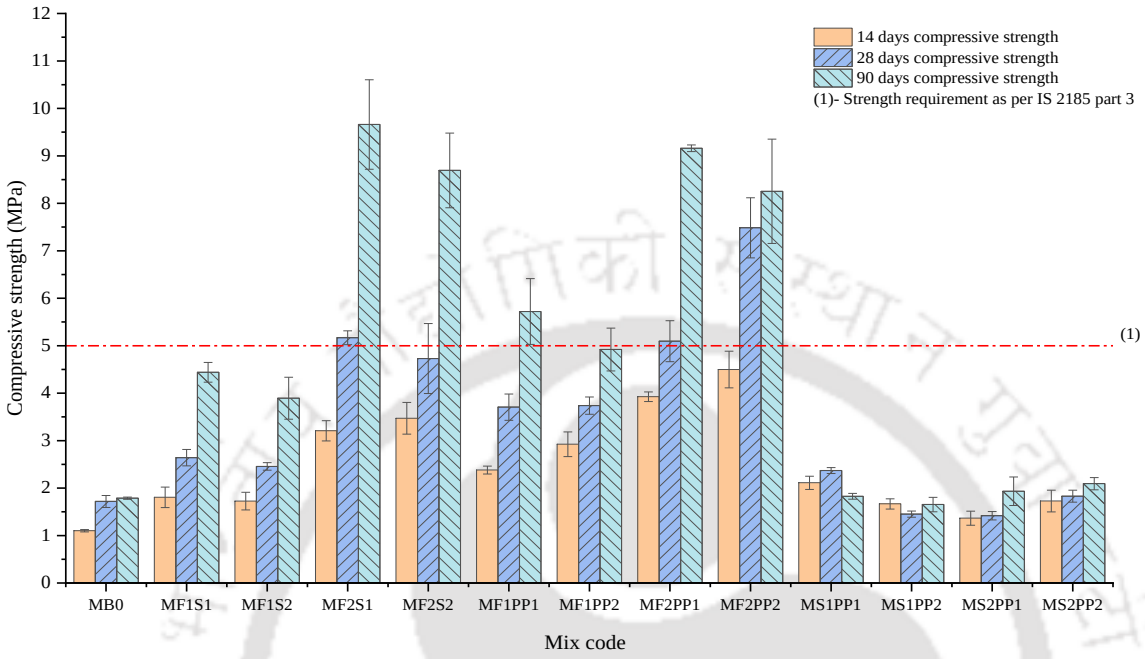

Figure 5-16: Effect of binary admixtures on compressive strength of foam concrete with design density 1000 kg/m^3

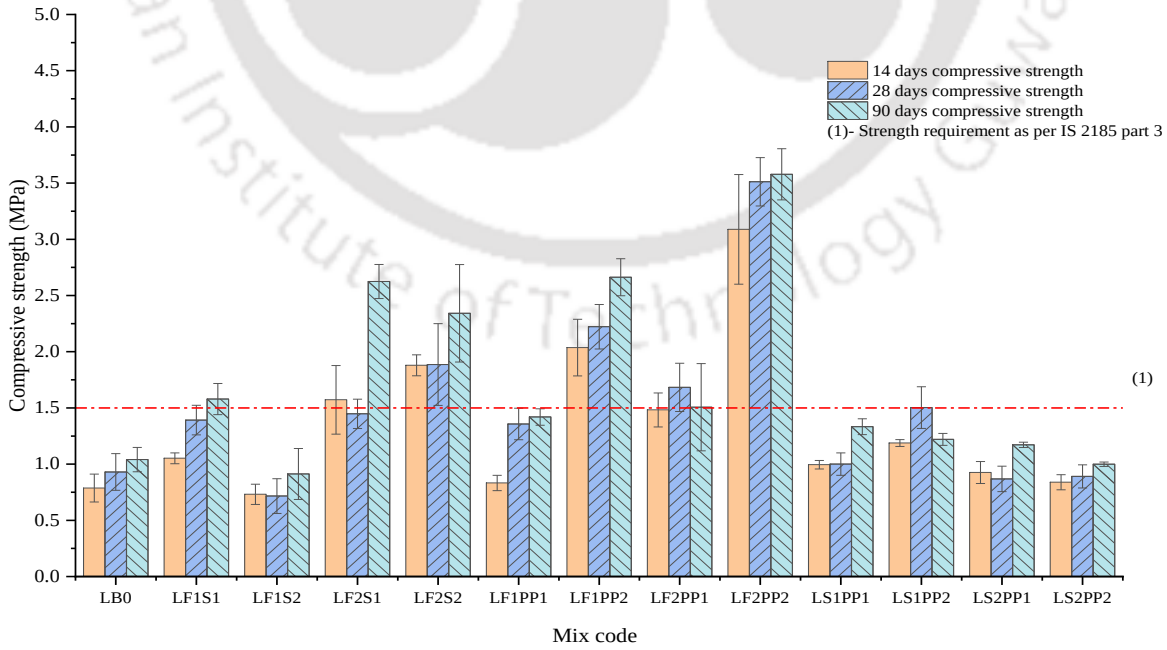

Figure 5-17: Effect of binary admixtures on compressive strength of foam concrete with design density 600 kg/m^3

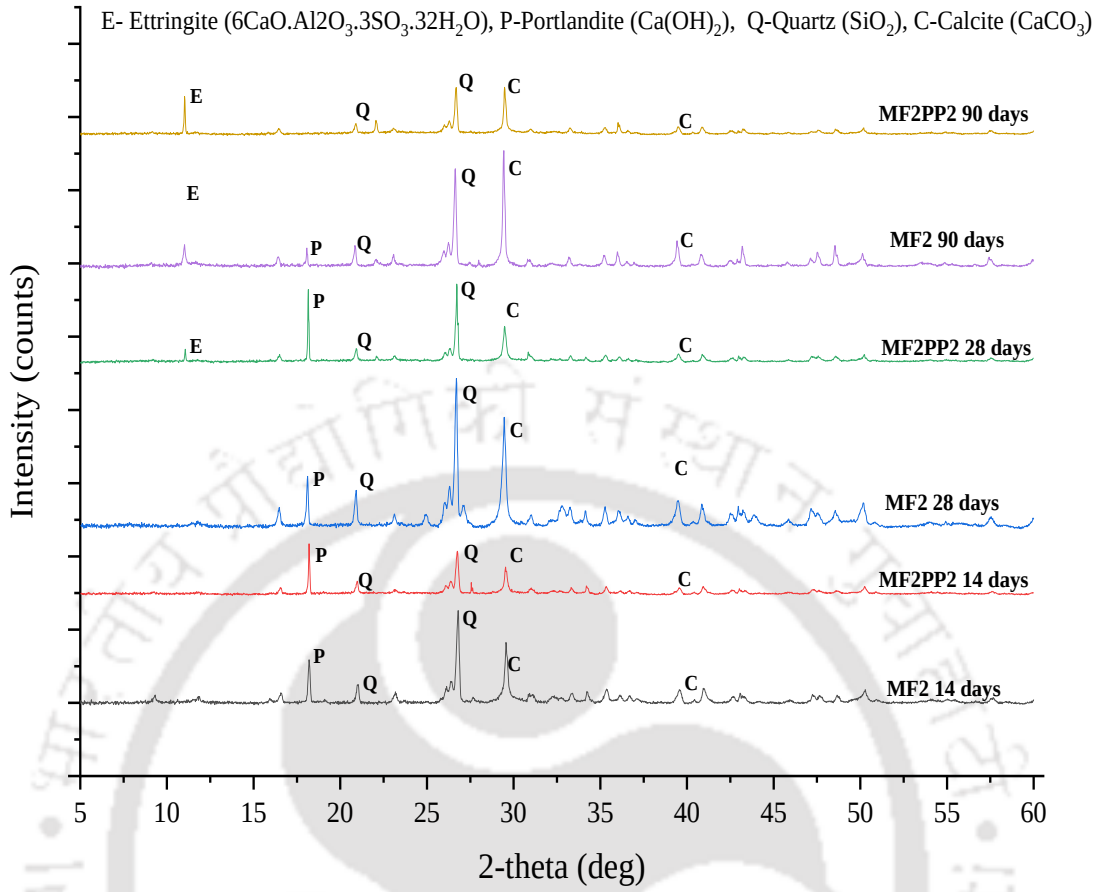

Figure 5-18: XRD pattern of MF2PP2 and MF2 at varying ages of 14 days, 28 days and 90 days

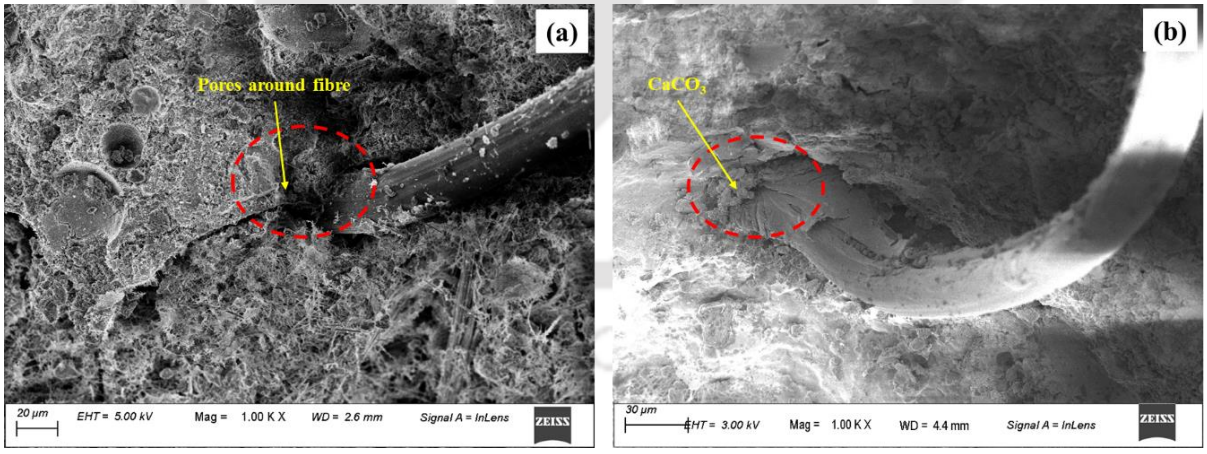

Figure 5-19: SEM image analysis of (a) MF2PP2 at 28 days age (b) MF2PP2 at 90 days age

Level 3 Replacement

Compressive strength for mixes incorporating ternary (combination of three) admixture along with its % increase in strength with respect to base mix at the corresponding ages is represented in Table 5.11. Figure 5.20 and Figure 5.21 represents the effect of incorporation of ternary

admixture i.e. FA + SF + PP fiber on the compressive strength of FC (at ages 14 days, 28 days and 90 days) with densities 1000 kg/m^3 and 600 kg/m^3 respectively.

Table 5-11: Results of Compressive Strength of FC with ternary admixture

Mix code	Compressive strength at 14 days (N/mm^2)	% increase w.r.t base mix (14days)	Compressive strength at 28 days (N/mm^2)	% increase w.r.t base mix (28days)	Compressive strength at 90 days (N/mm^2)	% increase w.r.t base mix (90days)
M0	1.10	0.00	1.72	0.00	1.79	0.00
MF1S1PP1	2.16	96.13	2.57	49.65	4.39	145.52
MF1S1PP2	2.32	110.90	3.10	80.22	4.84	170.90
MF1S2PP1	1.21	10.17	2.28	32.66	4.61	158.21
MF1S2PP2	2.23	102.30	2.75	59.97	4.80	168.66
MF2S1PP1	4.01	263.92	5.11	197.13	9.83	450.00
MF2S1PP2	4.75	331.23	6.58	282.85	8.99	402.99
MF2S2PP1	2.84	157.51	3.71	115.90	6.88	285.07
MF2S2PP2	3.44	212.35	4.46	159.74	6.99	291.04
LB0	0.79	0.00	0.93	0.00	1.04	0.00
LF1S1PP1	1.11	40.97	1.51	62.15	1.59	52.50
LF1S1PP2	1.32	68.28	1.62	74.64	1.93	86.00
LF1S2PP1	0.99	26.43	1.11	19.10	1.48	42.00
LF1S2PP2	1.33	69.16	1.64	75.94	1.90	82.67
LF2S1PP1	2.20	180.18	2.62	181.99	2.97	185.33
LF2S1PP2	2.17	175.33	3.27	251.51	3.93	277.67
LF2S2PP1	1.48	88.55	1.84	97.94	2.16	107.50
LF2S2PP2	2.00	154.63	2.74	194.85	2.81	169.83

The ternary mixes reported the highest compressive strength among all replacement levels for both the design densities1000 kg/m^3 and 600 kg/m^3. This can be ascribed to the synergistic effect of all three admixtures due to which a strength of 9.827 MPa is reported for mix MF2S1PP1 (100%FA + 10SF + 0.2% PP) and a strength of 3.93 MPa is reported for mix LF2S1PP2 (100%FA + 10SF + 0.4% PP) at the age of 90 days for densities 1000 kg/m^3 and 600 kg/m^3 respectively. The mixes MF2S1PP1 and LF2S1PP2 reports an increment in strength of 450% and 278% higher than that of the base mixes. Also the aforementioned mixes in Level 3 replacement category reports 18% and 15% improvement in strength when compared to the mixes exhibiting highest strength in level 1 replacement category for densities 1000 kg/m^3 and 600 kg/m^3 respectively.

In case of M series i.e. 1000 kg/m^3 density, mix MF2S1PP2 reports a higher early age strength of 4.75 MPa and 6.58 MPa at age of 14 days and 28 days respectively. However, at 90 days the MF2S1PP1 reports the highest ultimate strength of 9.827 MPa among all the combinations for

M series. For L series, the highest strength reported is for the combination of 100% FA + 10% SF + 0.4% PP fiber, at all ages. The strength reported for mix LF2S1PP2 is 2.20 MPa, 3.27 MPa and 3.93 MPa at ages 14 days, 28 days and 90 days respectively. The corresponding increment in strength when compared to base mix is found to be 182%, 252% and 278%. The above observations are in line with the results of level 2 replacement category where it is stated that paste plays a predominant role in M series mixes while in L series, mesh network of the fibers with the paste is the major strength governing factor. Similar to level 2 replacement category, the mixes in level 3 replacement category in combination of 100% FA reports 47% to 105% higher compressive strength than mixes in combination with 50%FA for both the densities. The adverse effect of incorporation of the higher % of SF can be noted in the mixes of level 3 replacement category also, where all the corresponding mixes with 20%SF reports decrement in the range of 5% to 52% in compressive strength when compared to mixes with 10% SF. Also it is to be noted that combination mixes with 100%FA and 20%SF shows much more decrement in strength when compared to mixes with 50% FA and 20% SF. This can be ascribed to the increased water demand of the mixes with 20% SF which does not get satisfied thus affecting the progress of hydration of the cement causing strength decrement and this effect gets further intensified in the mixes with 100% of sand replaced with FA.

Here all the M-series mixes in combination with 100%FA are able to meet the strength requirement criteria as per guidelines of IS 2185 part3. While in case of L series except LF1S2PP1 all other mixes are able to satisfy the minimum strength requirement as per IS 2185 part 3.

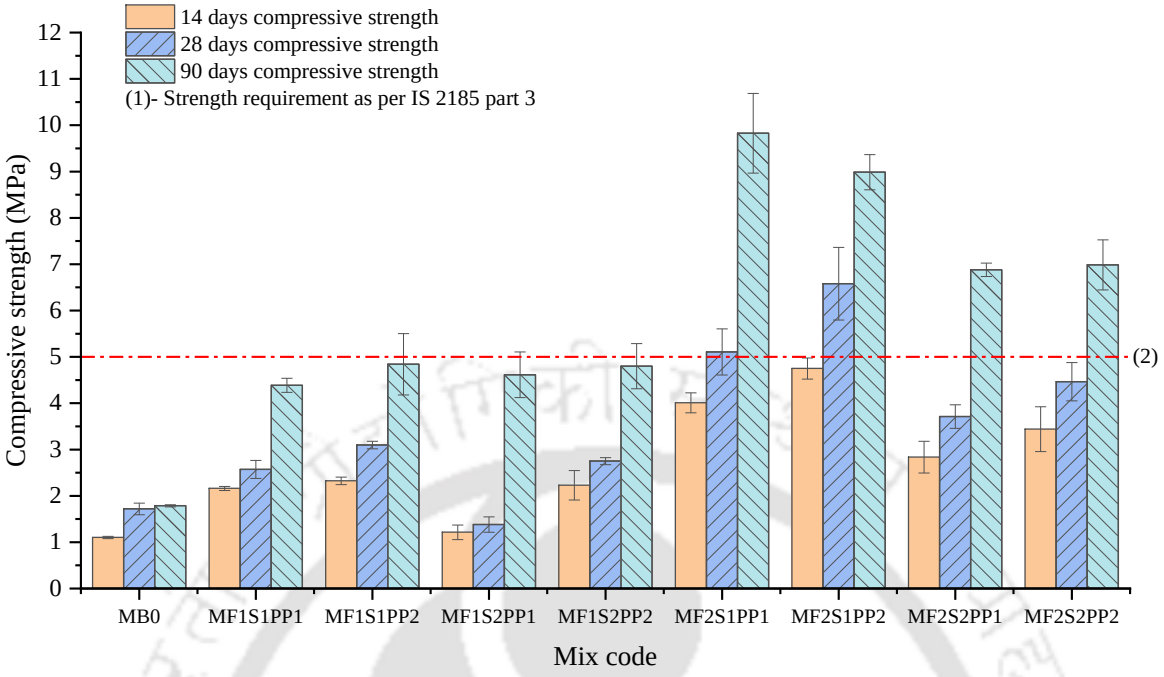

Figure 5-20: Effect of ternary admixtures on compressive strength of foam concrete with design density 1000 kg/m^3

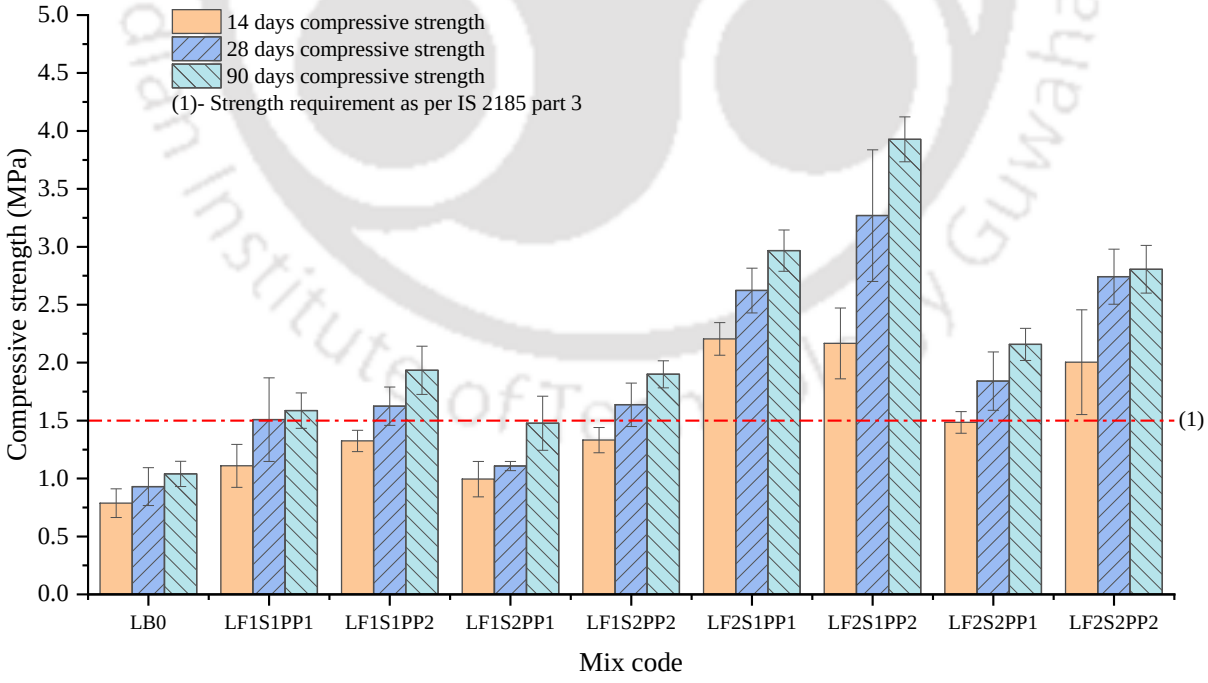

Figure 5-21: Effect of ternary admixtures on compressive strength of foam concrete with design density 600 kg/m^3

5.6.2 Splitting tensile strength

Level 1 Replacement

Table 5.12 provides the results for split tensile strength for mixes incorporating single admixture. Table 5.12, also provides the percentage increment in strength w.r.t. base mix at the respective ages. Figure 5.22 and Figure 5.23 represents the effect of incorporation of single admixture i.e. FA or SF or PP fiber on the split tensile strength of FC (at ages 28 days and 90 days) with densities 1000 kg/m^3 and 600 kg/m^3 respectively.

Table 5-12: Results on split tensile strength of FC with single admixture

Mix code	Split tensile strength at 28 days (N/mm^2)	% Increase w.r.t. base mix (28 Days)	Split tensile strength at 90 days (N/mm^2)	% Increase w.r.t. base mix (90 days)
MB0	0.24	0.00	0.28	0.00
MF1	0.31	32.16	0.68	138.20
MF2	0.45	92.87	0.94	233.15
MS1	0.22	-7.17	0.30	6.18
MS2	0.23	-0.81	0.31	7.87
MPP1	0.24	0.86	0.28	0.00
MPP2	0.25	5.37	0.33	15.17
LB0	0.15	0.00	0.18	0.00
LF1	0.20	29.85	0.33	76.95
LF2	0.26	73.77	0.45	143.56
LS1	0.20	33.85	0.22	21.14
LS2	0.09	-42.38	0.10	-47.43
LPP1	0.26	69.96	0.23	27.21
LPP2	0.28	82.49	0.27	46.45

From Figures 5.22 and 5.23, it can be noted that for base mixes corresponding to FC of design density 1000 kg/m^3 and 600 kg/m^3, the splitting tensile strength of FC increases exponentially with increase in density. The base mix of design density 1000 kg/m^3 reports a 90-day splitting tensile strength of 0.283 MPa, while the corresponding value for the base mix of design density 600 kg/m^3 is 0.184 MPa. The increase in density from 600 kg/m^3 to 1000 kg/m^3 in case of base mixes results in increase of splitting tensile strength by 60% and 54% at ages 28 days and 90 days respectively. The highest splitting tensile strength with single admixture replacement for both the densities i.e. 1000 kg/m^3 and 600 kg/m^3 is reported for mixes MF2 (100% FA replacement) and LF2 (100% FA replacement) at 90-day age which came out to be 0.944 MPa and 0.447 MPa respectively.

The impact of incorporation of FA at varying percentages on splitting tensile strength can be noted in Figures 5.22 and 5.23. Replacement of 50% of sand with FA results in increase in splitting tensile strength by 29% and 138% for M series mix and 33% and 76% for L series

mix, at a testing ages of 28 days and 90 days respectively when compared with corresponding base mixes. Further increase in replacement level say 100% FA results in significant increase of splitting tensile strength by 87% and 234% for M series mixes and 73% and 143% for L series mixes at testing ages of 28 days and 90 days respectively. The increment in the strength reported at 28 days can be primarily ascribed to the particle packing effect of FA resulting from the smaller size FA particles when compared to sand, which densifies the microstructure resulting in higher tensile strength. However, significant increase in splitting tensile strength observed at 90 days can be attributed to the combined effect of delayed pozzolanic reaction of FA particles along with superior particle packing ability. This combined physical and chemical effect further leads to pore structure improvement and subsequent enhancement of the splitting tensile strength of the FC mixtures (Al-Shwaiter et al., 2022; Jones and McCarthy, 2005c).

The effect of incorporation of SF on the splitting tensile strength is represented in Figures 5.22 and 5.23. The partial replacement of cement by SF causes a slight increase in splitting tensile strength when compared to base mixes. M series mixes with 10% SF and 20% SF incorporation reported an almost 12% and 8% increase in splitting tensile strength while for similar SF % incorporation, mixes for L series registered a 20% and 11% increment when compared to base mix at 90-day age. The increase in splitting tensile strength is ascribed to the filler effect and pozzolanic activity of fine silica particles of SF that bring the better and refined distribution of pore structure (S. Zhang et al., 2020).

The trend followed by splitting tensile strength with incorporation of PP fiber can be noted in Figures 5.22 and 5.23. The splitting tensile strength of FC does not show a significant improvement due to addition of PP fibers when compared to addition of FA and SF in case of M series. The mix MPP1 did not show any appreciable improvement in the splitting tensile strength while mix MPP2 showed a 15% improvement in the splitting tensile strength at the age of 90 days. However, when evaluating the effect of PP fiber incorporation on lower density mix i.e. L-series a considerable improvement can be noted. When compared to base mix, mix LPP1 reported 70% and 27% improvement in strength at ages 28 days and 90 days respectively while mix LPP2 reported a significant improvement of 82% and 46% in the splitting tensile strength at ages 28 days and 90 days respectively. Similar results were observed by Bing et.al. where they found that the effect of PP fibers upon increment of splitting tensile strength was more dominant in mixes with higher foam volume (Bing et al., 2012). The increment in splitting tensile strength can be assigned to the enhancement of bonding between the fibres and paste in

L series concrete mixes due to adoption of cement to sand ratio of 1:1 as compared to 1:2 of M series which results in homogenous incorporation of three dimensional PP fibre mesh network into the cement mortar paste system (Jhatial et al., 2021; Mydin et al., 2022). Further, the strength gain can be attributed to the tendency of PP fibres to bridge the micro crack and limit the propagation of the crack when it is subjected to external tensile stress, preventing the cracks from leading to a sudden failure (Jhatial et al., 2020).

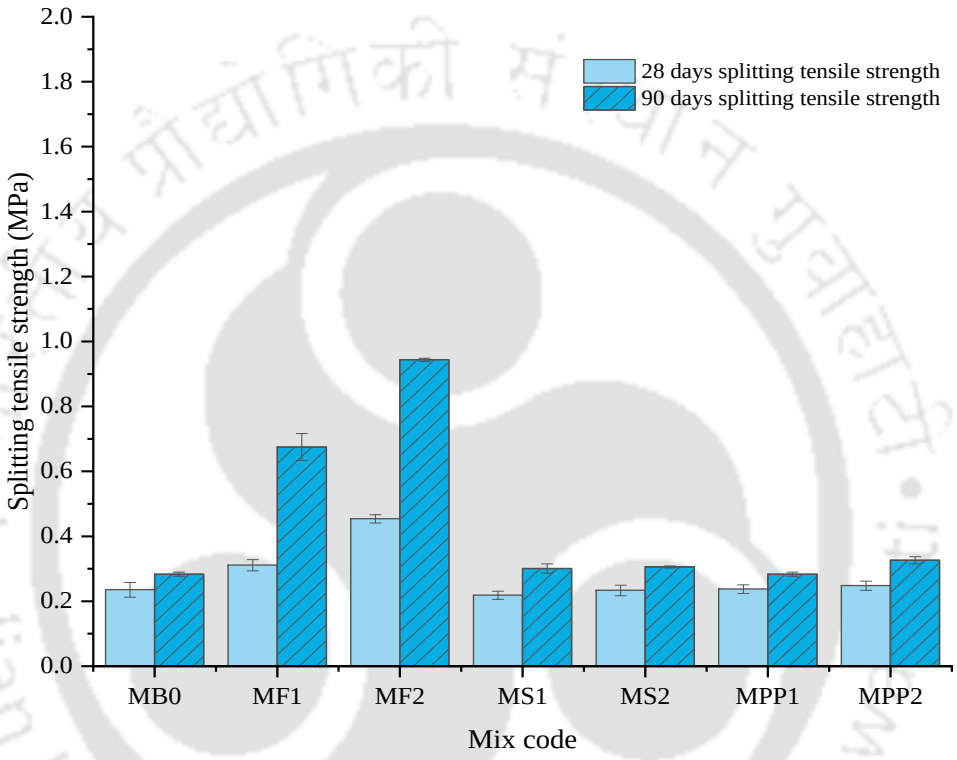

Figure 5-22: Effect of single admixture on split tensile strength of foam concrete with design density 1000 kg/m^3

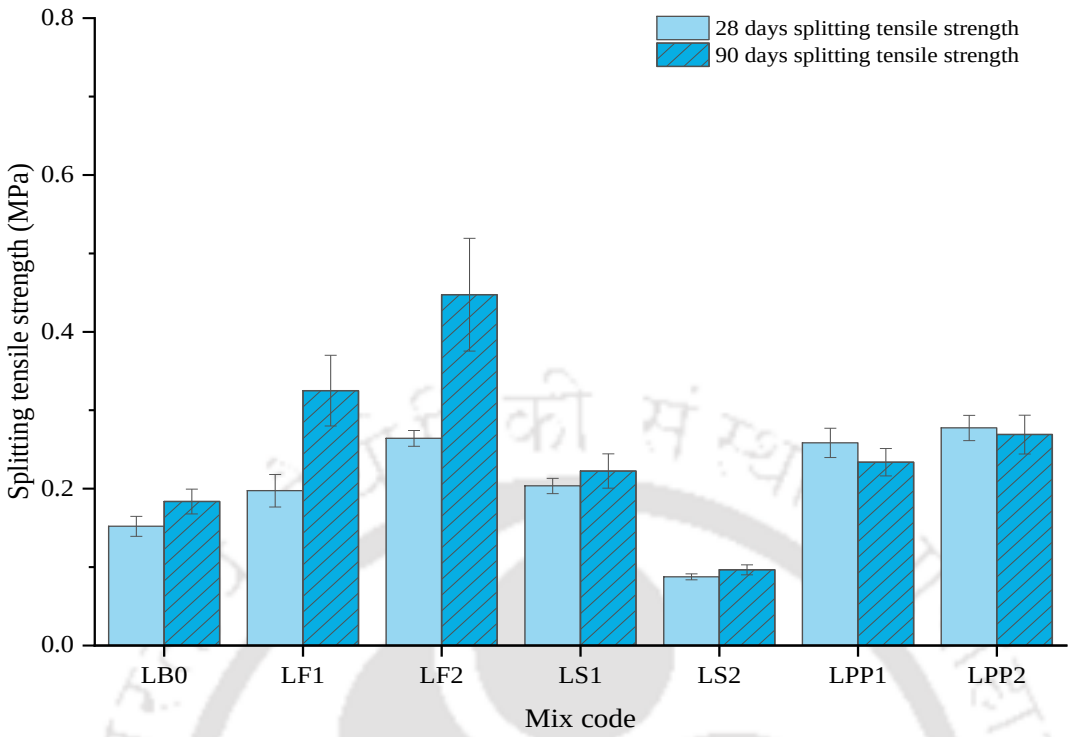

Figure 5-23: Effect of single admixture on split tensile strength of foam concrete with design density 600 kg/m^3

Level 2 Replacement

The results for mixes comprising binary (combination of two) admixtures for Split tensile strength are shown in Table 5.13. Additionally, Table 5.13 shows the % increase in strength with regard to base mix at the corresponding ages. Figure 5.24 and Figure 5.25 represents the effect of incorporation of binary admixture i.e. FA + SF or FA + PP fiber or SF + PP fiber on the Split tensile strength of FC (at ages 28 days and 90 days) with densities 1000 kg/m^3 and 600 kg/m^3 respectively.

The highest split tensile strength for binary admixture replacement for both the densities 1000 kg/m^3 and 600 kg/m^3 is reported for mix with 100% FA and 0.4% PP fibre (F2PP2), at 90-day age. The strengths reported for mixes MF2PP2 and LF2PP2 are 1.658 MPa and 0.694 MPa respectively, which is about 485% and 277% higher than that of the corresponding base mixes. Also the aforementioned mixes in Level 2 replacement category reports 76% and 55% improvement in strength when compared to the mixes exhibiting highest strength in level 1 replacement category for densities 1000 kg/m^3 and 600 kg/m^3 respectively. This can be assigned to the synergistic effect of admixtures in the level 2 replacement category which is discussed further in detail.

Table 5-13: Results on split tensile strength of FC with binary admixture

Mix code	Split tensile strength at 28 days (N/mm^2)	% Increase w.r.t. base mix (28 Days)	Split tensile strength at 90 days (N/mm^2)	% Increase w.r.t. base mix (90Days)
MB0	0.24	0.00	0.28	0.00
MF1S1	0.43	81.60	0.62	118.54
MF1S2	0.28	17.73	0.58	103.93
MF2S1	0.57	142.04	1.36	380.34
MF2S2	0.45	91.38	0.98	247.19
MF1PP1	0.57	140.46	0.94	232.58
MF1PP2	0.60	156.29	0.99	248.31
MF2PP1	0.90	280.51	1.49	424.49
MF2PP2	1.03	336.58	1.66	485.39
MS1PP1	0.41	75.78	0.31	9.55
MS1PP2	0.28	20.66	0.37	30.34
MS2PP1	0.30	28.69	0.35	24.16
MS2PP2	0.31	30.36	0.39	36.52
LB0	0.15	0.00	0.18	0.00
LF1S1	0.24	57.26	0.21	12.65
LF1S2	0.10	-32.30	0.17	-6.24
LF2S1	0.27	79.95	0.45	143.67
LF2S2	0.27	80.85	0.35	89.40
LF1PP1	0.31	102.00	0.36	96.24
LF1PP2	0.46	202.63	0.52	180.50
LF2PP1	0.46	204.17	0.53	187.26
LF2PP2	0.64	318.69	0.59	223.57
LS1PP1	0.26	68.06	0.23	27.21
LS1PP2	0.27	79.40	0.28	50.06
LS2PP1	0.18	21.60	0.24	32.06
LS2PP2	0.24	57.80	0.24	30.67

The effect of incorporation of combination of FA and SF in FC mixes with densities 1000 kg/m^3 and 600 kg/m^3 on splitting tensile strength can be observed in Figure 5.24 and Figure 5.25 respectively. The incorporation of 100% FA (F2) and 10% SF (S1) is reported to be optimum dosage in case of combination of FA and SF mixes for both the design densities. For instance, MF2S1 and LF2S1 mixes reported a maximum splitting tensile strength of 1.36 MPa and 0.45 MPa at the age of 90 days. The corresponding strength recorded an increment of 380% and 144% higher than that of base mixes with similar densities. This can be due to the delayed pozzolanic reaction occurring in the F2S1 mixes leading to the significant increase in the strength. Similar to level 1 replacement mixes, here in level 2 replacement category also mixes in combination with 100% FA provides better strength than that of mixes with 50% FA. This is mainly due to the higher FA content producing additional calcium silicate hydrate (C-S-H)

gel, which has the potential to fill the existing voids and enhance the resulting pore structure. Also its to be noted that in level 2 replacement category, mixes in combination with 10% SF provides better results than that of 20%SF.

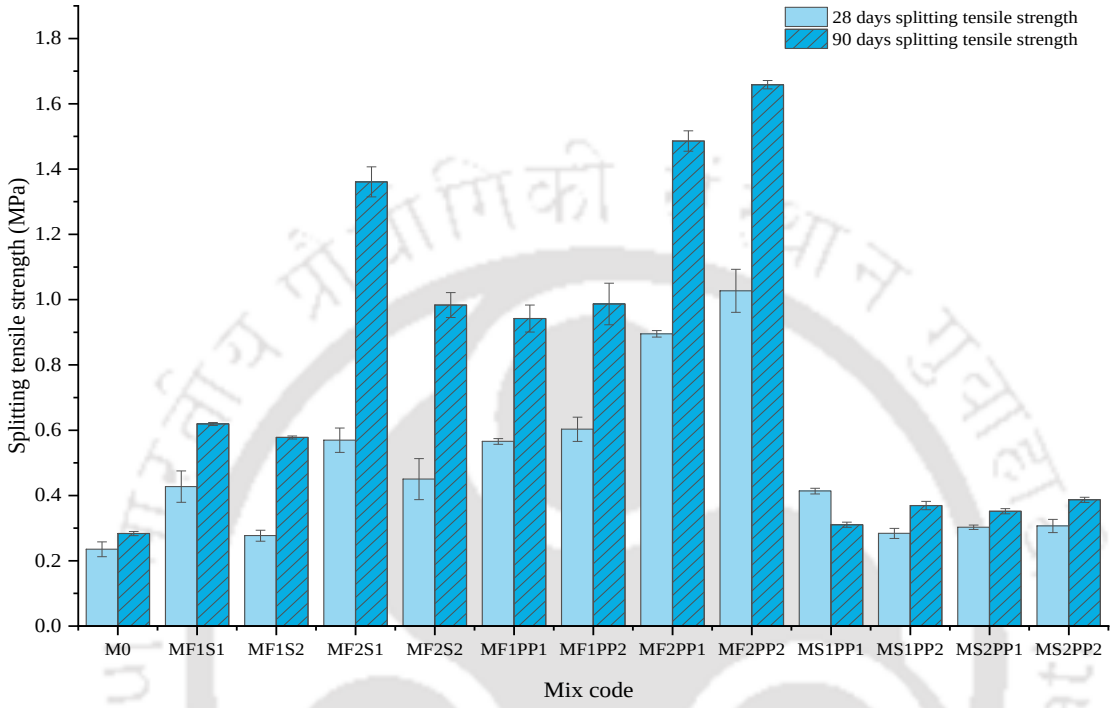

Figure 5-24: Effect of binary admixtures on split tensile strength of foam concrete with design density 1000 kg/m^3

Figures 5.24 and 5.25 describes the effect of incorporation of FA in combination with PP fibers on splitting tensile strength development of FC with densities 1000 kg/m^3 and 600 kg/m^3. In case of M series i.e. 1000 kg/m^3 density, mix MF2PP2 (100% FA and 0.4% PP) reported the highest split tensile strength in level 2 replacement category. The strength observed for MF2PP2 is 1.03 MPa and 1.66 MPa at the age of 28 days and 90 days respectively. The corresponding increment in strength is found to be 337% and 485% more than that of base mix. For L series, the highest strength reported in entire Level 2 replacement category is for the combination of 100% FA and 0.4% PP fiber, at all ages. The strength reported for mix LF2PP2 is 0.64 MPa, and 0.69 MPa at ages 28 days and 90 days respectively. The corresponding increment in strength is found to be 319% and 278% more than that of the base mix. The splitting tensile strength reported for LF2PP2 and MF2PP2 is almost 55% to 75% more than that of only F2

mixes while 158% to 408% more than that of only PP2 mixes. This can be attributed to the increased fiber and paste bond of the FA and PP fiber mixes.

Experimental outcomes indicate that the combination of SF and PP fibre show significant impact on splitting tensile strength development of FC when compared to mixes with only SF. The highest splitting tensile strength achieved in this combination is by mixes MS2PP2 and LS1PP2 which is 0.39 MPa and 0.28 MPa at the age of 90 days respectively. The corresponding increment in strength reported is 37% and 50% when compared to base mix at same age and similar densities. Similar to FA and PP fibres mixes the increment in the splitting tensile strength can be attributed to the enhanced fibre matrix interface as discussed in literature (Gencel et al., 2022b).

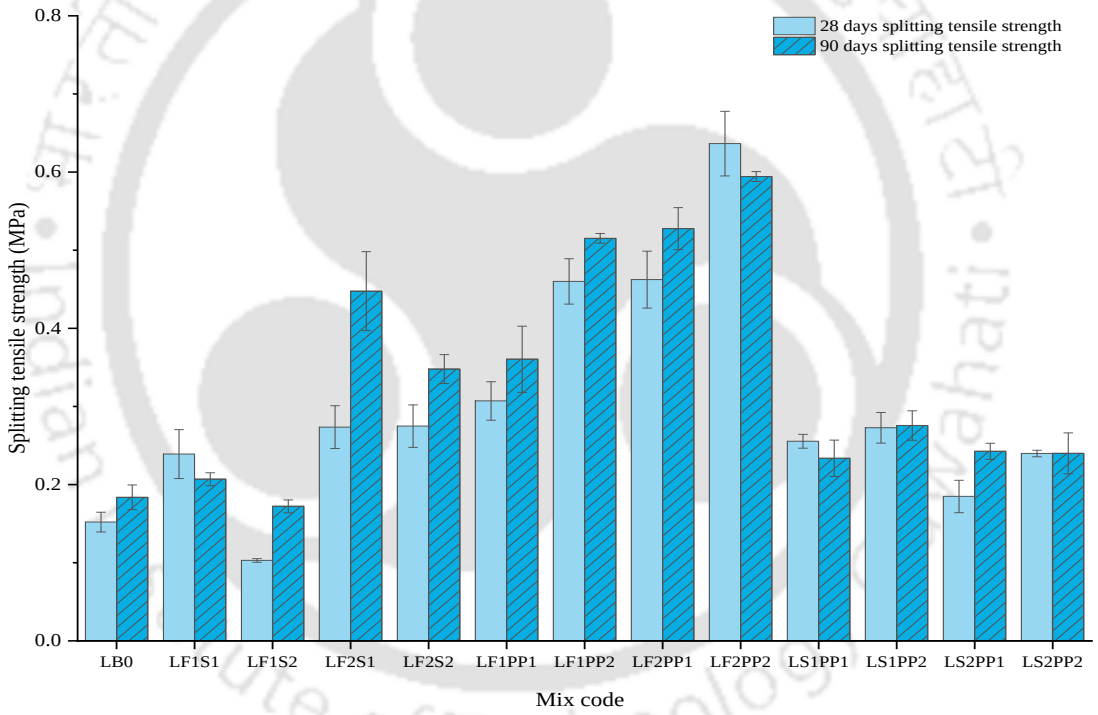

Figure 5-25: Effect of binary admixtures on split tensile strength of foam concrete with design density 600 kg/m^3

Level 3 Replacement

Split tensile strength for mixes incorporating ternary (combination of three) admixture along with its % increase in strength with regard to base mix at the corresponding ages is represented in Table 5.14. Figure 5.26 and Figure 5.27 represents the effect of incorporation of ternary admixture i.e. FA + SF + PP fiber on the Split tensile strength of FC (at ages 28 days and 90 days) with densities 1000 kg/m^3 and 600 kg/m^3 respectively. The ternary mixes reported the

highest splitting tensile strength among all replacement levels for both the design densities1000 kg/m^3 and 600 kg/m^3. The mixes MF2S1PP2 (100%FA + 10SF + 0.4% PP) and mix LF2S1PP2 (100%FA + 10SF + 0.4% PP) reported a splitting tensile strength of 1.67 MPa and 0.70 MPa at the age of 90 days for densities 1000 kg/m^3 and 600 kg/m^3 respectively. This can be ascribed to the synergistic effect of all three admixtures due to which mixes MF2S1PP2 and LF2S1PP2 reported an increment of 490% and 281% in strength when compared to base mixes. Also the aforementioned mixes in Level 3 replacement category reports 77% and 57% improvement in strength when compared to the mixes exhibiting highest strength in level 1 replacement category for densities 1000 kg/m^3 and 600 kg/m^3 respectively.

Table 5-14: Results on split tensile strength of FC with ternary admixture

Mix code	Split tensile strength at 28 days (N/mm^2)	% Increase w.r.t. base mix (28 Days)	Split tensile strength at 90 days (N/mm^2)	% Increase w.r.t. base mix (90Days)
MB0	0.24	0.00	0.28	0.00
MF1S1PP1	0.48	103.65	0.89	215.17
MF1S1PP2	0.57	140.60	0.91	221.91
MF1S2PP1	0.42	78.55	0.86	202.81
MF1S2PP2	0.54	130.27	0.90	219.10
MF2S1PP1	0.70	199.05	1.44	409.55
MF2S1PP2	0.92	292.56	1.67	489.89
MF2S2PP1	0.60	153.99	1.37	382.02
MF2S2PP2	0.81	244.56	1.34	373.60
LB0	0.15	0.00	0.18	0.00
LF1S1PP1	0.27	78.68	0.29	55.69
LF1S1PP2	0.37	143.74	0.40	118.48
LF1S2PP1	0.22	42.01	0.29	59.67
LF1S2PP2	0.38	152.36	0.41	120.39
LF2S1PP1	0.42	174.50	0.56	205.85
LF2S1PP2	0.54	252.00	0.66	259.04
LF2S2PP1	0.37	146.46	0.44	139.51
LF2S2PP2	0.49	225.05	0.57	209.79

Figures 5.26 and 5.27 illustrates the pattern of splitting tensile strength development with the incorporation of FA in combination with SF and PP fibers for densities 1000 kg/m^3 and 600 kg/m^3 respectively. In case of M series i.e. 1000 kg/m^3 density mix MF2S1PP2 reported highest splitting tensile strength of 0.92 and 1.671 MPa at age of 28 days and 90 days respectively. For L series, the highest splitting tensile strength reported is by the mix LF2S1PP2 which is observed to be 0.54 and 0.701 MPa at ages 28 days and 90 days respectively. The corresponding increment in strength is found to be 252% and 281% when compared with corresponding base

mixes. Similar to the results observed in compressive strength, of level 3 replacement category combination of 100% FA reported 54% to 83% higher splitting tensile strength than mixes in combination with 50%FA for both the densities. The adverse effect of incorporation of the higher % of SF can be noted in the mixes of level 3 replacement category also, where all the corresponding mixes with 20%SF reported a decrement of up to 25% in splitting tensile strength when compared to mixes with 10% SF.

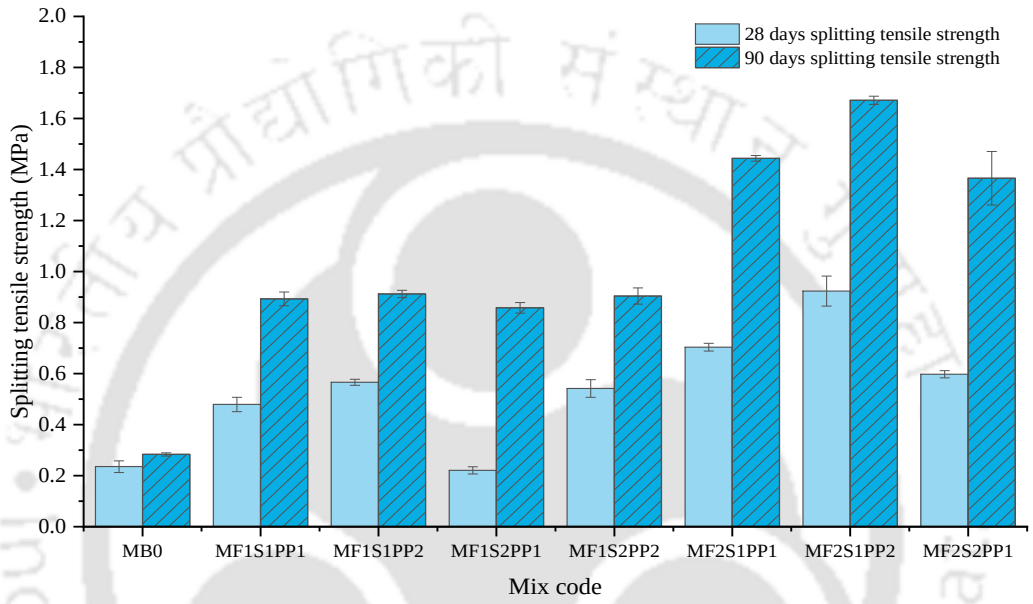

Figure 5-26: Effect of ternary admixtures on split tensile strength of foam concrete with design density 1000 kg/m^3

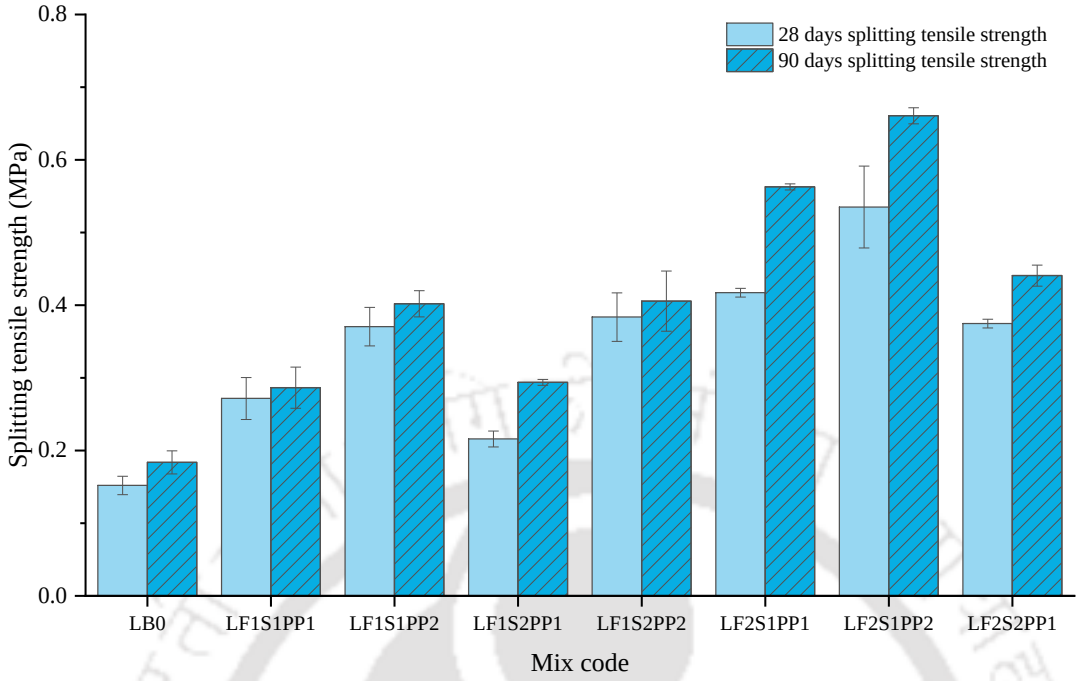

Figure 5-27: Effect of ternary admixtures on split tensile strength of foam concrete with design density 600 kg/m^3

5.6.3 Thermal Properties

The following sections are going to discuss the influence of admixtures (FA, SF, PP fibre) at different levels of replacement on the various thermal properties of FC like thermal conductivity (k-value) measured in W/m K, thermal diffusivity (α-value) expressed in terms of m^2/s and specific heat (C-value) expressed in terms of J/kg K.

Level 1 Replacement

The thermal properties of mixes incorporating single admixture is presented in Table 5.15. Figure 5.28 represents the effect of incorporation of single admixture i.e. FA or SF or PP fiber on the thermal conductivity (TC) of FC with design fresh densities 600 kg/m^3 and 1000 kg/m^3. In Figure 5.28, two limits are provided in accordance to IS 2185 part 3. Line no. 1 represented by blue color, is the maximum TC limit (0.37 W/mK) for the autoclaved cellular concrete blocks with oven dry density 751 kg/m^3 to 850 kg/m^3. This category is in close resemblance to the FC with design fresh density 1000 kg/m^3 having oven dry density in the similar range. Line no. 2 represented by red color, is the maximum TC limit (0.21 W/mK) for AAC blocks with oven dry density ranging from 451 to 550 kg/m^3. This category is in close resemblance to the FC with design density 600 kg/m^3 having oven dry density in the similar range.

Table 5-15: Thermal properties of FC with single admixture

Mix code	Thermal Conductivity (W/mK)	Thermal Diffusivity (m^2/s)	Specific Heat (J/kgK)	Oven dry density (kg/m^3)
MB0	0.3435	8.10E-07	523.30	810.67
MF1	0.3056	6.42E-07	639.84	744.00
MF2	0.2869	5.23E-07	685.16	800.00
MS1	0.3120	6.58E-07	546.81	866.67
MS2	0.3154	6.82E-07	587.46	786.67
MPP1	0.3234	7.17E-07	556.06	810.67
MPP2	0.3243	7.78E-07	522.51	797.33
LB0	0.2476	9.88E-07	406.29	616.83
LF1	0.2598	7.43E-07	503.85	694.29
LF2	0.2373	7.17E-07	509.06	650.13
LS1	0.2292	6.80E-07	553.78	608.43
LS2	0.2239	6.77E-07	633.28	522.56
LPP1	0.2438	8.33E-07	521.04	561.81
LPP2	0.2394	9.01E-07	538.64	493.12

Considering the effect of mix composition on thermal conductivity of FC, it is observed that density plays an important role as established in literature (Wagh et al., 2021). It is to be noted that, in case of thermal conductivity, the foam volume i.e. air content is the major governing factor. For base mix, with the increase in density from 600 kg/m^3 to 1000 kg/m^3 the TC of FC increases from 0.2476 W/mK to 0.3435 W/mK. This accounts for about 39% increment in TC with density. Although the incorporation of the admixtures affects the microstructure of the FC which in turn affect the TC but the density has a major influence on the thermal properties of FC.

Figure 5.28 shows that replacement of sand with FA results in decrement in TC of FC. In case of M series, a replacement of 50% of sand with FA results in reduction of 11% in TC of FC. Upon further increase in replacement level by 100% TC reduces by 17% when compared to base mix MB0. The improvement of concrete microstructure with reduced pore diameter and formation of more number of smaller pores due to particle packing effect of fine FA particles contributes to the above mentioned decrease in TC. The above observations supports the well-established fact that TC is highly dependent on the pore microstructure (Al-Shwaiter et al., 2022; Hajimohammadi et al., 2018; X. Zhang et al., 2020). These results are in line with the previous findings of research which have replaced filler with FA and rice husk ash etc. (Al-Shwaiter et al., 2022; Jones et al., 2003; Yue and Bing, 2015). In case of L series similar observation is reported where a reduction of 5% in TC can be observed for FC with 100% of

sand replaced with FA. However, in case of F1 (50% FA) mix due to the instability of fresh FC leading to increased demoulded density, a slight increment of 5% in TC is noted.

Incorporation of SF as a partial replacement of cement lead to slight decrement in TC of FC. Incorporation of SF provided up to 10% decrement in TC of FC for both the design densities 1000 kg/m^3 and 600 kg/m^3. This decrement can be attributed to the creation of the finer pores due to addition of SF in the mixture (Cong and Bing, 2015). Similar results were reported by Demirboğa and Gül, (2003) and Şeker et al., (2022). Further while evaluating the effect of addition of PP fibre on TC of FC a similar trend is observed. A decrement of 6% in TC is observed for M series mixes while a reduction in TC up to 3% is reported for L series mixes. This slight decrement in TC can be assigned due to the generation of additional voids and increase in porosity of FC after incorporation of PP fibres. Generally, the hydrophobic nature of PP fibres tends to retain water on its surface leading to creation of additional pores as the concrete solidifies, and this can be attributed to the above mentioned slight reduction in TC of FC (Gencel et al., 2021; Jhatial et al., 2020). Also it is to be noted that all the M-series mixes are able to fulfil the TC criteria as per IS 2185 part 3 and the reported TC values are lower than the requirement. While none of the L series mixes are able to meet the required criteria of the IS 2185 Part 3.

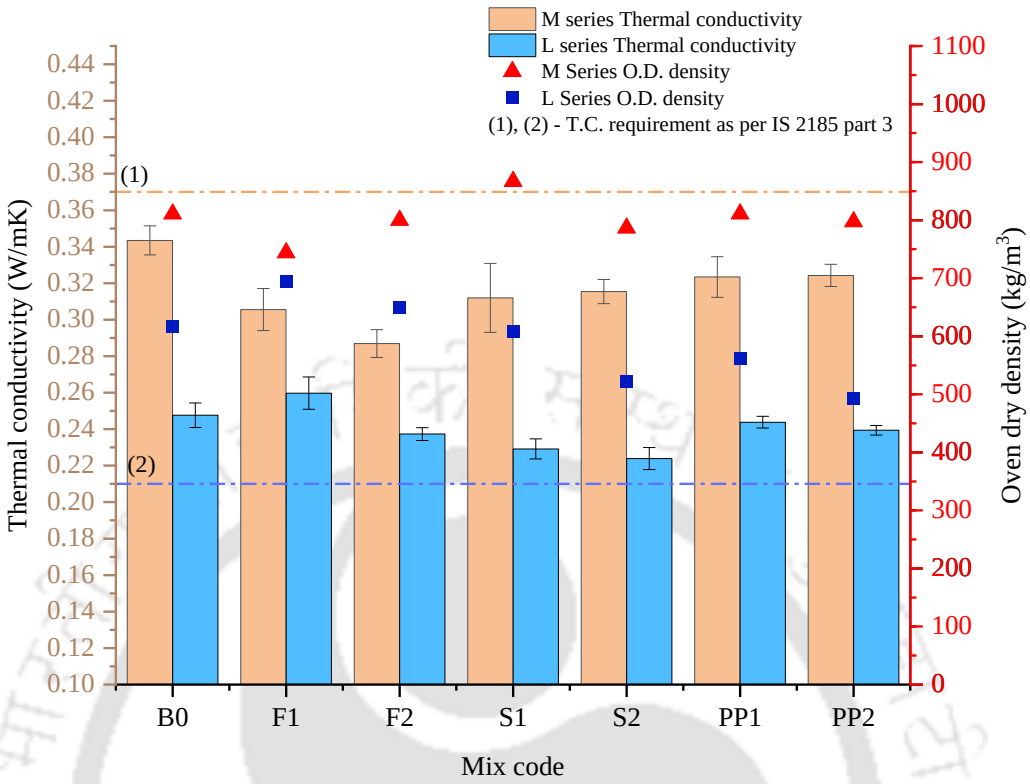

Figure 5-28: Effect of Single admixture on thermal conductivity of FC with design density 600 kg/m^3 and 1000 kg/m^3

Level 2 Replacement

The TC results of mixes comprising binary (combinations of two) admixtures are shown in Table 5.16. Figure 5.29 represents the effect of incorporation of binary admixture i.e. FA + SF or FA + PP fiber or SF + PP fiber on the TC of FC with design densities 1000 kg/m^3 and 600 kg/m^3.

The synergistic effect of the combination of two admixtures causes the further additional decrement in the TC of the both M series and L series mixes compared to Level 1 replacement mixes. The mixes with the combination of 100% FA and 0.4% PP fibre (F2PP2) shows the lowest TC of 0.2959 W/mK for M series mixes and 0.1973 W/mK in case of L series mixes. The corresponding percentage decrement reported is 14% and 20% with respect to base mix. This reduction can be assigned to the better pore structure created by the incorporation of FA and creation of additional voids due to PP fibres addition. Further, the mixes with combination of FA and SF also shows a significant reduction in TC values, with MF2S1 and LF2S1 reporting

the lowest TC in this particular combination. The reported percentage decrement in TC values of MF2S1 and LF2S1 when compared to base mixes are 12% and 18% respectively. In addition, all the M-series mixes are able to meet the requirement of the IS 2185 part 3 and some of the L series mixes are also able meet the criteria. LF2S1, LF2S2, LF1PP1, LF1PP2, LF2PP1, LF2PP2, LS1PP1, LS1PP2, LS2PP1 and LS2PP2 are able to meet the TC requirement set by IS 2185 part 3.

Table 5-16: Thermal properties of FC with binary admixture

Mix code	Thermal Conductivity (W/mK)	Thermal Diffusivity (m^2/s)	Specific Heat (J/kgK)	Oven dry density (kg/m^3)
MB0	0.3435	8.10E-07	523.30	810.67
MF1S1	0.3067	7.34E-07	530.88	786.67
MF1S2	0.3398	6.37E-07	682.60	781.33
MF2S1	0.2911	5.45E-07	643.87	829.33
MF2S2	0.3056	5.51E-07	659.61	840.00
MF1PP1	0.3264	6.68E-07	565.48	864.00
MF1PP2	0.3411	7.28E-07	576.22	813.33
MF2PP1	0.3073	5.03E-07	695.77	877.33
MF2PP2	0.2959	5.68E-07	616.23	845.33
MS1PP1	0.3296	7.60E-07	533.34	813.33
MS1PP2	0.3264	8.21E-07	490.50	810.67
MS2PP1	0.3188	6.52E-07	626.12	781.33
MS2PP2	0.3268	6.22E-07	637.82	824.00
LB0	0.2476	9.88E-07	406.29	616.83
LF1S1	0.2204	8.53E-07	519.12	498.03
LF1S2	0.2105	8.32E-07	477.42	529.92
LF2S1	0.1919	5.91E-07	678.51	478.40
LF2S2	0.1967	5.87E-07	675.97	495.57
LF1PP1	0.2207	7.37E-07	678.04	441.60
LF1PP2	0.2166	6.11E-07	656.96	539.73
LF2PP1	0.2120	6.20E-07	737.74	463.68
LF2PP2	0.1973	6.82E-07	574.92	502.93
LS1PP1	0.1986	8.76E-07	473.60	478.40
LS1PP2	0.2014	7.77E-07	518.00	500.48

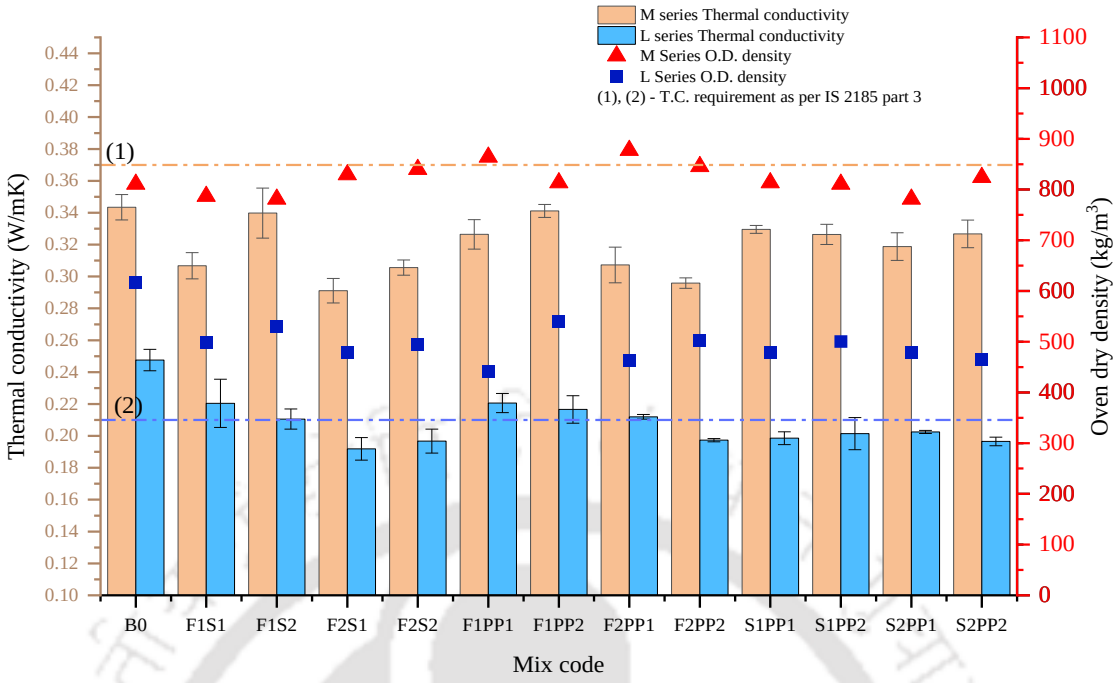

Figure 5-29: Effect of binary admixtures on thermal conductivity of FC with design density 600 kg/m^3 and 1000 kg/m^3

Level 3 Replacement

Thermal conductivity for mixes incorporating ternary (combination of three) admixtures is represented in Table 5.17. Figure 5.30 represents the effect of incorporation of ternary admixture i.e. FA + SF + PP fiber on the TC of FC with design densities 1000 kg/m^3 and 600 kg/m^3.

The results on the TC of FC mixes comprising of ternary admixture i.e. combination of FA + SF + PP fiber is shown in Figure 5.30. Due to synergistic effect of all three admixtures, the TC values reported for level 3 category mixes are lower when compared to level 1 and level 2 mixes. The lowest TC value of 0.2869 W/mK is noted for M series mix with F2S2PP2 (100%FA+20%SF+0.4%PP fiber) combination, while the lowest TC value for L series mix is 0.1880 W/mK for F2S2PP1 (100%FA+20%SF+0.2%PP fiber) combination. Since all the mixes in this category incorporates FA replacement in the range of 50% or 100% the effect of FA can be clearly noted in TC values of all the level 3 mixes. Similar to level 2 replacement category, the mixes in level 3 replacement category with combination of 100% FA reported much lower TC values than mixes in combination with 50% FA for both the densities. Mixes with 100% FA are able to report about 5% lower TC values than that of mixes with 50%FA. In level 3 replacement category all the M-series mixes as well as all the L-series mixes are below the maximum TC limit set by IS 2185 part 3.

Table 5-17: Thermal properties of FC with ternary admixture

Mix code	Thermal Conductivity (W/mK)	Thermal Diffusivity (m^2/s)	Specific Heat (J/kgK)	Oven dry density (kg/m^3)
MB0	0.3435	8.10E-07	523.30	810.67
MF1S1PP1	0.3196	6.40E-07	627.40	837.33
MF1S1PP2	0.3092	6.82E-07	612.44	778.67
MF1S2PP1	0.3109	6.64E-07	634.97	776.00
MF1S2PP2	0.3005	6.69E-07	563.13	840.00
MF2S1PP1	0.2966	5.32E-07	618.78	901.33
MF2S1PP2	0.2963	5.16E-07	691.70	829.33
MF2S2PP1	0.2896	5.38E-07	685.76	776.00
MF2S2PP2	0.2869	5.26E-07	692.48	792.00
LB0	0.2476	9.88E-07	406.29	616.83
LF1S1PP1	0.2058	8.21E-07	535.06	468.59
LF1S1PP2	0.2095	7.22E-07	635.60	456.32
LF1S2PP1	0.2039	8.00E-07	535.75	475.95
LF1S2PP2	0.1998	6.98E-07	604.72	473.49
LF2S1PP1	0.1961	6.69E-07	656.07	446.51
LF2S1PP2	0.1914	5.84E-07	652.12	502.93
LF2S2PP1	0.1880	5.47E-07	766.04	448.96
LF2S2PP2	0.1995	5.53E-07	709.68	507.84

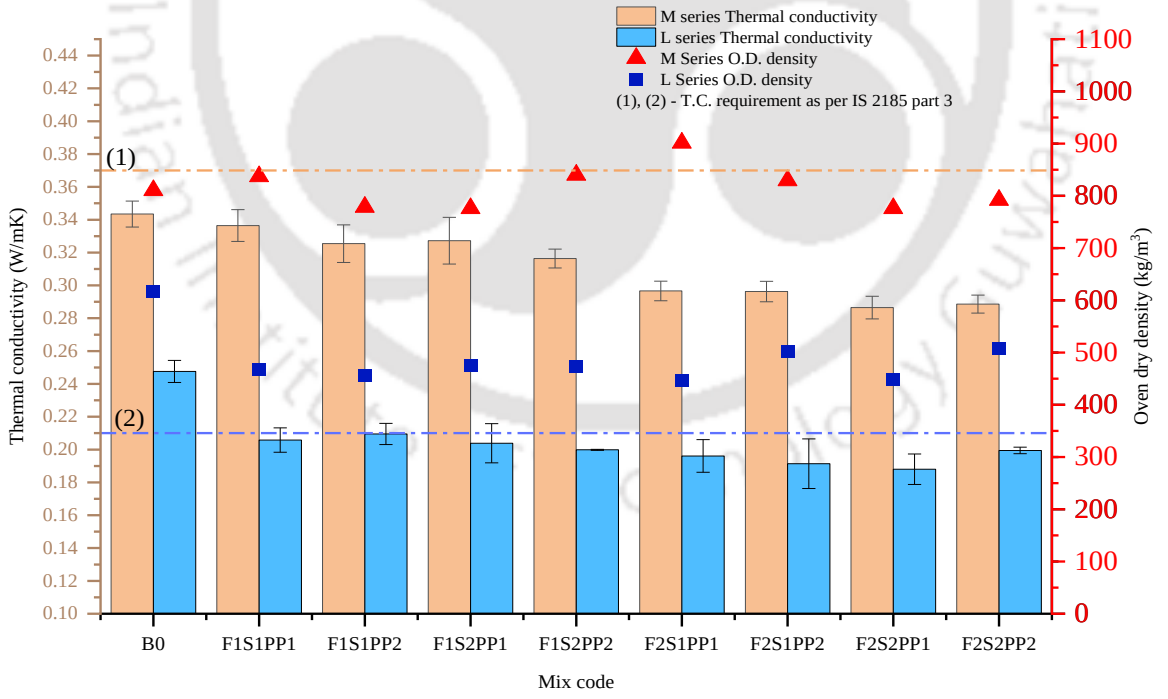

Figure 5-30: Effect of ternary admixtures on thermal conductivity of FC with design density 600 kg/m^3 and 1000 kg/m^3

5.7 Selection of the suitable optimum mix

To evaluate the effect of different admixtures (FA, SF and PP fibre) on various properties of FC, 27 mixes are casted each for density 600 kg/m^3 and 1000 kg/m^3. These mixes comprised of single admixture, combination of binary admixtures as well as ternary admixtures. Out of these variety of mixes, one best optimum mix shall be selected for each density, based upon the material cost and performance shown in fresh state, compressive strength test, split tensile test, Thermal conductivity test and various characteristics shown in microstructural properties. Table 5.18 provides the material cost of each ingredient used for the production of the FC mixes. The material cost is considered based upon the price quoted at the retailer's end. The following section discusses in detail with respect to the various parameters considered for the selection of the best optimum mix. The criteria and the corresponding weightage assigned for the optimization process are listed below.

Criteria: -

1) To achieve a minimum compressive strength of 5MPa and 1.5 MPa for FC with design density 1000 kg/m^3 and 600 kg/m^3 respectively (IS 2185 Part 3).
2) To attain the thermal conductivity, below the maximum prescribed limit of 0.37 W/mK and 0.21 W/mK for FC mixes with design density 1000 kg/m^3 and 600 kg/m^3 respectively (IS 2185 Part 3).

Optimization: -

All the mixes which are able to meet the aforementioned codal guidelines are considered for the further optimization process as listed in Table 5.19 and Table 5.20. The parameter considered for the optimization process are as follows: -

1) To minimize the material cost required for the production of per cubic meter of the FC mix (Weightage: 4/5)
2) To maximize the 28 days and 90 days compressive strength of FC mix (Weightage: - 3/5)
3) To maximize the 28 days and 90 days split tensile strength of FC mix (Weightage: - 3/5)
4) To minimize thermal conductivity of the FC mix samples (Weightage: - 5/5)

   Finally, the best optimum mixes are then selected based upon the average weighted score obtained.

Table 5.19 and Table 5.20 also provides the per cubic meter cost incurred by the FC mixes along with the various properties of those mixes. Weighted average score out of 100 for the mixes are represented in the last column based upon which the best optimum mix selection is carried out.

Table 5-18: Material cost of the mix ingredients

Cement	Sand	Flyash	Silica fume	PP fibre	Water	SP	Surfactant
₹ 8.6/kg	₹ 2/kg	₹ 2.5/ kg	₹ 38/kg	₹ 180/kg	₹ 0.1/litre	₹ 90/kg	₹ 6.83/kg

Table 5-19: Selection of optimised mix for FC with design density 1000 kg/m^3

Mix code	Cost (₹/m^3)	28-day compressive strength (MPa)	90-day compressive strength (MPa)	28-day split tensile (MPa)	90-day split tensile (MPa)	Thermal conductivity (W/mK)	Weighted average score
MF2	3794.84	4.40	8.360	0.45	0.94	0.2869	55.21
MF2S1	4639.60	5.17	9.661	0.57	1.36	0.3011	58.70
MF2S2	5484.36	4.73	8.693	0.45	0.98	0.3056	34.46
MF1PP1	4040.09	3.71	5.720	0.57	0.94	0.3264	20.84
MF2PP1	4137.89	5.09	9.160	0.90	1.49	0.3073	67.21
MF2PP2	**4664.73**	**7.48**	**8.253**	**1.03**	**1.66**	**0.2959**	**82.44**
MF2S1PP1	5097.51	5.11	9.827	0.70	1.44	0.2966	63.15
MF2S1PP2	5461.53	6.58	8.987	0.92	1.67	0.2963	73.06
MF2S2PP1	5893.06	3.71	6.880	0.60	1.37	0.2896	41.87
MF2S2PP2	6301.44	4.46	6.987	0.81	1.34	0.2869	48.36

Table 5-20: Selection of optimised mix for FC with design density 600 kg/m^3

Mix code	Cost (₹/m^3)	28-day compressive strength (MPa)	90-day compressive strength (MPa)	28-day split tensile (MPa)	90-day split tensile (MPa)	Thermal conductivity (W/mK)	Weighted average score
LF2S1	3632.67	1.95	2.62	0.3	0.45	0.2019	40.42
LF2S2	4325.43	1.89	2.34	0.3	0.35	0.2067	23.31
LF2PP1	3261.93	1.68	2.51	0.5	0.53	0.2120	41.37
LF2PP2	**3743.32**	**3.79**	**3.90**	**0.6**	**0.69**	**0.1973**	**84.21**
LF1S1PP1	3781.76	1.51	1.59	0.3	0.29	0.2058	22.74
LF1S1PP2	4262.04	1.62	1.93	0.4	0.40	0.2095	22.80
LF1S2PP2	4245.34	1.64	1.90	0.4	0.41	0.1998	34.11
LF2S1PP1	3993.79	2.62	2.97	0.4	0.56	0.1961	57.88
LF2S1PP2	4394.03	3.27	3.93	0.5	0.70	0.1914	75.75
LF2S2PP1	4724.51	1.84	2.16	0.4	0.44	0.1880	44.63
LF2S2PP2	5123.20	2.74	2.81	0.5	0.57	0.1995	45.15

Based on the optimization studies, the mixes satisfying the above mentioned criteria's and showing overall best performance across all the parameters are MF2PP2 and LF2PP2 for design densities 1000 kg/m^3 and 600 kg/m^3 respectively. For the next chapter, which provides

an in-depth investigation into the operational energy analysis for G+3 residential building and its LCA the abovementioned optimum mixes shall be considered along with the base mixes (for comparative analysis purposes).

5.8 Summary

The influence of incorporation of FA, PP fibers (PP), and SF in FC mixes is compared with base mixes (FC without any admixture), for two different design densities (600 kg/m^3 and 1000 kg/m^3). It is observed that all the mixes with target density 1000 kg/m^3 are able to achieve the allowable density ratios (0.95 to 1.05), while some of the mixes in much lower density i.e. 600 kg/m^3 exceeded the allowable density ratio. Incorporation of FA, SF and PP fibres reduces the spread flow of the FC to a great extent and hence demands the use of SP to maintain the flow. The incorporation of foam has significant effect on the spread flow of FC, and the spread flow% decreases with the increase in foam volume. The most significant impact of addition of admixtures is observed on the hardened properties of FC i.e. compressive strength and split tensile strength. The incorporation of FA as a replacement to filler had the most significant effect on the mechanical properties of FC by improving the compressive strength and splitting tensile strength to a great extent compared to other admixtures. This strength is further increased when used in combination with other admixtures like SF and PP fibre. Although the incorporation of the admixtures affects the microstructure of the FC which in turn affect the TC, but the density has a major influence on the thermal properties of FC. Based on the experimental outcomes and taking into consideration the economic perspective, mixes MF2PP2 (FC of 1000 kg/m^3 density with 100% FA + 0.4% PP fiber) and LF2PP2 (FC of 600 kg/m^3 density with 100% FA + 0.4% PP fiber) are selected as optimum mixes.

Chapter 6 LIFECYCLE ASSESSMENT OF FOAM CONCRETE AND OPERATIONAL ENERGY COST ANALYSIS

6.1 General

The previous chapter dealt with the influence of the admixtures (FA, SF and PP fiber) on the properties of FC, from which FC mix with optimum dosage of admixtures was selected which provided the desired properties. This chapter further offers an in-depth investigation on the performance of selected optimum mixes (MF2PP2 and LF2PP2) with respect to LCA and operational energy analysis. This chapter is divided in two parts. The first part specifically deals with the lifecycle assessment of FC. One of the primary concerns regarding FC production is the environmental impact generated throughout its upstream, i.e., during its production phase. The pursuit of a sustainable environment, necessitates an assessment of environmental impact of FC which can be effectively executed through the utilisation of the LCA methodology. Hence, in the first section **(6.2 Lifecycle assessment of Foam concrete)** LCA studies are carried out for optimum mixes (MF2PP2 and LF2PP2) as well as for base mixes in accordance with ISO 14040 and ISO 14044:2006 guidelines with SimaPro software where cradle to gate boundary conditions were applied, for which various environmental impact assessment categories involved in the production of $1m^3$ of FC are evaluated. In this section first the LCA studies of Hingot and NPE surfactant is carried out. Further the obtained LCA results of the optimum FC mixes prepared with hingot surfactant are compared with the pre-existing LCA results of AAC block and standard clay brick available in Ecoinvent 3.3 database for Indian context.

Further, the building construction sector is known around the world for its huge energy consumption with a significant proportion contributed by the building's operations phase alone. Studies carried out by various researchers have showed that the annual energy consumption of building can be reduced significantly by 27% to 77% through simpler means of incorporation of better thermal insulating materials for roof and wall during construction (Marwan, 2020; Mohsen and Akash, 2001). Therefore, Section 2 **(6.3 Operational energy analysis of building)** of this chapter analyses the performance of selected FC mixes as a walling and roofing material with varying densities (600 kg/m^3 to 1000 kg/m^3) in G+3 residential building from perspective

of operational energy. Additionally, comparative analysis of performance of selected FC mixes with conventional walling materials like standard clay brick and AAC block along with base mixes of FC (MB0 and LB0) is also carried out. DesignBuilder software used in this study serve as a suitable analysis tool for calculation of operational energy cost of the building. Simulation is carried out to calculate the total annual operational energy consumption of G+3 residential building for different study locations viz., Guwahati, Bangalore, Dehradun, Jodhpur, Mumbai and New Delhi representing the various climatic zones of India. While it is important to note that DesignBuilder software is employed only to assess the operational energy cost for an entire G+3 building where foam concrete is utilized as a walling material. The LCA of G+3 building is not carried out.

6.2 Lifecycle assessment of Foam concrete

6.2.1 Lifecycle assessment Methodology

Lifecycle assessment has been carried out with the help of SimaPro software version 9.3. SimaPro is the most widely used LCA program, with a 30-year reputation in business and academia in over 80 countries. SimaPro is a professional tool for collecting, analysing, and monitoring data on company's products and services sustainability performance. The software can be used for a variety of applications, such as carbon foot printing, sustainability reporting, product design, generating environmental product declarations, and determining key performance indicators.

Many LCI databases are included in SimaPro, including the well-known ecoinvent v3 database, the new Agri-footprint database, and the ELCD database. The ecoinvent database is the world's leading LCI database which delivers both in terms of transparency and consistency. The ecoinvent database contains detailed process data for thousands of products, allowing users to make properly informed decisions about their environmental impact. The ecoinvent database is an ISO 14040 and ISO 14044 compliant data source for studies and assessment. Ecoinvent v3.6 is one of the most comprehensive international LCI databases, with over 15,000 LCI datasets in the areas of energy supply, agriculture, transportation, biomaterials and biofuels, bulk and specialty chemicals, construction materials, packaging materials, textiles, basic and precious metals, metals processing, ICT and electronics, dairy, wood, and waste treatment. The ecoinvent LCI data can be used for different analysis such as life cycle management, LCA, carbon footprint assessment, water footprint assessment, product design and eco-design (DfE), or environmental product declarations (EPD). ISO 14040 and ISO 14044 specifies requirements

and provide guidelines and a framework for LCA. As per this LCA is performed in four stages. The four steps include: goal and scope definition; inventory analysis; life-cycle impact assessment (LCIA); and interpretation

6.2.2 Goal and scope

This is a crucial step and the ISO specifications require that LCA's purpose and scope to be clearly defined and consistent with the intended application. Therefore, the goal and scope document includes technical details which direct subsequent work.

The goal of this study aims to perform the LCA of the FC produced in Guwahati using locally available materials and to determine the impact that FC will deliver on the environment due to its production. The results will highlight the sustainability of FC as a building material and comparison of its impact with similar building materials will be carried out. This study also identifies the materials and manufacturing processes that have a significant impact on various environmental categories. All the calculations and evaluations are done for $1m^3$ of FC produced. For materials, their impact per kg of production will be used for comparison. For this study, all processes including the extraction of raw materials, production of electricity, transportation of materials to IIT Guwahati laboratory, and the processes involved in the production of concrete in the IIT Guwahati laboratory is considered. Secondary processes like transportation systems, distillation, processing, storage and transportation of fuel, construction of manufacturing plant and laboratory are excluded from this study. Cradle to gate approach, which is an assessment of a *partial* product life cycle from resource extraction (*cradle*) to the factory gate (i.e. before it is transported to the consumer), is selected for this study. The choice of this specific boundary condition was made based on several key considerations:

***Focus on Production Phase**:* The primary objective of this study is to produce a sustainable low density cost effective foam concrete which could perform better than the traditionally available walling materials like standard clay brick and AAC block. For this it was necessary to evaluate the environmental impacts associated with the production of foam concrete. The 'cradle to gate' approach effectively captures all relevant processes from raw material extraction (cradle) through to the manufacturing process and up to the factory gate, before the product is transported to the consumer (Colangelo et al., 2018). This boundary is suitable for assessing the environmental burdens of material production, which is the most significant phase in terms of energy consumption and emissions.

Significant Environmental Impacts: The production phase typically contributes significantly to the overall environmental footprint of concrete materials. By focusing on the 'cradle to gate' phase, it is possible to identify major hotspots and opportunities for impact reduction within the production processes, such as optimizing material use or improving energy efficiency of the process.

Standardization and Comparability: Using a 'cradle to gate' LCA model is a standardized practice in LCA studies, facilitating the comparison of environmental impacts across different materials and products. By limiting the scope to 'cradle to gate,' the results of this study can be compared with other studies and industry benchmarks, which often use the same boundary for their assessments as discussed in the literature review. Many LCA studies in the construction materials sector use similar boundaries, facilitating direct comparison of results and contributing to a broader understanding of the environmental impacts of different materials.

Data Availability and Quality: Reliable and detailed data for the use phase and end-of-life phase are often challenging to obtain and can vary significantly depending on specific use scenarios and geographical factors (Yazdanbakhsh and Lagouin, 2019). The 'cradle to gate' boundary allows us to utilize well-documented and high-quality data, ensuring the robustness and credibility of the LCA results.

Scope and Feasibility: Limiting the analysis to the 'cradle to gate' stage makes the study more feasible and manageable. Conducting a full 'cradle to grave' LCA, which includes the use phase and end-of-life treatment, requires extensive resources, time, and often involves significant uncertainties. The 'cradle to gate' boundary was chosen to ensure a thorough and manageable analysis within the scope of this study while still providing valuable insights into the environmental performance of foam concrete production.

SimaPro software version 9.3 is used for modelling and analysis.

6.2.3 Life cycle inventory analysis of FC

Life cycle inventory analysis involves, collection of data and the analysis of material and energy flows for each stage of the product life cycle. SimaPro relies on life cycle inventory data to quantify the inputs and outputs associated with each life cycle stage of a product. Information regarding materials, such as their source, composition, density, and transportation distances, serves as essential input data for constructing the life cycle inventory. By accurately characterizing materials and their sources, we ensure the reliability and representativeness of the LCI data, thus enhancing the credibility of the LCA results. SimaPro assesses the entire

lifecycle of a product—from raw material extraction through manufacturing, use, and disposal. Hence, detailed material data is essential for evaluating environmental impacts across all lifecycle stages comprehensively. For eg. the origin of materials (e.g., primary raw materials vs. recycled materials) influences various environmental parameters, such as energy consumption and emissions associated with extraction, processing, and transportation. Sourcing materials locally can reduce transportation-related emissions significantly. Table 6.1 provides the information about all the materials involved in the production of FC and its sources.

For foam generation, the data is derived considering the foam generation process at IIT Guwahati laboratory. Transportation distance information is collected from the suppliers. Most of the required data are collected in empirical form, and the inputs and outputs of raw materials of FC (OPC, fine aggregates, fly ash, polypropylene fibres water, foaming agents), transportation and electricity are extracted from Ecoinvent 3.8 database. However, suitable modifications based on available Indian data are made to the values obtained from the generic database. Since, the FC with hingot surfactant is yet to be commercialized, for assessment of some of the environmental impact inventories, inputs are assumed at laboratory scale. Fly ash being a waste material, only the energies involved and environmental impacts caused by the transportation of the FA to the IITG laboratory facility is considered. Further, due to the non-availability of data related to XG in the LCA inventory, environmental impact analysis of the XG is not included in this study. Also XG being natural compound produced from corn-starch and is used in very small quantities, and hence it is assumed that it will not have significant environmental impact. For NPE surfactant, data corresponding to non-ionic surfactant production (ethylene oxide derivate) is used, as this is the only available data in the inventory which closely resembles NPE surfactant. In case of Hingot surfactant, the hingot fruit is abundantly available in the wild forest and generally there is no special cultivation being done to produce it. Hence apart from the hingot fruit production all other steps like procurement, transportation and surfactant preparation process are considered in the LCA inventory. To assess the environmental loads in the transportation phase, the vehicles assumed are (a) freight, lorry 16-32 metric ton, euro4 (similar to BSIV) for cementitious materials, fine aggregate and fly ash (b) freight train for Hingot fruit, NPE surfactant and PP fibres. The electricity used for the surfactant preparation, foam generation and FC mixing and production process is assumed to be medium voltage from India's North-eastern grid. The process corresponding to direct filtration treatment of tap water for Indian scenario as available in ecoinvent database is used

for further calculations. Figure 6.1 shows the system boundary (Cradle to Gate) adopted for the current LCA of FC

Table 6-1: Information pertaining to materials, their characteristics and source.

Materials	Remark	Source	Travel distance (km)	Vehicle used
Cement	OPC 43 conforming to IS 8112 – 2013, Specific Gravity = 3.15	Dalmia cement plant Morigaon, Baghjhap, Assam	80	Truck
Sand	IS 383-2016, Pulverized and finer than 300 microns, Specific Gravity = 2.65	Brahmaputra river sand from Dudhnoi, Goalpara Assam	120	Dumper Truck, Truck
Hingot (Balanites aegyptiaca)	Desert fruit contains extractable saponin	Indore, Madhya Pradesh	2160	Rail / Truck (2100 km + 60 km)
Xanthan Gum (Nonylphenol ethoxylate)	Anionic additive	From Loba Chemie. PVT. Ltd. Mumbai, Maharashtra.	2780	Rail / Truck (2600 km + 180 km)
Water	-	Tap water from IITG Facility received after subjecting to direct filtration process	-	-
Fly ash	Class F passing through 75 µm sieve conforming to ASTM C 618, Bulk Density = 995 kg/m^3	NTPC Bongaigaon, Kokrajhar Assam	200	Truck
Polypropylene Fibers	PP fibers with length 12 mm and 22 µm diameter, synthetic, monofilament, alkali resistant with tensile strength of 400-500 MPa	Jogani Reinforcement, Mumbai.	2540	Rail / Truck (2400 km+140 km)

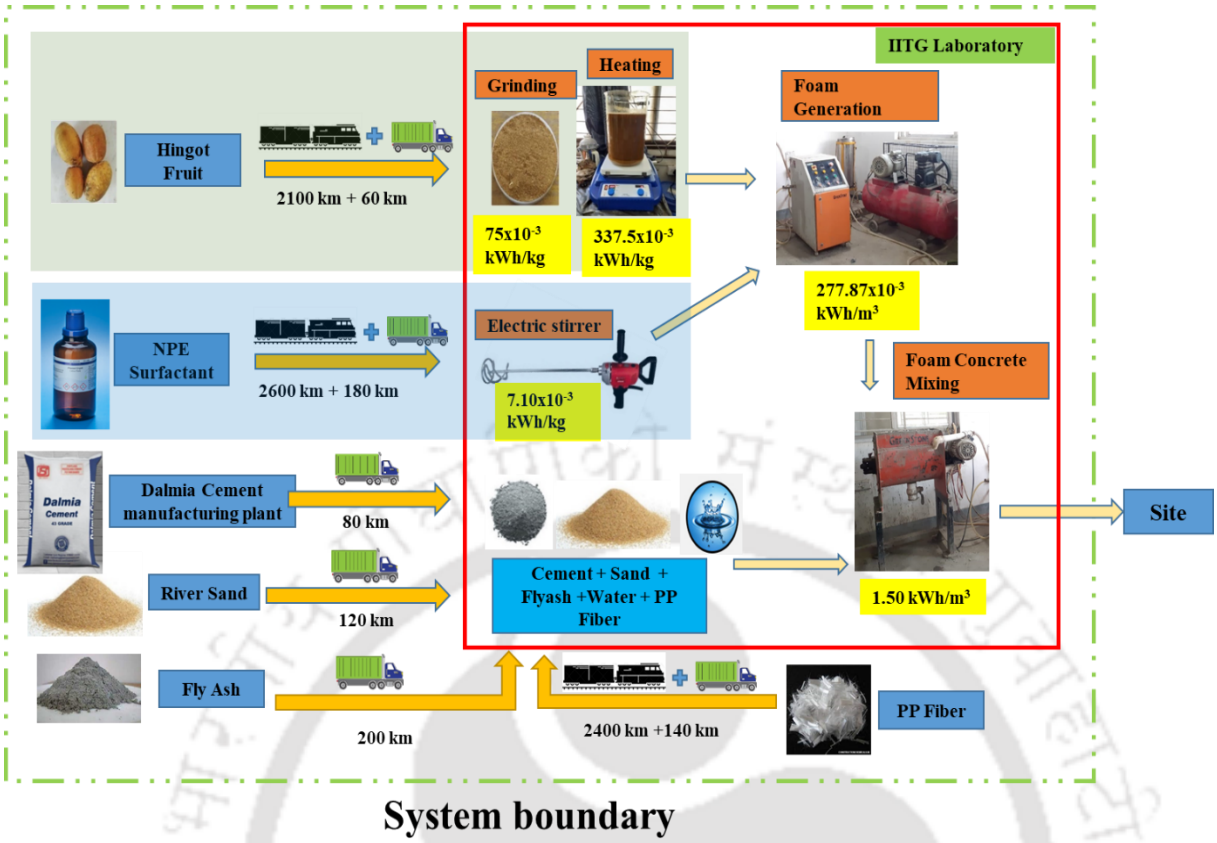

Figure 6-1: System boundary (Cradle to Gate) for LCA of FC

6.2.4 Processes for LCA of FC

The various processes needed to make FC with hingot fruit as a foaming agent, and their electricity consumption calculations, are described below.

Hingot solution preparation

The process for hingot solution preparation starts with the procurement of hingot (Balanites aegyptiaca) fruit. As this fruit is abundantly found in most of the wild areas of Madhya pradesh and no pre-processing is done before it is being transported to IITG facility, hence only the energies involved and the environmental impact caused by its transportation is considered for supply of raw Hingot fruit. The preparation of Hingot solution is carried out as per the methodology suggested by Khwairakpam et.al (Khwairakpam and Ranjani Gandhi, 2020). Hingot fruit is sun dried and then ground with the help of grinder. The hingot powder is then added in water at 6% concentration level followed by heating and stirring for 5 hours at 75^{o}C with the help of hot plate magnetic stirrer. After subjecting to heat treatment, the hingot is filtered to extract the foaming solution. The various components involved in the hingot solution preparation and its quantity is presented in Table 6.2.

Table 6-2: Parameters involved in the Hingot surfactant production process

Output:- Hingot Solution : 20 kg			
			Input:-
1.	Hingot Powder	1.2 kg	At 6% concentration
2.	Tap water	20 kg	By direct filtration treatment
3.	Transportation	2180 km	By Train and Truck (2100 +80) km
4.	Electricity required for Grinding 1.2 kg of Hingot	0.0625 kWh	For grinding 1.2 kg powder, time duration of 5 min is taken on 750 watts Grinder.
5.	Electricity required for Heating 20 litres of solution	6.75 kWh	Solution sample is heated at once for 5 hours on Hot plate magnetic stirrer of 1350 watts.

NPE solution preparation

The process for NPE solution preparation is rather simple. NPE solution is prepared by adding viscous NPE surfactant into water. As the surfactant is viscous it needs to be mixed in water with the help of power stirrer. The impact values for production of 1 kg of non-ionic surfactant, ethylene oxide derivative is selected from Simapro database and adopted for NPE surfactant which is also a non-ionic ethylene oxide based derivative. The various components involved in the NPE solution preparation and the corresponding quantity is presented in Table 6.3.

Table 6-3: Parameters involved in the NPE surfactant production process

Output:- NPE Solution : 20 kg			
			Input:-
1.	NPE	1.2 kg	At 6% concentration
2.	Tap water	20 kg	By direct filtration treatment
3.	Transportation	2780 km	By Train and Truck (2600 +180) km
4.	Electricity required for power mixing of 1.2 kg of NPE liquid surfactant.	0.142 kWh	For mixing 1.2 kg of NPE surfactant, time duration of 10 min is taken by using 850 watts power stirrer.

Electricity required for foam generation

The solution of hingot prepared is poured into foam generator vessel keeping the minimum indicated level and foam of desired density is produced by a foam generator with FGP of 550 kPa. Table 6.4 provides the results of the trails performed for determining foam output rate. As per ASTM C796-97

$$T = \frac{t_1 X W_1}{W_2 X V} \quad \ldots\ldots \text{ Eqn. 1}$$

T = Time to discharge cubic meter of foam (sec/m^3)
t_1 = time to fill the container (sec).
W_1= Weight of a container with foam before strike off.
W_2 = Weight of a container with foam after strike off.
V= Volume of a container (m^3)

Table 6-4: Experimental results on foam output rate.

S no	t (sec)	W_1 (gm)	W_2 (gm)	T(sec/m^3)
1	6.1	558.29	517.6	441.13
2	6.05	559.25	530	445.69
3	6.15	557.38	570	447.06

V=12250ml, T_{avg}= 444.62 sec/ m^3

Density of foam = 45kg/ m^3, T_{avg} = 9.88 sec/kg

Power rating – 750W (foam generator) + 1500W (compressor) = 2250W

Consumption of electricity/kg = $\frac{2250 \text{ X } 9.88}{60 \text{ X} 60 \text{ X} 1000}$ **= 6.175 x 10^{-3} kWh/kg**

= 277.87 x 10^{-3} kWh/m^3

Electricity required for FC mixing

Firstly, a homogeneous mortar mix of cement sand slurry is prepared using a horizontal shaft paddle-style mixer, followed by the addition of the measured quantity of foam to the mortar mix. The complete mixing operation is carried out for at least 5 minutes before the foam is blended evenly in the slurry.

Power rating of mixer = 750 watt

Quantity of FC mixed in one cycle = 50 liter

Time of mixing = (5 min +1 min for pouring) = 6 min

Power consumption involved in mixing of 50 liter of FC = 750 X 6/60 = 75Wh/50litres

Power consumption associated with mixing per cubic meter = 1500 Wh/m^3 = **1.50 kWh/m^3**

6.2.5 Lifecycle impact assessment of FC

The purpose of a life cycle impact assessment (LCIA) is to convert emissions and resource extractions into a small number of environmental impact scores using a characterization factor. Several approaches have been developed to calculate environment impact scores. Generally, majority of LCA experts do not create impact assessment methods, however they prefer to

choose that are already published. Each method has several impact categories; some allow for aggregation into a single score and some do not.

Evaluation of the magnitude and significance of the environmental impacts for each design mix throughout its life cycle is conducted focusing particularly on cumulative energy demand (MJ) and global warming potential in terms of equivalent carbon emission (kg eq. of CO_2). Other parameters like stratospheric ozone depletion, marine eutrophication, terrestrial ecotoxicity, freshwater ecotoxicity, marine ecotoxicity which are relevant in the current scenario are also considered. The above mentioned are the impact categories of major concern. In order to evaluate the aforementioned impact categories ReCiPe 2016 Midpoint (H) V1.06 / World and Cumulative Energy Demand V1.11 are used for impact assessment. Basically, Cumulative Energy Demand (CED) refers to the total amount of primary energy consumed throughout the entire life cycle of a product or service. This includes both direct and indirect energy use, encompassing various stages such as raw material extraction, manufacturing, transportation, and disposal. Global warming potential (GWP) is the amount of additional radiative forcing integrated caused by the emission of 1 kg of greenhouse gasses relative to the radiative forcing integrated caused by the emission of 1 kg of carbon dioxide (CO_2) over the same time horizon. Stratospheric ozone depletion is the gradual thinning of the ozone layer in the Earth's upper atmosphere, primarily caused by the release of ozone-depleting substances such as chlorofluorocarbons (CFCs). Marine eutrophication is the excessive enrichment of water with nutrients, leading to increased primary production and often resulting in harmful algal blooms, dead zones, and negative ecological impacts. Terrestrial ecotoxicity involves the impact of pollutants on land ecosystems, freshwater ecotoxicity pertains to the adverse effects of substances on freshwater environments, and marine ecotoxicity addresses the toxicity of pollutants in marine ecosystems.

6.2.6 Uncertainty Analysis

In the context of LCA several factors contribute to the uncertainties involved in the process of evaluating the environmental impacts of Hingot surfactant, NPE surfactant, and the resulting FC produced using these surfactants., Sources of uncertainty typically stem from various stages, including data collection, modelling assumptions, and parameter variability. For instance, uncertainties may arise from the accuracy of data regarding material inputs, energy consumption, emissions factors, and end-of-life scenarios. Furthermore, modelling assumptions such as system boundaries, allocation methods, and choice of impact assessment methods can introduce additional uncertainties. Similarly, in operational energy analysis, uncertainties may

arise from factors such as variability in energy consumption patterns, efficiency of equipment, and weather conditions. To address the uncertainties related to inventory data and the application of characterization models, the most commonly adopted technique of Monte Carlo simulation method is utilized in the present study. Monte Carlo simulation identifies potential impacts by substituting a set of design variables. The level of uncertainty associated with each variable is determined by the probabilistic distribution of the chosen factors (Mooney, 1997). The estimation of variability is conducted through the utilization of a pedigree matrix, which effectively characterizes the quality of the data based on its source, collection methodology, as well as its geographical, temporal, and technological representativeness (Weidema and Wesnaes, 1997). The simulations involved 1,000 iterations of independent variables, establishing a 95% confidence interval to ensure robustness.

6.2.7 Results on LCA of FC

Result on LCA analysis related to comparison of Hingot surfactant with NPE Surfactant

Table 6.5 summarizes the magnitude of environmental loads determined for production and transportation of a batch of two different surfactant solutions. Results of LCA analysis show us that the total cumulative energy demand associated with 1 kg of production of Hingot solution (5.237 GJ) is less than that of 1 kg of NPE surfactant solution (6.084 GJ) while GWP of NPE (0.205 kg CO_2) is less than that of Hingot solution (0.314 kg CO_2). The higher GWP of hingot solution could be probably due to the significant amount of energy consumed in the form of electricity from northeast Indian grid for heating (Figure 6.2). Also majority of the electricity produced in the Northeast Indian grid is dependent on the thermal power plants which uses coal for its electricity generation and this might have led to rise in the GWP of the hingot surfactant. Further, it should be noted that the value derived for hingot solution preparation is for laboratory scale model and the energy consumption and GWP of hingot solution can be further reduced using more efficient industrial scale heaters or boilers for preparation of hingot solution. Also, the other outcomes of environmental hazard impact analysis, such as stratospheric ozone depletion, marine eutrophication, terrestrial ecotoxicity, freshwater ecotoxicity, marine ecotoxicity. exhibits higher values for NPE when compared to hingot. This is due to the fact that NPE degrade into nonylphenol (NP), which “is persistent in the aquatic environment, moderately bio accumulative, and extremely toxic to aquatic organisms” (US EPA, Shah et. al 2016). Foaming agents, especially bio-based ones, have been shown to reduce the environmental impact of foam concrete production. They can enhance the properties of foam

concrete while lowering its GWP and other environmental impacts compared to conventional admixtures (Lai et al., 2023). Considering all the above pros and cons, it can be concluded that hingot surfactant may be deemed noteworthy as sustainable alternative to the NPE. Hence for the further lifecycle assessment of FC, mixes prepared with hingot surfactant are considered for analysis.

Table 6-5: Impact of one kg of surfactant across different environmental categories

Impact category	Unit	Hingot	N.P.E
Total Cumulative Energy demand	MJ	5.237	6.083497
Global warming	kg CO_2 eq	3.14E-01	2.05E-01
Stratospheric ozone depletion	kg CFC11 eq	9.61E-08	22.18E-08
Marine eutrophication	kg N eq	6.01E-06	105.83E-06
Terrestrial ecotoxicity	kg 1,4-DCB	1.97E-01	6.33E-01
Freshwater ecotoxicity	kg 1,4-DCB	4.92E-03	9.36E-03
Marine ecotoxicity	kg 1,4-DCB	6.60E-03	10.54E-03

*MJ- Mega Joule, kg CO_2 eq- kilograms equivalent of carbon dioxide (CO_2), kg CFC11 eq- kilograms equivalent of trichlorofluoromethane, kg N eq- kilograms equivalent of nitrogen (N), kg 1,4-DCB- kilograms equivalent of dichlorobenzene.

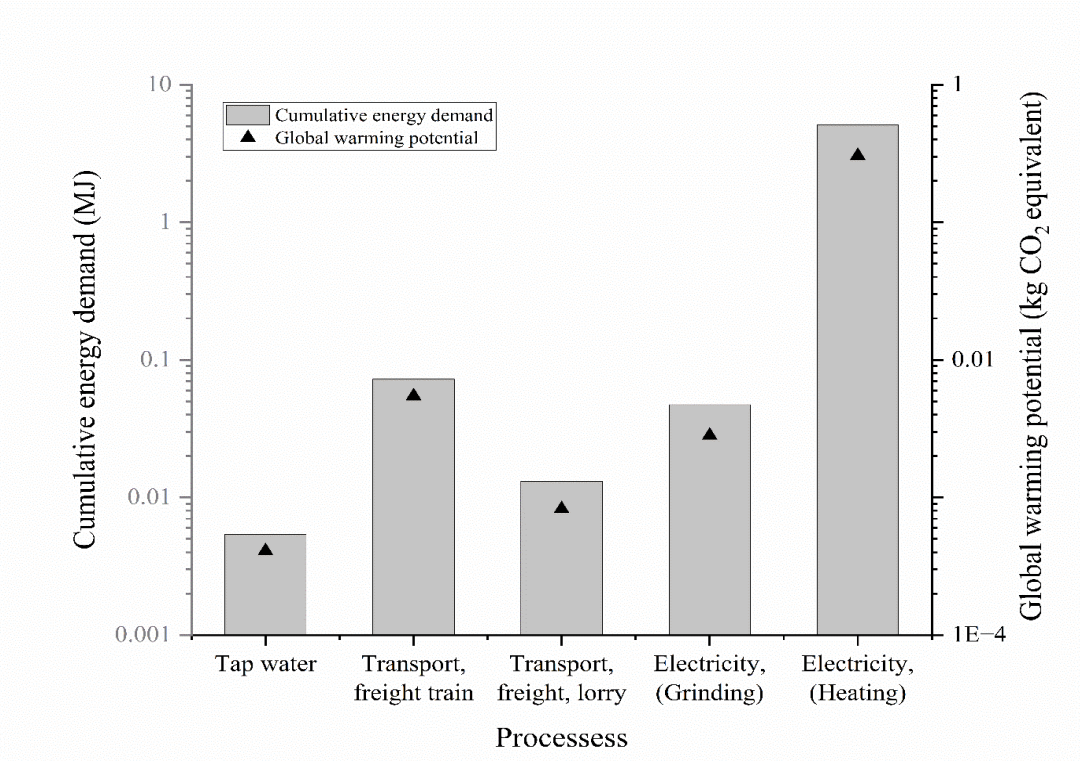

Figure 6-2: Cumulative energy demand for production of 1 kg of hingot surfactant solution

Results on LCA analysis related to comparison of performance of Hingot based FC with AAC block and clay brick

Figure 6.3 shows the distribution of the cumulative energy demand of production of various constituents involved in the FC production. In case of FC mixes of both the design densities (600 kg/m^3, 1000 kg/m^3 and 1500 kg/m^3), maximum cumulative energy demand can be observed for cement, which accounts for almost 70% of total embodied energy required for FC. Similar such observations were also reported by other researchers who have highlighted that higher cumulative energy consumption came from the extensive use of ordinary Portland cement (OPC) in FC (Tiong et al., 2020; Zimele et al., 2019). Hence, the above issue can be addressed through the partial replacement of OPC with other pozzolanic materials which can help to lower the energy demand, CO_2 emissions and the other negative environmental impact of FC (Gettu et al., 2019; Panesar et al., 2019; Yao et al., 2019). The contribution of surfactant to total energy demand is found to range from 11.73 to 2.4% for densities from 600 kg/m^3 to 1500 kg/m^3. Hence the energy demand is higher for low density mixes (600 kg/m^3) as their foam consumption is high and foam volume comprises of the 70% of total FC volume. Further Table 6.6 provides the comparison of the current LCA results (GWP and CED) with relevant literature where it can be noted that the results obtained aligns with the existing values.

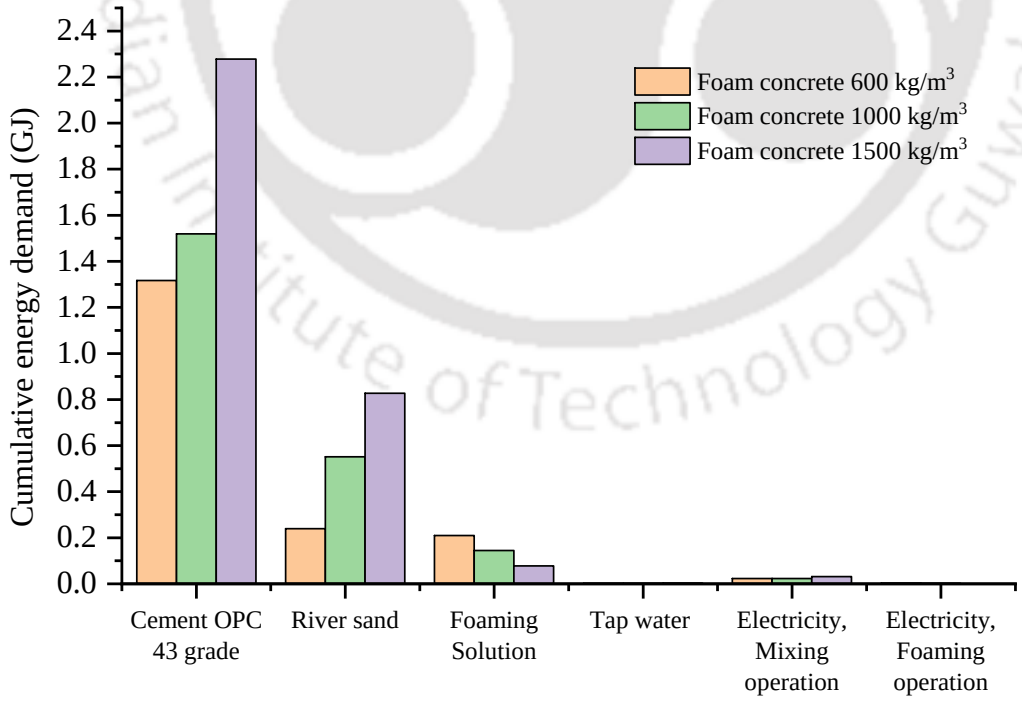

Figure 6-3: Distribution of cumulative energy for 1 m^3 of FC with densities 600 kg/m^3, 1000 kg/m^3 and 1500 kg/m^3

Table 6-6: Comparison of the current LCA results with relevant literature

Parameters	Unit	Comparison with relevant literature					
		Current study	**Current study**	**Current study**	**(Lim et al., 2017)**	**(Tiong et al., 2020)**	**(Ahmadi et al., 2022)**
Total Cumulative Energy demand	GJ	1.75	2.238	3.214	2.99 to 3.95	2.019 to 2.183	–
Global warming	kg CO_2 eq	233.86	284.074	417.694	558.95 to 619.17	455.27 to 505.54	330 to 488
Density	Kg/m^3	600	1000	1500	1300 ±50	1300 ±50	1400 to 2000

Table 6.7 and Figure 6.4 presents the comparative analysis of LCA of the FC with other commonly used building materials like AAC blocks and standard clay brick. The values for the AAC blocks and Standard clay brick are taken from the predefined library of the SimaPro software for comparison. Results of LCA analysis indicate that FC with density 600 kg/m^3 (LB0) and 1000 kg/m^3 (MB0) shows better performance than AAC block and standard clay brick. When comparing with base mixes i.e. LB0 and MB0, standard clay brick showed 153% and 95% more cumulative energy demand respectively. Similarly, AAC block showed 65% and 30% higher cumulative energy demand when compared to LB0 and MB0 respectively. The GWP in terms of kg CO_2 eq. is also 70% to 90% higher for Clay brick and 16% to 36% higher for AAC block when compared with FC. This higher cumulative energy demand and GWP can be ascribed to the process of kiln burning and autoclaving involved in manufacturing of clay brick and AAC block respectively. Apart from the above mentioned lifecycle assessment categories, the FC also outperformed clay brick and AAC block in other environmental impact categories like stratospheric ozone depletion, marine eutrophication, terrestrial ecotoxicity, freshwater ecotoxicity and marine ecotoxicity.

The effect of density can also be clearly noted on the LCA performance of the FC. The total cumulative energy involved in production of FC with 600 kg/m^3 density is almost 21% less than that of FC with density 1000 kg/m^3. On similar lines the GWP i.e. kg equivalent CO_2 emission for 600 kg/m^3 is 17% lower than that of FC with density 1000 kg/m^3. This is due to the lower amount of OPC cement required for the production of FC with density 600 kg/m^3. In our study cement accounted for almost 70% of the total cumulative energy demand and 84% of the total GWP. Admixtures, although used in smaller quantities, can significantly impact the environmental profile of the foam concrete, especially when using chemical based or synthetic. While the exact degree of impact can vary depending on factors such as composition, usage

rates, and production processes, our findings consistently underscore the significance of chemical admixtures in influencing environmental performance. This can be predominantly assigned to their usage rate as admixtures are used in very small quantities. For eg. In the present study, a PCE-based superplasticizer is utilized as a chemical admixture to ensure the flowability. Though the GWP of per kg of PCE based SP is 2.5 times higher than that of cement but still it only accounts for 3% of the total GWP of the FC while cement still contributes to more than 80% of the GWP. Similar is the case of PP fibre which reports 3 times higher per kg CO_2 emissions compared to cement. This can be assigned due to higher usage rate of cement while admixtures accounting for very small proportion of the total mix proportion constituents. Hence it should be worth noting that performance of LCA of FC can be further improved by decreasing the density and use of various mineral admixtures like FA, SF, GGBS which are waste by products derived from various industries. This will lead to reduction of overall cement consumption of the FC mixes which accounts for the major part of the cumulative energy consumption for FC mixes. A slight increase in cumulative energy consumption of the LF2PP2 mix can be observed, when compared to LB0 and this can be ascribed mainly to the polypropylene fibers incorporated in the mix. As discussed earlier, the PP fiber production have multiple times more energy requirement compared to other constituent materials in FC. Also it should be taken into consideration that the replacement of the sand with FA results in better performance of optimum mixes with respect to environmental impact analysis in LCA. However, this is overcome by the incorporation of the PP fibers. Nonetheless the optimum mixes LF2PP2 and MF2PP2 shows better performance in lifecycle assessment when considering all the impact categories.

Table 6-7: Comparison of performance of FC with clay brick and AAC block across different environmental categories

Impact category	Unit	LB0	LF2PP2	MB0	MF2PP2	AAC Block	Clay brick
Total Cumulative Energy demand	GJ	1.75	1.95	2.22	2.22	2.89	4.68
Global warming	kg CO_2 eq	233.86	232.96	282.95	269.88	317.43	462.72
Stratospheric ozone depletion	kg CFC11 eq	3.24E-05	3.04E-05	4.36E-05	3.60E-05	5.67E-05	6.89E-05
Marine eutrophication	kg N eq	2.62E-03	2.68E-03	3.09E-03	3.09E-03	3.90E-03	4.31E-03
Terrestrial ecotoxicity	kg 1,4-DCB	405.09	303.61	650.79	411.22	805.73	714.52

Freshwater ecotoxicity	kg 1,4-DCB	2.57	2.33	3.38	2.81	3.86	8.36
Marine ecotoxicity	kg 1,4-DCB	3.63	3.26	4.85	3.96	5.61	11.10

*MJ- Mega Joule, kg CO_2 eq- kilograms equivalent of carbon dioxide (CO_2), kg CFC11 eq- kilograms equivalent of trichlorofluoromethane, kg N eq- kilograms equivalent of nitrogen (N), kg 1,4-DCB- kilograms equivalent of dichlorobenzene.

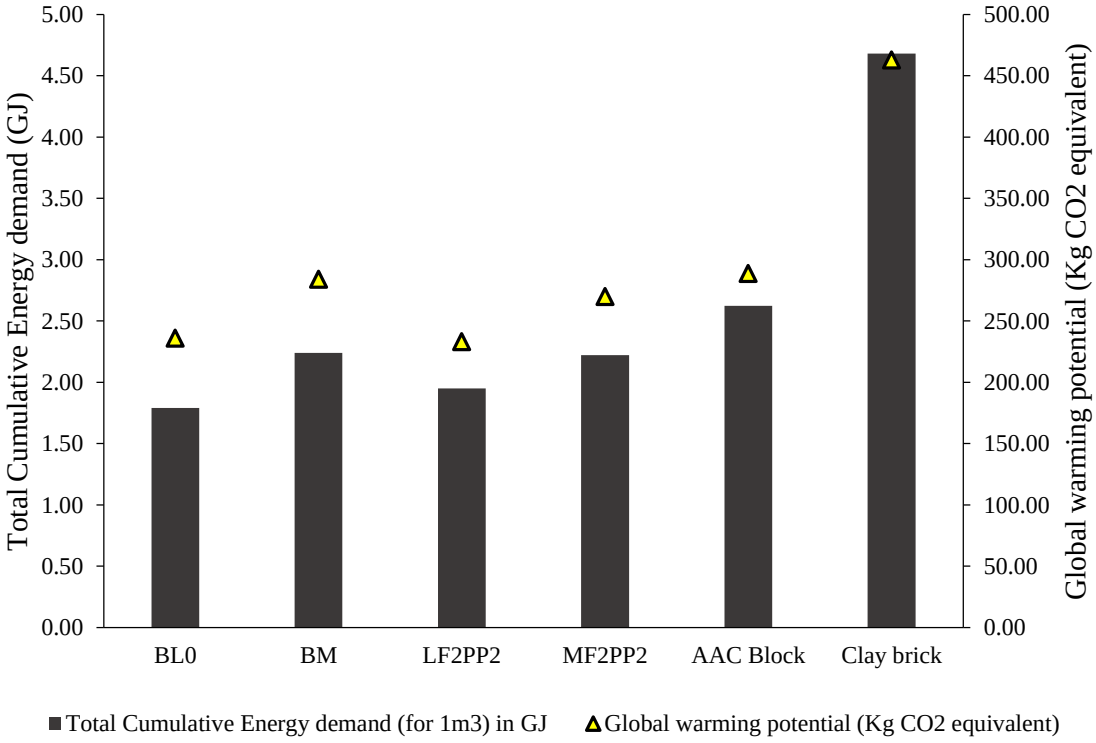

Figure 6-4: Cumulative energy demand and GWP of FC and commonly used similar building materials

Uncertainty analysis results and discussion

Uncertainty related to data variability is assessed through five uncertainty analyses: (i) Hingot Surfactant solution and NPE surfactant solution; (ii) FC1000 kg/ m^3 (Hingot) and FC1000 kg/ m^3 (NPE); (iii) FC1000 kg/ m^3 (Hingot) and AAC Block; (iv) FC1500 kg/ m^3 (Hingot) and FC1500 kg/ m^3 (NPE); (v) FC1500 kg/ m^3 (Hingot) and standard clay brick. The results derived from the Monte Carlo simulations are listed in Table 6.8. The simulation performs the subtraction of two compared systems, where results also indicate the probability that one option generates more impact or damage than the other. The amount of data containing uncertainty values is 80.90% and the remaining 19.10% of the data contained no uncertainty and were therefore considered as fixed data since they are derived from direct calculation. These results are on par with the uncertainty analyses carried out in literature (Cuenca-Moyano et al., 2019; Maia de Souza et al., 2016; Souza et al., 2015).

In case of first uncertainty analysis i.e. Hingot Surfactant solution vs NPE surfactant solution, the results showed that the probability that the production of 1 kg Hingot surfactant solution could generate more impact than the production of 1 kg of NPE surfactant solution is 100 % for GWP, 10.6% for total cumulative energy demand, 13.8% for marine ecotoxicity, 6.5% for freshwater ecotoxicity, 0.3% for stratospheric ozone depletion and 0% for marine eutrophication and terrestrial ecotoxicity.

For second uncertainty analysis i.e. for the probability that $1m^3$ of "FC1000 kg/ m^3 (Hingot)" could generate more impact than $1m^3$ of "FC1000 kg/ m^3 (NPE)" are 98.7% for GWP, 0.4% for cumulative energy demand, 7.3% for marine ecotoxicity, 3% for Freshwater ecotoxicity, 0.1% for Stratospheric ozone depletion and 0% for Marine eutrophication and Terrestrial ecotoxicity. As, FC 1000 kg/m^3 density mix with Hingot surfactant performed better in majority of the environmental impact categories, it is selected to be the best suitable option for comparison with the AAC block in further uncertainty analysis.

On comparing the "FC1000 kg/ m^3 (Hingot)" vs "AAC block" for the third uncertainty analysis, the probability that the production of $1m^3$ of "FC1000 kg/ m^3 (Hingot)" could generate more impact than the production of $1m^3$ AAC block is 45.2 % for GWP, 5.5% for total cumulative energy demand, 44.6% for marine ecotoxicity, 48.6% for freshwater ecotoxicity, 14% for stratospheric ozone depletion, 21.80% for marine eutrophication and 43.1% for terrestrial ecotoxicity. The probability of the occurrence of an inversion "FC1000 kg/ m^3 (Hingot)" ≥ AAC block for Fresh water ecotoxicity is of 51.4%. This uncertainty analysis thus indicates that it is not possible to differentiate between these two scenarios as to which predominantly evaluates the toxic effects of chemicals on aquatic life during all life cycle stages (Oginah et al., 2023). As for fresh water ecotoxicity is concerned, the Monte-Carlo assessment indicates a high uncertainty associated with respect to "FC1000 kg/ m^3 (Hingot)" vs "AAC block", and, therefore, conclusions cannot be made based on this indicator.

For the fourth uncertainty analysis the probability that the production of $1m^3$ of "FC1500 kg/m^3 (Hingot)" generates more impact than "FC1500 kg/ m^3 (NPE) is: 100 % for GWP, 12.1% for total cumulative energy demand, 15.5% for marine ecotoxicity, 6.7% for freshwater ecotoxicity, 0.1% for stratospheric ozone depletion and 0% for marine eutrophication and terrestrial ecotoxicity.

For the fifth and last comparison, the probability that the production of $1m^3$ of "FC1500 kg/ m^3 (Hingot)" could generate more impact than the production of $1m^3$ of standard clay brick is 28.5 % for GWP, 0.1% for total cumulative energy demand, 15.5% for marine ecotoxicity, 12.5% for freshwater ecotoxicity, 26.2% for stratospheric ozone depletion, 62.90% for marine eutrophication and 83.6% for terrestrial ecotoxicity.

The uncertainty assessment performed using Monte-Carlo iterations, have shown that the conclusions of this LCA are robust. Results showed a high probability that the production of Hingot surfactant and the corresponding FC showed the least impact than all the other alternatives discussed in the current study.

Table 6-8: Results of Monte Carlo uncertainty analysis

Category	Probability	Mean	Median	SD	CV (Coefficient of variation)	2.5%	97.50%	Standard error of mean
Hingot surfactant ≥ NPE surfactant								
CED	10.60%	-8.46E-01	-8.80E-01	6.40E-01	-7.56E+01	-2.03E+00	4.86E-01	2.02E-02
F_{ET}	6.50%	-4.47E-03	-4.06E-03	3.44E-03	-7.70E+01	-1.28E-02	1.50E-03	1.09E-04
GWP	100.00%	1.08E-01	1.07E-01	3.29E-02	3.04E+01	4.75E-02	1.74E-01	1.04E-03
M_{ET}	13.80%	-3.98E-03	-3.51E-03	4.44E-03	-1.11E+02	-1.44E-02	3.89E-03	1.40E-04
M_{EU}	0.00%	-9.82E-05	-9.56E-05	2.47E-05	-2.51E+01	-1.56E-04	-5.94E-05	7.81E-07
SOD	0.30%	-1.25E-07	-1.24E-07	3.73E-08	-2.98E+01	-1.98E-07	-5.33E-08	1.18E-09
T_{ET}	0.00%	-4.31E-01	-3.67E-01	2.55E-01	-5.91E+01	-1.10E+00	-1.43E-01	8.06E-03
FC1000 kg/ m3 (Hingot) ≥ FC1000 kg/ m3 (NPE)								
CED	0.40%	-4.93E+01	-5.02E+01	1.55E+01	-3.14E+01	-7.70E+01	-1.59E+01	4.90E-01
F_{ET}	3.00%	-1.48E-01	-1.35E-01	9.91E-02	-6.72E+01	-3.89E-01	1.39E-02	3.13E-03
GWP	98.70%	1.62E+00	1.60E+00	7.66E-01	4.72E+01	2.47E-01	3.24E+00	2.42E-02
M_{ET}	7.30%	-1.40E-01	-1.26E-01	1.28E-01	-9.17E+01	-4.52E-01	7.35E-02	4.06E-03
M_{EU}	0.00%	-2.87E-03	-2.78E-03	7.21E-04	-2.52E+01	-4.59E-03	-1.72E-03	2.28E-05
SOD	0.10%	-4.07E-06	-4.03E-06	1.02E-06	-2.49E+01	-6.23E-06	-2.23E-06	3.21E-08
T_{ET}	0.00%	-1.33E+01	-1.12E+01	8.15E+00	-6.14E+01	-3.43E+01	-4.96E+00	2.58E-01
FC1000 kg/ m3 (Hingot) ≥ AAC block								
CED	5.50%	-3.98E+02	-3.74E+02	2.70E+02	-6.79E+01	-9.72E+02	8.83E+01	8.54E+00

F_{ET}	48.60%	-1.46E-01	-4.04E-02	1.53E+00	-1.05E+03	-3.82E+00	2.71E+00	4.83E-02
GWP	45.20%	-5.90E+00	-4.86E+00	3.84E+01	-6.51E+02	-8.95E+01	6.03E+01	1.21E+00
M_{ET}	44.60%	-2.82E-01	-1.74E-01	2.03E+00	-7.21E+02	-5.24E+00	3.43E+00	6.42E-02
M_{EU}	21.80%	-4.63E-04	-3.74E-04	6.38E-04	-1.38E+02	-2.03E-03	5.57E-04	2.02E-05
SOD	14.00%	-8.36E-06	-6.80E-06	9.06E-06	-1.08E+02	-3.13E-05	5.60E-06	2.86E-07
T_{ET}	43.10%	-8.23E+01	-3.39E+01	2.29E+02	-2.78E+02	-6.73E+02	2.22E+02	7.23E+00
FC1500 kg/ m3 (Hingot) ≥ FC1500 kg/ m3 (NPE)								
CED	12.10%	-1.13E+01	-1.20E+01	8.97E+00	-7.96E+01	-2.61E+01	7.35E+00	2.84E-01
F_{ET}	6.70%	-5.90E-02	-5.87E-02	5.41E-02	-9.16E+01	-1.64E-01	3.60E-02	1.71E-03
GWP	100.00%	1.54E+00	1.54E+00	4.46E-01	2.89E+01	6.49E-01	2.46E+00	1.41E-02
M_{ET}	15.50%	-5.10E-02	-5.18E-02	7.18E-02	-1.41E+02	-1.87E-01	8.15E-02	2.27E-03
M_{EU}	0.00%	-1.40E-03	-1.34E-03	3.61E-04	-2.59E+01	-2.23E-03	-8.12E-04	1.14E-05
SOD	0.10%	-1.76E-06	-1.74E-06	5.39E-07	-3.06E+01	-2.87E-06	-7.62E-07	1.70E-08
T_{ET}	0.00%	-6.01E+00	-5.11E+00	3.98E+00	-6.63E+01	-1.48E+01	-2.04E+00	1.26E-01
FC1500 kg/ m3 (Hingot) ≥ Clay brick								
CED	0.10%	-1.47E+03	-1.43E+03	4.94E+02	-3.37E+01	-2.51E+03	-5.62E+02	1.56E+01
F_{ET}	12.50%	-3.60E+00	-2.79E+00	4.42E+00	-1.23E+02	-1.53E+01	2.44E+00	1.40E-01
GWP	28.50%	-4.74E+01	-4.20E+01	7.99E+01	-1.69E+02	-2.19E+02	8.77E+01	2.53E+00
M_{ET}	15.50%	-4.25E+00	-3.20E+00	5.76E+00	-1.36E+02	-1.90E+01	3.86E+00	1.82E-01
M_{EU}	62.90%	2.17E-04	2.98E-04	8.19E-04	3.77E+02	-1.61E-03	1.64E-03	2.59E-05
SOD	26.20%	-6.27E-06	-5.58E-06	1.06E-05	-1.69E+02	-2.90E-05	1.19E-05	3.34E-07
T_{ET}	83.60%	2.38E+02	3.14E+02	3.42E+02	1.44E+02	-5.97E+02	6.27E+02	1.08E+01

*CED- Cumulative Energy Demand, F_{ET}- Freshwater Ecotoxicity, GWP- Global Warming Potential, M_{ET}- Marine Ecotoxicity, M_{EU}- Marine Eutrophication, SOD- Stratospheric Ozone Depletion, T_{ET}- Terrestrial Ecotoxicity.

By acknowledging and addressing these uncertainty, we aim to enhance the robustness and validity of our research findings, thus contributing to the advancement of knowledge in the field of sustainability assessment. Further it is to be noted that, SimaPro software is a widely used tool for conducting LCA studies, and its validation typically involves several key aspects like:

Methodological Consistency: SimaPro follows established LCA methodologies and standards, such as ISO 14040 and ISO 14044, ensuring methodological consistency and compatibility with international best practices.

Data Quality and Transparency: SimaPro provides access to a comprehensive database of life cycle inventory data, emission factors, and impact assessment methods, enabling users to select data sources that align with their specific study requirements. Additionally, SimaPro allows for the transparent documentation of data sources, assumptions, and modelling parameters, facilitating peer review and validation. Further I would like to add that the there are two types of inputs primary inputs and secondary inputs, primary inputs reflect the data related to the transportation distances from sources, actual energy usages over the different process etc. This data was collected on site. Also the secondary inputs which reflects the data collected from the simapro software database was Indian region specific data.

Benchmarking and Comparison: SimaPro enables benchmarking and comparison of LCA results against industry benchmarks, peer-reviewed studies, and regional or sectoral averages. By comparing SimaPro results with external sources, users can validate the software's performance and assess the reliability of the findings.

User Feedback and Software Updates: SimaPro regularly solicits user feedback and incorporates software updates to address user concerns, improve functionality, and enhance the accuracy of LCA results. This iterative process of software development and refinement contributes to the ongoing validation and improvement of SimaPro's performance.

In summary, SimaPro software undergoes validation through methodological consistency, data quality, benchmarking, user feedback, and software updates to ensure the accuracy and reliability of LCA results.

6.3 Operational energy analysis of building

6.3.1 Methodology adopted for operational energy analysis of building

Building plan and site selection

A typical G+3-building floor plan is designed with the help of AutoCAD 2020. The building consists of residential apartments along with commercial shops and a dedicated car park area. A staircase width of 2 m connects all floors. The plan shown in Figure 6.5 is used for the further building energy analysis. This study simulates the performance of building in different climatic zones of India (Table 6.9) as per the NBC (National Building Code) 2016 Vol. 2. and estimates the corresponding operational energy cost of the building. Table 6.10 and Figure 6.6 represents the different cities selected for the present study across India and their corresponding climatic zones. As climatic zones in design builder are assigned based upon ASHRAE 90.1 codal guidelines, the Table 6.10 also provides the correlation of the Indian climatic zones (as per NBC 2016) with the ASHRAE 90.1.

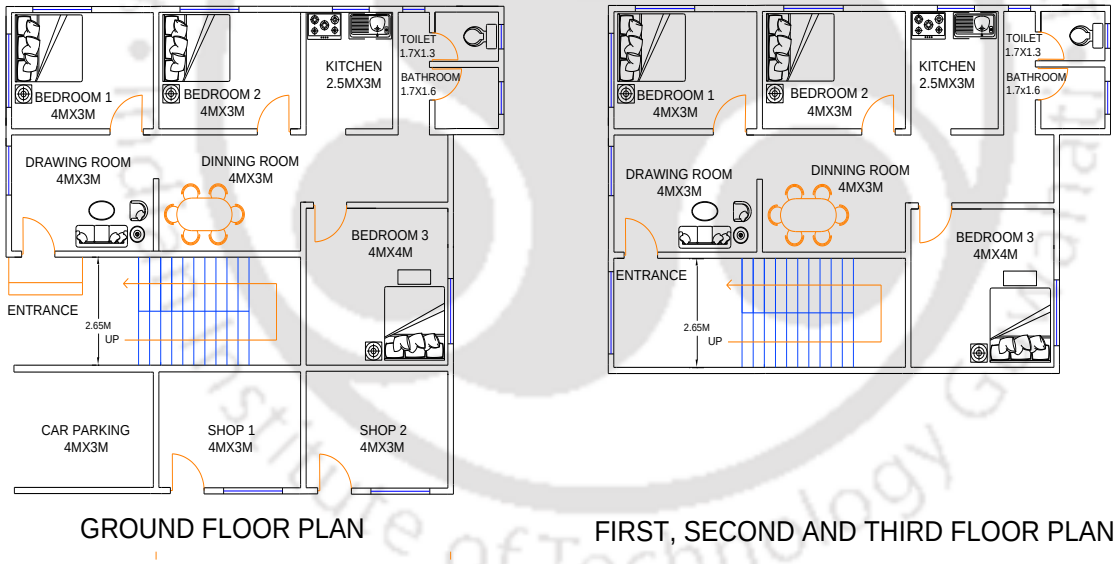

Figure 6-5: G+3 Residential building plan for the analysis

Table 6-9: Climatic zones as per NBC 2016

Sr. No.	Climatic Zone	Mean monthly maximum temperature (°C)	Mean monthly relative humidity (%)
1.	Hot-Dry	Above 30	Below 55
2.	Warm-Humid	Above 30	Above 75
		Above 25	Above 75
3.	Temperate	25-30	Below 75
4.	Cold	Below 25	All values
5.	Composite	A climatic zone that does not have any season for more than six months can be called as composite	

Table 6-10: Climatic Zones for the selected study locations for analysis

Sr. No.	City Name	Climatic Zone as per NBC 2016	Climatic Zone as per ASHRAE 90.1
1.	Bengaluru	Temperate	2B
2.	Dehradun	Cold	3A
3.	Guwahati	Warm and Humid	1A
4.	Jodhpur	Hot and Dry	1B
5.	Mumbai	Warm and Humid	1A
6.	New Delhi	Composite	1B

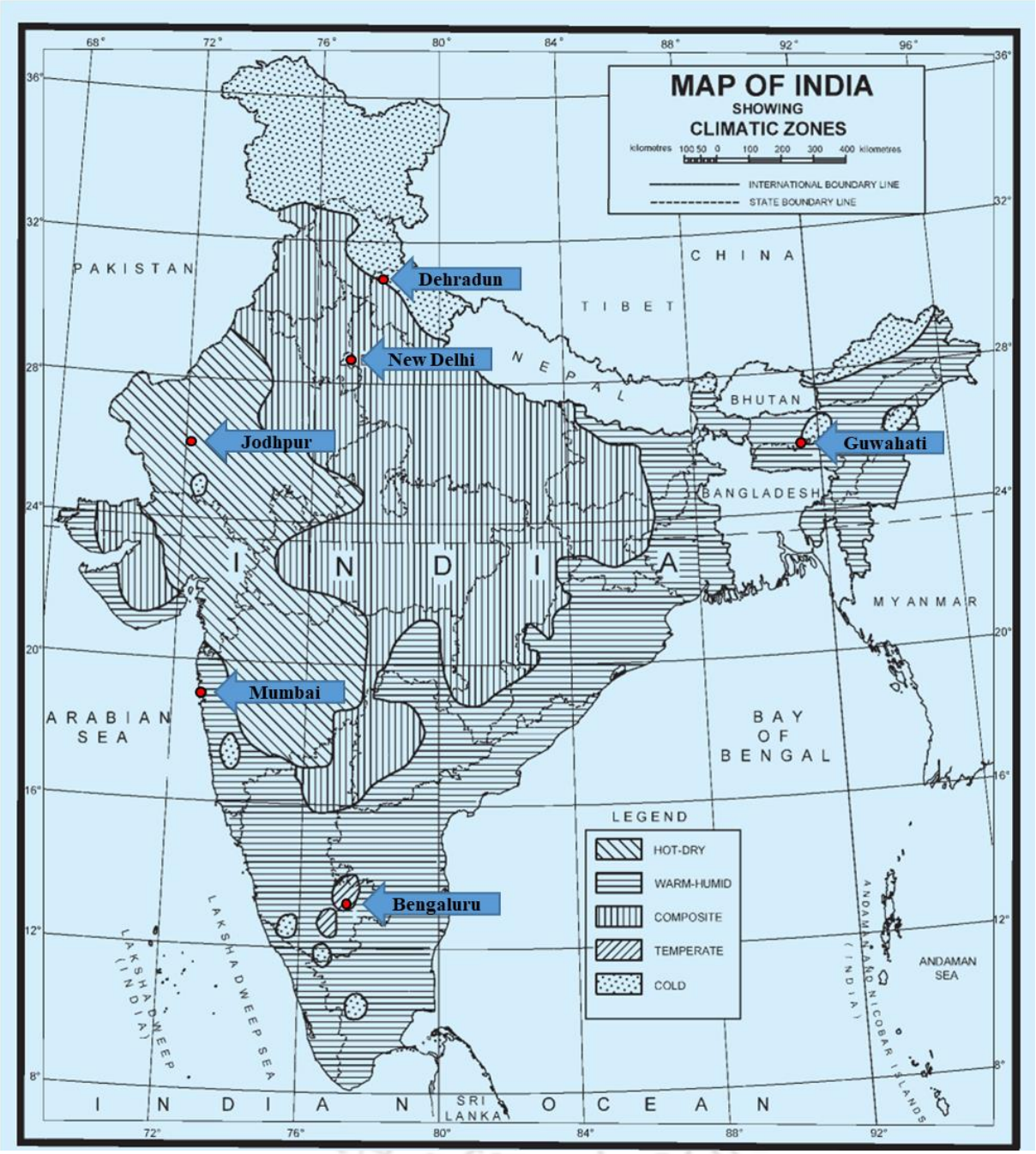

Figure 6-6: Pictorial representation of the selected study locations across India (modified from National building code (NBC vol. 2, 2016)

DesignBuilder methodology

Estimation of building's operational energy consumption is the primary objective of this chapter. Hence for this, a review of various software's available was carried out as mentioned in literature review and DesignBuilder software is chosen as suitable option among them. DesignBuilder software used in this study serve as a suitable analysis tool for calculation of operational energy cost of the building. Some of the important modules in Design Builder which

are worth mentioning are 3-D Modeler, visualization module used to render image, simulation module which uses EnergyPlus simulations for energy and comfort analysis, HVAC module which provides a powerful and flexible interface to EnergyPlus HVAC. Other modules include CFD, LEED, and Daylighting etc. EnergyPlus is the industry standard building energy simulation tool and has simulation capabilities which covers various parameters such as building fabric, thermal mass, glazing, shading, renewable and the most important component of simulation namely HVAC and financial analysis. EnergyPlus simulations provides data on energy consumption, carbon emissions and room comfort in the user mentioned timestamps. It also provides detailed reports on temperature distribution, heating and cooling systems and whole life-cycle cost of the building. It calculates heating and cooling loads using the ASHRAE-approved 'Heat Balance' method. It is also capable of calculating the heat transmitted through building fabrics which includes walls, roofs, ventilation, infiltration etc. It also enables to check the difference in annual energy consumption and other data when design alternatives are used.

The operational energy cost assessment in DesignBuilder software involves various parameters such as building envelope materials, building design, building orientation, HVAC systems, lighting, occupancy patterns, and climatic conditions. These factors collectively influence the building's energy performance over its lifecycle. These parameters are finalised as per the National building code 2016 and central public works department (CPWD) specifications handbook 2019 and considered for evaluation of operational energy cost of building over its life time. Here it is to be noted that the main point of concerned study is the performance of foam concrete as a walling material compared to traditionally available materials like AAC block and Standard clay brick. Hence to have fair analysis a basic model of G+3 building is prepared and keeping all other parameters constant only walling material (for both internal and external wall) as well as roofing material is changed. Figure 6.7 shows the schematic representation of methodology adopted for typical energy simulation modelling for building using DesignBuilder software. Further the step wise methodology adopted is discussed below. Figure 6.8 provides the cross sectional representation of different options of walling materials (AAC Block, FC, standard clay brick) assigned to building model considering different scenarios.

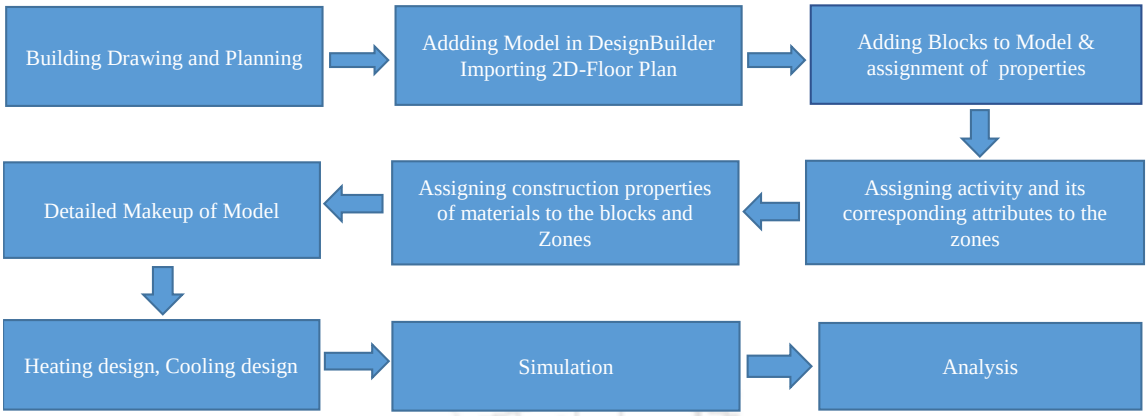

Figure 6-7:Schematic representation for a typical Building Modelling in design-builder

Stepwise methodology adopted for typical energy simulation modelling for building using DesignBuilder software: -

1. Residential bungalow G+3 as represented earlier in Figure 6.5 is designed using AutoCAD.
2. New Model is created in DesignBuilder, and the corresponding site location is assigned as mentioned earlier, and a new building is added.
3. 2D-DXF floor plan created using AutoCAD is imported in DesignBuilder. With the imported floor plan, block perimeters and partitions are tracked easily in less time to create the model.
4. Building blocks are created using the perimeter of imported plans and the height of the block refers to floor-floor height. Building Blocks are divided into several zones by drawing partitions inside the block according to their usage as shown in Figure 6.9.
5. Doors, windows, vent are added to the model according to the Floor plan in respective Zones. The size and material required for doors, windows and vent are assigned as per the National building code 2016 and central public works department (CPWD) specifications handbook 2019.
6. Activity is assigned for each zone and its occupancy is assigned as per the utility of that room. The heating set points and cooling set points are assigned accordingly. Typically for human comfort the heating temperature is set at 18°C and cooling at 25°C. The lighting tab adjusts lighting in each zone as represented in Figure 6.10.
7. Construction tab is used to edit the detailed makeup of the construction of walls, roofs, floors, ceilings, partitions, etc., used in the building. Table 6.11 provides the thermo-mechanical properties of the different walling materials used in the current study. The

properties are measured as per the methodology conforming to the relevant codal provision as discussed in the earlier chapter.

8. All the elements of the building are assigned with the proper layers and with corresponding properties as shown in Table 6.12 and represented by Figure 6.8. Building design drawing hand book is used to finalise the layers and their corresponding thickness.
9. The heating and cooling design sections calculate the equipment required to meet the coldest and hottest conditions at the chosen study location. The source of energy for heating and cooling is set accordingly for Indian subcontinent which is predominantly electricity from power grid. Annual energy consumption of buildings is calculated in the simulation section.

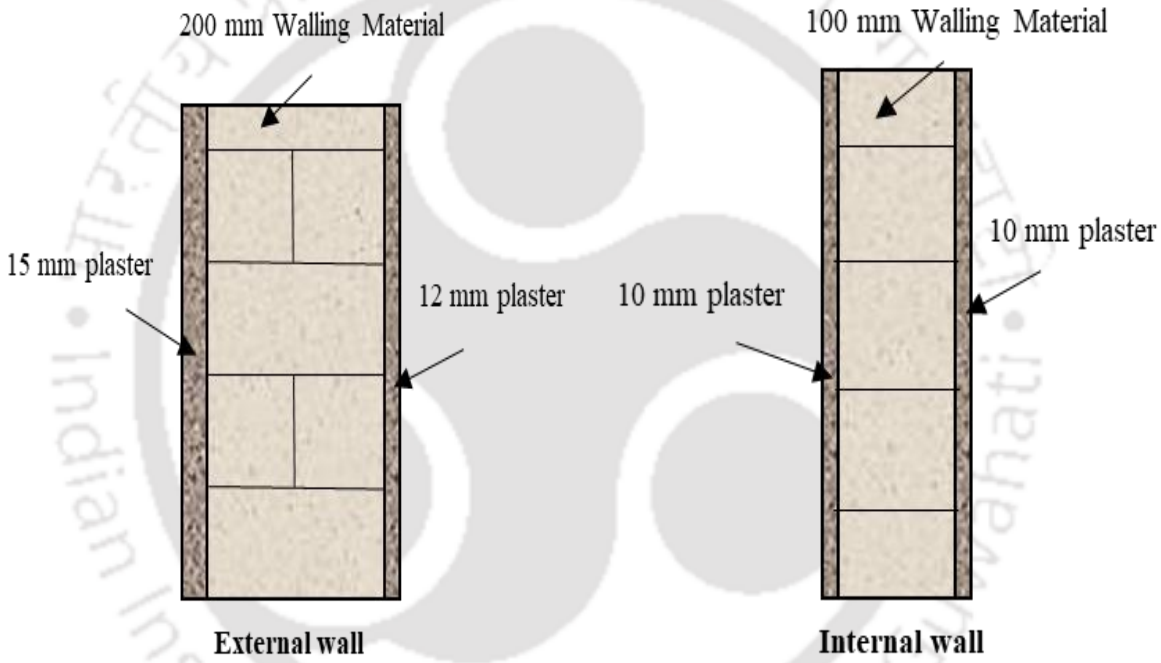

Figure 6-8: Representational cross sectional view of the external and internal wall assigned to the building

Figure 6-9: 3-D rendered view of the model, zones and partitions created for the building

Activity Template	
Template	**Domestic Bedroom**
Sector	Residential spaces
Zone type	1-Standard
Zone multiplier	1
☑ Include zone in thermal calculations	
☑ Include zone in Radiance daylighting calculations	
Floor Areas and Volumes	
Occupancy	
Occupancy density (people/m2)	0.0229
Schedule	Dwell_DomBed_Occ
Heating Setpoint Temperatures	
Heating (°C)	18.0
Heating set back (°C)	12.0
Cooling Setpoint Temperatures	
Cooling (°C)	25.0
Cooling set back (°C)	**30.0**
Lighting	
Target Illuminance (lux)	100
Default display lighting density (W/m2)	0

Figure 6-10: Activity template showing assignment of various parameters for the typical bedroom of the created residential model

Table 6-11: Thermo-Mechanical properties of the different walling materials selected for the study

Material	Oven dry Density (kg/m^3)	Avg. thermal conductivity (W/m-K)	Average thermal diffusivity ($m^2/s \times 10^{-7}$)	Average Specific Heat (J/kg-K)	Average Compressive strength (MPa)
LB0 (FC)	616.83	0.2476	9.88	406.29	1.04
MB0 (FC)	810.62	0.3435	8.10	523.30	1.79
LF2PP2 (FC)	502.93	0.1973	6.82	574.92	3.90
MF2PP2 (FC)	845.33	0.2959	5.68	616.23	8.25
AAC	685.56	0.3165	5.68	812.79	4.08
Clay Brick	1795.26	0.9597	5.71	840.00	9.87

Table 6-12: Details on various Cross Sections

Construction Unit	Number of Layers	Cross Sections (In Order)
Walls	3	15 mm plaster, 200 mm Block*, 12 mm plaster (External) 10 mm plaster, 100 mm Block*, 10 mm plaster (Internal)
Intermediate Floor	5	15 mm tiles, 10 mm cement Screed, 25 mm mortar, 150 mm reinforced concrete, 10 mm plaster
Roof	3	5 mm water proof coating, 25 mm mortar, 100 mm block* coba, 150 mm reinforced concrete Slab, 10 mm plaster
Ground Floor	4	15 mm Tiles, 10 mm cement Screed, 50 mm damp proof course, 100 mm lean concrete, 250 mm compacted earth

* here block refers to the various walling materials used (AAC Block, Foam concrete, Standard clay brick)

6.3.2 Results on Operational energy simulation

Figure 6.11 provides the Sunpath diagram along with energy consumption for a residential building considering its placement in various cities with different climatic conditions. The Sunpath diagram can be closely correlated to the energy consumption of the building throughout the year. The winter months typically showing shorter day duration tends to show lower monthly energy consumption. This phenomenon can be clearly noted from the Sunpath diagram of New Delhi city where lowest energy consumption can be recorded for the winter months from November to March. In general, a significant amount of energy consumption is allocated to cooling operations, while a relatively smaller proportion is dedicated to heating operations. This is mostly due to the fact that, during the majority of the winter season in the selected study locations in India, temperatures do not typically drop below a particular threshold

level, with the exception of Dehradun. Dehradun city, situated in the northern region of India and at the foothills of the Himalayas, shows a significant level of energy consumption specifically for heating operations during the winter period spanning from November to March. The energy consumption for heating operations in Dehradun city is approximately 6% of the whole annual energy consumption, whereas in other cities, this proportion varies from 0% to 2%. Thus, the major consumer of energy in operational phase of the building are cooling mechanisms, day-to-day lightings, domestic hot water and other electrical equipment. Table 6.13 summarizes the energy simulation output of Design build software for a typical G+3 residential building located in selected cities in India. Simulation results shows that, the highest total annual operational energy consumption is reported for Mumbai city while lowest is reported for Bangalore city for all the walling and roofing materials adopted in this study. For example, when considering standard clay brick as walling and roofing material the total annual operational energy recorded for Bangalore city is 43810.12 KWh while Mumbai reported an annual energy consumption of 84537.48 KWh. The energy consumption reported for Mumbai city is almost twice that of Bangalore. This can be attributed to the warm and humid climate type of Mumbai city with temperature varying between 24°C to 32°C throughout the year while that of Bangalore the temperature variation is from 20°C to 27°C.

Of all the materials used in the present study as a walling material, clay brick exhibits highest annual energy consumption while FC mix LF2PP2 reports the lowest annual energy consumption irrespective of study locations. For instance, in case of Mumbai city clay brick reports an annual operational energy consumption of 84537.48 kWh while FC mix LF2PP2 reports 68357.99 kWh (Table 6.13). This accounts for about 19% overall annual energy savings for a residential building in Mumbai city. The increased annual energy consumption of clay brick wall can be attributed to its higher thermal conductivity value, which allows higher average thermal transmittance through the structure (Aste et al., 2009; Ficco et al., 2015). Though Mumbai city reports the highest operational energy, but the realization of savings in energy consumption due to use of appropriate walling and roofing material with low thermal conductivity is found to be significant for New Delhi city. For example, mere use of FC mix LF2PP2 as a walling and roofing material instead of clay brick walls and conventional brick bat roof results in 21.00% of saving in operational energy in New Delhi city. Similarly, the corresponding saving for FC mix MF2PP2 with density 1000 kg/m^3 is observed to be 16.00%. When compared with performance of AAC block, FC mix LF2PP2 outperforms by showing average. annual energy saving of 11% while MF2PP2 results in savings of 4.5% in New Delhi

city. This can be attributed to the higher daily thermal fluctuations experienced in the New Delhi city. The lowest % energy saving of 11% is shown by Bangalore city while Guwahati and Dehradun showed an energy saving of 17% when mix LF2PP2 is used instead of standard clay brick.

Table 6.14 provides a detailed cost estimate considering the annual energy charges incurred by the building utilizing region-specific costs over the facility's lifetime. In accordance to BS 7543:2015 (Guide to durability of buildings and building parts, products and components), the building's expected lifespan is assumed as sixty years. For the building located in Guwahati, the energy costs adopted in the estimation (₹8.15/ kWh for year 2023) pertain to the state of Assam and conform to LT-III housing type. Similarly, for the buildings in different study locations, the costs pertaining to corresponding region is considered for analysis as shown in Table 6.14. In addition, ten years of financial data are analysed, and the average rate of increase in electricity rates is determined to be 6.1% and used for cost analysis (Jaganmohan, 2022). Results indicate that when compared to clay brick, the lifecycle operational energy cost of building with FC is found to be significantly lower. For instance, with respect to Guwahati city, FC mixes LF2PP2 and MF2PP2 with target densities of 600 and 1000 kg/m^3 results in cost savings of ₹4,76,80,928.76 and ₹3,51,23,850.70 respectively when compared to clay brick as walling material. However, the savings in operational energy achieved with FC when compared to AAC blocks is slightly lesser. For example, the use of LF2PP2 and MF2PP2 as a walling material instead of AAC block lead to total lifecycle operational energy cost savings of ₹2,14,15,957.35 and ₹88,58,879.29 for a residential building at Guwahati city. These savings will be much more when considering the same building in New Delhi city. As anticipated and confirmed by the report, it can be concluded that FC with a lower density can dramatically cut the operational energy usage leading to significant saving in the operational energy cost throughout the life of the building.

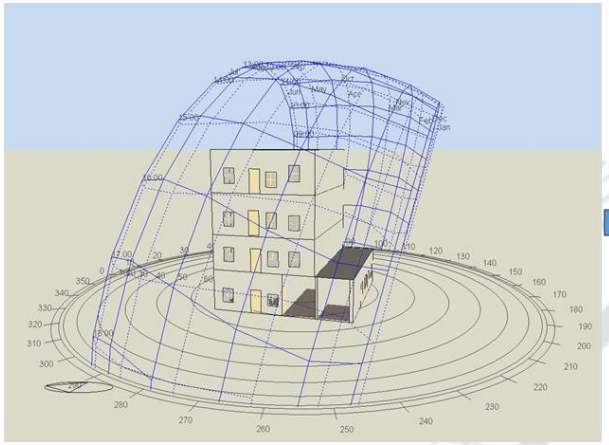

Bengaluru

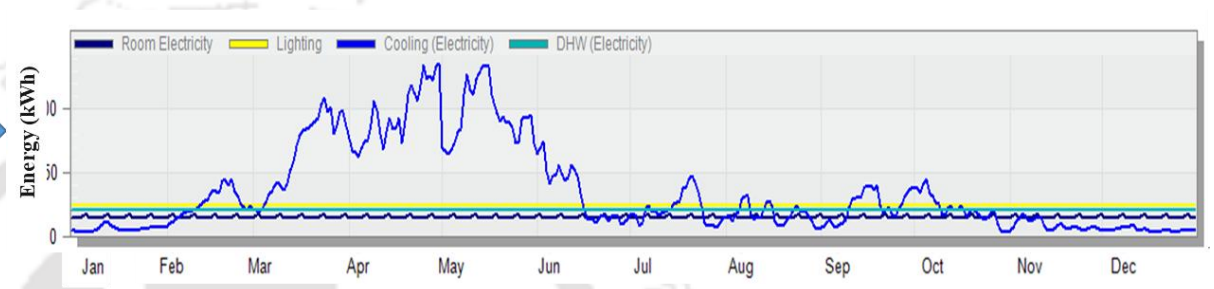

(a)

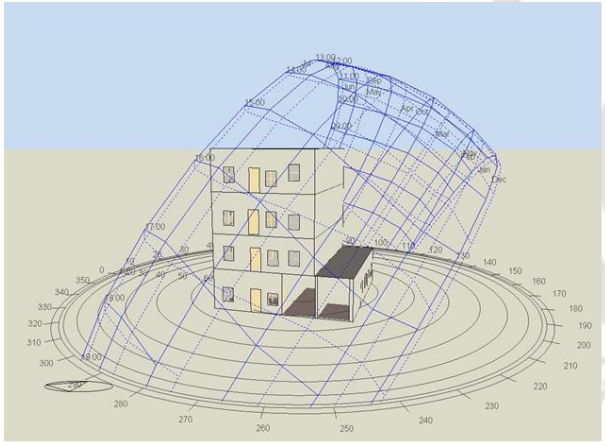

Dehradun

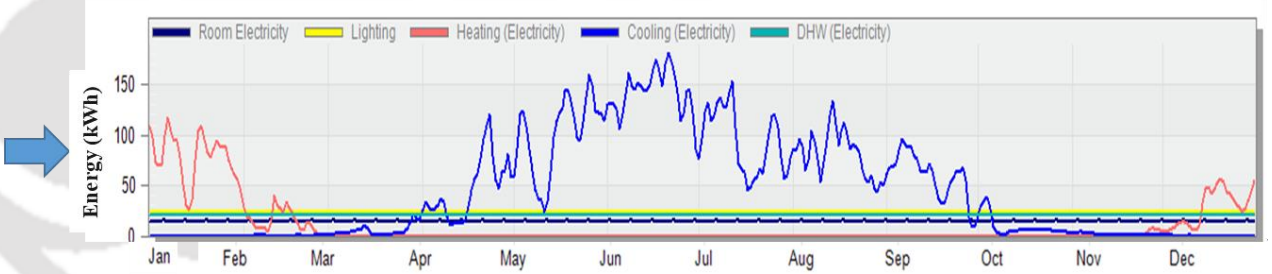

(b)

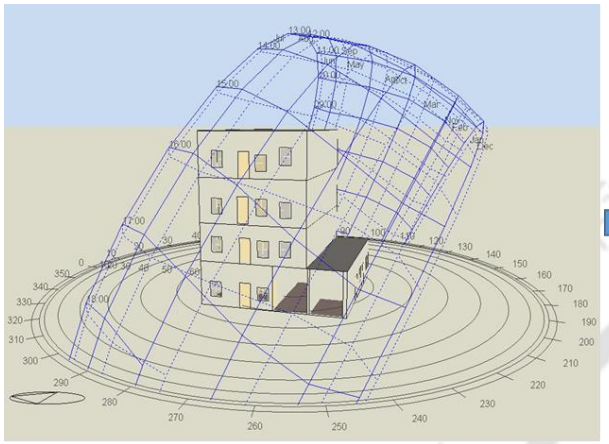

Guwahati

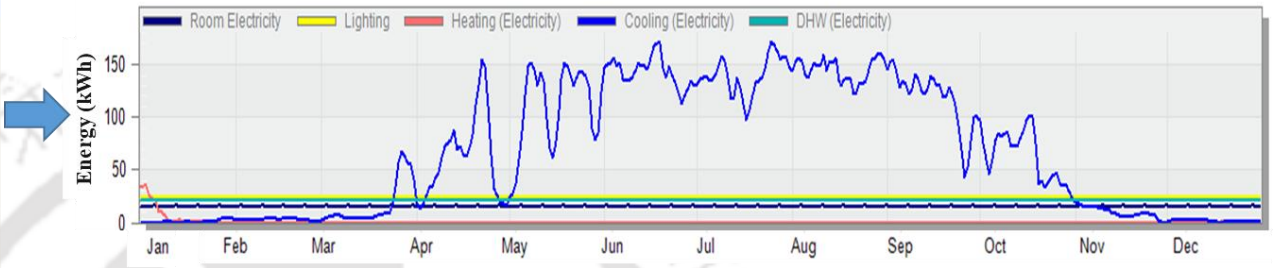

(c)

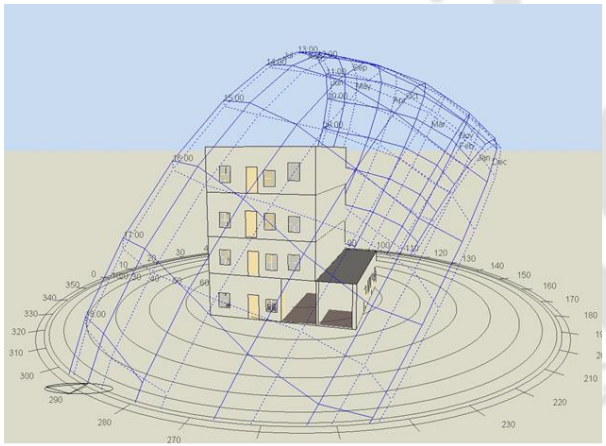

Jodhpur

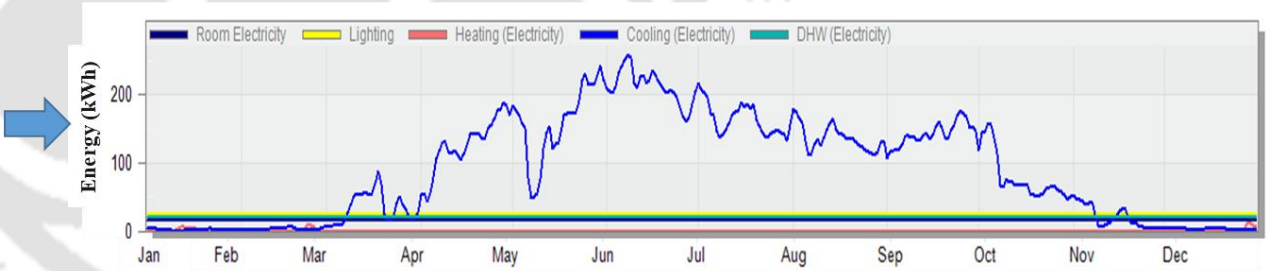

(d)

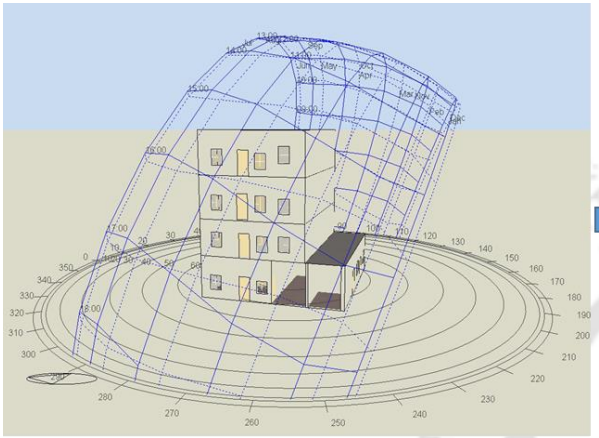

Mumbai

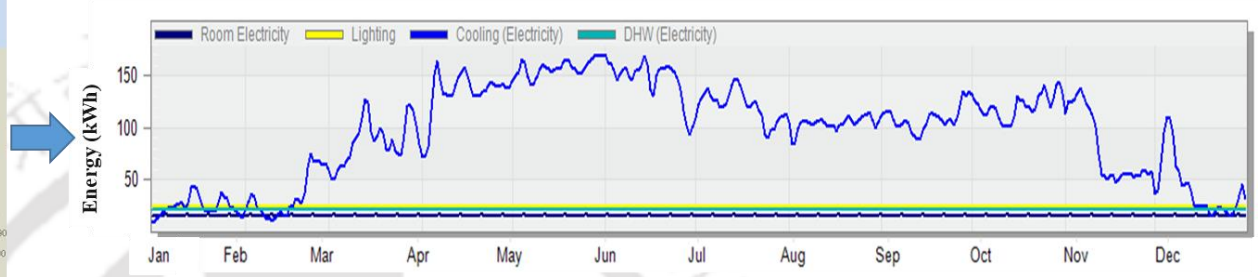

(e)

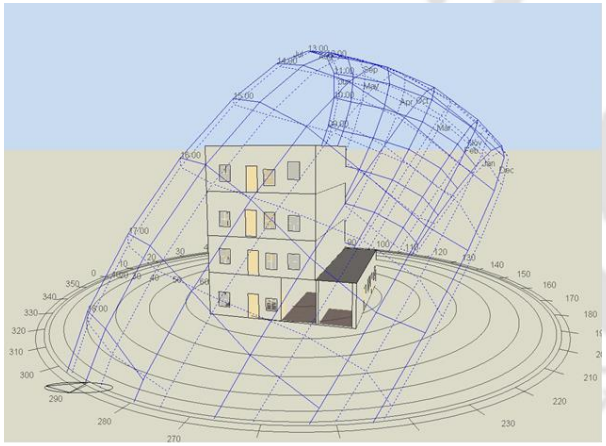

New Delhi

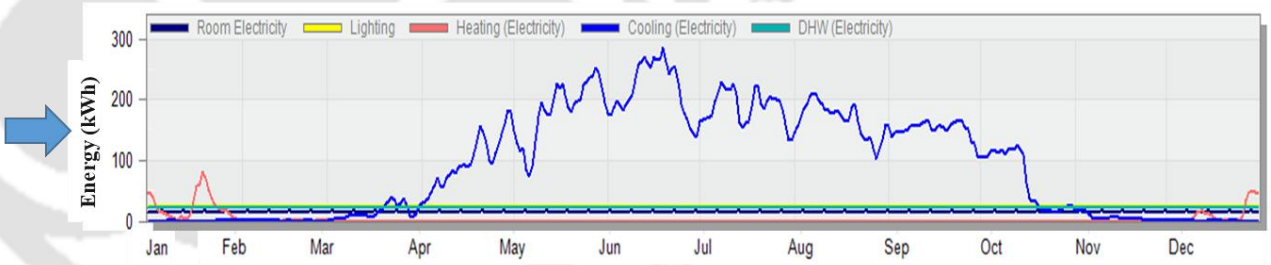

(f)

Figure 6-11: Sunpath diagram and Energy consumption for a residential building locate in various cities (a) Bengaluru (b) Dehradun (c) Guwahati (d) Jodhpur (e) Mumbai (f) New Delhi

Table 6-13: Annual operational energy consumption of G+3 residential building with different walling and roofing materials

Mix Code	TC (W/mK)	Annual Operational Energy consumption across various cities (kWh)					
		Bangalore	Dehradun	Guwahati	Jodhpur	Mumbai	New Delhi
LB0 (FC)	0.2476	39739.35	45965.12	56113.76	66133.85	70208.81	66938.45
MB0 (FC)	0.3435	40868.11	47963.10	58484.34	69671.52	73661.43	70644.47
LF2PP2 (FC)	0.1973	38778.12	44475.03	54807.53	63928.66	68357.99	64615.49
MF2PP2 (FC)	0.2959	40108.52	46903.97	57697.54	68152.05	72512.35	69074.15
AAC	0.3165	41731.93	48973.10	59736.41	71070.18	75315.01	72257.21
Clay Brick	0.9597	43810.12	53794.49	65781.29	80252.89	84537.48	81821.24

Table 6-14: Operational energy Cost analysis over entire life cycle of G+3 residential building with different walling and roofing materials

Mix Code	Type	Operational Energy cost across various cities (unit cost per kWh)					
		Bangalore (₹ 8.20/kWh)	Dehradun (₹ 6.95/kWh)	Guwahati (₹ 8.15/kWh)	Jodhpur (₹ 7.95/kWh)	Mumbai (₹ 13.70/kWh)	New Delhi (₹ 8.00/kWh)
LB0	Annual	₹ 3,25,862.67	₹ 3,19,457.58	₹ 4,57,327.14	₹ 5,25,764.11	₹ 9,61,860.70	₹ 5,35,507.60
	Life cycle	₹ 1737,26,572.48	₹ 1703,11,840.63	₹ 2438,13,988.35	₹ 2802,99,662.21	₹ 5127,95,043.66	₹ 2854,94,192.64
MB0	Annual	₹ 3,35,118.50	₹ 3,33,343.55	₹ 4,76,647.37	₹ 5,53,888.58	₹ 10,09,161.59	₹ 5,65,155.76
	Life cycle	₹ 1786,61,117.35	₹ 1777,14,837.76	₹ 2541,14,145.83	₹ 2952,93,613.20	₹ 5380,12,483.23	₹ 3013,00,462.25
LF2PP2	Annual	₹ 3,17,980.58	₹ 3,09,101.46	₹ 4,46,681.37	₹ 5,08,232.85	₹ 9,36,504.46	₹ 5,16,923.92
	Life cycle	₹ 1695,24,410.31	₹ 1647,90,698.28	₹ 2381,38,425.96	₹ 2709,53,253.19	₹ 4992,76,920.75	₹ 2755,86,709.13
MF2PP2	Annual	₹ 3,28,889.86	₹ 3,25,982.59	₹ 4,70,234.95	₹ 5,41,808.80	₹ 9,93,419.20	₹ 5,52,593.20
	Life cycle	₹ 1753,40,454.91	₹ 1737,90,506.01	₹ 2506,95,504.02	₹ 2888,53,538.60	₹ 5296,19,768.29	₹ 2946,03,007.49
AAC	Annual	₹ 3,42,201.83	₹ 3,40,363.05	₹ 4,86,851.74	₹ 5,65,007.93	₹ 10,31,815.64	₹ 5,78,057.68
	Life cycle	₹ 1824,37,436.99	₹ 1814,57,131.02	₹ 2595,54,383.31	₹ 3012,21,650.44	₹ 5500,89,993.57	₹ 3081,78,839.39
Clay Brick	Annual	₹ 3,59,242.98	₹ 3,73,871.71	₹ 5,36,117.51	₹ 6,38,010.48	₹ 11,58,163.48	₹ 6,54,569.92
	Life cycle	₹ 1915,22,558.56	₹ 1993,21,542.24	₹ 2858,19,354.71	₹ 3401,41,364.19	₹ 6174,49,587.13	₹ 3489,69,670.71

6.4 Summary

This chapter provided a comprehensive examination of the performance of two optimum mixes (MF2PP2 and LF2PP2) in relation to LCA and operational energy analysis. The LCA studies were conducted on optimal mixes, adhering to the requirements outlined in ISO 14040 and ISO 14044:2006, and utilizing SimaPro software. Comparison of the LCA analyses of Hingot and NPE surfactant proved that the hingot surfactant is a sustainable option. Further, comparison of the LCA results of the optimum FC mixes produced using hingot surfactant with the results of conventional materials available in market such as AAC block and Standard clay brick for Guwahati city is carried out. It has been found that performance of FC is better across all LCA impact categories discussed, when compared to clay brick and AAC block. Also, in particular the lower density FC mix i.e. 600 kg/m^3 outperformed all the other alternatives. Further it should be noteworthy that performance of LCA of FC cane be further improved by decreasing the density and through use of various mineral admixtures like FA, SF, GGBS etc. as replacement for cement.

The operational energy analysis of a G+3 residential building using optimal FC mixes, compared to traditional clay bricks and AAC blocks, showed promising results. A simulation is conducted using DesignBuilder software to determine the overall annual operational energy usage of a G+3 residential building in six different locations, namely Guwahati, Bangalore, Dehradun, Jodhpur, Mumbai, and New Delhi, representing distinct climate zones in India. Simulation results shows that Mumbai has the greatest annual operational energy usage considering all materials used in the study, whereas Bangalore has the lowest. Clay brick as walling material has higher thermal conductivity and average thermal transmittance, which increases their annual energy consumption and thus performed worst among all the materials analysed. The study also reported that usage of FC LF2PP2 instead of clay brick provided the highest annual operational energy saving of 21.37% for New Delhi has city, for mix MF2PP2 with density 1000 kg/m^3, the corresponding saving is 15.52%. Further on comparing with AAC block the average yearly energy savings for LF2PP2 and MF2PP2 are 11%, and 4.5% respectively in New Delhi. While considering Guwahati city, the energy saving can result in life time cost saving of up to ₹4,76,80,928.76 and ₹3,51,23,850.70 for FC mixes LF2PP2 and MF2PP2 respectively when compared to clay brick as walling and roofing material. The corresponding savings when compared to AAC block are ₹2,14,15,957.35 and ₹88,58,879.29 respectively. Thus this study proves the potential of FC to become an sustainable and cost efficient alternative as a walling and roof insulating material in building construction.

Chapter 7 CONCLUSIONS AND SCOPE FOR FUTURE WORK

7.1 Conclusions

The significant conclusions resulting from this research are outlined in this section. The studies conducted on foam concrete can be categorized into four sections:

(i) Investigations on the performance of xanthan gum (XG) as a foam stabilizer in FC production;

(ii) Influence of various admixtures on FC behaviour;

(iii) Lifecycle assessment of FC; and

(iv) Operational energy analysis of G+3 residential building.

The findings derived from the experimental studies are categorized into these four parts, which are relevant to the properties of the materials employed and the scope of the parameters examined.

Objective 1 :- Investigations on the performance of xanthan gum as a foam stabilizer in foam concrete production

1. The addition of XG significantly enhances the viscosity of both Hingot and NPE surfactant solutions, leading to a substantial reduction in bubble size and an increase in lamella thickness. Notably, the combination of Hingot and XG reduces bubble coarsening more effectively than the NPE and XG combination due to the synergistic effect of increased viscosity and lower surface tension, which improves lamella drainage time and decreases bubble coalescence.

2. The addition of XG significantly reduces spread flow and enhances demoulding time for FC mixes with Hingot FC showing higher demoulding time due to the retarding nature of saponin surfactant further intensified by XG addition. Remarkably, XG addition increases compressive strength by 51% in Hingot FC and 22% in NPE FC, while also decreasing thermal conductivity by 13% and 17% respectively.

3. The superior mechanical and thermal characteristics attributed to the enhanced pore structure, combined with its cost-effectiveness, emphasize that Hingot + 0.1XG stands out as a better and sustainable surfactant option than NPE for the production of FC.

Objective 2 :- Investigations on the Influence of various admixtures on foam concrete behaviour

1. Incorporating fly ash (FA), silica fume (SF), and polypropylene (PP) fibres into FC significantly influences its fresh and mechanical properties. The spread flow of the FC decreases with these admixtures, necessitating the use of superplasticizers for proper flow. Replacing sand entirely with FA results in substantial improvements in compressive strength—by 368% for a density of 1000 kg/m³ and 228% for 600 kg/m³—compared to the base mix. When FA is combined with SF and PP fibers, compressive strength further increases, achieving maximum values of 9.83 MPa and 3.93 MPa for densities of 1000 kg/m³ and 600 kg/m³, respectively. Additionally, this combination results in remarkable enhancements in splitting tensile strength, with increments of 490% and 260%, achieving values of 1.671 MPa and 0.661 MPa for the respective densities after 90 days.
2. The thermal conductivity (TC) of FC increases with its density, rising from 0.2476 W/mK at 600 kg/m³ to 0.3435 W/mK at 1000 kg/m³. While the incorporation of FA, SF, and PP fibres improves the microstructure and reduces TC by up to 28%, the density remains the primary factor influencing the thermal properties of FC.
3. Considering mechanical and thermal performance as well as economic viability, the mixes MF2PP2 (FC of 1000 kg/m^3 density with 100% FA + 0.4% PP fiber) and LF2PP2 (FC of 600 kg/m^3 density with 100% FA + 0.4% PP fiber) are identified as the optimal FC mixes.

Objective 3 :- Life cycle assessment of Foam concrete

1. The Hingot surfactant is a more sustainable and environmentally friendly alternative to the NPE surfactant, demonstrating lower cumulative energy demand and better performance across various environmental indicators, including marine eutrophication, marine ecotoxicity, stratospheric ozone depletion, terrestrial ecotoxicity, and freshwater ecotoxicity.

2. Reducing cement consumption in FC mixes through the use of supplementary cementitious materials can significantly lower the embodied energy and global warming potential, as cement constitutes nearly 70% and 84% of it respectively. Life Cycle Assessment (LCA) analysis shows that the optimum mixes MF2PP2 and LF2PP2 outperform standard clay bricks and AAC blocks across all environmental impact categories. Notably, the LF2PP2 mix demonstrated a 33% lower cumulative energy demand and a 27% lower global warming potential compared to AAC blocks.

3. It should be worth noting that the performance of LCA for foam concrete can be improved further by lowering the density and incorporating mineral admixtures (as replacement to cement), thus decreasing the overall cement consumption, nevertheless FC still comes out to be more sustainable and ecofriendly alternative to traditional walling materials like clay brick and AAC block.

Objective 4 :- Operational energy analysis of G+3 residential building

1. The FC mixes MF2PP2 (1000 kg/m^3) and LF2PP2 (600 kg/m^3) demonstrated annual operational energy savings of 16% and 21%, respectively, when compared to standard clay bricks. On similar lines, savings of 4.5% and 11% are observed compared to AAC blocks when utilized as walling and roofing materials for New Delhi's climatic zone.

2. The operational energy requirement of buildings varies significantly across climatic zones, with potential increases of up to 80%. For instance, using MF2PP2 as walling and roofing material, Bengaluru city under temperate climatic zone showed an annual operational energy consumption of 40,108.52 kWh while Mumbai city with warm and humid climate showed an energy consumption of 72,512.35 kWh.

3. Clay brick when used as a walling and roofing material demanded the highest operational energy consumption while LF2PP2 required the lowest, for instance, in case of Mumbai city clay brick reported an annual operational energy consumption of 84537.48 kWh while mix LF2PP2 reported 68357.99 kWh.

4. The results of the operational energy analysis highlight the significance of building material selection for climate-specific considerations to optimize operational energy efficiency. Additionally, it is worth noting that FC shows promise as an energy-efficient alternative compared to clay brick and AAC block for building construction.

7.2 Scope for Future Work

This study serves as the initial phase of the subsequent long-term investigations on FC. Future investigations which can focus on specific areas to enhance our comprehension of the material, contributing to its increased utility in the construction industry are as follows: -

i) Investigations on other mechanical properties like modulus of elasticity and properties related to dimensional stability such as creep and shrinkage, functional properties like sound insulation, fire resistance and durability related properties can be carried out.

ii) LCA studies can be done for complete life cycle from cradle to grave for building constructed with FC as walling and roofing material.

iii) Lifecycle cost analysis can be done for all the building life cycle phases including construction phase, operational phase, maintenance phase and demolition phase.

iv) The DesignBuilder model used in our study can be validated through comparison with empirical data, field measurements, or by constructing actual small scale models.

REFERENCES

ACI Committee 523, 2014. ACI PRC-523.3-14 Guide for cellular concretes above 50 lb/ft^3 (800 kg/m^3), Norma del American Concrete Institute. American Concrete Institute.

Ahmad, M.H., Awang, H., 2013. Effect of steel and alkaline-resistance glass fibre on mechanical and durability properties of lightweight foamed concrete. Adv. Mater. Res. 626, 404–410. https://doi.org/10.4028/www.scientific.net/AMR.626.404

Ahmad, M.R., Chen, B., Farasat Ali Shah, S., 2019. Investigate the influence of expanded clay aggregate and silica fume on the properties of lightweight concrete. Constr. Build. Mater. 220, 253–266. https://doi.org/10.1016/j.conbuildmat.2019.05.171

Ahmad, S., Baghabra Al-Amoudi, O.S., Khan, S.M.S., Maslehuddin, M., 2022. Effect of silica fume inclusion on the strength, shrinkage and durability characteristics of natural pozzolan-based cement concrete. Case Stud. Constr. Mater. 17, e01255. https://doi.org/10.1016/j.cscm.2022.e01255

Ahmadi, S.F., Reisi, M., Amiri, M.C., 2022. Reusing granite waste in eco-friendly foamed concrete as aggregate. J. Build. Eng. 46, 103566. https://doi.org/10.1016/j.jobe.2021.103566

Al-Shwaiter, A., Awang, H., Khalaf, M.A., 2022. Performance of sustainable lightweight foam concrete prepared using palm oil fuel ash as a sand replacement. Constr. Build. Mater. 322, 126482. https://doi.org/10.1016/j.conbuildmat.2022.126482

Aldridge, D., n.d. INTRODUCTION TO FOAMED CONCRETE: WHAT, WHY, HOW?, in: Use of Foamed Concrete in Construction. pp. 1–14. https://doi.org/10.1680/uofcic.34068.0001

Aldridge, D., Ansell, T., 2001. Foamed concrete: production and equipment design, properties, applications and potential, in: Proceedings of One Day Seminar on Foamed Concrete: Properties, Applications and Latest Technological Developments, Loughborough University. pp. 1–7.

Aleksandr I. Kudyakov; Aleksei B. Steshenko, 2014. Heat insulating reinforced air hardened foamed concrete. Vestn. TSUAB 60–65.

Amran, Y.H.M., Farzadnia, N., Ali, A.A.A., 2015. Properties and applications of foamed concrete; A review. Constr. Build. Mater. 101, 990–1005.

https://doi.org/10.1016/j.conbuildmat.2015.10.112

Angarska, J.K., Tachev, K.D., Ivanov, I.B., Mehreteab, A., Brose, G., 1997. Effect of magnesium ions on the properties of foam films stabilized with sodium dodecyl sulfate. J. Colloid Interface Sci. 195, 316–328. https://doi.org/10.1006/jcis.1997.5133

Antonelli, J.F.C., Erba, L.A., Azambuja, M.D.A., 2020. Walls composed of different materials: a brief review on thermal comfort. Rev. Nac. Gerenciamento Cid. 8, 57–73. https://doi.org/10.17271/2318847286620202699

Arabloo, M., Ghazanfari, M.H., Rashtchian, D., 2015. Spotlight on kinetic and equilibrium adsorption of a new surfactant onto sandstone minerals: a comparative study. J. Taiwan Inst. Chem. Eng. 50, 12–23.

Asnacios, A., Klitzing, R., Langevin, D., 2000. Mixed monolayers of polyelectrolytes and surfactants at the air-water interface. Colloids Surfaces A Physicochem. Eng. Asp. 167, 189–197. https://doi.org/10.1016/S0927-7757(99)00475-6

Aste, N., Angelotti, A., Buzzetti, M., 2009. The influence of the external walls thermal inertia on the energy performance of well insulated buildings. Energy Build. 41, 1181–1187. https://doi.org/10.1016/j.enbuild.2009.06.005

ASTM C230/C230M-21, 2021. Standard Specification for Flow Table for Use in Tests of Hydraulic Cement. ASTM Int. 4–9.

ASTM C495/C495M-12, 2019. Standard test method for compressive strength of concrete. ASTM Int.

ASTM C796-19, 2019. Standard Test Method for Foaming Agents for Use in Producing Cellular Concrete Using Preformed Foam. Astm C796/C796M.

ASTM C796/C796M − 19, 1967. Standard Test Method for Foaming Agents for Use in Producing Cellular Concrete Using Preformed Foam. Connect 3, 1–5. https://doi.org/10.1520/C0796

Awang, H., Mydin, A.O., Roslan, A.F., 2012. Effect of additives on mechanical and thermal properties of lightweight foamed concrete. Adv. Appl. Sci. Res. 3, 3326–3338.

Bagheri, A., Samea, S.A., 2018. Parameters Influencing the Stability of Foamed Concrete. J. Mater. Civ. Eng. 30, 04018091. https://doi.org/10.1061/(asce)mt.1943-5533.0002290

Bajpai, R., Choudhary, K., Srivastava, A., Singh, K., 2020. Environmental impact assessment of fl y ash and silica fume based geopolymer concrete. J. Clean. Prod. 254, 120147. https://doi.org/10.1016/j.jclepro.2020.120147

Bejan, A., 1995. Heat transfer, second edition.

Berninger, T., Dietz, N., González López, Ó., 2021. Water-soluble polymers in agriculture:

xanthan gum as eco-friendly alternative to synthetics. Microb. Biotechnol. 14, 1881–1896. https://doi.org/10.1111/1751-7915.13867

Bessenouci, M.Z., Bibi-Triki, N.E., Bendimerad, S., Nakoul, Z., Khelladi, S., Hakem, A., 2014. Influence of humidity on the apparent thermal conductivity of concrete pozzolan. Phys. Procedia 55, 150–156. https://doi.org/10.1016/j.phpro.2014.07.022

Bhatia, N., 2014. Life Cycle Assessment as a tool for Material Selection - A comparison of Autoclaved Aerated Concrete and VSBK Brick Wall Assembly . 30th Int. PLEA Conf. Sustain. Habitat Dev. Soc. Choos. W. Forw. 1–8.

Bindiganavile, V., Batool, F., Suresh, N., 2012. Effect of fly ash on thermal properties of cement based foams evaluated by transient plane heat source. Indian Concr. J. 86, 7–14.

Bing, C., Zhen, W., Ning, L., 2012. Experimental Research on Properties of High-Strength Foamed Concrete. J. Mater. Civ. Eng. 24, 113–118. https://doi.org/10.1061/(ASCE)MT.1943-5533.0000353

Braga, A.M., Silvestre, J.D., de Brito, J., 2017. Compared environmental and economic impact from cradle to gate of concrete with natural and recycled coarse aggregates. J. Clean. Prod. 162, 529–543. https://doi.org/10.1016/j.jclepro.2017.06.057

Brown, N., Ubbelohde, M.S., Loisos, G., Philip, S., 2014. Quick design analysis for improving building energy performance. Energy Procedia 57, 3041–3050. https://doi.org/10.1016/j.egypro.2014.10.340

Bueno, V.B., Freitas, D., Petri, S., 2014. Xanthan hydrogel films : Molecular conformation , charge density and protein carriers. Carbohydr. Polym. 101, 897–904. https://doi.org/10.1016/j.carbpol.2013.10.039

Celik, K., Meral, C., Gursel, A.P., Mehta, P.K., Horvath, A., Monteiro, P.J.M., 2015. Cement & Concrete Composites Mechanical properties , durability , and life-cycle assessment of self-consolidating concrete mixtures made with blended portland cements containing fly ash and limestone powder. Cem. Concr. Compos. 56, 59–72. https://doi.org/10.1016/j.cemconcomp.2014.11.003

Chen, B., Liu, N., 2013. A novel lightweight concrete-fabrication and its thermal and mechanical properties. Constr. Build. Mater. 44, 691–698. https://doi.org/10.1016/j.conbuildmat.2013.03.091

Chen, X., Wang, H., Najm, H., Venkiteela, G., Hencken, J., 2019. Evaluating engineering properties and environmental impact of pervious concrete with fly ash and slag. J. Clean. Prod. 237, 117714. https://doi.org/10.1016/j.jclepro.2019.117714

Chica, L., Alzate, A., 2019. Cellular concrete review: New trends for application in

construction. Constr. Build. Mater. 200, 637–647. https://doi.org/10.1016/j.conbuildmat.2018.12.136

Chung, S.Y., Kim, J.S., Lehmann, C., Stephan, D., Han, T.S., Elrahman, M.A., 2020. Investigation of phase composition and microstructure of foamed cement paste with different supplementary cementing materials. Cem. Concr. Compos. 109, 103560. https://doi.org/10.1016/j.cemconcomp.2020.103560

Coakley, D., Raftery, P., Molloy, P., 2012. Calibration of Whole Building Energy Simulation Models: Detailed Case Study of a Naturally Ventilated Building Using Hourly Measured Data. Build. Simul. Optim. 57–64.

Colak, A., 2000. Density and strength characteristics of foamed gypsum. Cem. Concr. Compos. 22, 193–200.

Colangelo, F., Forcina, A., Farina, I., Petrillo, A., 2018. Life Cycle Assessment (LCA) of different kinds of concrete containing waste for sustainable construction. Buildings 8. https://doi.org/10.3390/buildings8050070

Cong, M., Bing, C., 2015. Properties of a foamed concrete with soil as filler. Constr. Build. Mater. 76, 61–69. https://doi.org/10.1016/j.conbuildmat.2014.11.066

Costa, A., Keane, M.M., Torrens, J.I., Corry, E., 2013. Building operation and energy performance: Monitoring, analysis and optimisation toolkit. Appl. Energy 101, 310–316. https://doi.org/10.1016/j.apenergy.2011.10.037

Cox, L.S., 2005. Major road and bridge projects with foam concrete, in: Proceedings of the International Conference on the Use of Foamed Concrete in Construction. Thomas Telford Publishing, pp. 105–112.

Cuenca-Moyano, G.M., Martín-Morales, M., Bonoli, A., Valverde-Palacios, I., 2019. Environmental assessment of masonry mortars made with natural and recycled aggregates. Int. J. Life Cycle Assess. 24, 191–210. https://doi.org/10.1007/s11367-018-1518-9

Cui, Y.L., Qian, F.G., Liu, S.X., Yin, H.T., 2014. Effects of hydrogen peroxide on foam concrete performances, in: Applied Mechanics and Materials. pp. 1746–1749. https://doi.org/10.4028/www.scientific.net/AMM.584-586.1746

Dandautiya, R., Singh, A.P., 2019. Utilization potential of fly ash and copper tailings in concrete as partial replacement of cement along with life cycle assessment. Waste Manag. 99, 90–101. https://doi.org/10.1016/j.wasman.2019.08.036

Dário, A.F., Hortêncio, L.M.A., Rita, M., Queiroz, J.C., Petri, D.F.S., 2011. The effect of calcium salts on the viscosity and adsorption behavior of xanthan. Carbohydr. Polym. 84, 669–676. https://doi.org/10.1016/j.carbpol.2010.12.047

Demirboğa, R., Gül, R., 2003. Thermal conductivity and compressive strength of expanded perlite aggregate concrete with mineral admixtures. Energy Build. 35, 1155–1159. https://doi.org/10.1016/j.enbuild.2003.09.002

Dhasindrakrishna, K., Ramakrishnan, S., Pasupathy, K., Sanjayan, J., 2021. Collapse of fresh foam concrete: Mechanisms and influencing parameters. Cem. Concr. Compos. 122, 104151. https://doi.org/10.1016/j.cemconcomp.2021.104151

Dissanayake, D.M.K.W., Jayasinghe, C., Jayasinghe, M.T.R., 2017. A comparative embodied energy analysis of a house with recycled expanded polystyrene (EPS) based foam concrete wall panels. Energy Build. 135, 85–94. https://doi.org/10.1016/j.enbuild.2016.11.044

Djabbarah, N.F., Wasan, D.T., 1985. Foam stability: The effect of surface rheological properties on the lamella rupture. AIChE J. 31, 1041–1043. https://doi.org/10.1002/aic.690310623

Duval, R., Kadri, E.H., 1998. Influence of Silica Fume on the Workability and the. Cem. Concr. Res. 28, 533–547.

Ezema, I.C., 2019. Chapter 9 - Materials, in: Tam, V.W.Y., Le, K.N.B.T.-S.C.T. (Eds.), . Butterworth-Heinemann, pp. 237–262. https://doi.org/https://doi.org/10.1016/B978-0-12-811749-1.00007-9

Fabien, A., Sebaibi, N., Boutouil, M., 2019. Effect of several parameters on non-autoclaved aerated concrete: use of recycling waste perlite. Eur. J. Environ. Civ. Eng. 0, 1–18. https://doi.org/10.1080/19648189.2019.1647465

Falliano, D., De Domenico, D., Ricciardi, G., Gugliandolo, E., 2018. Experimental investigation on the compressive strength of foamed concrete: Effect of curing conditions, cement type, foaming agent and dry density. Constr. Build. Mater. 165, 735–749. https://doi.org/10.1016/j.conbuildmat.2017.12.241

Falliano, D., Parmigiani, S., Suarez-Riera, D., Ferro, G.A., Restuccia, L., 2022. Stability, flexural behavior and compressive strength of ultra-lightweight fiber-reinforced foamed concrete with dry density lower than 100 kg/m3. J. Build. Eng. 51, 104329. https://doi.org/10.1016/j.jobe.2022.104329

Ficco, G., Iannetta, F., Ianniello, E., D'Ambrosio Alfano, F.R., Dell'Isola, M., 2015. U-value in situ measurement for energy diagnosis of existing buildings. Energy Build. 104, 108–121. https://doi.org/10.1016/j.enbuild.2015.06.071

Folmer, B.M., Kronberg, B., 2000. Effect of surfactant-polymer association on the stabilities of foams and thin films: Sodium dodecyl sulfate and poly(vinyl pyrrolidone). Langmuir 16, 5987–5992. https://doi.org/10.1021/la991655k

Gandhi, I.S.R., Boddepalli, U., Bisht, R., Wagh, C., 2023. Impact of Addition of Fly Ash (as Sand Replacement) and Polypropylene Fibers on Energy Absorption Characteristics of Foam Concrete. Adv. Civ. Eng. Mater. 12, 127–144. https://doi.org/10.1520/ACEM20220131

Gandhi, I.S.R., Ramamurthy, K., 2012. Behaviour of foam concrete under sulphate environments. Cem. Concr. Compos. 34, 825–834. https://doi.org/10.1016/j.cemconcomp.2012.03.007

Ganesan, S., Othuman Mydin, M.A., Mohd Yunos, M.Y., Mohd Nawi, M.N., 2015. Thermal Properties of Foamed Concrete with Various Densities and Additives at Ambient Temperature. Appl. Mech. Mater. 747, 230–233. https://doi.org/10.4028/www.scientific.net/amm.747.230

Gelman, R.A., Barth, H.G., 1981. Atypical viscosity behavior of dilute solutions of xanthan gum. J. Appl. Polym. Sci. 26, 2099–2101. https://doi.org/https://doi.org/10.1002/app.1981.070260632

Gencel, O., Bilir, T., Bademler, Z., Ozbakkaloglu, T., 2022a. A Detailed Review on Foam Concrete Composites: Ingredients, Properties, and Microstructure. Appl. Sci. 12. https://doi.org/10.3390/app12115752

Gencel, O., Kazmi, S.M.S., Munir, M.J., Kaplan, G., Bayraktar, O.Y., Yarar, D.O., Karimipour, A., Ahmad, M.R., 2021. Influence of bottom ash and polypropylene fibers on the physico-mechanical, durability and thermal performance of foam concrete: An experimental investigation. Constr. Build. Mater. 306, 124887. https://doi.org/10.1016/j.conbuildmat.2021.124887

Gencel, O., Nodehi, M., Yavuz Bayraktar, O., Kaplan, G., Benli, A., Gholampour, A., Ozbakkaloglu, T., 2022b. Basalt fiber-reinforced foam concrete containing silica fume: An experimental study. Constr. Build. Mater. 326, 126861. https://doi.org/10.1016/j.conbuildmat.2022.126861

Gettu, R., Patel, A., Rathi, V., Prakasan, S., Basavaraj, A.S., Palaniappan, S., Maity, S., 2019. Influence of supplementary cementitious materials on the sustainability parameters of cements and concretes in the Indian context. Mater. Struct. Constr. 52, 1–11. https://doi.org/10.1617/s11527-019-1321-5

Gettu, R., Pillai, R.G., Santhanam, M., Basavaraj, A.S., 2018. Sustainability-based decision support framework for choosing concrete mixture proportions. Mater. Struct. 0123456789. https://doi.org/10.1617/s11527-018-1291-z

Giannakou, A., Jones, M.R., 2002. Potential of foamed concrete to enhance the thermal

performance of low-rise dwellings. Innov. Dev. Concr. Mater. Constr. Proc. Int. Conf. held Univ. Dundee, Scotland, UK 9--11 Sept. 2002 533–544.

Gökçe, H.S., Hatungimana, D., Ramyar, K., 2019. Effect of fly ash and silica fume on hardened properties of foam concrete. Constr. Build. Mater. 194, 1–11. https://doi.org/10.1016/j.conbuildmat.2018.11.036

Gołaszewski, J., Klemczak, B., Smolana, A., Gołaszewska, M., Cygan, G., Mankel, C., Peralta, I., Röser, F., Koenders, E.A.B., 2022. Effect of Foaming Agent, Binder and Density on the Compressive Strength and Thermal Conductivity of Ultra-Light Foam Concrete. Buildings 12. https://doi.org/10.3390/buildings12081176

Gomes, R., Silvestre, J.D., de Brito, J., 2020. Environmental life cycle assessment of the manufacture of EPS granulates, lightweight concrete with EPS and high-density EPS boards. J. Build. Eng. 28. https://doi.org/10.1016/j.jobe.2019.101031

Gong, J., Zhu, L., Li, J., Shi, D., 2020. Silica Fume and Nanosilica Effects on Mechanical and Shrinkage Properties of Foam Concrete for Structural Application. Adv. Mater. Sci. Eng. 2020. https://doi.org/10.1155/2020/3963089

Hajimohammadi, A., Ngo, T., Mendis, P., 2018. Enhancing the strength of pre-made foams for foam concrete applications. Cem. Concr. Compos. 87, 164–171. https://doi.org/10.1016/j.cemconcomp.2017.12.014

Hajimohammadi, A., Ngo, T., Mendis, P., Kashani, A., van Deventer, J.S.J., 2017. Alkali activated slag foams: The effect of the alkali reaction on foam characteristics. J. Clean. Prod. 147, 330–339. https://doi.org/10.1016/j.jclepro.2017.01.134

Hajimohammadi, A., Ngo, T., Provis, J.L., Kim, T., Vongsvivut, J., 2019. High strength/density ratio in a syntactic foam made from one-part mix geopolymer and cenospheres. Compos. Part B Eng. 173, 106908. https://doi.org/10.1016/j.compositesb.2019.106908

Hamidul Islam D, 2012. Use of Material in Residential House Design: An Optimisation Approach Balancing Life Cycle Cost & Life Cycle Environmental Impact 275.

Hashim, M., Tantray, M., 2021. Case Studies in Construction Materials Comparative study on the performance of protein and synthetic-based foaming agents used in foamed concrete. Case Stud. Constr. Mater. 14, e00524. https://doi.org/10.1016/j.cscm.2021.e00524

Hilal, Ameer A, Howard, N., Robert, A., 2015. On entrained pore size distribution of foamed concrete. Constr. Build. Mater. 75, 227–233. https://doi.org/10.1016/j.conbuildmat.2014.09.117

Hilal, Ameer A., Thom, N.H., R. Dawson, A., 2015. The Use of Additives to Enhance Properties of Pre- Formed Foamed Concrete. Int. J. Eng. Technol. 7, 286–293.

https://doi.org/10.7763/ijet.2015.v7.806

Huang, H., Yuan, Q., Deng, D., Peng, J., Huang, Y., 2019. Effects of chemical and mineral admixtures on the foam indexes of cement-based materials. Case Stud. Constr. Mater. 11, e00232. https://doi.org/10.1016/j.cscm.2019.e00232

Ibrahim, N.M., Salehuddin, S., Amat, R.C., Rahim, N.L., Izhar, T.N.T., 2013. Performance of Lightweight Foamed Concrete with Waste Clay Brick as Coarse Aggregate. APCBEE Procedia 5, 497–501. https://doi.org/10.1016/j.apcbee.2013.05.084

IS 2185:1984, 1984. Concrete masonry units, Part 3: Autoclaved cellular Aerated concrete blocks. Bureau of Indian Standards, New Delhi, India.

IS 269:2015, 2015. Ordinary Portland cement – Specification, Bureau of Indian Standards. Bureau of Indian Standards, New Delhi, India.

Islam, H., Jollands, M., Setunge, S., Ahmed, I., Haque, N., 2014. Life cycle assessment and life cycle cost implications of wall assemblages designs. Energy Build. 84, 33–45. https://doi.org/10.1016/j.enbuild.2014.07.041

ISO 14040, 2006. International Standard ISO 14040 Environmental management — Life cycle assessment — Requirements and guidelines Management.

ISO 14040 2006, n.d. Environmental management - Life cycle assessment - Principles and framework.

ISO 14044, 2006. International Standard ISO 14044 Environmental management — Life cycle assessment — Requirements and guidelines Management. Work 0–90.

ISO 14044 2006, n.d. Environmental Management- Life cycle assessment- Requirements and guidelines.

ISO 22007-2, 2008. Plastics — Determination of thermal conductivity and thermal diffusivity — Part 2: Transient plane heat source (hot disc) method. Int. Stand.

Jaganmohan, M., 2022. Average cost of state electricity supply in India from financial year 2009 to 2020 [WWW Document]. URL https://www.statista.com/statistics/808201/india-cost-of-state-electricity-supply/ (accessed 9.8.22).

Jhatial, A.A., Goh, W.I., Mastoi, A.K., Rahman, A.F., Kamaruddin, S., 2021. Thermo-mechanical properties and sustainability analysis of newly developed eco-friendly structural foamed concrete by reusing palm oil fuel ash and eggshell powder as supplementary cementitious materials. Environ. Sci. Pollut. Res. 28, 38947–38968. https://doi.org/10.1007/s11356-021-13435-2

Jhatial, A.A., Goh, W.I., Mohamad, N., Rind, T.A., Sandhu, A.R., 2020. Development of Thermal Insulating Lightweight Foamed Concrete Reinforced with Polypropylene Fibres.

Arab. J. Sci. Eng. 45, 4067–4076. https://doi.org/10.1007/s13369-020-04382-0

Ji, J., Liu, X., Tan, S., Ni, W., 2019. Preparation and properties of waste-solid based foam concrete energy-saving materials, in: IOP Conference Series: Earth and Environmental Science. https://doi.org/10.1088/1755-1315/295/4/042140

Jiang, J., Lu, Z., Niu, Y., Li, J., Zhang, Y., 2016. Study on the preparation and properties of high-porosity foamed concretes based on ordinary Portland cement. Mater. Des. 92, 949–959. https://doi.org/10.1016/j.matdes.2015.12.068

Joglekar, S.N., Kharkar, R.A., Mandavgane, S.A., Kulkarni, B.D., 2018. Sustainability assessment of brick work for low-cost housing : A comparison between waste based bricks and burnt clay bricks. Sustain. Cities Soc. 37, 396–406. https://doi.org/10.1016/j.scs.2017.11.025

Johnson Alengaram, U., Al Muhit, B.A., bin Jumaat, M.Z., Jing, M.L.Y., 2013. A comparison of the thermal conductivity of oil palm shell foamed concrete with conventional materials. Mater. Des. 51, 522–529. https://doi.org/10.1016/j.matdes.2013.04.078

Jones, M.R., McCarthy, A., 2006. Heat of hydration in foamed concrete: Effect of mix constituents and plastic density. Cem. Concr. Res. 36, 1032–1041. https://doi.org/10.1016/j.cemconres.2006.01.011

Jones, M.R., McCarthy, A., 2005a. Behaviour and assessment of foamed concrete for construction applications, in: Proceedings of the International Conference on the Use of Foamed Concrete in Construction. Thomas Telford Publishing, University of Dundee, Scotland, UK, pp. 61–88.

Jones, M.R., McCarthy, A., 2005b. Preliminary views on the potential of foamed concrete as a structural material. Mag. Concr. Res. 57, 21–31. https://doi.org/10.1680/macr.2005.57.1.21

Jones, M.R., McCarthy, A., 2005c. Utilising unprocessed low-lime coal fly ash in foamed concrete. Fuel 84, 1398–1409. https://doi.org/10.1016/j.fuel.2004.09.030

Jones, M.R., Mccarthy, M.J., Mccarthy, A., 2003. Moving fly ash utilisation in concrete forward : A UK perspective. Proc. Int. ash Util. Symp. Cent. Appl. energy Res. Univ. Kentucky #113.

Jones, M.R., Zheng, L., Ozlutas, K., 2016. Stability and instability of foamed concrete. Mag. Concr. Res. 68, 542–549. https://doi.org/10.1680/macr.15.00097

Jusoh, N., Bakar, R.A., Ismail, A.R., Ali, T.Z.S., 2015. Computational analysis of thermal building in a no-uniform thermal environment. Energy Procedia 68, 438–445. https://doi.org/10.1016/j.egypro.2015.03.275

Just, A., Middendorf, B., 2009. Microstructure of high-strength foam concrete. Mater. Charact. 60, 741–748. https://doi.org/10.1016/j.matchar.2008.12.011

Kalyana, S., Jyosyula, R., Surana, S., Raju, S., 2020. Materials Today : Proceedings Role of lightweight materials of construction on carbon dioxide emission of a reinforced concrete building. Mater. Today Proc. https://doi.org/10.1016/j.matpr.2020.01.294

Kamisetty, A., Gandhi, I.S.R., Kumar, A., 2023. Combined effect of fly ash and fiber on spreadability, strength and water permeability of foam concrete. J. Build. Eng. 78, 107607. https://doi.org/10.1016/j.jobe.2023.107607

Karl, S., Worner, J.D., 1993. Foamed concrete-mixing and workability, in: Special Concrete-Workability and Mixing. E&FN Spon London, pp. 217–224.

Kashani, A., Ngo, T.D., Mendis, P., Black, J.R., Hajimohammadi, A., 2017. A sustainable application of recycled tyre crumbs as insulator in lightweight cellular concrete. J. Clean. Prod. 149, 925–935. https://doi.org/10.1016/j.jclepro.2017.02.154

Kearsley, E.P., Mostert, H.F., 1997. Foamcrete in Developing Communities, in: FIP Symposium. The Concrete Society of Southern Africa, Johannesburg, South Africa, pp. 735–745.

Kearsley, E.P., Mostert, H.F., n.d. Designing Mix Composition of Foamed Concrete.

Kearsley, E.P., Wainwright, P.J., 2002. The effect of porosity on the strength of foamed concrete. Cem. Concr. Res. 32, 233–239. https://doi.org/10.1016/S0008-8846(01)00665-2

Kearsley, E. P., Wainwright, P.J., 2001a. The effect of high fly ash content on the compressive strength of foamed concrete. Cem. Concr. Res. 31, 105–112. https://doi.org/10.1016/S0008-8846(00)00430-0

Kearsley, E. P., Wainwright, P.J., 2001b. The effect of high fly ash content on the compressive strength of foamed concrete. Cem. Concr. Res. 31, 105–112. https://doi.org/10.1016/S0008-8846(00)00430-0

Kearsley, E P, Wainwright, P.J., 2001. Porosity and permeability of foamed concrete 31.

Khan, M.W., Ali, Y., 2019. Sustainable construction Lessons learned from life cycle assessment (LCA) and life cycle cost analysis (LCCA). Sustain. Constr. https://doi.org/10.1108/CI-05-2019-0040

Khwairakpam, S., Gandhi, I.S.R., Wagh, C., 2023a. Investigations on Optimization of Extraction Process of Surfactant from Hingot Fruit (Balanites aegyptiaca) and Sesame Seed (Sesamum indicum) and Its Suitability in Foam Concrete Production. Arab. J. Sci. Eng. 48, 14119–14152. https://doi.org/10.1007/s13369-023-08098-9

Khwairakpam, S., Ranjani Gandhi, I.S., 2020. Assessment of the potential of a naturally available foaming agent for use in the production of foam concrete. Mater. Today Proc. 32, 896–903. https://doi.org/10.1016/j.matpr.2020.04.528

Khwairakpam, S., Siva, I., Gandhi, R., Gandhi, I.S.R., Wagh, C., 2023b. Investigations on Optimization of Extraction Process of Surfactant from Hingot Fruit (Balanites aegyptiaca) and Sesame Seed (Sesamum indicum) and Its Suitability in Foam Concrete Production. Arab. J. Sci. Eng. https://doi.org/10.1007/s13369-023-08098-9

Kossecka, E., Kosny, J., 2002. Influence of insulation configuration on heating and cooling loads in a continuously used building. Energy Build. 34, 321–331. https://doi.org/10.1016/S0378-7788(01)00121-9

Kováts, P., Thévenin, D., Zähringer, K., 2020. International Journal of Multiphase Flow Influence of viscosity and surface tension on bubble dynamics and mass transfer in a model bubble column 123. https://doi.org/10.1016/j.ijmultiphaseflow.2019.103174

Krstonošić, V., Milanović, M., Dokić, L., 2019. Application of different techniques in the determination of xanthan gum-SDS and xanthan gum-Tween 80 interaction. Food Hydrocoll. 87, 108–118. https://doi.org/10.1016/j.foodhyd.2018.07.040

Kumar, A., Suman, B.M., 2013. Experimental evaluation of insulation materials for walls and roofs and their impact on indoor thermal comfort under composite climate. Build. Environ. 59, 635–643. https://doi.org/10.1016/j.buildenv.2012.09.023

Kumar, R., Lakhani, R., Tomar, P., 2018. A simple novel mix design method and properties assessment of foamed concretes with limestone slurry waste. J. Clean. Prod. 171, 1650–1663. https://doi.org/10.1016/j.jclepro.2017.10.073

Kunhanandan Nambiar, E.K., Ramamurthy, K., 2008. Fresh State Characteristics of Foam Concrete. J. Mater. Civ. Eng. 20, 111–117. https://doi.org/10.1061/(asce)0899-1561(2008)20:2(111)

Kurda, R., Silvestre, J.D., de Brito, J., 2018. Life cycle assessment of concrete made with high volume of recycled concrete aggregates and fly ash. Resour. Conserv. Recycl. 139, 407–417. https://doi.org/10.1016/j.resconrec.2018.07.004

Kuzielová, E., Pach, L., Palou, M., 2016. Effect of activated foaming agent on the foam concrete properties. Constr. Build. Mater. 125, 998–1004. https://doi.org/10.1016/j.conbuildmat.2016.08.122

Lai, G., Liu, X., Li, S., Xu, Y., Zheng, Y., Guan, J., Gao, R., Wei, Z., Wang, Z., Cui, S., 2023. Development of chemical admixtures for green and environmentally friendly concrete: A review. J. Clean. Prod. 389, 136116. https://doi.org/10.1016/j.jclepro.2023.136116

Laukaitis, A., Žurauskas, R., Kerien, J., 2005. The effect of foam polystyrene granules on cement composite properties. Cem. Concr. Compos. 27, 41–47.

Lewis, M.A., 1991. Chronic and sublethal toxicities of surfactants to aquatic animals: A review and risk assessment. Water Res. 25, 101–113. https://doi.org/10.1016/0043-1354(91)90105-Y

Li, J., Chen, Z., Chen, W., Xu, Z., 2020. Seismic performance of pre-cast self-insulation shear walls made by a new type of foam concrete with high strength and low thermal conductivity. Structures 24, 124–136. https://doi.org/10.1016/j.istruc.2020.01.001

Li, P., Wu, H., Liu, Y., Yang, J., Fang, Z., Lin, B., 2019. Preparation and optimization of ultra-light and thermal insulative aerogel foam concrete. Constr. Build. Mater. 205, 529–542. https://doi.org/10.1016/j.conbuildmat.2019.01.212

Li, T., Wang, Z., Zhou, T., He, Y., Huang, F., 2019. Preparation and properties of magnesium phosphate cement foam concrete with H 2 O 2 as foaming agent. Constr. Build. Mater. 205, 566–573. https://doi.org/10.1016/j.conbuildmat.2019.02.022

Lim, S.K., Tan, C.S., Li, B., Ling, T.C., Hossain, M.U., Poon, C.S., 2017. Utilizing high volumes quarry wastes in the production of lightweight foamed concrete. Constr. Build. Mater. 151, 441–448. https://doi.org/10.1016/j.conbuildmat.2017.06.091

Lim, S.K., Tan, C.S., Lim, O.Y., Lee, Y.L., 2013. Fresh and hardened properties of lightweight foamed concrete with palm oil fuel ash as filler. Constr. Build. Mater. 46, 39–47. https://doi.org/10.1016/j.conbuildmat.2013.04.015

Liu, C., Luo, J., Li, Q., Gao, S., Su, D., Zhang, J., Chen, S., 2019. Calcination of green high-belite sulphoaluminate cement (GHSC) and performance optimizations of GHSC-based foamed concrete. Mater. Des. 182, 107986. https://doi.org/10.1016/j.matdes.2019.107986

Liu, M.Y.J., Alengaram, U.J., Jumaat, M.Z., Mo, K.H., 2014. Evaluation of thermal conductivity, mechanical and transport properties of lightweight aggregate foamed geopolymer concrete. Energy Build. 72, 238–245. https://doi.org/10.1016/j.enbuild.2013.12.029

Ma, C., Chen, B., 2016. Properties of foamed concrete containing water repellents. Constr. Build. Mater. 123, 106–114. https://doi.org/10.1016/j.conbuildmat.2016.06.148

Magrabi, S.A., Dlugogorski, B.Z., Jameson, G.J., 2002. A comparative study of drainage characteristics in AFFF and FFFP compressed-air fire-fighting foams. Fire Saf. J. 37, 21–52.

Magrabi, S.A., Dlugogorski, B.Z., Jameson, G.J., 1999. Bubble size distribution and coarsening of aqueous foams. Chem. Eng. Sci. 54, 4007–4022.

Mahlia, T.M.I., Taufiq, B.N., Ismail, Masjuki, H.H., 2007. Correlation between thermal conductivity and the thickness of selected insulation materials for building wall. Energy Build. 39, 182–187. https://doi.org/10.1016/j.enbuild.2006.06.002

Maia de Souza, D., Lafontaine, M., Charron-Doucet, F., Chappert, B., Kicak, K., Duarte, F., Lima, L., 2016. Comparative life cycle assessment of ceramic brick, concrete brick and cast-in-place reinforced concrete exterior walls. J. Clean. Prod. 137, 70–82. https://doi.org/10.1016/j.jclepro.2016.07.069

Majinda, R.R.T., 2012. Extraction and isolation of saponins. Methods Mol. Biol. 864, 415–426. https://doi.org/10.1007/978-1-61779-624-1_16

Maria, A. Di, Maria, A. Di, 2018. Life cycle assessment to evaluate the environmental performance of new construction material from stainless steel slag. Int. J. Life Cycle Assess.

Marwan, M., 2020. The effect of wall material on energy cost reduction in building. Case Stud. Therm. Eng. 17, 100573. https://doi.org/10.1016/j.csite.2019.100573

Mccormick, B.F.C., 1967. Ratioanl Proportioning of Preformed Foam Cellular Concrete. ACI J. Proc. 64. https://doi.org/10.14359/7547

Miles, G.D., Shedlovsky, L., Ross, J., 1945. Foam drainage. J. Phys. Chem. 49, 93–107.

Moffat, J., Morris, V.J., Al-assaf, S., Gunning, A.P., 2016. Visualisation of xanthan conformation by atomic force microscopy. Carbohydr. Polym. 148, 380–389. https://doi.org/10.1016/j.carbpol.2016.04.078

Mohanan, A., Nickerson, M.T., Ghosh, S., 2020. Utilization of pulse protein-xanthan gum complexes for foam stabilization: The effect of protein concentrate and isolate at various pH. Food Chem. 316, 126282. https://doi.org/10.1016/j.foodchem.2020.126282

Mohsen, M.S., Akash, B.A., 2001. Some prospects of energy savings in buildings. Energy Convers. Manag. 42, 1307–1315. https://doi.org/10.1016/S0196-8904(00)00140-0

Mooney, C.Z., 1997. Monte carlo simulation. Sage.

Mydin, A.O., 2011. Effective thermal conductivity of foamcrete of different densities. Concr. Res. Lett. 2, 181–189.

Mydin, A.O., Awang, H., Roslan, A.F., 2012. Determination of lightweight foamed concrete thermal properties integrating various additives. Elixir Cem. Con. Com. 48, 9286–9291.

Mydin, M.A.O., Abdullah, M.M.A.B., Mohd Nawi, M.N., Yahya, Z., Sofri, L.A., Baltatu, M.S., Sandu, A.V., Vizureanu, P., 2022. Influence of Polyformaldehyde Monofilament Fiber on the Engineering Properties of Foamed Concrete. Materials (Basel). 15. https://doi.org/10.3390/ma15248984

Myers, D., 2020. Surfactant science and technology. John Wiley & Sons, New Jersey.

Nambiar, E.K., Ramamurthy, K., 2006. Influence of filler type on the properties of foam concrete. Cem. Concr. Compos. 28, 475–480. https://doi.org/10.1016/j.cemconcomp.2005.12.001

Nambiar, E.K.K., Ramamurthy, K., 2009. Shrinkage Behavior of Foam Concrete. J. Mater. Civ. Eng. 21, 631–636. https://doi.org/10.1061/(asce)0899-1561(2009)21:11(631)

Nambiar, E.K.K., Ramamurthy, K., 2007a. Sorption characteristics of foam concrete. Cem. Concr. Res. 37, 1341–1347. https://doi.org/10.1016/j.cemconres.2007.05.010

Nambiar, E.K.K., Ramamurthy, K., 2007b. Air-void characterisation of foam concrete. Cem. Concr. Res. 37, 221–230. https://doi.org/10.1016/j.cemconres.2006.10.009

Nambiar, E.K.K., Ramamurthy, K., 2006a. Influence of filler type on the properties of foam concrete. Cem. Concr. Compos. 28, 475–480. https://doi.org/10.1016/j.cemconcomp.2005.12.001

Nambiar, E.K.K., Ramamurthy, K., 2006b. Models relating mixture composition to the density and strength of foam concrete using response surface methodology. Cem. Concr. Compos. 28, 752–760. https://doi.org/10.1016/j.cemconcomp.2006.06.001

Namsone, E., Korjakins, A., Sahmenko, G., Sinka, M., 2017. The environmental impacts of foamed concrete production and exploitation. IOP Conf. Ser. Mater. Sci. Eng. 251. https://doi.org/10.1088/1757-899X/251/1/012029

NBC vol. 2, -16, 2016. National Building code of India 2016 Volume 2. Bureau of Indian Standards.

Ng, S.C., Low, K.S., 2010. Thermal conductivity of newspaper sandwiched aerated lightweight concrete panel. Energy Build. 42, 2452–2456. https://doi.org/10.1016/j.enbuild.2010.08.026

Nguyen, T.T., Bui, H.H., Ngo, T.D., Nguyen, G.D., 2017. Materials & Design Experimental and numerical investigation of in fl uence of air-voids on the compressive behaviour of foamed concrete. Mater. Des. 130, 103–119. https://doi.org/10.1016/j.matdes.2017.05.054

Nnanna, I.A., Cheng, G.Y., Xia, J., 2001. Potential applications of protein-based surfactants, in: Nnanna, I.A., Xia, J. (Eds.), Protein-Based Surfactants; Synthesis: Physicochemical Properties, and Applications (Surfactant Science Series). New York, Marcel Dekker, pp. 227–260.

Oginah, S.A., Posthuma, L., Maltby, L., Hauschild, M., Fantke, P., 2023. Linking freshwater ecotoxicity to damage on ecosystem services in life cycle assessment. Environ. Int. 171, 107705. https://doi.org/10.1016/j.envint.2022.107705

Oleszek, W., Hamed, A., 2010. Saponin-based surfactants. Surfactants from Renew. Resour. 1, 239–251.

Oren, O.H., Gholampour, A., Gencel, O., Ozbakkaloglu, T., 2020. Physical and mechanical properties of foam concretes containing granulated blast furnace slag as fine aggregate. Constr. Build. Mater. 238, 117774. https://doi.org/10.1016/j.conbuildmat.2019.117774

Osei-Bonsu, K., Shokri, N., Grassia, P., 2016. Fundamental investigation of foam flow in a liquid-filled Hele-Shaw cell. J. Colloid Interface Sci. 462, 288–296.

Othman, R., Jaya, R.P., Muthusamy, K., Sulaiman, M., Duraisamy, Y., Mustafa, M., Bakri, A., Przybył, A., Sochacki, W., Skrzypczak, T., Vizureanu, P., Sandu, A.V., 2021. Relation between Density and Compressive Strength of Foamed Concrete.

Othuman, M.A., Wang, Y.C., 2011. Elevated-temperature thermal properties of lightweight foamed concrete. Constr. Build. Mater. 25, 705–716. https://doi.org/10.1016/j.conbuildmat.2010.07.016

Pallas, N.R., Harrison, Y., 1990. An automated drop shape apparatus and the surface tension of pure water. Colloids and Surfaces 43, 169–194. https://doi.org/10.1016/0166-6622(90)80287-E

Palod, R., Ramtekkar, S.V.D.G.D., 2019. Utilization of waste from steel and iron industry as replacement of cement in mortars. J. Mater. Cycles Waste Manag. https://doi.org/10.1007/s10163-019-00889-3

Pan, Z., Hiromi, F., Wee, T., 2007. Preparation of high performance foamed concrete from cement, sand and mineral admixtures. J. Wuhan Univ. Technol. Mater. Sci. Ed. 22, 295–298. https://doi.org/10.1007/s11595-005-2295-4

Pan, Z., Li, H., Liu, W., 2014. Preparation and characterization of super low density foamed concrete from Portland cement and admixtures. Constr. Build. Mater. 72, 256–261. https://doi.org/10.1016/j.conbuildmat.2014.08.078

Panesar, D K, 2013. Cellular concrete properties and the effect of synthetic and protein foaming agents. Constr. Build. Mater. 44, 575–584.

Panesar, D. K., 2013. Cellular concrete properties and the effect of synthetic and protein foaming agents. Constr. Build. Mater. 44, 575–584. https://doi.org/10.1016/j.conbuildmat.2013.03.024

Panesar, D.K., Kanraj, D., Abualrous, Y., 2019. Effect of transportation of fly ash: Life cycle assessment and life cycle cost analysis of concrete. Cem. Concr. Compos. 99, 214–224. https://doi.org/10.1016/j.cemconcomp.2019.03.019

Pendergrass, B., Darwin, D., Feng, M., Khajehdehi, R., 2017. Compatibility of shrinkage-

reducing and air-entraining admixtures. ACI Mater. J. 114, 809–818. https://doi.org/10.14359/51689900

Pillai, R.G., Gettu, R., Santhanam, M., Rengaraju, S., Dhandapani, Y., Rathnarajan, S., Basavaraj, A.S., 2019. Service life and life cycle assessment of reinforced concrete systems with limestone calcined clay cement (LC3). Cem. Concr. Res. 118, 111–119. https://doi.org/10.1016/j.cemconres.2018.11.019

Piotrowski, T., Prochoń, P., 2018. Influence of water to solid ratio on mechanical properties of GBFS-based geopolymer foam concrete. MATEC Web Conf. 163, 6–11. https://doi.org/10.1051/matecconf/201816306003

Porter, M.R., 1994. Handbook of Surfactants, Handbook of Surfactants. Springer. https://doi.org/10.1007/978-94-011-1332-8

Pradhan, S., Tiwari, B.R., Kumar, S., Barai, S. V, 2019. Comparative LCA of recycled and natural aggregate concrete using Particle Packing Method and conventional method of design mix. J. Clean. Prod. 228, 679–691. https://doi.org/10.1016/j.jclepro.2019.04.328

Praseeda, K.I., Reddy, B.V.V., Mani, M., 2015a. Embodied and operational energy of urban residential buildings in India. Energy Build. https://doi.org/10.1016/j.enbuild.2015.09.072

Praseeda, K.I., Reddy, B.V.V., Mani, M., 2015b. Embodied energy assessment of building materials in India using process and input – output analysis. Energy Build. 86, 677–686. https://doi.org/10.1016/j.enbuild.2014.10.042

Pugh, R.J., 1996. Foaming, foam films, antifoaming and defoaming. Adv. Colloid Interface Sci. 64, 67–142. https://doi.org/10.1016/0001-8686(95)00280-4

Pushkar, S., 2019. The Effect of Different Concrete Designs on the Life-Cycle Assessment of the Environmental Impacts of Concretes Containing Furnace Bottom-Ash Instead of Sand. Sustainability.

Q.X. Wang*, Y.X. Shi*, J.B. Shi, Y.G. Zhang, W.L., 2015. An Experimental Study on Thermal Conductivity of Ceramsite Cellular Concrete, in: International Conference on Structural, Mechanical and Materials Engineering. pp. 64–69.

Qi, Y., Li, S., Li, Z., Zhang, J., Li, H., 2019. Hydration effect of sodium silicate on cement slurry doped with xanthan. Constr. Build. Mater. 223, 976–985. https://doi.org/10.1016/j.conbuildmat.2019.07.327

Raj, A., Sathyan, D., Mini, K.M., 2019. Physical and functional characteristics of foam concrete: A review. Constr. Build. Mater. 221, 787–799. https://doi.org/10.1016/j.conbuildmat.2019.06.052

Raj, S., Krishnan, J.M., Ramamurthy, K., 2022. Influence of admixtures on the characteristics

of aqueous foam produced using a synthetic surfactant. Colloids Surfaces A Physicochem. Eng. Asp. 643, 128770. https://doi.org/10.1016/j.colsurfa.2022.128770

Ram, V.G., Kishore, K.C., Kalidindi, S.N., 2020. Environmental benefits of construction and demolition debris recycling: Evidence from an Indian case study using life cycle assessment. J. Clean. Prod. 255, 120258. https://doi.org/10.1016/j.jclepro.2020.120258

Ramamurthy, K., Kunhanandan Nambiar, E.K., Indu Siva Ranjani, G., 2009. A classification of studies on properties of foam concrete. Cem. Concr. Compos. 31, 388–396. https://doi.org/10.1016/j.cemconcomp.2009.04.006

Ramesh, T., Prakash, R., Shukla, K.K., 2012. Life cycle energy analysis of a residential building with different envelopes and climates in Indian context. Appl. Energy 89, 193–202. https://doi.org/10.1016/j.apenergy.2011.05.054

Ranjani, G.I.S., 2011. Investigations on behavior of preformed foam concrete using two synthetic surfactants. Civ. Eng. . IIT Madras, Chennai .

Ranjani, G.I.S., Ramamurthy, K., 2010. Analysis of the Foam Generated Using Surfactant Sodium Lauryl Sulfate. Int. J. Concr. Struct. Mater. 4, 55–62. https://doi.org/10.4334/ijcsm.2010.4.1.055

Ranjani, I.S., Ramamurthy, K., 2010. Relative assessment of density and stability of foam produced with four synthetic surfactants. Mater. Struct. Constr. 43, 1317–1325. https://doi.org/10.1617/s11527-010-9582-z

Reddy, T.A., Deng, S., Claridge, D.E., 1999. Development of an inverse method to estimate overall building and ventilation parameters of large commercial buildings. J. Sol. Energy Eng. Trans. ASME 121, 40–46. https://doi.org/10.1115/1.2888141

Reisi, M., Dadvar, S.A., Sharif, A., 2017. Microstructure and mixture proportioning of non-structural foamed concrete with silica fume. Mag. Concr. Res. 69, 1218–1230. https://doi.org/10.1680/jmacr.17.00066

Retta, N., 1991. Extract from Endod (phytolacea dodecandra), a soap berry plant, in the making of concrete. Cem. Concr. Res. 21, 401–409. https://doi.org/10.1016/0008-8846(91)90089-Z

Richard, T.G., Dobogai, J.A., Gerhardt, T.D., Young, W.C., 1975. Cellular concrete – a potential load-bearing insulation for cryogenic applications? IEEE Trans. Magn. 11, 500–503. https://doi.org/10.1109/TMAG.1975.1058746

Roslan, A.F., Awang, H., Mydin, M.A.O., 2013. Effects of various additives on drying shrinkage, compressive and flexural strength of lightweight foamed concrete (LFC). Adv. Mater. Res. 626, 594–604. https://doi.org/10.4028/www.scientific.net/AMR.626.594

Sahu, S.S., Gandhi, I.S.R., 2021a. Studies on influence of characteristics of surfactant and foam on foam concrete behaviour. J. Build. Eng. 40. https://doi.org/10.1016/j.jobe.2021.102333

Sahu, S.S., Gandhi, I.S.R., 2021b. Studies on influence of characteristics of surfactant and foam on foam concrete behaviour. J. Build. Eng. 40, 102333. https://doi.org/10.1016/j.jobe.2021.102333

Sahu, S.S., Gandhi, I.S.R., Khwairakpam, S., 2018. State-of-the-Art Review on the Characteristics of Surfactants and Foam from Foam Concrete Perspective. J. Inst. Eng. Ser. A 99, 391–405. https://doi.org/10.1007/s40030-018-0288-5

Salvini, V.R., Luz, A.P., Pandolfelli, V.C., 2012. Foam Sprayed Porous Insulating Refractories. Refract. WORLDFORUM 4, 93–97.

Samson, G., Phelipot-Mardelé, A., Lanos, C., 2017. Thermal and mechanical properties of gypsum–cement foam concrete: effects of surfactant. Eur. J. Environ. Civ. Eng. 21, 1502–1521. https://doi.org/10.1080/19648189.2016.1177601

Sang, G., Zhu, Y., Yang, G., Zhang, H., 2015. Preparation and characterization of high porosity cement-based foam material. Constr. Build. Mater. 91, 133–137. https://doi.org/10.1016/j.conbuildmat.2015.05.032

Sangwan, K.S., Choudhary, K., Batra, C., 2018a. Environmental impact assessment of a ceramic tile supply chain–a case study. Int. J. Sustain. Eng. 11, 211–216. https://doi.org/10.1080/19397038.2017.1394398

Sangwan, K.S., Choudhary, K., Batra, C., 2018b. Environmental impact assessment of a ceramic tile supply chain–a case study. Int. J. Sustain. Eng. 11, 211–216. https://doi.org/10.1080/19397038.2017.1394398

Saucier, F., Pigeon, M., Plante, P., 1990. Air-Void Stability , Part Ill : Field Tests of Superplasticized Concretes. ACI Mater. J. 3–11.

Schindelin, J., Arganda-Carreras, I., Frise, E., Kaynig, V., Longair, M., Pietzsch, T., Preibisch, S., Rueden, C., Saalfeld, S., Schmid, B., 2012. Fiji: an open-source platform for biological-image analysis. Nat. Methods 9, 676–682.

Şeker, B.Ş., Gökçe, M., Toklu, K., 2022. Investigation of the effect of silica fume and synthetic foam additive on cell structure in ultra-low density foam concrete. Case Stud. Constr. Mater. 16. https://doi.org/10.1016/j.cscm.2022.e01062

Selija, K., Gandhi, I.S.R., 2022. Comprehensive investigation into the effect of the newly developed natural foaming agents and water to solids ratio on foam concrete behaviour. J. Build. Eng. 58, 105042. https://doi.org/10.1016/j.jobe.2022.105042

Shahri, M.P., Shadizadeh, S.R., Jamialahmadi, M., 2012. Applicability test of new surfactant

produced from Zizyphus Spina-Christi leaves for enhanced oil recovery in carbonate reservoirs. J. Japan Pet. Inst. 55, 27–32. https://doi.org/10.1627/jpi.55.27

Sharma, M.K., Shah, D.O., Brigham, W.E., 1984. Correlation of Chain Length Compatibility and Surface Properties of Mixed Foaming Agents with Fluid Displacement Efficiency and Effective Air Mobility in Porous Media. Ind. Eng. Chem. Fundam. 23, 213–220. https://doi.org/10.1021/i100014a013

Sheng, J., 2013. Enhanced oil recovery field case studies. Gulf Professional Publishing, USA.

Sheng, Y., Lu, S., Xu, M., Wu, X., Li, C., 2016. Effect of Xanthan Gum on the Performance of Aqueous Film-Forming Foam. J. Dispers. Sci. Technol. 37, 1664–1670. https://doi.org/10.1080/01932691.2015.1124341

Sheng, Y., Xue, M., Zhang, S., Wang, Y., Zhai, X., Ma, L., Hu, D., Huang, X., 2021. Effect of xanthan gum and silica nanoparticles on improving foam properties of mixed solutions of short-chain fluorocarbon and hydrocarbon surfactants. Chem. Eng. Sci. 245. https://doi.org/10.1016/j.ces.2021.116952

Short, A., Kinniburgh, W., 1963. Lightweight concretes 1–2.

Shrivastava, O.P., 1977. Lightweight aerated concrete – a review. Indian Concr. J 10–23.

Silva, M.A.G., 2004. Influence of Environmental Aging on Properties of Polymeric Mortars. J. Mater. Civ. Eng. 16, 461–468. https://doi.org/10.1061/(ASCE)0899-1561(2004)16

Singh, A., Vaddy, P., Biligiri, K.P., 2020. Resources , Conservation & Recycling Quantification of embodied energy and carbon footprint of pervious concrete pavements through a methodical lifecycle assessment framework. Resour. Conserv. Recycl. 161, 104953. https://doi.org/10.1016/j.resconrec.2020.104953

Singh, G.B., 2005. Site Produced Cellular Lightweight Concrete - a Boon for Housing [WWW Document]. URL https://eco-web.com/edi/050113.html

Singh, M., Chaudhary, K., Srivastava, A., Sangwan, K.S., Bhunia, D., 2017. A study on environmental and economic impacts of using waste marble powder in concrete. J. Build. Eng. https://doi.org/10.1016/j.jobe.2017.07.009

Siva, M., Ramamurthy, K., Dhamodharan, R., 2017. Development of a green foaming agent and its performance evaluation. Cem. Concr. Compos. 80, 245–257. https://doi.org/10.1016/j.cemconcomp.2017.03.012

Siva, M., Ramamurthy, K., Dhamodharan, R., 2015. Sodium salt admixtures for enhancing the foaming characteristics of sodium lauryl sulphate. Cem. Concr. Compos. 57, 133–141. https://doi.org/10.1016/j.cemconcomp.2014.12.011

Souza, D.M. De, Lafontaine, M., Charron-Doucet, F., Bengoa, X., Chappert, B., Duarte, F.,

Lima, L., 2015. Comparative Life Cycle Assessment of ceramic versus concrete roof tiles in the Brazilian context. J. Clean. Prod. 89, 165–173. https://doi.org/10.1016/j.jclepro.2014.11.029

Sritam Swapnadarshi, S., Indu Siva Ranjani, G., Kumar, A., Garg, S., 2021. Evaluation of suitability of carboxymethyl cellulose in performance improvement of sodium lauryl sulfate foam and compressive strength of foam concrete. Adv. Civ. Eng. Mater. 10, 74–92. https://doi.org/10.1520/ACEM20200083

Standard, D., n.d. 42-40 (2002) Foam liquids, fire extinguishing (concentrates, foam, fire extinguishing), issue 2. UK Minist. Def.

Stevenson, P., 2012. Foam engineering: fundamentals and applications. John Wiley & Sons.

Stolz, J., Boluk, Y., Bindiganavile, V., 2018. Mechanical, thermal and acoustic properties of cellular alkali activated fly ash concrete. Cem. Concr. Compos. 94, 24–32. https://doi.org/10.1016/j.cemconcomp.2018.08.004

Subbarao, K.P., 1988. PSTAR - Primary and Secondary Terms Analysis and Renormalization. A Unifed Approach to Building Energy Simulation and Short-Term Monitoring. Sol. Energy Res. Inst. Golden, CO, USA SERI/TR-25.

Sun, C., Zhu, Y., Guo, J., Zhang, Y., Sun, G., 2018. Effects of foaming agent type on the workability, drying shrinkage, frost resistance and pore distribution of foamed concrete. Constr. Build. Mater. 186, 833–839. https://doi.org/10.1016/j.conbuildmat.2018.08.019

Sun, G., Gan, Y., Xu, A., Zhang, Y., Shi, Q., 2022. PHYSICAL REVIEW E 106 , 035101 (2022) Thermodynamic nonequilibrium effects in bubble coalescence : A discrete Boltzmann study. Phys. Rev. E 106, 35101. https://doi.org/10.1103/PhysRevE.106.035101

Tait, M.W., Cheung, W.M., 2016. A comparative cradle-to-gate life cycle assessment of three concrete mix designs. Int. J. Life Cycle Assess. 21, 847–860. https://doi.org/10.1007/s11367-016-1045-5

Tarasov, A.S., Kearsley, E.P., Kolomatskiy, A.S., Mostert, H.F., 2010. Heat evolution due to cement hydration in foamed concrete. Mag. Concr. Res. 62, 895–906. https://doi.org/10.1680/macr.2010.62.12.895

Tiong, H.Y., Lim, S.K., Lee, Y.L., Ong, C.F., Yew, M.K., 2020. Environmental impact and quality assessment of using eggshell powder incorporated in lightweight foamed concrete. Constr. Build. Mater. 244, 118341. https://doi.org/10.1016/j.conbuildmat.2020.118341

Tong, X.C., 2011. Characterization Methodologies of Thermal Management Materials, in: Advanced Materials for Thermal Management of Electronic Packaging. Springer New

York, New York, NY, pp. 59–129. https://doi.org/10.1007/978-1-4419-7759-5_2

Tran, N.P., Nguyen, T.N., Ngo, T.D., Le, P.K., Le, T.A., 2022. Strategic progress in foam stabilisation towards high-performance foam concrete for building sustainability: A state-of-the-art review. J. Clean. Prod. 375, 133939. https://doi.org/10.1016/j.jclepro.2022.133939

Udawattha, C., Halwatura, R., 2017. Life cycle cost of different Walling material used for affordable housing in tropics. Case Stud. Constr. Mater. 7, 15–29. https://doi.org/10.1016/j.cscm.2017.04.005

Udawattha, C., Halwatura, R., 2016. Embodied energy of mud concrete block (MCB) versus brick and cement blocks. Energy Build. 126, 28–35. https://doi.org/10.1016/j.enbuild.2016.04.059

Valore, R.C., 1954a. Cellular Concretes Part 1 Composition and Methods of Preparation. ACI J. Proc. 50, 773–796. https://doi.org/10.14359/11794

Valore, R.C., 1954b. Cellular Concretes Part 2 Physical Properties. ACI J. Proc. 50, 817–836. https://doi.org/10.14359/11795

Vananuvat, P., Kinsella, J.E., 1975. Functional properties of protein isolates from yeast, Saccharomyces fragilis. J. Agric. Food Chem. 23, 613–616.

Varun, Sharma, A., Shree, V., Nautiyal, H., 2012. Life cycle environmental assessment of an educational building in Northern India: A case study. Sustain. Cities Soc. 4, 22–28. https://doi.org/10.1016/j.scs.2012.03.002

Vijayaraghavan, K., Nikolov, A., Wasan, D., Henderson, D., 2009. Foamability of liquid particle suspensions: a modeling study. Ind. Eng. Chem. Res. 48, 8180–8185.

Wagh, C.D., Indu Siva Ranjani, G., Kamisetty, A., 2021. Thermal Properties of Foamed Concrete: A Review. RILEM Bookseries 29, 113–137. https://doi.org/10.1007/978-3-030-51485-3_9

Walstra, P., 1989. Principles of Foam Formation and Stability, in: Wilson, A. (Ed.), Foams: Physics, Chemistry and Structure. Springer, London, pp. 1–15. https://doi.org/10.1007/978-1-4471-3807-5_1

Wang, D., Yu, W., Zhao, X., Dai, W., Ruan, Y., 2016. The influence of thermal insulation position in building exterior walls on indoor thermal comfort and energy consumption of residential buildings in Chongqing. IOP Conf. Ser. Earth Environ. Sci. 40. https://doi.org/10.1088/1755-1315/40/1/012081

Wei, S., Yiqiang, C., Yunsheng, Z., Jones, M.R., 2013. Characterization and simulation of microstructure and thermal properties of foamed concrete. Constr. Build. Mater. 47, 1278–

1291. https://doi.org/10.1016/j.conbuildmat.2013.06.027

Weidema, B.P., Wesnaes, M.S., 1997. example of using data quality indicators * 4, 167–174.

Weigler, H., Karl, S., 1980. Structural lightweight aggregate concrete with reduced density-lightweight aggregate foamed concrete. Int. J. Cem. Compos. Light. Concr. 2, 101–104. https://doi.org/10.1016/0262-5075(80)90029-9

Westphal, F.S., Lamberts, R., 2005. BUILDING SIMULATION CALIBRATION USING SENSITIVITY ANALYSIS Energy Efficiency in Buildings Laboratory (LabEEE) Federal University of Santa Catarina (UFSC) Florianópolis - Santa Catarina - Brazil. 9Th 1331–1338.

Wiley, J., 2010. Surfactants from Renewable.

Wimpenny, D.E., 1996. Some Aspects of the Design and Production of Foamed Concrete, in: Concrete in the Service of Mankind: Appropriate Concrete Technology. University of Dundee, Dundee, pp. 243–252.

Xian, G., Liu, Z., Wang, Z., Zhou, X., 2022. Study on the Performance and Mechanisms of High-Performance Foamed Concrete. Materials (Basel). 15. https://doi.org/10.3390/ma15227894

Yang, K.H., Lee, K.H., Song, J.K., Gong, M.H., 2014. Properties and sustainability of alkali-activated slag foamed concrete. J. Clean. Prod. 68, 226–233. https://doi.org/10.1016/j.jclepro.2013.12.068

Yao, X., Wang, W., Liu, M., Yao, Y., Wu, S., 2019. Synergistic use of industrial solid waste mixtures to prepare ready-to-use lightweight porous concrete. J. Clean. Prod. 211, 1034–1043. https://doi.org/10.1016/j.jclepro.2018.11.252

Yazdanbakhsh, A., Lagouin, M., 2019. The effect of geographic boundaries on the results of a regional life cycle assessment of using recycled aggregate in concrete. Resour. Conserv. Recycl. 143, 201–209. https://doi.org/10.1016/j.resconrec.2019.01.002

Yoon, J., Lee, E.J., Claridge, D.E., 2003. Calibration procedure for energy performance simulation of a commercial building. J. Sol. Energy Eng. Trans. ASME 125, 251–257. https://doi.org/10.1115/1.1564076

Yu, X., Jiang, N., Miao, X., Zong, R., Sheng, Y., Li, C., Lu, S., 2020. Formation of stable aqueous foams on the ethanol layer : Synergistic stabilization of fluorosurfactant and polymers. Colloids Surfaces A 591, 124545. https://doi.org/10.1016/j.colsurfa.2020.124545

Yuanliang, X., Baoliang, L., Chun, C., Yamei, Z., 2021. Properties of foamed concrete with Ca(OH)2 as foam stabilizer. Cem. Concr. Compos. 118, 103985.

https://doi.org/10.1016/j.cemconcomp.2021.103985

Yue, L., Bing, C., 2015. New Type of Super-Lightweight Magnesium Phosphate Cement Foamed Concrete. J. Mater. Civ. Eng. 27, 1–8. https://doi.org/10.1061/(asce)mt.1943-5533.0001044

Zhang, H., Shang, C., Tang, G., 2022. Measurement and identification of temperature-dependent thermal conductivity for thermal insulation materials under large temperature difference. Int. J. Therm. Sci. 171, 107261. https://doi.org/10.1016/j.ijthermalsci.2021.107261

Zhang, J., Gao, X., Yu, L., 2020. Improvement of viscosity-modifying agents on air-void system of vibrated concrete. Constr. Build. Mater. 239, 117843. https://doi.org/10.1016/j.conbuildmat.2019.117843

Zhang, S., Cao, K., Wang, C., Wang, X., Wang, J., Sun, B., 2020. Effect of silica fume and waste marble powder on the mechanical and durability properties of cellular concrete. Constr. Build. Mater. 241, 117980. https://doi.org/10.1016/j.conbuildmat.2019.117980

Zhang, W., Min, H., Gu, X., Xi, Y., Xing, Y., 2015. Mesoscale model for thermal conductivity of concrete. Constr. Build. Mater. 98, 8–16. https://doi.org/10.1016/j.conbuildmat.2015.08.106

Zhang, X., Yang, Q., Shi, Y., Zheng, G., Li, Q., Chen, H., Cheng, X., 2020. Effects of different control methods on the mechanical and thermal properties of ultra-light foamed concrete. Constr. Build. Mater. 262, 120082. https://doi.org/10.1016/j.conbuildmat.2020.120082

Zhang, Y., Chang, Z., Luo, W., Gu, S., Li, W., An, J., 2015. Effect of starch particles on foam stability and dilational viscoelasticity of aqueous-foam. Chinese J. Chem. Eng. 23, 276–280. https://doi.org/10.1016/j.cjche.2014.10.015

Zhang, Z., Provis, J.L., Reid, A., Wang, H., 2015. Mechanical, thermal insulation, thermal resistance and acoustic absorption properties of geopolymer foam concrete. Cem. Concr. Compos. 62, 97–105. https://doi.org/10.1016/j.cemconcomp.2015.03.013

Zhao, X., Lim, S.K., Tan, C.S., Li, B., Ling, T.C., Huang, R., Wang, Q., 2015. Properties of foamed mortar prepared with granulated blast-furnace slag. Materials (Basel). 8, 462–473. https://doi.org/10.3390/ma8020462

Zhou, W., Wang, X., Chen, C., Zhu, L., 2013. Enhanced soil washing of phenanthrene by a plant-derived natural biosurfactant, Sapindus saponin. Colloids Surfaces A Physicochem. Eng. Asp. 425, 122–128.

Zhu, H., Chen, L., Xu, J., Han, Q., 2020. Experimental study on performance improvement of anionic surfactant foaming agent by xanthan gum. Constr. Build. Mater. 230, 116993.

https://doi.org/10.1016/j.conbuildmat.2019.116993

Zimele, Z., Sinka, M., Korjakins, A., Bajare, D., Sahmenko, G., 2019. Life Cycle Assessment of Foam Concrete Production in Latvia. Environ. Clim. Technol. 23, 70–84. https://doi.org/10.2478/rtuect-2019-0080

Zulkarnain, F., Ramli, M., 2011. Durability of performance foamed concrete mix design with silica fume for housing development. J. Mater. Sci. Eng. 5.

PUBLICATIONS/ CONFERENCE/ SYMPOSIUM BASED ON RESEARCH

Publications –

1. **Wagh, C.D.**, Gandhi, I.S.R., Shrivastava, V. (2024). Analysis of Operational Energy Cost of Typical Residential Building (in Guwahati Located in Northeastern India) with Foam Concrete as Walling Material. In: Hazarika, H., Haigh, S.K., Chaudhary, B., Murai, M., Manandhar, S. (eds) Climate Change Adaptation from Geotechnical Perspectives. CREST 2023 2023. Lecture Notes in Civil Engineering, vol 447. Springer, Singapore. https://doi.org/10.1007/978-981-99-9215-7_1
2. **Wagh, C. D**., & Gandhi, I. S. R. (2024). "Investigations on the performance of xanthan gum as a foam stabilizer and assessment of economic and environmental impacts of foam concrete production". *Journal of Building Engineering*, Vol. 82, 108286. https://doi.org/10.1016/j.jobe.2023.108286
3. **Wagh, C. D.**, Gandhi, I. S. R., and Neti, K. V. (2023). "Impact of addition of fly ash (as sand replacement) and polypropylene fires on shrinkage and thermal characteristics of foam concrete", *The Indian Concrete Journal*, Vol. 97, No. 9, pp. 25-34.
4. Khwairakpam, S., Gandhi, I. S. R., & **Wagh, C.D.,** (2023). "Investigations on Optimization of Extraction Process of Surfactant from Hingot Fruit (Balanites aegyptiaca) and Sesame Seed (Sesamum indicum) and Its Suitability in Foam Concrete Production." *Arabian Journal for Science and Engineering*, 48(10), 14119–14152. https://doi.org/10.1007/s13369-023-08098-9
5. Gandhi, I. S. R., Boddepalli, U., Bisht, R. & **Wagh, C.D.,** (2023). "Impact of Addition of Fly Ash (as Sand Replacement) and Polypropylene Fibers on Energy Absorption Characteristics of Foam Concrete". *Advances in Civil Engineering Materials*, 12(1), 127-144. https://doi.org/10.1520/ACEM20220131
6. **Wagh, C.D.**, Gandhi, I.S.R., Kamisetty, A., (2020), "Thermal properties of foamed concrete; a review", 3rd International Conference on Innovative Technologies for Clean and Sustainable development (ITCSD2020), Chandigarh, India, Feb 2020, *Springer-RILEM Bookseries, Proceedings.* https://doi.org/10.1007/978-3-030-51485-3_9

7. Banolia Akshay, **Wagh, C.D**., Das Rahul, Gandhi, I. S. R & Muthukumar P., "Investigations on the Mechanical and Functional behaviour of Mortar Boards Incorporated with Macro Encapsulated Phase Change Materials". *Journal of Materials in Civil Engineering, (Under review)*

Planned for Publication in Refereed Journals: -

1. **Wagh, C. D**., & Gandhi, I. S. R., "Assessment of sustainability of foam concrete as an insulation material for various Indian climatic zones". *Journal of Cleaner Production,*

Conference/Symposium

1. **Wagh, C.D.**, Gandhi, I.S.R., Shrivastava,V., "Analysis of Operational Energy Cost of Typical Residential Building (in Guwahati located in North Eastern India) with Foam Concrete as Walling Material", Construction Resources for Environmentally Sustainable Technologies (CREST 2023). Fukuoka International Congress Centre, 20-22 November 2023, Fukuoka Japan.
2. **Wagh, C.D.**, Gandhi, I.S.R., Kamisetty, A.,"Thermal properties of foamed concrete; a review", 3rd International Conference on Innovative Technologies for Clean and Sustainable Development on 19-21 February 2020, organized by organized by National Institute of Technical Teachers Training & Research, Chandigarh and Maharaja Agrasen University, Baddi, Chandigarh, India
3. **Wagh, C.D.**, and Gandhi, I. S. R. "State-of-the-Art Review on Thermal Properties of Lightweight Foamed Concrete." in Symposium - Concrete Research in India (CRI) on 14th September 2019, organized by IIT Madras, Chennai.

Achievements

1. Won the Best Poster award at Indian Urban Housing Conclave (IUHC 2022) on theme of " Future of Affordable Housing in India" organized under Pradhan Mantri Awas Yojana by Ministry of urban affairs, Govt. of India.